THE UNIVERSITY
of EDINBURGH

A Functional Analysis of RP2 and ARL3 in X-Linked Retinitis Pigmentosa

Abigail Little

Thesis submitted for the degree of Doctor of Philosophy

The University of Edinburgh 2018

igmm
INSTITUTE OF GENETICS & MOLECULAR MEDICINE

Declaration

The work presented in this thesis is my own work except when explicitly stated. This work has not been submitted for any other degree or professional qualification.

Abigail Little, September 2018

Acknowledgements

For the past four years, I have undertaken my PhD studies at the Institute of Genetic and Molecular Medicine, Human Genetics Unit and I feel very lucky to have completed my PhD studies in an institute with such a friendly and collaborative atmosphere. Special thanks has to be given to my PhD supervisor Toby Hurd who for the last four years has spent countless hours teaching me lab techniques and advising on project ideas. Thank you for always listening to my suggestions, however unfeasible and providing advice and support throughout my studies, without which I wouldn't be here today with a completed thesis. I would also like to thank the other lab members who have come and gone in my time as a PhD student Rodanthi Lyraki, Matthieu Vermeren, Jilly Hope and other members of W2 for providing a fun lab environment and always being happy to provide the odd protocol or reagent. I am also grateful to Ian Jackson, Pleasantine Mill, Roly Megaw and their lab members whose suggestions and criticisms in lab meetings have helped shape this project.

During my four years as a PhD student, I have had the pleasure of making wonderful friends in fellow students Gabi Olley, Zoe Crane-Smith, Jane Fraser and Luke Williamson. I credit these friends for keeping me sane throughout my PhD, always providing a person to vent to and a story to laugh at. Thanks for being my lunch buddies, drinking partners, travel buddies, flat mates and best friends for the last four years, a friendship that I'm sure will last for many more years to come as we take our next steps into the future.

I am forever grateful to all my family and friends for their endless support, encouragement and belief in me. Thank you to my parents, Peter and Yvonne, and my sisters Kerry, Holly and Eilidh for listening to my stories of PhD life despite never understanding my project or what my work involves. No matter what the ups and downs I knew I could always rely on my Mum's encouragement from her favourite moto "What's meant for you won't go by you" an attitude which proved invaluable during my PhD studies and one which I'm sure will serve me well in my next steps in life.

Abstract

Retinitis Pigmentosa (RP) is a disease of the retina, which causes progressive retinal degeneration. X-linked RP is one of the most severe subtypes with an estimated 15% of cases caused by mutations in *RP2*. RP2 functions as a GTPase Activating Protein (GAP) for the small G protein ARL3, which is proposed to regulate the traffic of lipid-modified proteins within photoreceptors. It is hypothesised that mutations in *RP2* result in dysregulation of ARL3 and therefore protein mis-trafficking. In order to elucidate the contribution of ARL3 dysregulation to the pathogenesis of RP, I have established new mouse models by CRISPR-mediated genome editing. These include an *Rp2h* knockout line and a line, which harbours a human pathogenic missense mutation, E135G, which abolishes interaction with ARL3.

Furthermore, I have generated mice carrying a Q71L missense mutation in *Arl3*. This mutation locks ARL3 in the active GTP-bound state, and hence is predicted to phenocopy *Rp2h* knockout. Histological examination has revealed that *Rp2h* knockout, *Rp2h* E135G and *Arl3* Q71L/+ mutant animals display progressive retinal degeneration evident from age 6 months. *Arl3* Q71L/Q71L animals display retinal degeneration at age 3 months demonstrating that elevated levels of ARL3-GTP is a driver of retinal degeneration in mice. Immunofluorescence analysis has shown *ARL3 Q71L* mice, *Rp2h* knockout mice and *Rp2h* E135G/Y mice show mislocalisation of lipid modified proteins likely driving retinal degeneration, however further analysis has shown that these mice do not completely phenocopy each other suggesting that levels of ARL3-GTP may not be the only mechanism contributing to retinal degeneration in *Rp2h* mutant mice.

The mechanisms of RP2 regulation are not well understood; therefore to identify potential interactors of RP2 a BIO-ID proximity labelling assay in RPE-1 cells was performed. A top hit from this assay was palmitoyltransferase ZDHHC5. I confirmed this interaction in cells and using a click chemistry based approach demonstrated that it is unlikely that this enzyme functions to palmitoylate RP2. Using immunofluorescence in HeLa cells I have shown that overexpression of ZDHHC5 can rescue the localisation of human pathogenic RP2 mutants C3S and G2A, which are normally mislocalised *in vivo*, independent of its catalytic activity. SiRNA knockdown of ZDHHC5 in cells leads to mislocalisation of RP2 demonstrating ZDHHC5 has a role in trafficking RP2. Results from these studies have provided new knowledge

regarding the mechanisms that cause retinal degeneration and new insights into the potential mechanisms that regulate the trafficking of lipid-modified proteins in photoreceptors.

Lay Summary

The retina is the part of the eye that is responsible for detecting light and sending signals to the brain. Within the retina, the specialised cells which detect light, are called photoreceptors. Inherited Retinal Degenerations are a group of diseases that lead to death of these photoreceptor cells and cause blindness in humans. One specific disease called Retinitis Pigmentosa can be caused by a defect in a molecule called RP2. It is not understood why defects in RP2 cause death of photoreceptors, therefore research into the function of RP2 is essential for the development of treatments for patients. Previous research has suggested that RP2 controls the localisation of other molecules in the photoreceptors by working with another molecule called ARL3. RP2 acts as a switch to inactivate ARL3 in cells, therefore defects in RP2 are thought to lead to photoreceptors which have too much active ARL3. It is thought that this active ARL3 disrupts photoreceptor function eventually leading to cell death. In order to determine if high levels of active ARL3 is the only issue in photoreceptors with defective RP2 I used mouse models that had been designed to have no RP2, defective RP2 or only active ARL3. If having high levels of active ARL3 is the only issue in photoreceptors with defective RP2 all of these mice should become progressively blind at the same rate. Analysis of visual function and photoreceptor health in these animals revealed that they do not all become blind at the same time and that the issues in the photoreceptors leading to blindness are not identical, suggesting RP2 may have other roles in photoreceptors, which when missing also contribute to photoreceptor cell death.

The mechanisms which control RP2 in photoreceptors are not understood, therefore an experiment which identifies new molecules which regulate RP2 was performed. This revealed a new molecule, which controls where RP2 is located in cells and provides new insights into the ways the localisation of molecules in photoreceptors are controlled. Overall, the research described in this thesis provides new knowledge into the causes of photoreceptor death when RP2 is defective in patients with Retinitis Pigmentosa.

Abbreviations

17- ODYA: 17- Octadecynoic Acid
8-oxoG: 8-Oxoguanine
A2: Annexin 2
AD: Activating domain
ADRP: Autosomal Dominant Retinitis Pigmentosa
AIF: Apoptosis Inducing Factor
Aipl1: Aryl Hydrocarbon Receptor Interacting Protein Like 1
Akt: Cellular Homolog of Murine Thymoma virus akt8 Oncogene
AP-1: Activator Protein- 1
AP2: Adaptor Complex 2
ARF: ADP Ribosylation Factor
ARL13B: Arf- like Protein 13B
ARL2: Arf-like Protein 2
ARL3: Arf-like Protein 3
ARL6: Arf-like Protein 6
ARPE19: Adherent Retinal Pigment Epithelium 19
Arr: Arrestin
ARRP: Autosomal Recessive Retinitis Pigmentosa
ATF6: Activating Transcription Factor 6
ATP: Adenosine Triphosphate
BCL2: B-cell lymphoma 2
BD: DNA binding domain
BIO-ID: Proximity Based Biotinylation
BRF: Biomedical Research Facility
BSA: Bovine Serum Albumin
C3: Cysteine 3
cAMP: Cyclic Adenosine Monophosphate
CC: Connecting Cilium
CD36: Cluster of Differentiation 36
cGMP: Cyclic Guanosine Monophosphate
CNG: Cyclic Nucleotide Gated
CNGA1: Cyclic Nucleotide Gated Alpha 1
CNGB1: Cyclic Nucleotide Gated Beta 1
CNTF: Ciliary Neurotrophic Factor
CO-IP: Co-Immunoprecipitation
COS: Cone Outer Segment
CREB: cAMP response element binding protein
CRISPR: Clustered Regularly Interspaced Short Palindromic Repeats
CTRL: Control
DEP: Dishevelled/Eg110/Pleckstrin
DHC2H1: Dynein Heavy Chain 2
DMEM: Dulbecco's Modified Eagle Medium
DNA: Deoxyribonucleic Acid

DPX: Distyrene, Plasticiser and Xylene
DYNC2L11: Cytoplasmic Light Intermediate Chain
ECL: Enhanced Chemilluminescence
EIF2a: Eukaryotic translation initiation factor 2A
ER: Endoplasmic Reticulum
ERG: Electroretinography
ERK: Extracellular- signal Related Kinase
FAK: Focal Adhesion Kinase
FAM161A: Family with Sequence Similarity 161 Member A
FERMT2: Fermitin Family Member 2
FGF-2: Fibroblast growth factor 2
G*: Active Transducin Gα-GTP (Transducin subunit α-GTP)
G: Transducin
GAP: GTPase Activating Protein
GC: Guanyl Cyclase
GCAP: Guanyl Cyclase Activating Proteins
GCL: Ganglion Cell Layer
GDP: Guanosine Diphosphate
GEF: Guanine Nucleotide Exchange Factor
GFAP: Glial Fibrillary Acidic Protein
GFP: Green Florescent Protein
GMP: Guanosine Monophosphate
GOAT: Ghrelin O-acyltransferase
Gp130: Glycoprotein 130
GPCR: G- Protein Coupled Receptor
GRIP1: Glutamate Receptor Interacting Protein 1
GRK1/7: G- protein coupled Receptor Kinase 1/7
gRNA: Guide RNA
GRP78/BiP: Glucose Regulated Protein 78kDa/ Binding Immunoglobulin Protein
Gsn: Gelsolin
GTP: Guanosine Triphosphate
HA: Human influenza hemagglutinin
HCl: Hydrocholic Acid
HEK293T: Human Embryonic Kidney 293 T- antigen
HGU: Human Genetics Unit
HRP: Horseradish Peroxidase
IFT: Intraflagellar Transport
IFT20/88: Intraflagellar Transport Protein 20/88
IFTA/B: Intraflagellar Transport Complex A/B
IGMM: Institute of Genetic and Molecular Medicine
IL6: Interleukin 6
INL: Inner Nuclear Layer
INP55E: Inositol Polyphosphate 5-phosphatase E
IP: Immunoprecipitation
IPL: Inner Plexiform Layer
IRE1: Inositol Requiring 1

IS: Inner Segments
ISCEV: International Society for Clinical Electrophysiology of Vision
JAK: Janus associated kinases
KAP: Kinesin Associated Protein
Kif17: Kinase Like Protein 17
Kif3: Kinesin Family Member 3
L opsin: Long Wave Opsin
LCA: Leber Congenital Amaurosis
Lhx2: LIM Homeobox 2
LIF: Leukaemia Inhibitory Factor
LIFR: Leukaemia Inhibitory Factor Receptor
M opsin: Medium Wave Opsin
MBOAT: Membrane bound O-acyl transferase
MD: Macular Degeneration
MDCK: Madin-Darby Canine Kidney Cells
MERTK: MER proto-oncogene Tyrosine Kinase
MGF-EF: Milk Fat Globule–EF
MKS1/6: Meckel syndrome type 1/6
MMTS: S-methylmethanethiosulfonate
mRNA: Messenger RNA
NDKL: Nucleoside Diphosphate Kinase Like
NLS: Nuclear Localisation Sequence
NPHP: Nephrocystin
Nrl: Neural Retina Lucine Zipper
NSF: N-ethylmaleimide-sensitive factor
OCT: Optical Cutting Temperature
OFD1: Oral Facial Digital syndrome 1
OGG: Oxyguanine Glycosylase
ON: Optic Nerve
ONL: Outer Nuclear Layer
OPL: Outer Plexiform Layer
OS: Outer Segments
OSTF1: Osteoclast Stimulating Factor 1
PACAP: Pituitary adenylate cyclase-activating polypeptide
PAP-1: Pim-1-Associated protein 1
PARP: Poly ADP-ribose polymerase
PAT: Palmitoyltransferase
Pax6: Paired Box Protein 6
PBS: Phosphate- Buffered Saline
PCR: Polymerase Chain Reaction
PDE6*: Catalytically active PDE6
PDE6: Phosphodiesterase 6
PDE6α/β: Phosphodiesterase 6 α/β subunit
PDE6δ: Phosphodiesterase 6 δ
PERK: PKR-like ER kinase
PERK: Protein Kinase R (PKR)-like Endoplasmic Reticulum Kinase

PFA: Paraformaldehyde
pkd2: Polycystin 2
PLCβ1: Phospholipase C β1
PMSF: Phenylmethylsulfonyl Fluoride
PN: Post Natal day
PRPF: Pre-mRNA-Processing-Splicing Factor
PSD: Postsynaptic Density
PVDF: Polyvinylidene Fluoride
R*: Catalytically Active Rhodopsin
R9AP: RGS9-Anchoring Protein
Rax: Retina And Anterior Neural Fold Homeobox
rd1: Retinal Degeneration 1
rd10: Retinal Degeneration 10
rds: Retinal Degeneration Slow
Rec: Recoverin
RGS9-1: Regulator of G protein Signalling Proteins 9-1
Rheb: Ras homolog enriched in brain
RIP3: Receptor Interacting Protein Kinase 3
RIPA: Radioimmunoprecipitation Assay Buffer
RNA: Ribonucleic Acid
RNAi: RNA Interference
ROS: Reactive Oxidative Species
ROS: Rod Outer Segment
RP: Retinitis Pigmentosa
RP2/1: Retinitis Pigmentosa 2/1
Rp2h: Retinitis Pigmentosa 2 homologue
RPE: Retinal Pigment Epithelium
RPE65: Retinal Pigment Epithelium-specific 65 kDa
RPGR: Retinitis Pigmentosa GTPase Regulator
RPGRIP1: RPGR Interacting Protein 1
RPGRIP1L: RPGR Interacting Protein 1 Like
$RPGR^{ORF15}$: Retinitis Pigmentosa GTPase Regulator Open Reading Frame 15
S opsin: Short Wave Opsin
SDS: Sodium Dodecyl Sulphate
Shh: Sonic Hedgehog
siRNA: Small Interfering Ribonucleic Acid
Six3: Six Homeobox 3
SNAP: Synaptosomal-associated protein of 25kDa
SNARE: Soluble NSF Attachment Protein Receptor
snRNP: Small Nuclear Ribonuclear Proteins
SOC: Super Optimal broth with Catabolite repression
ssDNA: Single Stranded DNA
STAT3/1: Signal Transducer and Activator of Transcription 3/1
TALENs: Transcription Activator-like Effector Nucleases
TBCC: Tubulin Specific Chaperone C
TBE: Tris Borate EDTA

TBS: Tris Buffered Saline
TBST: Tris Buffered Saline and Tween 20/ Tx100
TGU: Transgenic Unit
TMEM 237: Transmembrane protein 237
UNC119: Uncoordinated 119
UPR: Unfolded Protein Response
USH1/2: Usher Syndrome Type 1/2
VPP: Rhodopsin V20G, P23H, P27L transgene
WT: Wild Type
XLRP: X- linked Retinitis Pigmentosa
Y2H: Yeast 2 Hybrid
ZDHHC: Zinc finger DHHC domain-containing protein

Contents

List of Figures

List of Tables

Chapter 1

Introduction

Chapter 1: Introduction

1.1 General Structure and Function of the Retina and Photoreceptor Cells

The mammalian eye facilitates vision by focusing light that passes through the lens and cornea to the retina. The retina is a layer of neural tissue at the back of the eye which captures light and sends signals to the brain to facilitate vison. Shortly after gastrulation, the eye field is specified in the medial anterior neural plate and contains all the progenitors required for the development of the neural retina (Heavner and Pevny 2012). Cells in the eye field express a set of eye field specific transcription factors that constitute a gene regulatory network required for the development of the eye. In mammals, these transcription factors include paired box protein 6 (*Pax6)*, retina and anterior neural fold homeobox *(Rax)*, six homeobox 3 *(Six3)* and LIM homeobox 2 *(Lhx2)* (Heavner and Pevny 2012). Both eyes develop from this single eye field which is split into two separate hemispheres, a process which is regulated by sonic hedgehog (*Shh)* and *Six3* (Chiang et al. 1996; Oliver et al. 1995). In mouse at E8.5-9, optic vesicles form from evagination of the embryonic tissue which is densely packed with retinal stem cells, which go on to form the neural retina (Heavner and Pevny 2012). At E9.5 the optic vesicle is reorganised into 3 tissue types: the retinal pigment epithelium (RPE), neural retina and the ventral optic stock which eventually becomes the optic nerve (Heavner and Pevny 2012). At E10.5 the optic vesicles invaginate centrally and create two optic cups from which the eye develops (Adler and Canto-Soler 2007). During development of the optic cup a wave of neurogenesis occurs from the retinal stem cells which gives rise to the cell types present in the adult retina. The first cell type produced is the retinal ganglion cells followed by horizontal cells, amacrine cells and cone photoreceptors. Post-natal retinal precursors give rise to rod photoreceptors, bipolar cells and Muller glial cells (Heavner and Pevny 2012). The precursor cells which give rise to the neural retina cell types migrate to their future destination prior to completing differentiation giving rise to the characteristic conserved laminal structure of the retina (Hoon et al. 2014; Heavner and Pevny 2012).

The retina is supported by the choroid that provides blood supply and nutrients required for cell function and survival (Figure 1.1 A). The retina has a highly conserved laminated structure and is oriented so that the photoreceptors, the light detecting cells,

are at the back of the eye (Thoreson W.B, 2017) (Figure 1.1 B). The photoreceptors are supported by a single layer of pigmented cells, the retinal pigment epithelium (RPE), which are essential for photoreceptor survival (Raymond and Jackson 1995). The RPE physically contact the photoreceptor outer segments and phagocytose the shed photoreceptor outer segment discs (Hall and Abrams 1987). They also contain photoprotective pigment granules, release neurotrophic factors, recycle 11-cis retinal, regulate the flow of ions and nutrients from the retinal blood supply to the outer retina and form the retinal blood-brain barrier (Strauss et.al 2005; Ming *et al.*, 2009). The photoreceptor layer consists of the outer segments (OS), inner segments (IS) and outer nuclear layer (ONL). The ONL contains the photoreceptor cell bodies and nuclei of rod and cone photoreceptors, the IS the region of the photoreceptor where proteins required for vision are synthesised and the OS is made up of OS disc membranes where light detection and phototransduction occurs. Below the ONL is the outer plexiform layer (OPL) which contains the synapses between photoreceptors and horizontal and bipolar cells. Photoreceptors use glutamate as a neurotransmitter and form synapses with the bipolar cells which respond to the neurotransmitter signals (Hoon et al. 2014). Synaptic transmission of this signal is controlled by horizontal cells (Hoon et al. 2014).

Bipolar cells exist in two functional classes the rod bipolar cells and cone bipolar cells where rod bipolar cells preferentially synapse with rod photoreceptors and cone bipolar cells with cones (Hoon et al. 2014). Two further subtypes of bipolar cell exist, ON bipolar cells and OFF bipolar cells. ON bipolar cells depolarise in response to light and all rod bipolar cells are ON bipolar cells. OFF bipolar cells hyperpolarise in response to light, cone bipolar cells can be either the ON or OFF subtypes (Hoon et al. 2014). The inner nuclear layer (INL) consists of the nuclei and cell bodies of the horizontal, bipolar and amacrine cells. The inner plexiform layer (IPL) contains the synaptic junctions between the bipolar, horizontal, amacrine and ganglion cells. The ganglion cell layer (GCL) contains the cell bodies of the ganglion cells. Ganglion cells are the output cells of the retina and their projections form nerve fibres which converge to form the optic nerve (ON) that carries signals from the retina to the brain where visual processing occurs (Thoreson W.B, 2017) (Figure 1.1 B). Excitation of ganglion cells is controlled by amacrine cells and two fast neurotransmitters, γ- aminobutyric acid and glycine. Either Amacrine cells form synapses which directly interact with ganglion cell dendrites, which enables a pathway of signal transduction called feedforward inhibition, or form synapses with axons of bipolar cells, which results in

feedback inhibition, which is responsible for the transmission of scotopic signals from rod cells. The two inhibition mechanisms result in regulation of ganglion cell activation in response to different light intensities (Marc et al. 2014; Hoon et al. 2014).

Figure 1. 1 Schematic of the Eye, Retina Layer and Rod and Cone Photoreceptor Cells

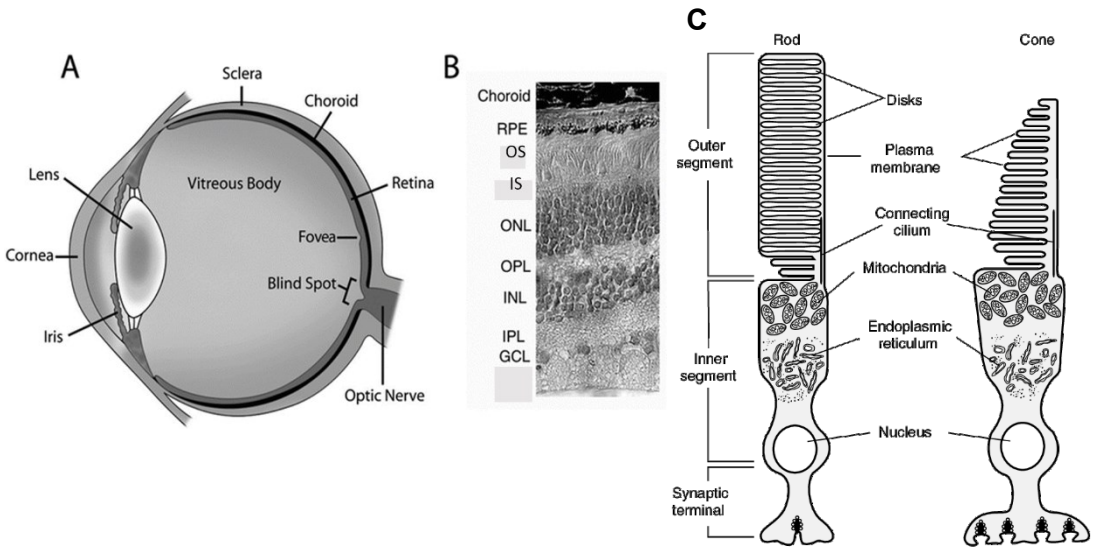

(A) Schematic of Mammalian Eye.
(B) Cross section of primate retina showing different layers.
(C) Schematic of rod and cone photoreceptor cells. Rods are the predominant cell type in the retina with the ratio of rods to cones about 20:1 in the humans. Rods and Cones differ in the organisation of OS discs. Both cell types contain many mitochondria in the IS directly below the OS. IS also contains the machinery required for protein synthesis.

RPE Retinal Pigment Epithelium **OS** Outer Segment **IS** Inner Segment **ONL** Outer Nuclear Layer **OPL** Outer Plexiform Layer **INL** Inner Nuclear Layer **IPL** Inner Plexiform Layer **GCL** Ganglion Cell Layer

Taken from (A and B) Thoreson W.B, 2017 (C) Rick, 2006

1.1.1 Photoreceptor OS Morphogenesis

Photoreceptors are the most abundant cells in the retina and function to detect light and initiate the phototransduction cascade (Kendal et.al 2013). Photoreceptors fall into two distinct cell types, rods and cones. Rods through the photopigment rhodopsin facilitate long wave light detection and night vision whilst cones contain M/L or S opsin photopigments and facilitate daytime and colour vision (Ferrari et al. 2011).

Photoreceptors are polarised neurons composed of two distinct compartments the OS, a modified sensory cilium, and the IS connected via a connecting cilium (CC) (Ferrari et.al 2011) (Figure 1.1 C). The IS is rich in factors involved in protein synthesis, energy generation and transport, whereas the OS contains proteins involved in phototransduction (Liu et.al, 2007). The proper regulation of protein trafficking from the IS to the OS via the CC is essential for photoreceptor function and survival (Besharse et al. 2003).

Rods and cones differ in the morphology of their OS. In rods, stacks of disc membranes are sealed and separated from the plasma membrane by cytosol and in cones the plasma membrane invaginates to form a tightly packed lamellae structure which is open and physically continuous with the plasma membrane (Kawamura and Tachibanaki 2008; Molday 1998) (Figure 1.1 C). In rods it was thought that OS discs develop by evagination of the plasma membrane at the OS base (Ding, Salinas, and Arshavsky 2015) however it was recently discovered that OS discs form as a result of inhibition of ciliary ectosome release (Salinas et al. 2017). Cilia contain the ability to produce ectosomes which are proposed to function to facilitate disposal of proteins from the cell or to transfer materials and genetic information between cells (Wood et al. 2013; Nager et al. 2017; Wood and Rosenbaum 2015). It was demonstrated that in peripherin knockout mice (retinal degeneration slow, *rds-/-*), which do not develop OS's, ciliary ectosomes accumulate at the tip of the connecting cilia during development of the first OS discs (Salinas et al. 2017). In WT retinas peripherin functions to inhibit the release of ciliary ectosomes and membrane structures trapped at the ciliary tip form OS discs through elongation and flattening (Salinas et al. 2017).

In cones, OS's develop from incomplete rim development of the connecting cilia. Evagination of the plasma membrane from the rim of the connecting cilia occurs at the OS base followed by multiple membrane invaginations to form the lamellae structure (Mustafi, Engel, and Palczewski 2009; Farjo et al. 2006). It was shown that although peripherin is essential for the development of the rod outer segments (ROS), absence of peripherin does not prevent cone outer segment (COS) development (Farjo et al. 2006). In order to specifically investigate the development of the COS a *Nrl-/-rds-/-* knockout mouse was generated (Farjo et al. 2006). *Nrl* (neural retina lucine zipper) is required for the development of Rods, thus the *Nrl-/-* mice develop a retina which contains only cones (Mears et al. 2001). This double knockout mouse revealed that in the absence of peripherin, COS's develop and are capable of

phototransduction but are morphologically disrupted suggesting peripherin is not required for the initial membrane evagination but is required for the subsequent membrane invaginations which lead to the lamellae structure of cone OS discs (Farjo et al. 2006).

1.1.2 OS Disc Shedding

Daily renewal of OS's is required for normal retina function (Kevany and Palczewski 2010). Throughout the day photoreceptors add new discs at the base of the OS whereas at the tip older discs are removed and phagocytosed by the adjacent RPE cells (Jonnal et al. 2010). This continual process is thought to counterbalance the light toxicity and metabolic demands endured by the photoreceptors (Organisciak and Winkler 1994; Daemen 1973). RPE cells are thought to recognise the OS by a receptor based mechanism (Kevany and Palczewski 2010). It has been shown that integrin avβ5 and its proposed ligand milk fat globule–EF (MGF-EF) and cluster of differentiation 36 (CD36) are important for OS binding, as mice deficient in these genes or treated with CD36 inhibitors develop retinal degeneration due to inefficient phagocytosis of OS discs (Silvia C Finnemann et al. 1997; S C Finnemann and Silverstein 2001; Nandrot et al. 2007).

Recognition of the OS is thought to trigger a phosphorylation cascade involving MER proto-oncogene tyrosine kinase (MERTK), focal adhesion kinase (FAK) and src kinases. This surge in protein phosphorylation activates signalling that leads to actin cytoskeleton reorganisation, which is required for engulfment of the OS by RPE cells (D'Cruz et al. 2000; Feng et al. 2002; Silvia C Finnemann 2003; Law et al. 2010; Kevany and Palczewski 2010). Internalisation of OS's by the RPE has been shown to require the actin regulator annexin 2 (A2) as knockdown of this gene results in reduced OS internalisation (Law et al. 2010). Formation of the pseudopod that is essential for phagocytosis requires myosin, and in RPE cells myosin II is known to interact with MERTK upon OS stimulation (Strick, Feng, and Vollrath 2009). After internalisation the OS are degraded in phagosomes containing cathepsin D (Deguchi et al. 1994).

1.1.3 Photoreceptor Connecting Cilia

The photoreceptor connecting cilium separates the IS from the OS of photoreceptors and is analogous to the transition zone in cilia (Besharse & Horst 1999). The connecting cilia contains nine microtubule doublets that originate from the basal body which resides in the IS (Greiner et al. 1981). Y shaped linkers connect the microtubules to the integral membrane forming the ciliary necklace which can be visualised by electron microscopy (Besharse and Horst 1990; Insinna and Besharse 2008). The connecting cilia is only 0.25μm in diameter forming a narrow passageway through which all outer segments proteins pass (Insinna and Besharse 2008). Proteins involved in phototransduction such as rhodopsin and the cyclic nucleotide gated (CNG) membrane channels are localised exclusively in the OS (Keady, Le, and Pazour 2011; Moritz et al. 2001; Deretic et al. 2005; Hüttl et al. 2005) and are not found in the IS suggesting the CC acts as a gatekeeper regulating protein entry to the OS. This was confirmed in a study using frogs in which rods that were isolated from the retina by mechanical dissociation were analysed for rhodopsin localisation. Mechanical dissociation causes fusion of the IS and OS and in these rods rhodopsin localised throughout the IS and OS demonstrating that with lack of the connecting cilia, proteins can freely diffuse between segments (Spencer, Detwiler, and Bunt-Milam 1988).

The regulation of protein trafficking in the connecting cilia is thought to occur through multiple mechanisms including intraflagellar transport (IFT) and other forms of regulated membrane trafficking (see 1.5.1 and 1.5.2) which is essential for the function and survival of photoreceptors. Many genes which are associated with human diseases which cause blindness encode for proteins which localise to the connecting cilia, for example Retinitis Pigmentosa GTPase Regulator (*RPGR*) and Retinitis Pigmentosa 2 (*RP2*) which cause X-linked Retinitis Pigmentosa (Hardcastle et al. 1999; Meindl et al. 1996) Nephrocystin 1 (*NPHP1*) which causes Nephronophthisis, a kidney disorder often associated with Retinitis Pigmentosa (Fliegauf 2006) and Usher Syndrome Type 1 (*USH1)* and Usher Syndrome Type 2 (*USH2),* the genes which cause Usher Syndrome which manifests as deafness and blindness in childhood (X. Liu et al. 2007; Maerker et al. 2008).

1.1.4 Phototransduction

1.1.4.1 Phototransduction in Rods

Phototransduction involves absorption of a photon by rhodopsin resulting in rhodopsin becoming catalytically active (R*). R* catalyses the activation of the G protein transducin (G), generating Gα-GTP (G*). G* then activates phosphodiesterase 6 (PDE6) generating PDE6* which hydrolyses cGMP to GMP. Decreased levels of cGMP causes hyperpolarisation in the cell as cGMP gated channels close due to reduced levels of cytoplasmic free cGMP (Yingbin Fu and Yau 2007). Closure of channels leads to decrease in cytoplasmic Ca^{2+} concentration which generates an action potential which stimulates downstream bipolar cells (Shiells and Falk 1990) (Figure 1.2).

Rhodopsin contains the chromophore 11-cis-retinal which binds K296 on mammalian rhodopsin (Yingbin Fu and Yau 2007). In darkness 11-cis-retinal locks rhodopsin in the inactive state however upon absorption of a photon a cis-trans transformation occurs which activates rhodopsin. Rhodopsin activation occurs within milliseconds of photon absorption and generates a series of intermediates which can be identified by their absorption spectra. Meta I describes the bathorhodopsin, lumirhodopsin and metarhodopsin I states this is followed by the metarhodopsin II state (Meta II), which is active rhodopsin also known as R* (Yingbin Fu and Yau 2007).

RPE cells also play an important role in the vision cycle. This was first discovered in *Rpe65* -/- mice which have progressive retinal degeneration and no photoreceptor response despite expression of rhodopsin (Redmond et al. 1998). *Rpe65* is a gene expressed exclusively in the RPE. An accumulation of all-trans retinal was detected in the RPE cells of these mice suggesting RPE65 is required for the generation of 11-cis retinal from all trans retinyl esters (Redmond et al. 1998). As expected RPE65 has isomerhydrolase activity and is required for the conversion of all trans retinal to 11 cis-retinal *in vivo* (Moiseyev et al. 2005).

Transducin activation is the first amplification step in phototransduction, as around 20 transducin molecules are activated by a single R* (Yingbin Fu and Yau 2007; Claudia M. Krispel et al. 2006). In rods the $G\alpha_{t1}G\beta_{1\gamma1}$ isoform of transducin is expressed (Lerea et al. 1986; Fung, Lieberman, and Lee 1992; Y. W. Peng et al. 1992). The $G\alpha_{t1}$ null

mouse (*gnat*-/-) has no detectable rod photoreceptor response, confirming transducin is essential for the propagation of signal from R* to PDE6 (Calvert et al. 2000).

PDE6 is a tetrameric protein made up of two catalytically active domains, α and β, and two γ subunits (Hurley and Stryer 1982). In dark conditions, the two γ subunits are bound to the two catalytic subunits ensuring they remain inactive. However in the light Gα-GTP displaces the γ subunits and frees the catalytic subunits to allow hydrolysis of cGMP (Yingbin Fu and Yau 2007). A mouse with specifically the PDE6γ subunit knocked out demonstrated that the γ subunit is not only required to supress α and β catalytic activity but is also essential for their stability, which in turn is essential for photoreceptor survival as *Pde6γ -/-* mice display rapid retinal degeneration (Tsang et al. 1996). In addition, the retinal degeneration 1 (*rd1)* mouse, a commonly used naturally occurring model of retinal degeneration that carries a nonsense mutation in the β subunit has a rapid severe retinal degeneration demonstrating the β subunit is also required for cell survival (Bowes et al. 1990; B. Chang et al. 2002).

Closure of CNG channels is the final amplification phase of phototransduction. cGMP-gated channels are plasma membrane localised non-cation specific channels that belong to the family of CNG channels present in most cell types (Yingbin Fu and Yau 2007). The rod CNG channel has a 3 CNGA1: 1 CNGB1 subunit ratio (Weitz et al. 2002; Zheng, Trudeau, and Zagotta 2002; Zhong et al. 2002). The baseline concentration of cGMP in the dark ensures channels stay open. However upon light absorption, reduction in cGMP stimulates rapid closure of the channels with sub-millisecond efficiency (Yau 1994; Karpen et al. 1988). *Cngb1* knockout mice revealed that CNGB1 is required to localise CNGA1 to the plasma membrane to form a functional channel, consequently only minimal levels of CNGA are present in these mice and photoreceptors do not respond to light (Hüttl et al. 2005). In humans mutation of *CNGA1* causes Retinitis Pigmentosa (Dryja et al. 1995) (Table 1.1).

1.1.4.2 Termination of Phototransduction in Rods

In order to respond to changes in illumination a rapid inactivation of each activated component is required so that photoreceptors can recover and respond to subsequent photons (Yingbin Fu and Yau 2007). R* is first phosphorylated at several sites by G-protein coupled receptor kinase 1 (GRK1), which lowers its activity, and then bound by arrestin which reduces any residual activity (Wilden, Hall, and Kuhn 1986; Kühn

and Wilden 1987). Six serine/threonine residues on rhodopsin's C-terminus are phosphorylated by GRK1 in mouse with 7 such residues identified in humans (Ohguro et al. 1995). Studies using transgenic mouse models with rhodopsin phosphorylation site mutations demonstrated that at least three sites are required for efficient deactivation of R*, however it was also shown that multiple phosphorylation sites may be required for reproducibility of the single photon response (Doan et al. 2006; Ana Mendez et al. 2000; Hamer et al. 2003; Rieke and Baylor 1998). In mice with multiple phosphorylation site deletions, the reproducibility of the single photon response is reduced with each phosphorylation site that is mutated and this does not depend on site identity (Ana Mendez et al. 2000; Doan et al. 2006). GRK1 mediated phosphorylation and deactivation of rhodopsin is very rapid occurring about ~100ms after the light exposure (Yingbin Fu and Yau 2007).

Recoverin is a calcium binding protein which is N-terminally myristoylated. This myristoylation facilitates interaction with the photoreceptor membrane when calcium levels in the cell are high (Calvert, Klenchin, and Bownds 1995). Recoverin-Ca^{2+} binds GRK1 and inhibits its ability to phosphorylate rhodopsin, this binding was shown to occur in a calcium dependant manner and does not require recoverin myristoylation (C. L. Makino et al. 2004; Calvert, Klenchin, and Bownds 1995). Upon light absorption intracellular calcium levels decrease and calcium free recoverin is unable to bind GRK1, leaving GRK1 free to phosphorylate rhodopsin and induce photoreceptor recovery after phototransduction (C. L. Makino et al. 2004). The phenotype of the recoverin knockout mice (*Rec-/-*) supports this mechanism as *Rec -/-* mice have a faster flash recovery time than WT mice indicating a reduced ability to deactivate R* (C. L. Makino et al. 2004)

Arrestin knockout mice (*Arr -/-*) have ERG responses similar to WT except in the recovery phase where responses only recover to half the baseline value, demonstrating that GRK1 phosphorylation can reduce R* activity but is not sufficient to return responses to baseline values (Xu et al. 1997). Two isoforms of arrestin are expressed in rods, full length p48 and a C-terminal truncated p44 version (Smith et al. 1994). P44 has faster on site binding than P48 and is more efficient than P48 at deactivation of R* *in vitro* and P44 is not transported from the OS during dark adaptation (Palczewski 1994; Philp, Chang, and Long 1987). P48 is expressed 10 times more abundantly than P44 but is translocated from the OS during dark adaptation (see 1.1.3.4) therefore is not present in the OS of active photoreceptors

(Whelan and McGinnis 1988; Philp, Chang, and Long 1987). Rescue experiments in *Arr-/-* mice with specific arrestin isoforms demonstrated that both p44 and p48 could rapidly bind phosphorylated R* however only p48 could inactivate unphosphorylated R* (M. E. Burns 2006).

G* is inactivated by hydrolysis of its bound GTP to GDP. As with many G proteins transducin has intrinsic GTPase activity which is amplified by a GTPase activating protein (GAP) complex (Yingbin Fu and Yau 2007). The GAP for transducin is a complex of regulator of G protein signalling proteins 9-1 (RGS9-1), the long form of Gβ5 subunit (Gβ5-L) and membrane anchor protein, RGS9-anchoring protein (R9AP). RGS9-1 has a G protein γ- like domain that interacts with Gβ5-L. Gβ5-L interacts with R9AP through its Dishevelled/Eg110/Pleckstrin (DEP) domain (W. He, Cowan, and Wensel 1998; E. R. Makino et al. 1999; G. Hu and Wensel 2002). Gα-GDP then dissociates from PDE6γ, allowing PDE6γ to again interact with PDE6α and PDE6β to inhibit their catalytic activity (Yingbin Fu and Yau 2007).

Transgenic mice lacking either RGS9-1, Gβ5-L or R9AP all show a similar phenotype of delayed recovery of the flash response with no effect on A-wave amplitude demonstrating all 3 members of the complex are obligatory for GTPase activity (Keresztes et al. 2004; C M Krispel et al. 2003; Ching Kang Chen et al. 2000). Disruption of any one component leads to reduction in the levels of other components through a post translational mechanism (C.-K. Chen et al. 2003; Ching Kang Chen et al. 2000; Keresztes et al. 2004). The GAP activity of transducin is also increased by PDE6γ thereby ensuring that termination of phototransduction cannot occur until after PDE6α and β have hydrolysed cGMP (Angleson and Wensel 1994; Skiba, Hopp, and Arshavsky 2000).

Guanyl cyclase (GC) enzymes synthesis cGMP and are essential for restoring dark levels of cGMP during recovery of phototransduction. GC activity is regulated by Ca^{2+} and guanyl cyclase activating proteins (GCAP) (Yau 1994). In mouse two gaunyl cyclase enzymes exist, GC1 and GC2. GC1 is expressed in both rods and cones and GC2 is expressed in only rods (Xinran Liu et al. 1994; Lowe et al. 1995). A *Gc1 -/-* mouse revealed that GC1 is required for cone survival as these mice exhibit cone degeneration (R. B. Yang et al. 1999). In the dark the high concentration of Ca^{2+} in the cell facilitates the formation of GCAP-Ca^{2+} which inhibits GCs however in the light the low level of Ca^{2+} results in Ca^{2+} free GCAP and GCs are free to generate more

cGMP (Yingbin Fu and Yau 2007). In mice there are two GCAPs, GCAP1 and GCAP2, both of which are expressed in rods (Cuenca et al. 1998; Howes et al. 1998). A double knockout mouse revealed GCAP deficient photoreceptors have an increased A-wave amplitude and decreased recovery rate after phototransduction in line with a decreased rate of cGMP restoration (A. Mendez et al. 2001). These mice were also used to determine that activation of GCs occurs 40ms after the flash much faster than phosphorylation of rhodopsin which occurs 80-100ms after flash (Marie E. Burns et al. 2002).

1.1.4.3 Phototransduction in Cones

Human cone photoreceptors express either M/L or S opsin photopigments which bind 11-cis retinal to facilitate colour vision. M/L opsin and S opsin have peak absorption spectra a 508nm and 360nm respectively and the Meta II state of cone opsins degrades 50 times faster than rhodopsin (Yingbin Fu and Yau 2007; Imai et al. 1997). After activation of opsin by light absorption, the downstream signalling process in cones is similar to that in rods however some differences in specific protein isoforms do exist (Yingbin Fu and Yau 2007). In cones signal amplification from a single photon is 250 times less efficient than in rods and 30 times less efficient at activating transducin (Kawamura and Tachibanaki 2008). In cones the $G\alpha_{t2}G\beta_3\gamma_8$ isoform of transducin is expressed and the CNG channel in cones has a 2 CNGA3: 2 CNGB3 stoichiometry (Lee et al. 1992; C. Peng, Rich, and Varnum 2004; Fung, Lieberman, and Lee 1992). As expected CNGA3 deficient mice show no cone photoreceptor responses and are commonly used in studies as a method of blocking cone photoreceptor responses (Biel et al. 1999; Y. Fu et al. 2005). In humans, mutations in *CNGA3* and *CNGB3* cause achromatopsia, a condition in which patients have no colour vision (S Kohl et al. 1998; Susanne Kohl et al. 2000). Rod PDE6 consists of the PDE6α and PDE6β catalytic subunits and two identical PDE6γ inhibitory subunits however in cones the catalytic core of PDE6 contains two identical PDE6α subunits and cone PDE6 also contains two cone specific PDE6γ subunits. AAV delivery of cone PDE6α in the *rd10* mouse, which carries a point mutation in *Pde6β* (B. Chang et al. 2002), demonstrated that cone PDE6α can form a functional complex with rod PDE6γ which restores rod photoreceptor responses. Rods expressing cone PDE6α were two times more sensitive to light that WT rods demonstrating that cone PDE6α

has distinct physiological properties which contribute to the functional differences between rods and cones (Deng et al. 2013).

To terminate phototransduction in cones, cone opsin pigments are phosphorylated on more residues than rhodopsin, on human M/L opsin 10 phosphorylation sites have been identified (Yingbin Fu and Yau 2007). In all species studied except mice and rats, two GRKs are expressed, GRK1 in rods and GRK7 in cones, mice and rats express only GRK1 in both rods and cones (Lyubarsky et al. 2000; C K Chen et al. 1999; Yingbin Fu and Yau 2007). GRK7 is present at a much higher concentration in cones than GRK1 is in rods and the specific activity of GRK7 has been shown to be higher than that of GRK1 (Weiss et al. 2001; Tachibanaki et al. 2005; Wada et al. 2006). Phosphorylation of opsin occurs 50 times faster in carp cones compared to rods and the presence of more phosphorylation sites and expression of GRK7 rather than GRK1 is thought explain this difference (Kawamura and Tachibanaki 2008).

Cone photoreceptors also express their own arrestin known as cone arrestin or X-arrestin, however in mice both rod and cone arrestin are expressed in cones (Cheryl M. Craft and Whitmore 1995; Zhu et al. 2005). A cone arrestin knockout mouse demonstrated that cone arrestin is essential for recovery of cone response and even though rod arrestin is expressed in cones it does not compensate for cone arrestin (C M Craft et al. 2006). In rods overexpression of the RGS9-1 R9AP Gβ5-L GAP complex established that termination of G*-PDE6* is the rate limiting step in recovery of the photoresponse as no effect on rate of recovery was detected with GRK1 overexpression but increased recovery was observed with overexpression of the GAP complex (Claudia M. Krispel et al. 2006). It is thought that this is also the rate limiting step in cones however the concentration of RGS9-1 R9AP Gβ5-L is much higher in cones than in rods indicating that this may not necessarily be the rate limiting step in cone photoreceptors (Yingbin Fu and Yau 2007).

Figure 1. 2 Molecular Mechanism of Phototransduction

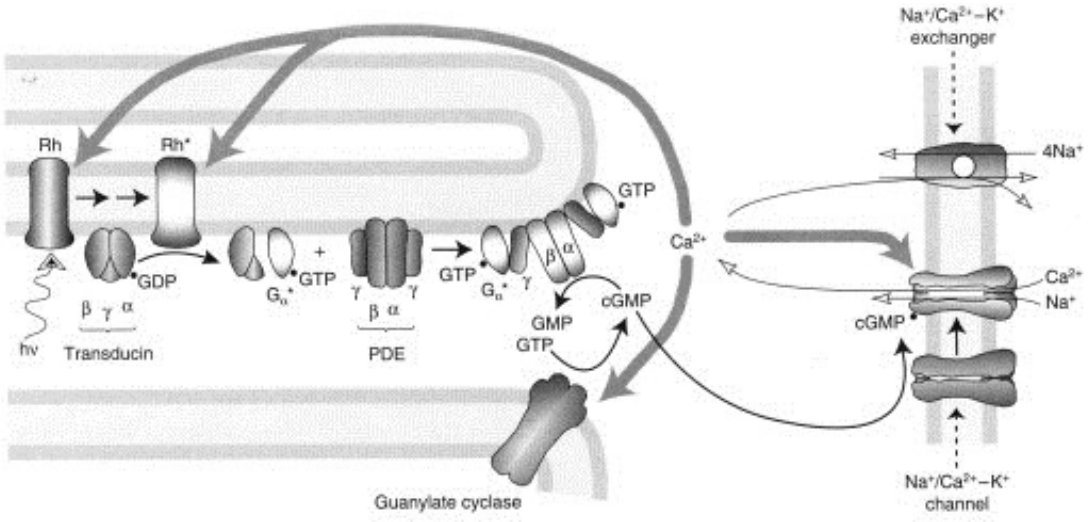

Schematic of the steps of phototransduction in rods. Rhodopsin is activated by absorption of a photon becoming R*. R* then hydrolyses the Gα subunit of transducin generating G*. G* then displaces PDE6γ freeing catalytically active PDE6α and PDE6β to hydrolyse cGMP. The resulting decrease in cGMP levels lead to closure of the CNG channels which decreases cytoplasmic Ca^{2+} levels. The decrease in cytoplasmic Ca^{2+} levels stimulates the production of cGMP from GC which in turn leads to re-opening of the CNG channels and restoration of intracellular Ca^{2+} levels.

Taken from Fain et.al 1996

1.1.4.4 Light and Dark Adaptation

After exposure to bright light photopigment bleaching occurs resulting in reduced photoreceptor sensitivity. This process occurs due to delay in the renewal of photopigment and the presence of a steady decreased cytoplasmic Ca^{2+} concentration (Fain, Matthews, and Cornwall 1996). Under steady background light rods become gradually desensitised, this is known as background or light adaptation. After photobleaching, the slow recovery of the dark current is known as dark adaptation (Fain, Matthews, and Cornwall 1996). Some proteins undergo light induced translocation from the OS to the IS after exposure to bright light (Whelan and McGinnis 1988). The most well studied example of this phenomenon is transducin. In rods the $G\alpha_{t1}$ and the $G\beta_1\gamma_1$ subunits of transducin translocate to the IS upon light

stimulation (Brann and Cohen 1987; Sokolov et al. 2002). This process is thought to prevent rod photoreceptor activation under bright light and to protect against light induced toxicity (Elias et al. 2004; Sokolov et al. 2002). $G\alpha_{t2}$ does not translocate from the cone OS under light stimulation, thus cone phototransduction can occur under bright light conditions (Kennedy, Dunn, and Hurley 2004). Transducin is lipid modified at both the N and C terminus, the N Terminal Gα subunit is acylated and the C terminal Gγ subunit is farnesylated (Y. Fukada et al. 1990; Kokame et al. 1992; Neubert et al. 1992). These post translational lipid modifications regulate its ability to translocate under light adaption as Kassai et.al demonstrated in mice where the farnesylated group on Gγ1 was replaced with a geranylgeranyl group the ability of Gγ1 to translocate under light adaption was reduced and consequently these mice were unable to facilitate proper light adaptation (Kassai et al. 2005). In electroretinography (ERG) studies, to analyse rod responses, subjects are firstly dark adapted so that maximum sensitivity can be detected however when cone function is to be studied rod responses are shut off through photobleaching by exposure to a bright background light.

1.1.5 Comparison of Human and Mouse Retina

The mouse retina is rod dominated, as only 3% of photoreceptors are cones (Carter-Dawson and LaVail 1979). One of the most pertinent differences between the human and the mouse retina is the absence of the macula or fovea in the mouse (Carter-Dawson and LaVail 1979). The macula is a region in the central retina of humans and many other non-primates that facilitates the sharp central vision which is required for reading, driving and seeing fine details. The centre of the macula contains the fovea centrialis where cone photoreceptors are most densely packed and no rod photoreceptors are found (Curcio et al. 1990; Hendrickson 2005). Although the mouse retina does not have a fovea it does have a region of high cone cell density present near the central retina (Volland et al. 2015). The mouse has large RPE cells which facilitate 3 times the phagocytic load of human RPE cells (Volland et al. 2015). Given that OS phagocytosis is essential for survival of photoreceptors, this may be an important feature to consider when analysing disease progression in the mouse. Mouse cone photoreceptors differ from human cones in that humans have three subtypes of cones, one which expresses L opsin, one which expresses M opsin and one which expresses S opsin (Hunt et.al 2005), however in the mouse only one type

of cone cell exists that expresses both M/L and S opsin (Applebury et al. 2000). In this study, it was demonstrated that all mouse cones express M/L and S opsins but the level of expression of each per cone cell varies from the peripheral to the central retina. In extremely peripheral regions S opsin expression was stochastic and some cones expressed only M/L opsin (Applebury et al. 2000). Mice are the most commonly used model of human retinal degenerations therefore, it is important to consider these differences in the retina when comparing findings to human patients.

1.2 Inherited Retinal Degeneration

Retinal degeneration can be associated with either syndromic or non-syndromic ciliopathies, with non-syndromic inherited retinal degeneration displaying a huge amount of genetic and clinical heterogeneity. Mutations in approximately 250 genes are associated with inherited retinal degenerations meaning a specific diagnosis is often not possible based on clinical phenotype alone (Hafler 2017). The shear amount of genetic heterogeneity that exists in diseases of inherited retinal degeneration suggests photoreceptor cell death may be a common outcome resulting from the disruption of multiple biochemical processes (Sullivan and Daiger 1996). Non-syndromic inherited retinal degenerations include Retinitis Pigmentosa (RP), Macular Degeneration (MD), Startgardt's Disease, Leber Congenital Amaurosis (LCA) and Cone-Rod Dystrophies (Daiger, Sullivan, and Bowne 2013; de Jong 2006; den Hollander et al. 2008; C. P. Hamel 2007) which differ by rate of disease progression and age of onset. Syndromic forms of retinal degeneration include the ciliopathies Joubert syndrome and Bardet Bidel syndrome which involve retinal degeneration in combination with kidney, lung and brain phenotypes. Another well known syndromic form of RP is Usher syndrome which manifests as retinal degeneration in combination with hearing impairment in childhood (Saraiva and Baraitser, n.d.; Forsythe and Beales 2013; Boughman, Vernon, and Shaver 1983). Table 1.1 lists various non-syndromic forms of inherited retinal degenerations, examples of genes which when mutated cause the condition and patient phenotypes.

Table 1. 1 Non-Syndromic and Syndromic Inherited Retinal Degenerations

Disease	Genes Mutated	Patient Phenotype
Retinitis Pigmentosa	Examples of some causative genes: Autosomal Dominant: *CRX*, *PRPF3, BEST1, CA4, ARL3* Autosomal Recessive: *CNGA1*, *CNGB1*, *CRB1, IDH3B* X-linked: *RPGR*, *RP2* Over 100 genes known to cause the disease (Strom et al. 2016; Daiger, Sullivan, and Bowne 2013; Galan et al. 2011)	Loss of night vision followed by progressive loss of peripheral and central vision (Daiger, Sullivan, and Bowne 2013)
Macular Degeneration	*CFH*, *APOE*, *ABCA4* Environmental risk factor is smoking. (de Jong 2006)	Late onset loss of central vision occurs in adulthood. Wet form caused by haemorrhage in the eye which causes detachment of the RPE. Occurs rapidly and vison loss occurs after a few weeks. Dry form progresses slowly over time. (de Jong 2006)
Stargardt's Disease	*ABCA4* (Kong et al. 2008)	Occurs in second decade of life leads to progressive loss of central vision and development of macular lesions. (Querques and Souied 2016)

Leber Congenital Amaurosis	*CEP290, GUCY2D, CRB1, RPE65* (den Hollander et al. 2008)	Autosomal recessive blindness from birth or before 1 year of age. No ability to follow light and flat line ERG response. In childhood retinal degeneration occurs and is observed by appearance of pigmented deposits in the retina. (den Hollander et al. 2008)
Cone-Rod Dystrophy	*ABCA4, CRX, GUCY2D, RPGR* (C. P. Hamel 2007)	Loss of central vison, photosensitivity followed by later onset of night blindness (C. P. Hamel 2007)

List of non-syndromic forms of Inherited Retinal Degenerations. Inherited Retinal Degenerations are highly heterogenous as mutations in many genes have been identified as causative. Phenotypes vary between conditions but consistently photoreceptor cells die causing blindness in children or adults.

1.2.1 X-Linked Retinitis Pigmentosa

Retinitis Pigmentosa (RP) is a leading cause of inherited blindness worldwide affecting around 1:3000-1:7000 people (C. Hamel 2006). RP firstly presents as night blindness in childhood, adolescence or adulthood caused by the degeneration of rod photoreceptors followed by secondary cone cell death which leads to loss of central vision (Daiger, Sullivan, and Bowne 2013). Retinitis Pigmentosa is genetically heterogeneous, as over 100 genes have been identified as being causative for the condition (Galan et al. 2011) (see Table 1.1 for examples). A huge amount of clinical heterogeneity exists in RP with age of onset and rate of disease progression varying even between patients from the same families, which harbour the same pathogenic mutation (Sullivan and Daiger 1996; Daiger, Sullivan, and Bowne 2013). RP has three sub-types attributed to the mode of inheritance autosomal dominant (ADRP), autosomal recessive (ARRP) and X-linked (XLRP). Autosomal recessive and X-linked have the most severe clinical phenotype in terms of age of onset and disease

progression (Daiger, Sullivan, and Bowne 2013). Most cases of X-linked RP (70-90%) are caused by mutations in Retinitis Pigmentosa GTPase Regulator (*RPGR*), mutations in Retinitis Pigmentosa 2 (*RP2*) account for the remaining 7-18% (see 1.3 for detailed discussion of RP2 function) however an intronic mutation in Oral Facial Digital syndrome 1 (*OFD1)* has also been reported to cause X-linked RP in one family (Sahel, Marazova, and Audo 2015; Webb et al. 2012).

1.2.2 RPGR Function in the Photoreceptor

Initial isolation of *RPGR* identified a transcript containing 19 exons that is expressed in multiple tissues (Meindl et al. 1996; Yan et al. 1998). Identification of a second splice isoform originating from a splice site within intron 15 lead to the identification of $RPGR^{ORF15}$ (Vervoort et al. 2000). Further studies have shown that the $RPGR^{ORF15}$ isoform is specifically expressed in the retina and is a mutational hotspot in patients with XLRP (Kirschner et al. 1999). $RPGR^{ORF15}$ contains a highly GC rich sequence and Glu-Gly rich repetitive C-terminal domain which is glutamylated prior to anchoring to the membrane of the CC *in vivo* (Sergouniotis et al. 2014; Hong et al. 2000, 2003). The *Rpgr* knockout mouse displayed mislocalisation of opsins generating the hypothesis that RPGR has a role in trafficking opsins from the IS to the OS via the CC (Hong et al. 2000). This was also observed in autopsy samples from human XLRP patients (Adamian et al. 2006). The N-terminal region of RPGR has guanine nucleotide exchange factor (GEF) activity for the small GTPase Rab8 (Murga-Zamalloa et al. 2010). Rab8 is involved in trafficking rhodopsin to the OS implying RPGR may regulate rhodopsin trafficking through this mechanism (Moritz et al. 2001).

RPGR has also been shown to interact with PDE6δ (Linari, Hanzal-Bayer, and Becker 1999), a highly conserved chaperone protein that functions to traffic prenylated proteins to the OS (H Zhang et al. 2007). RPGR also interacts with RPGRIP1 (RPGR Interacting Protein 1) at the CC of photoreceptors (Boylan and Wright 2000; Roepman et al. 2000) and RPGRIP1 also interacts with PDE6δ (Wätzlich et al. 2013). The binding sites on RPGR for PDE6δ and RPGRIP1 overlap (Remans et al. 2014) indicating that PDE6δ may be involved in trafficking RPGR to the CC where RPGRIP1 stimulates release of RPGR from PDE6δ. However this also alludes to the possibility that RPGR may have a role in regulating trafficking of prenylated OS proteins, a phenomenon that when disrupted causes photoreceptor cell death (Houbin Zhang et al. 2015; Z. C. Wright et al. 2016; H Zhang et al. 2007).

The ORF15 domain interacts with the scaffolding protein Whirlin which has been shown to regulate actin dynamics in the ear through its interaction with epsin (R. N. Wright, Hong, and Perkins 2012; J. Yang et al. 2010). Rhodopsin trafficking is controlled by the actin based motor protein myosin VIIa (Wolfrum and Schmitt 2000) implying RPGR could regulate rhodopsin trafficking through regulation of actin dynamics. It has recently been demonstrated that a human XLRP mutation in *RPGR* disrupts the interaction of RPGR with the actin cleavage protein gelsolin. *Rpgr* knockout mice and retinal cultures derived from human *RPGR* mutation carrying patient induced pluripotent stem cells (iPSC) displayed increased actin polymerisation in the CC and mislocalisation of rhodopsin. Furthermore, this phenotype is also present in the gelsolin (*Gsn*-/-) knockout mouse demonstrating that RPGR is required for regulation of gelsolin, which regulates actin polymerisation in the CC, thus regulating rhodopsin trafficking which is essential for photoreceptor maintenance (Megaw *et al.*, 2017).

1.2.3 Mechanisms of Cell Death in RP

The mechanism of photoreceptor cell death in humans is not well understood however studies of cell death mechanism in multiple animal models has revealed that photoreceptors commonly die by apoptosis (Travis 1998). This finding has been observed in studies focussing on the *rd1* mouse, which carries a nonsense mutation in *Pde6β*, the *rds* mouse, which carries a mutation in peripherin, and engineered mice containing human rhodopsin mutations associated with ADRP (G. Q. Chang, Hao, and Wong 1993; Portera-Cailliau et al. 1994). However in retinal degeneration 10 (*rd10)* mice, which carry a point mutation in exon 13 of *Pde6β* and have a slower, later onset degeneration than the *rd1* mouse (B. Chang et al. 2002), ablation of necrosis factor receptor interacting protein kinase 3 (RIP3) protected against cone cell death. Further analysis of the morphology of cone cells during retinal degeneration in *rd10* retinas revealed the presence of both apoptotic nuclei and necrotic cells (Murakami et al. 2012). In human patients the method of cell death as well as the mechanisms which drive cell death are unclear, in order to preserve vision in patients with inherited retinal degenerations it is essential that the mechanisms which drive cell death are deciphered so that effective treatment options can be developed.

1.2.3.1 Phototransduction Defects

In *rd1 -/-* mice the levels of cGMP are 10 fold higher than WT leading to a huge influx of Ca^{2+} from the cGMP-gated channels. The large increase in Ca^{2+} levels is thought to directly activate apoptosis (Farber and Lolley 1977; Bowes et al. 1990). Continuous exposure to light causes photoreceptor cell death and blindness (Travis 1998) and many mutations associated with retinal degeneration constitutively activate the phototransduction cascade. Homozygous mutations in cGMP gated channels (Dryja et al. 1995) and human rhodopsin mutations G90, T94, A292, are all thought to lead to constitutive activation of transducin (Mendes et al. 2005). The hyper- activation of phototransduction is thought to cause oxidative stress in the photoreceptor however the exact mechanism which triggers apoptosis is not completely understood (Travis 1998). In salamander rods it was shown that mislocalised rhodopsin is still able to activate the phototransduction cascade and this initiates apoptosis through a caspase-3 mechanism (Alfinito and Townes-Anderson 2002). Many human pathogenic mutations in rhodopsin lead to rhodopsin mislocalisation (Mendes et al. 2005) and therefore it is possible that these mislocalised rhodopsin molecules can aberrantly activate phototransduction (Alfinito and Townes-Anderson 2002) and stimulate apoptosis.

1.2.3.2 ER Stress

The ER performs essential functions in protein synthesis, regulation of protein post translational modifications and protein sorting (Bravo et al. 2013). An accumulation of misfolded or misprocessed proteins can activate the unfolded protein response (UPR) which exists to protect against ER stress. UPR involves multiple mechanisms which are activated to restore ER homeostasis including upregulation of factors to assist protein folding, inhibition of protein translation and increased degradation of misfolded proteins (Bravo et al. 2013). If the insult to the ER cannot be contained by the UPR ER stress ensues and this can trigger apoptosis through caspase 12 (Szegezdi et al. 2006). Multiple human rhodopsin mutations, which cause RP, have been shown to result in rhodopsin retention in the ER (Mendes et al. 2005). It has been demonstrated in the *rd1* mouse that degenerating photoreceptors have increased expression of the ER stress factors glucose regulated protein 78kDa/ binding immunoglobulin protein (GRP78/BiP), eukaryotic translation initiation factor

2A (EIF2a) and protein kinase R (PKR)-like endoplasmic reticulum kinase (PERK) furthermore caspase 12 can translocate from the IS to the nuclei of degenerating photoreceptors (L. P. Yang et al. 2007; Sanges and Marigo 2006).

1.2.3.3 Oxidative Stress

Generation of reactive oxidative species (ROS) and oxidative stress is the natural biproduct of mitochondrial ATP generation, consequently cells contain multiple mechanisms to protect against oxidative damage known as the antioxidant network (Sancho-Pelluz et al. 2008). Increased oxidative stress can result from increases in the ATP demand in cells, defects in oxidative phosphorylation or deficiencies in defence mechanisms (Halliwell 2006). In other forms of neurodegeneration oxidative stress is prompted by loss of apoptosis inducing factor (AIF) localisation to mitochondria. AIF has high redox activity therefore depletion of AIF results in an increase in ROS (Yamashima 2004). Downregulation of the oxidative stress protective proteins glutathione-*S*-transferase and glutathione peroxidase has been reported to contribute to retinal degeneration in the *rd1* mouse (Ahuja-Jensen et al. 2007; Ahuja et al. 2005). The major biproduct in DNA resulting from ROS's is oxidation of guanine to generate 8-oxoguanasine (8-oxoG) (Kasai and Nishimura 1984). 8-oxoG is able to base pair with either adenine or cytosine so is highly mutagenic (Maki 2002), the accumulation of multiple mis-matched bases if not repaired can lead to apoptosis (Hickman and Samson 1999). Interestingly, samples of visceral fluid from eyes of human RP patients demonstrated increased oxidative stress as measured by increased levels of carbonyl adducts on proteins which occurs as a result of oxidative stress (Campochiaro et al. 2015). Furthermore antioxidant treatment increased photoreceptor survival in *rd1* mice (Sanz et al. 2007) together suggesting oxidative stress induced apoptosis may be an attractive therapeutic target in patients.

1.2.3.4 DNA Damage and Transcription

DNA damage induces the expression of multiple repair enzymes such as poly ADP-ribose polymerase (PARP) and oxyguanine glycosylase (OGG) (Shakibaei et al. 2007; Schreiber et al. 2006). OGG is required to repair mis-match lesions which result from ROS induced 8-oxoG generation (Hill, Hu, and Evans 2008). As PARP

functions to promote DNA repair (Schreiber et al. 2006) it is natural to assume that its activity is protective to the cell, however overexpression of PARP causes increased ATP consumption and oxidative stress (Du et al. 2003). In the *rd1* mouse excessive activity of PARP has been reported and may promote retinal degeneration (François Paquet-Durand et al. 2007). The increased survival of photoreceptors in antioxidant treated *rd1* retinas was partially attributed to a reduction in oxidative stress induced DNA damage (Sanz et al. 2007).

Onset of retinal degeneration is accompanied by huge changes in the transcriptome of the retina (Loscher et al. 2008). Changes in the transcription of transcription factors can influence a myriad of downstream signalling and can influence cell survival pathways. For example ablation of c-fos, a subunit of transcription factor complex activator protein- 1 (AP-1), completely prevented cell death in a light induced model of retinal degeneration (Eferl and Wagner 2003; Wenzel et al. 2000). cAMP response element binding protein (CREB) is a master transcription factor which controls the transcription of multiple genes involved the survival of neurons (CREB target gene database: http://natural.salk.edu/CREB). CREB regulates the transcription of OGG and the anti-apoptotic protein B-cell lymphoma *2 (*BCL2) (X. Zhang et al. 2005; Lonze and Ginty 2002). Reduced CREB expression was detected in the *rd1* mouse (Francois Paquet-Durand et al. 2006) and furthermore in a study in rats with retinal degeneration, the protective effect of antioxidant pituitary adenylate cyclase-activating polypeptide (PACAP) was attributed to increased CREB expression and signalling (Rácz et al. 2006).

1.2.3.5 Secondary Cone Cell Death

A hallmark of RP is loss of rod photoreceptors followed by secondary cone cell death. Currently four models exist which may explain why cone cells die after rod degeneration; 1. Death of rod cells releases toxic factors which kills cones (Ripps 2002), 2. As rod cells die microglial activation occurs and microglial cells migrate to the photoreceptor layer and secrete substances which kill cones (Gupta, Brown, and Milam 2003), 3. Rods secrete a factor that is required for cones for survival (Léveillard et al. 2004) 4. Death of rods causes increased oxidative stress in cones (Shen et al. 2005). The major flaw of the first three hypotheses is that in patients cones can survive for years after all rods have been lost (Shen et al. 2005) therefore

rod cell death resulting in increased oxidative stress in cones is currently the prevailing hypothesis.

As rods degenerate oxygen levels in the retina increase (D.-Y. Yu et al. 2000). This is because the retinal vasculature does not enter the outer retina instead, the outer retina is provided with oxygen by diffusion from choroidal vessels located behind the RPE (Figure 1.3). In the inner retina if oxygen levels are high vessels constrict, reducing blood flow however as the choroidal vessels do not enter the outer retina they do not adapt to changes in oxygen concentration (Campochiaro and Mir 2018) (Figure 1.3). This results in extremely elevated oxygen levels as rod cells die as the volume of oxygen supplied remains steady despite loss of the prevailing cell type. This effect was observed in a cat model of RP where photoreceptor oxygen consumption was reduced as retinal degeneration progressed causing high levels of oxygen throughout the outer retina that spread to the inner retina causing increased restriction of vessels (Padnick-Silver et al. 2006). Increased oxygen levels lead to oxidative stress which manifests via the mechanism described above (see 1.2.3.3). Further evidence supporting this hypothesis comes from multiple studies which have demonstrated decreasing oxidative stress protects against cone cell death *in vivo* (Komeima et al. 2006; Usui et al. 2009; Shen et al. 2005).

Figure 1. 3 Retinal Vasculature

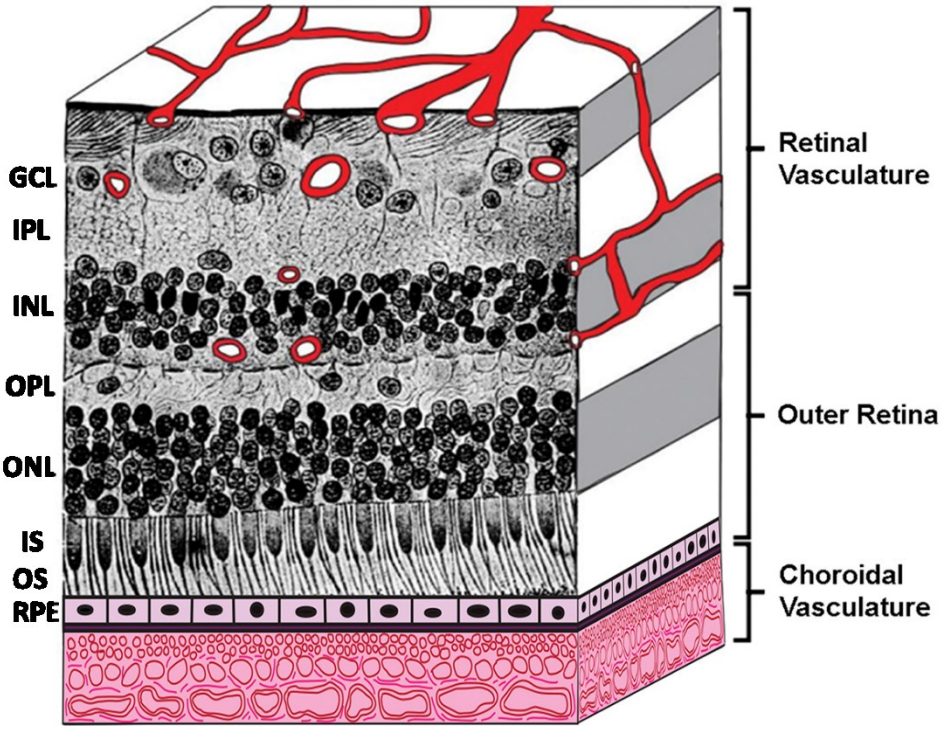

Schematic of Retinal Vasculature. The Retina has two blood supplies. The retinal vasculature supplies the inner retina with oxygen. The choroidal vasculature provides the outer retina with oxygen via diffusion through the RPE and inner and outer segments.

Adapted from Campochario et.al 2018

1.2.3.6 Loss of OS Targeting and OS Shortening

A common feature in mouse models of RP is mislocalisation of OS proteins within the photoreceptor (F. Liu et al. 2015; Houbin Zhang et al. 2015; Z. C. Wright et al. 2016; Hong et al. 2000). This phenotype is observed in mouse models harbouring mutations in *Rpgr* and *Rp2h* and precedes photoreceptor cell death (Houbin Zhang et al. 2015; L. Li et al. 2013; Hong et al. 2000). Many human pathogenic mutations in rhodopsin result in rhodopsin mislocalisation (Mendes et al. 2005). Furthermore in mice where the photoreceptor chaperone proteins PDE6δ and Uncoordinated 119 (UNC119), which function to traffic proteins to the OS, have been knocked out mislocalisation of various proteins is observed accompanied by progressive retinal degeneration (H Zhang et al. 2007; Ishiba et al. 2007). It is hypothesised that these mistargeted proteins may trigger apoptosis as; they overwhelm the normal

trafficking machinery and interrupt with the trafficking of normal cargos, the large amount of mistargeted proteins in the wrong cellular compartments may interfere with normal cellular processes or a metabolic burden may be put on photoreceptors due to continuous degradation of mutant proteins (Mendes et al. 2005).

Another common feature of mouse models of retinal degeneration is shortening of the OS prior to cell death (Travis 1998). Loss of the OS is accompanied by loss of the cGMP-gated channels leading to a decrease in cation influx. This then unloads the mitochondrial Na^+K^+ ATPase channels resulting in reduced oxygen consumption and reduced ATP generation by the IS mitochondria. With loss of the OS the IS and ONL are closer to the oxygen rich choroid capillaries (Figure 1.3) and may be exposed to higher oxygen concentrations which may in itself trigger oxidative stress and cell death (Mendes et al. 2005). Interestingly a double knockout of peripherin and β subunit of PDE6 (*rds -/-, rd1 -/-)* has a slower rate of cell death than the *rd1* -/- mutant alone demonstrating that loss of OS reduces cation influx which produces a protective effect against loss of PDE6β (Sanyal and Jansen 1989) as a dramatic increase in intracellular Ca^{2+} levels is avoided.

Mislocalisation of OS proteins is a common outcome of mutations in many genes which cause retinal degenerations. Mislocalised OS proteins and shortening of the OS likely stimulate apoptosis through various mechanisms as discussed above e.g. mistrafficked proteins may stimulate ER stress, shortening of the OS and mistargeting of proteins involved in phototransduction would likely cause phototransduction defects and loss of Ca^{2+} regulation, which in turn can affect mitochondrial function leading to oxidative stress and DNA damage. Therefore, in order to develop effective therapies for RP it is paramount that the functional defects caused by pathogenic mutations are understood as treatments that reduce oxidative stress may only be effective temporarily as ultimately apoptosis may be activated through alternative mechanisms. However, a treatment that directly prevents mislocalisation of proteins would be expected to be effective long term. It is important to note that mislocalisation of proteins may not be the only pathogenic mechanism which stimulates apoptosis in RP as mutations in genes which encode for splicing factors, which would be expected to affect RNA transcripts, not protein localisation, are causative of ADRP (Chakarova et al. 2002; McKie et al. 2001; Vithana et al. 2001).

1.3 RP2 and ARL3 Protein Structure and Function

1.3.1 The RP2 Protein

The *RP2* gene encodes the 350aa protein RP2 which is ubiquitously expressed at a low level in all tissues (Schwahn et al. 1998). The crystal structure of the RP2 protein revealed an amino-terminal β sheet domain which is homologous to the tubulin specific chaperone co-factor C (Kühnel et al. 2006). Co- factor C in conjunction with co factor D stimulates GTP hydrolysis during tubulin folding. *In vitro* assays by Bartolini et.al demonstrated RP2 also has GAP activity by establishing that RP2 is capable of stimulating the GTP hydrolysis of tubulin in conjunction with co factor D (Bartolini et al. 2002). A second C terminal domain of unknown function shows homology to nucleoside diphosphate kinase (NDK) (Kühnel et al. 2006). In renal epithelial cells, RP2 localised to the basal body and axoneme of primary cilia (Hurd, Fan and Margolis, 2011). In the mouse retina RP2 localises to the basal body of the photoreceptor connecting cilia, the periciliary ridge and Golgi (Evans et al. 2010). Localisation of RP2 is regulated by post translational modifications, palmitoylation at Cysteine 3 (C3) and myristolation at Glycine (G2)(Chapple *et al.*, 2000, 2002).

RP2 interacts with the small GTPase ARF Like Protein 3 (ARL3) (Figure 1.4). Biochemical studies demonstrated RP2 co-crystallises with ARL3-GTP and is capable of increasing ARL3 GTPase activity by about 90,000 times *in vitro* (Veltel, Gasper, et al. 2008). ARL3 is localised to microtubule structures throughout the human retina and is highly enriched at the CC (Grayson et al. 2002). Therefore similar to the function of ARF proteins in intracellular transport it is hypothesised that ARL3 and RP2 play an important role in the trafficking of cargo within the retina from the IS to the OS with disruptions in this process known to cause retinal degeneration (Kühnel et al. 2006). Ismail et.al demonstrated that ARL3 is capable of trafficking prenylated proteins in cells. Upon activation by its guanine nucleotide exchange factor (GEF) ARL13B (Gotthardt et al. 2015), ARL3 is converted from the inactive ARL3-GDP to the active conformation, ARL3-GTP. ARL3-GTP is able to bind to the chaperone phosphodiesterase 6 δ (PDE6δ), which forms a soluble complex with prenylated proteins, and uncoordinated 119 (UNC119) which solubilises myristolated proteins (Fansa et al. 2016; Ismail et al. 2011). Upon stimulation of GTP hydrolysis by RP2, ARL3-GTP is converted to ARL3-GDP resulting in a conformational change in either PDE6δ or UNC119 and the release of their cargo (Ismail et al. 2011; Wätzlich et al.

2013). RP2 and ARL3 also regulate the trafficking of transducin β1 (Gβ1) in ARPE19 cells. RP2 is required for membrane localisation of Gβ1 and expression of ARL3-Q71L, constitutively active ARL3, locked in the GTP bound form, disrupted this membrane localisation. RP2 is required for the incorporation of Gβ1 into Rab11 vesicles suggesting RP2 and ARL3 may regulate the trafficking of Gβ1 to the OS through this mechanism (Schwarz et al. 2012). Rab11 has been implicated in the trafficking of rhodopsin in drosophila photoreceptors and is essential for ciliogenesis in mammalian cells (Satoh 2005; Knodler et al. 2010). Rab11 mediates trafficking through the trans-Golgi network from early endosomes and stimulates the GEF activity of Rabin 8 for Rab8 (Wilcke et al. 2000; Knodler et al. 2010). As Rabin 8 and Rab8 mediate membrane trafficking during ciliogenesis and as rhodopsin is trafficked to the OS in Rab8 associated vesicles in mammalian photoreceptors (Nachury et al. 2007; Moritz et al. 2001), this suggests that RP2 and ARL3 could regulate the trafficking of other G proteins through this mechanism *in vivo*.

The ciliary localisation of RP2 is regulated by binding of importin β2 through the M9-core like sequence on RP2's N terminus (T. W. Hurd, Fan, and Margolis 2011). Importin β2 directly binds cargo and releases them upon binding of Ran-GTP (Pollard et al. 1996; Bonifaci et al. 1997; Siomi et al. 1997). As Importins classically regulate the trafficking of nuclear proteins (Stewart 2007) this demonstrated a new role for importins in the trafficking of cilia proteins. As mutations in the importin β2 M9-core like binding sequence are found in patients with XLRP, this suggests this interaction is required for the function of RP2 *in vivo* (D. Sharon et al. 2000; T. W. Hurd, Fan, and Margolis 2011). RP2 also interacts with N-ethylmaleimide-sensitive factor (NSF), a protein which facilitates membrane/vesicle fusion by promoting disassembly of the soluble NSF attachment protein receptor (SNARE) complex in an ATP-dependant manner (Holopainen et al. 2010). This interaction suggests that RP2 could play a role in regulating vesicular trafficking as disassembly of the SNARE complex is required for recycling of the complex to enable the next round of vesicle- membrane fusion (Littleton et al. 2001). In MDCK cells RP2 regulates the ciliary localisation of polycystin 2 and when either *rp2* or polycystin 2 (*pkd2*) is knocked down in zebrafish with morpholinos a similar phenotype of left-right asymmetry defects occurs and injection of morpholinos for both *rp2* and *pkd2* enhanced this phenotype suggesting both proteins function in the same pathway to regulate cilia function during zebrafish development (T. Hurd et al. 2010). Another study using *rp2* morpholinos to knockdown Rp2 expression in zebrafish demonstrated *rp2* is a maternal effect gene and

maternally derived *rp2* mRNA is required for normal embryo development (Desvignes et al. 2015). However this finding has not been replicated in zebrafish with *rp2* knocked out using transcription activator-like effector nucleases (TALENs) (F. Liu et al. 2015) or in mammals as no fertility defects have been reported in mouse models where *Rp2h* expression is knocked out (Li et al. 2013; Zhang et al. 2015).

1.3.2 RP2 Pathogenic Mutations

Many identified pathogenic mutations in RP2 are predicted to result in no protein expression, however multiple missense mutations have been reported which are not destabilising therefore must disrupt RP2 function (Dror Sharon et al. 2003; F. Liu et al. 2017). The *RP2* E135G and R118H mutations are predicted to disrupt the RP2-ARL3 interaction (Veltel, Gasper, et al. 2008). Mutations at C3 and G2 disrupt the residues which are post-translationally modified *in vivo* leading to mislocalised RP2 (Chapple et al. 2000, 2002). Expression of these mutants in cells has shown that mutations of C3 prevents palmitoylation and results in accumulation of RP2 at intracellular membranes, whereas mutation at G2 results in nuclear accumulation (Chapple et al. 2000). Mutation at G2 prevents myristoylation and palmitoylation of RP2 therefore nuclear accumulation is thought to occur as a result of the nuclear localisation sequence-like (NLS-like) sequence downstream from G2 (Chapple et al. 2000; T. W. Hurd, Fan, and Margolis 2011). The R211L mutation is not destabilising and does not disrupt the RP2-ARL3 interaction as this residue is not close to this interaction interface. R211L does disrupt the interaction of RP2 with osteoclast stimulating factor 1 (OSTF1) although whether loss of this interaction directly leads to retinal degeneration still needs to be determined (Lyraki et al. 2018).

1.3.3 RP2 vs RPGR Patient Phenotype

In a review of the clinical phenotype of patients with XLRP attributed to *RP2* mutation it was shown that early macular involvement was common in *RP2* disease and therefore may be a hallmark of *RP2* disease (Jayasundera et al. 2010). *RP2* patients have earlier loss of central vision compared to *RPGR* patients despite the similarity in disease progression as measured by ERG response (Dror Sharon et al. 2003). Rod photoreceptors do not appear to be more severely affected in *RP2* patients than in *RPGR* patients as onset of night blindness is similar (Flaxel et al. 1999). Early effects

on cone photoreceptors have also been recapitulated in mouse models where *RP2* is knocked out (Li et al. 2013).

1.3.4 The ARL3 protein

Small GTPases act as the molecular switches of the cell by binding and hydrolysing GTP and therefore converting from the active to the inactive state. ARF-like GTPases facilitate GDP-GTP exchange via interacting GEFs and GAPs. GEFs bind the inactive GDP bound ARLs and stimulate conversion to the active state, followed by GAPs which stimulate the hydrolysis of GTP reverting the ARLs back to the inactive GDP bound form (Figure 1.5).

The ARL family of small GTPases contains over 20 members which are conserved across eukaryotes (Yawei Li et al. 2004). A 3D conformation of ARL3 predicted it to have a similar structure to Ras GTPases with a six stranded β sheet surrounded by 5 α helices (Hillig et al. 2000). Human CAGE data reveals ARL3 is most highly expressed in eye, heart and pineal gland, the pineal gland is one of the most ancient features of the vertebrate brain suggesting that ARL3 may have an ancient functional role conserved across species. A comparative genomics study demonstrated that ARL3 and ARL6 are only found in ciliated organisms (Avidor-Reiss et al. 2004). ARL3 is a microtubule associated protein which localised to the CC and microtubules in the human retina (Grayson et al. 2002). In cell culture systems ARL3 localises to the centrosome, mitotic spindle, Golgi membranes, nucleus and is enriched in primary cilia (Enjalbert et al. 2006; Avidor-Reiss et al. 2004). Early functional studies in *C. elegans* demonstrated that ARL3 is a negative regulator of ciliogenesis as *Arl3*$^{-/-}$ worms form normal cilia however overexpression of constitutively active ARL3 (ARL3^{Q70L}) causes ciliogenesis defects (Yujie Li et al. 2010). SiRNA knockdown of ARL3 in mammalian cells caused a range of phenotypes including defects in ciliary trafficking (Lai et al. 2011), Golgi fragmentation and defective cytokinesis (Enjalbert et al. 2006) suggesting ARL3 may have other roles not related to cilia function.

A knockout of *Arl3* in mice has a severe ciliopathy like phenotype with abnormal renal, hepatic and pancreatic epithelial tube structures, defects in photoreceptor development and severe cystic kidney disease resulting in death by 3 weeks of age (Schrick et al. 2006).

Figure 1. 4 Crystal Structure of RP2 and ARL3-GTP Interaction

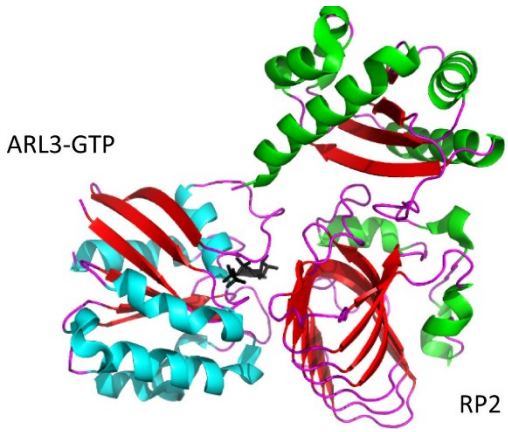

Crystal Structure of ARL3-GTP complexed with RP2. Ribbon diagram of the ARL3-GTP-RP2 complex (ARL3 Q71L): β-strands (red), α-helices (blue for ARL3 and green for RP2), and loops (purple) are shown with GTP bound to ARL3 (GTP, black). Figure was drawn with PyMOL (www.pymol.org, in the public domain).

Taken from Baehr 2014

Figure 1. 5 Small GTPase Activation

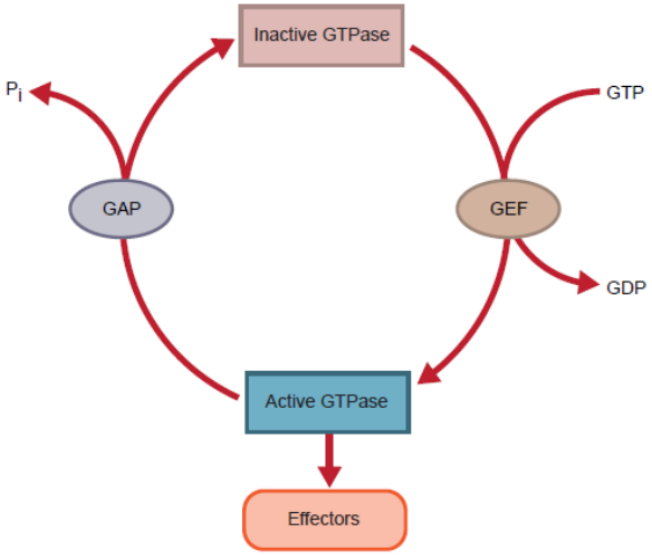

Small GTPases are activated through interaction with GEFs (Guanine Nucleotide Exchange Factors) which facilitate GTP to GDP exchange. Active GTPases can then interact with their effector proteins. GTPases are inactivated by GAPs (GTPase Activating Proteins) which stimulate the hydrolysis of GTP to revert the GTPase back to the inactive state.

1.4 Roles of RP2 and ARL3 in Ciliary Trafficking

1.4.1 General Principles of Cilia

Cilia are small hair like microtubule-based organelles which protrude from the surface of almost every mammalian cell type and exist in two forms motile and non-motile or primary. Primary cilia are the cells antenna to the extracellular environment with studies over the last two decades demonstrating their role as the signalling hub for sonic hedgehog, wnt and other G- protein coupled receptor (GPCR) signalling pathways (Singla and Reiter 2006). Motile cilia protrude from specialised cell types and use dynein motors to generate beating motions essential for facilitating fluid flow across the cell surface (Ibañez-Tallon, Heintz, and Omran 2003). Many genes related to cilia function have been identified as causative of human ciliopathies, a heterogeneous group of syndromic and non-syndromic conditions which manifest with phenotypes including retinal degeneration, cystic kidneys, obesity and mental retardation. Cilia do not contain ribosomes so require a specialised trafficking system to supply the protein load required for their formation and function. This process is known as intraflagellar transport (IFT) and involves the co-operation of IFT complex A and dynein motors and IFT complex B and kinesins which control retrograde and anterograde transport of cargo, respectively (Rosenbaum and Witman 2002). A role for small GTPases in the regulation of cilia formation and function including members from the ARF, ARF-like, Ran and Rab super families has been established (Yujie Li and Hu 2011). ARF-like GTPases are thought to have a particularly significant role with regards to cilia function demonstrated by the identification of human pathogenic mutations in these proteins, ARL13B in Joubert syndrome (Cantagrel et al. 2008), ARL6 in Bardet-beidl syndrome (Khan et al. 2013) and most recently a point mutation in ARL3 being linked to dominantly inherited Retinitis Pigmentosa (Strom et al. 2016).

1.4.2 Intraflagellar Transport

During IFT non-membrane, bound particles are moved across the axonemal doublet microtubules from the base to the tip of the cilia. Cargos moving in this anterograde direction carry cargo required for the maintenance of the axonemes and cilia membranes. In the retrograde direction particles travel from the tip to the basal body, movement of cargo in this direction is required for recycling of IFT particles and motors (Rosenbaum and Witman 2002) (Figure 1.6). Kinesin II is a heterotrimeric

complex of three subunits, two motor subunits kinesin family member 3A (Kif3a) and kinesin family member 3B (Kif3b) and the non-motor subunit kinesin associated protein (KAP) (Scholey 1996). Dynein's use ATP hydrolysis to produce force required to move cargo within cells (Roberts et al. 2013) (Figure 1.6). Ciliated organisms have 15 different dynein heavy chains however in mammals the dynein heavy chain required for IFT is dynein heavy chain 2 (DHC2H1) which exists in a complex with the cytoplasmic light intermediate chain 1 (DYNC2L11) (Pazour, Dickert, and Witman 1999). The kinesins and dynein's required for IFT associate with two large multiprotein intraflagellar transport complexes, IFTA and IFTB (Goetz and Anderson 2010). IFTB and kinesin II are required for anterograde trafficking and disruption of either one prevents cilia formation *in vivo*. IFTA and dynein's regulate retrograde trafficking and disruption of retrograde transport results in small bulged cilia (Goetz and Anderson 2010).

RP2 and ARL3 has also been shown to function in ciliary trafficking as demonstrated by the mislocalisation of ciliary polycystins in *Arl3* -/- worms and the requirement of RP2 for polycystin 2 cilia localisation in MDCK cells (Q. Zhang, Hu, and Ling 2013; T. Hurd et al. 2010). In cultured RPE cells it has been demonstrated that siRNA knockdown of RP2 does not affect ciliogenesis but causes Golgi fragmentation and consequently mislocalisation of intraflagellar transport protein 20 (IFT20) (Evans et al. 2010) and in MDCK cells RP2 knockdown again does not affect ciliogenesis but results in malformed cilia (T. Hurd et al. 2010). Golgi fragmentation was also observed with expression of constitutively active ARL3, ARL3 Q71L, and knockdown of Kif3a demonstrating RP2's GAP activity on ARL3 is required for Golgi cohesion which has a direct effect on the sorting of ciliary destined proteins such as IFT20 (Evans et al. 2010).

Figure 1. 6 Schematic of Intraflagellar Transport in Cilia

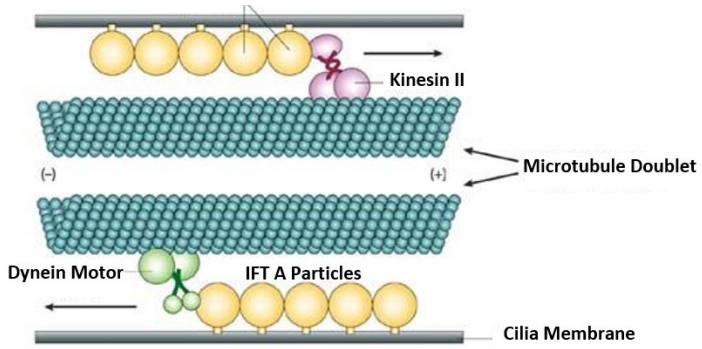

The kinesin II motor protein and IFTB particles travel in the anterograde direction carrying cargo essential for building and maintenance of cilia. IFTA particles and the dynein motor complex travel in the retrograde direction carrying particles out of cilia so that IFT particles and motors can be recycled.

Adapted from Rosenbaum and Witman 2003

1.4.3 Lipid Modified Protein Trafficking

Cilia contain a large amount of lipid modified proteins and many studies have demonstrated the necessity of various posttranslational acylations for cilia membrane targeting (Mick et al. 2015; Roy et al. 2017; Kokame et al. 1992; Chapple et al. 2000). The prenyl binding protein PDE6δ and the myristol binding protein UNC119 interact with the RP2-ARL3 complex (S. a Ismail et al. 2011; S. A. Ismail et al. 2012). Both ARL2 and ARL3 are able to interact with PDE6δ and induce the release of prenylated cargo (S. a Ismail et al. 2011). Recently a study by Fansa et.al sought to investigate the mechanism by which PDE6δ can selectively target some cargo to the cilia and some to the cell body. Using inositol polyphosphate 5-phosphatase E (INPP5E) as an example of a protein trafficked exclusively to the cilia and Ras homolog enriched in brain (Rheb) a protein localised to endomembranes by PDE6δ, they showed that INPP5E has a 100x higher affinity for PDE6δ than Rheb. Using *in vitro* kinetic assays they demonstrated that ARL2 and ARL3 were both able to release Rheb from PDE6δ, however only ARL3 could release INPP5E. This has been confirmed in RPE-1 cells where it has been shown that only ARL3 and not ARL2 can release INPP5E from PDE6δ (S. Thomas et al. 2014). Furthermore siRNA knockdown of ARL3 caused INPP5E to be partially mislocalised to the cell body (Fansa et.al 2016). Together this

evidence suggests a model of ciliary trafficking such that prenylated cargos are solubilised by PDE6δ, complexes binding with high affinity are trafficked to the cilia. ARL3 is activated by it's GEF ARL13b, cargo is then released by ARL3-GTP in the cilia and low affinity complexes are released in the cytosol by ARL2-GTP (Fansa et al. 2016)(Figure 1.7). Only ARL3-GTP can efficiently release cargo from UNC119 (S. A. Ismail et al. 2012; K. J. Wright et al. 2011) and this is required for ciliary localisation of nephrocystin 3 (NPHP3) (K. J. Wright et al. 2011). The exact mechanism of cargo release differs slightly between PDE6δ and UNC119 such that when ARL3-GTP binds UNC119 it induces opening of the hydrophobic binding pocket resulting in release of cargo, whereas for PDE6δ ARL3-GTP binding induces closure of the hydrophobic binding pocket and subsequent cargo release (S. a Ismail et al. 2011; S. A. Ismail et al. 2012).

Figure 1. 7 The Role of RP2-ARL3-PDE6δ in Cilia Trafficking

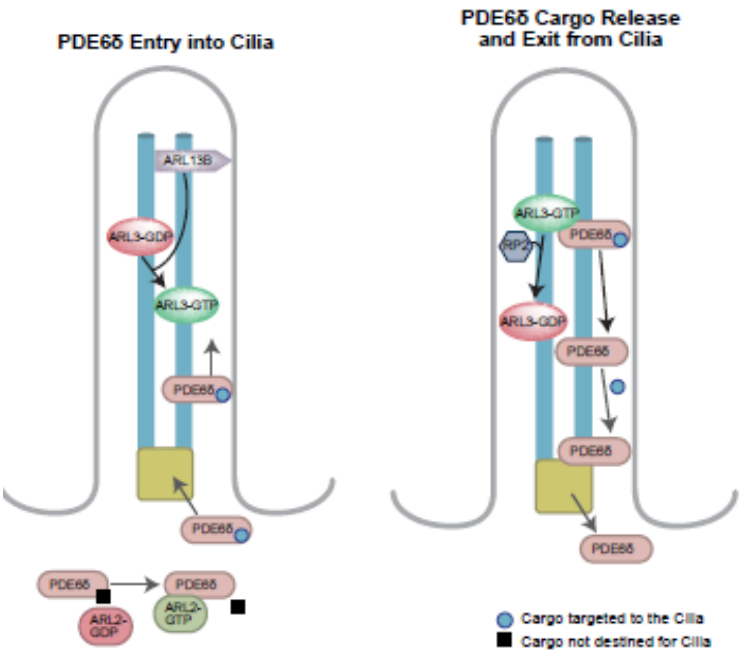

Schematic of RP2-ARL3-PDE6δ trafficking in Cilia. High affinity cargo such as proteins destined for cilia e.g. INP55E bind tightly to PDE6δ so are trafficked to the cilia. At the cilia, ARL3-GDP is activated to ARL3-GTP by ARL13B. ARL3-GTP then interacts with PDE6δ and causes closure of the hydrophobic pocket and release of INP55E in the cilia. ARL3-GTP is converted back to ARL3-GDP by RP2. Low affinity binding cargo e.g. Rheb is released by ARL2-GTP outside the cilia. Rheb then localises to the ER membranes.

1.5 The Role of RP2 and ARL3 in Photoreceptor Protein Trafficking

1.5.1 Intraflagellar Transport in Photoreceptors

Intraflagellar transport occurs in photoreceptors and has important roles in the morphogenesis and maintenance of the OS (Marszalek et al. 2000; Pazour et al. 2002) (Figure 1.8). IFT proteins, IFT20, IFT88, kinesin II and dynein's have been detected at the ciliary axoneme of the connecting cilia in photoreceptors (Baker et al. 2003; Insinna et al. 2008; Mikami 2002; Pazour et al. 2002). IFT complexes have been identified in photoreceptors containing kinesin II, dynein's, rhodopsin and GC1 suggesting IFT is required for the trafficking of these proteins to the photoreceptor OS (Bhowmick et al. 2009). Transgenic mice where *Kif3a*, *Ift20* or *Ift88* were knocked out in photoreceptors confirmed IFT is required for rhodopsin and GC1 trafficking *in vivo,* as all of these mice display defects in OS development, mislocalised rhodopsin and rapid retinal degeneration (Keady, Le, and Pazour 2011; Marszalek et al. 2000; Pazour et al. 2002).

Evidence for a role of RP2 and ARL3 in IFT mediated trafficking in photoreceptors comes from a mouse in which *Rp2h* was knocked out (L. Li et al. 2013) and resulted in mislocalisation of M/L opsin prior to onset of retinal degeneration (L. Li et al. 2013). M/L opsin is thought to be trafficked to the OS by an IFT mediated mechanism involving Kif3a and the homomeric kinesin kinase like protein 17 (Kif17) (Avasthi et al. 2009; Insinna et al. 2008). It has since been demonstrated that RP2 and ARL3 interact with Kif17 and regulate its localisation at ciliary tips *in vitro* (Schwarz et al. 2017) suggesting a mechanism by which RP2 and ARL3 may regulate the localisation of Kif17 and thus regulate M/L opsin trafficking *in vivo*. In a *rp2* knockout zebrafish mislocalisation of rhodopsin and M/L opsin was not observed casting doubt on the importance of RP2 and ARL3 in IFT mediated trafficking *in vivo*. In another *Rp2h* knockout mouse model no mislocalisation of rhodopsin or M/L opsin was observed even at late stages of retinal degeneration casting further doubt on the role RP2 and ARL3 play in IFT *in vivo* (Houbin Zhang et al. 2015). *Rp2h* knockout mouse phenotypes discussed in detail in 3.1.

Figure 1. 8 Schematic of IFT in Photoreceptors

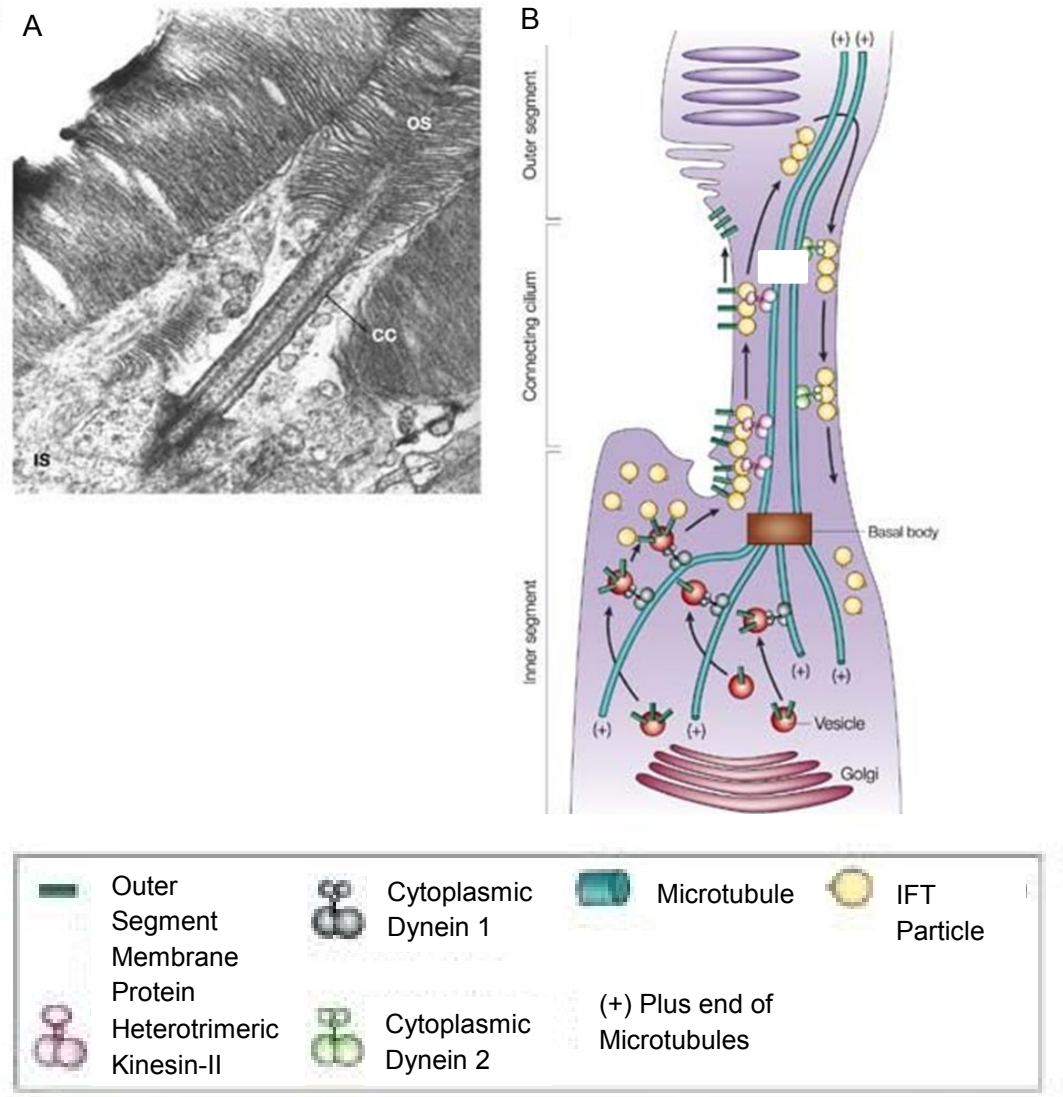

(A) Electron micrograph showing the photoreceptor connecting cilia (CC) between the Inner Segment (IS) and Outer Segment (OS) in a rod photoreceptor.

(B) Schematic of IFT in photoreceptors. Cargo is sorted into vesicles destined for the OS and transported to the base of the connecting cilia via cytoplasmic Dynein 1 on microtubules. Once at the base of the CC IFT particles associate with vesicles and vesicles fuse with the ciliary or plasma membrane. IFT particles and their attached cargo are transported through the CC by kinesin II. At the tip of the CC IFT particles disassociate from their cargo and are taken back to the IS by cytoplasmic dynein 2.

Adapted from Pazour et.al 2002

1.5.2 Trafficking of OS Proteins in Photoreceptors

The function of RP2 and ARL3 in photoreceptors has been studied in depth using mouse models. Retina ($Ret^{ARL3-/-}$) and rod specific *Arl3* knockout ($Rod^{ARL3-/-}$) mice were generated using cre-lox system in order to investigate the roles of ARL3 pre and post ciliogenesis in the mouse retina (Hanke-Gogokhia et al. 2016). Mice were generated by crossing into two different transgenic lines, iCre75 which expresses Cre in rods (S. Li et al. 2005) and six3Cre which expresses Cre in retinal progenitors (Furuta et.al 2002). $Rod^{ARL3-/-}$ retinas developed normally with normal connecting cilia. These mice showed normal photopic and scotopic ERG responses at p15, demonstrating normal function of photoreceptors, however ERG responses were reduced at 1 month of age and by 2 months of age both rods and cones were severely degenerated. Global mislocalisation of lipid modified proteins was reported in these mice with lipid modified outer segment proteins; GRK1, PDE6 and Transducin α,β and γ, detected in the IS and ONL (Hanke-Gogokhia et al. 2016). It has been previously reported that PDE6δ interacts strongly with GRK1 (Houbin Zhang et al., 2004) and that this is required for its localisation in photoreceptors (H Zhang et al. 2007). UNC119 interacts with transducin α and may function in dissociating Gα from membranes to facilitate its diffusion back to the OS during dark adaption (Zhang et al. 2011). Therefore, this supports the hypothesis that the RP2-ARL3 complex controls the localisation of lipid-modified proteins in the photoreceptors through the GDI effector activity of ARL3-GTP for PDE6δ and UNC119 (Figure 1.9 A).

Pde6δ knock out mice are viable however they are 20-30% smaller than their WT littermates and display a slow progressive rod/cone dystrophy with shortening of the OS evident from 4 weeks and thinning of the ONL evident from 5 months of age (H Zhang et al. 2007). *Pde6δ* -/- retina's show loss of GRK1 in the OS and have PDE6 mislocalised to the inner segments (H Zhang et al. 2007). Similarly *Unc119* -/- mice have progressive retinal degeneration evident from 5 months of age and almost complete at 20 months (Ishiba et al. 2007). The mechanism of degeneration is unclear in *Unc119* -/- mice therefore a *Pde6δ*, *Unc119* double knockout was generated (Houbin Zhang, Frederick, and Baehr 2014). In these mice expression of GRK1 is undetectable in rods however appears to be increased in cones, compared to *Pde6δ* single knockout. This increase in GRK1 was enough to partially rescue cone scotopic ERG responses compared to *Pde6δ*-/- but was not enough to restore WT responses. The authors speculate that the increase in GRK1 expression in *Pde6*-/- *Unc119* -/-

cones compared to *Pde6δ*-/- cones may be attributed to an increase in the levels ARL3-GTP as it is free from binding UNC119. This would then allow ARL3-GTP to transport GRK1 via an alternative mechanism independent of PDE6δ (Houbin Zhang, Frederick, and Baehr 2014). A possible mechanism for this has yet to be elucidated and it is currently unknown how GRK1 can traffic to the cone OS in the absence of PDE6δ.

A retinal specific knockout of ARL3, $Ret^{ARL3-/-}$, mice have severe retinal degeneration evident from P15 and almost complete by 2 months of age shown by severely reduced ERG responses and significant thinning of the retina (Hanke-Gogokhia et al. 2016). These mice fail to develop photoreceptor OSs and do not form connecting cilia suggesting a role for ARL3 in ciliogenesis in photoreceptors (Hanke-Gogokhia et al. 2016). As a result of lack of OS formation, mislocalisation of OS pigments rhodopsin and M/L opsin, as well as the progressive accumulation of GRK1, PDE6 and rod transducin α (Gα) in the inner segments and ONL was observed (Hanke-Gogokhia et al. 2016). This is similar to the phenotype of *Arl3* -/- mice which also fail to develop proper photoreceptor OS, form only rudimentary CC and have mislocalised rhodopsin (Schrick et al. 2006). This phenotype suggests defects in both IFT and membrane protein trafficking implying ARL3 may play essential roles in both pathways.

The role of RP2 in photoreceptors has also been studied using animal models. As previously discussed two *Rp2h* knockout mice have been generated which show contradictory phenotypes. The first *Rp2h* knockout mouse, $Rp2h^{null}$, generated by gene trap cassette displayed progressive retinal degeneration attributed to early mislocalisation of M/L opsin. No mislocalisation of lipid modified OS proteins was observed suggesting a pathogenic mechanism which is not be attributed to RP2's regulation of ARL3-GTP and subsequent regulation of PDE6δ (L. Li et al. 2013). The second *Rp2h* knockout mouse, *Rp2h* -/-, generated by the cre lox system displayed progressive retinal degeneration attributed to mislocalisation of GRK1, transducin α and other lipid modified proteins (Houbin Zhang et al. 2015). No mislocalisation of rhodopsin or M/L opsin was observed suggesting retinal degeneration is driven by increased ARL3-GTP levels and aberrant release of PDE6δ cargo (Houbin Zhang et al. 2015) (Figure 1.9 B) (*Rp2h* knockout mice phenotypes discussed in detail in 3.1).

The hypothesis that mutation of RP2 results in increased levels of ARL3-GTP and aberrant trafficking of lipid modified OS proteins is also supported by the phenotype of a transgenic mouse with expression of ARL3-GTP driven by the rhodopsin

promoter, Rod^{ARL3Q71L}. This mouse demonstrated severe, rapid retinal degeneration attributed to mislocalisation of lipid modified OS proteins. Rhodopsin or GC1 were not mislocalised in this model demonstrating increased levels of ARL3-GTP specifically caused mislocalisation of lipid modified OS proteins (Z. C. Wright et al. 2016) (Phenotype of Rod ^{ARL3Q71L} mouse discussed in detail in 4.1).

The mechanism by which mutation in *RP2* causes retinal degeneration in patients with XLRP remains unclear however increased levels of ARL3-GTP and subsequent mistrafficking of lipid modified OS protein is the prevailing hypothesis (Figure 1.9). The two opposing phenotypes of the *Rp2h* knockout mice mean the function of RP2 in the retina remains unclear. Some proteins reported to be mislocalised in *Rp2h* -/- mice and Rod^{ARL3Q71L} mice overlap however these models do not phenocopy each other as would be expected if increased levels of ARL3-GTP was the pathogenic mechanism in both cases. The Rod^{ARL3Q71L} mouse is a transgenic model which expresses ARL3 Q71L under the rhodopsin promoter thus it is only expressed in rods and overexpressed compared to the endogenous locus. Therefore, to study the contribution of levels of ARL3-GTP to retinal degeneration this mouse may not be an ideal model as it is not clear whether the phenotypes present occur because of increased ARL3-GTP levels or because ARL3 Q71L is overexpressed compared to the endogenous locus. Therefore, the question remains as to whether retinal degeneration in the cases of *RP2* mutations is solely attributed to increased levels of ARL3-GTP.

Figure 1. 9 Schematic of GRK1 Trafficking in WT and Rp2h Knockout Photoreceptors

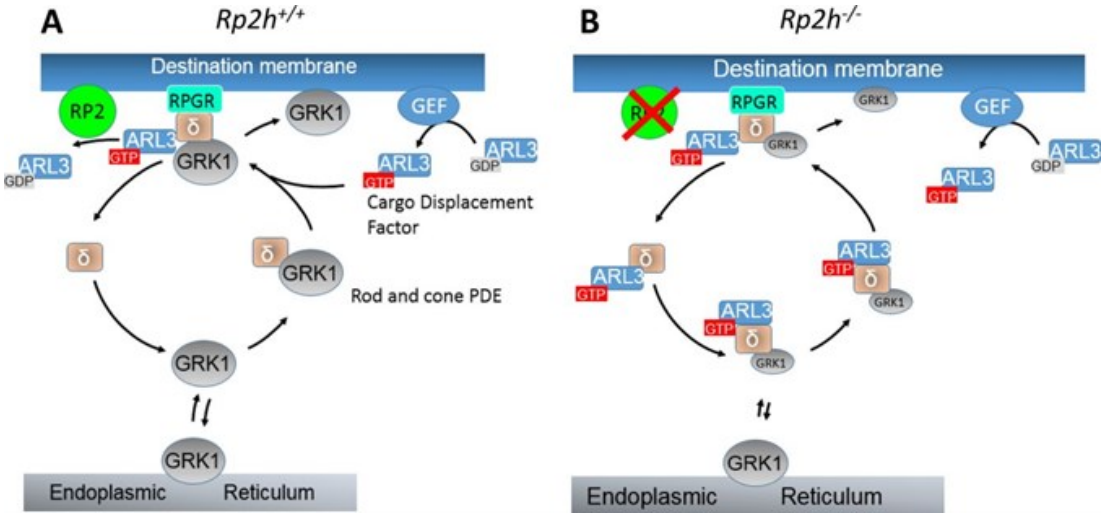

(A) Schematic of GRK1 trafficking in WT photoreceptors. After translation and post-translational prenylation, GRK1 anchors at the ER membrane. PDE6δ extracts GRK1 from the ER membrane and forms a soluble complex. PDE6δ-GRK1 traffic to the destination membrane which is the CC or OS membrane. PDE6δ-GRK1 may dock to the destination membrane via its interaction with RPGR. After docking PDE6δ-GRK1 form a tertiary complex with ARL3-GTP which stimulates a conformational change in PDE6δ converting its hydrophobic pocket from the open conformation to the closest conformation resulting in release of GRK1. ARL3-GTP then interacts with RP2 which stimulates ARL3's intrinsic GTPase activity converting ARL3-GTP to ARL3-GDP. ARL3-GDP is converted to ARL3-GTP via its GEF which has recently been identified as ARL13b.

(B) Absence of RP2 prevents hydrolysis of ARL3 so ARL3 remains in the GTP bound state as ARL3-GDP continues to be activated to ARL3-GTP by the GEF. PDE6δ can still extract prenylated GRK1 from the ER membrane but ARL3-GTP is able to stimulate release of GRK1 before PDE6δ-GRK1 reach the destination membrane leading to GRK1 mislocalisation.

Taken from Baehr et.al 2014

1.6 Aims:

In order to determine whether the pathogenesis of XLRP in cases of RP2 mutation is attributed to dysregulation of ARL3 new mouse models of RP were generated using CRISPR genome editing. A new *Rp2h* knockout model was generated (*Rp2h* DEL26/Y), a mouse lacking RP2 GAP activity (*Rp2h* E135G/Y) and mice expressing constitutively active ARL3 (*Arl3* Q71L/+ and *Arl3* Q71L/Q71L).

The first aim of this study was to characterise the phenotype of the *Rp2h* DEL26/Y, *Rp2h* E135G/Y, *Arl3* Q71L/+ and *Arl3* Q71L/Q71L mice. By characterising, the phenotype of these mice and analysing genotype to phenotype correlations insights into the contribution of ARL3 mis-regulation to Retinitis Pigmentosa could be made. The mice were analysed continually until 12 months of age to fully observe the process of retinal degeneration over time using both invasive and non-invasive techniques. Analysis also facilitated the comparison of *Rp2h* DEL26/Y and *Rp2h* E135G/Y to the previously published *Rp2h* knockout mice providing information about the function of RP2 in the retina.

As *Rp2h* and *Arl3* mutant mice were generated using the same CRISPR technique on the same background strain they could be directly compared to each other in order to assess whether increased levels of ARL3-GTP phenocopy *Rp2h* knockout and loss of RP2 GAP activity. This allowed the question of whether the pathogenesis of XLRP in patients with *RP2* mutations is solely due to dysregulation of ARL3 to be directly addressed.

The function of RP2 was further analysed via a study of the interactions RP2 is involved in retinal pigment epithelium cells (RPE-1). To analyse RP2 interactions *in vitro* the proximity based biotinylation (BIO-ID) method was used. This identified ZDHHC5 as a novel RP2 interactor and the functional consequence of this interaction was investigated with the aim of providing further insights into the mechanisms that regulate RP2 *in vivo*.

Chapter 2

Materials and Methods

Chapter 2: Materials and Methods

2.1 Mouse Studies Methods

2.1.1 Animal Husbandry

Mice used in this study were housed in the University of Edinburgh Transgenic Unit (TGU) mouse facility. Mice used for ERG studies were transferred through to the University of Edinburgh Biomedical Research Facility (BRF) facility. Where required, all procedures were performed under a Personal and Project Home Office Licence. PIL: SAB/SCT-E/145/15, PPL: 60-4424, P1914806F

2.1.2 Generation of *Rp2h* and *Arl3* mutant mouse lines

Constructs used to generate the *Rp2h* and *Arl3* mutant lines were designed and synthesised by Dr Hurd before I joined the lab. CRISPR gRNA guides were designed to target *Rp2h* and *Arl3*. To generate *Rp2h* mice, paired guides were used in conjunction with Cas9n mRNA (Sigma Aldrich). To generate *Arl3* mice, a single guide with conventional Cas9 mRNA (Sigma Aldrich) was used. Repair templates (ssDNA) were provided to allow the introduction of *Rp2h* E135G and *Arl3* Q71L point mutations (ssDNA repair template sequences provided in Table 2.1). CRISPR guides, Cas9/Cas9n mRNA and rescue ssDNA (25ng/ul per Guide; 50ng/ul ssDNA; 150ng/ul ssDNA) were injected into the cytosol of single cell C57BL6/J embryos by staff in the University of Edinburgh Transgenic (TGU) mouse facility. Founder (F0) pups generated from these injections were genotyped and those carrying appropriate mutations were outbred to C57BL6/J control mice in order to establish the F1 animals to establish lines.

2.1.3 Genotyping of *Rp2h* and *Arl3* mouse lines

Genomic DNA generated from mouse ear clips was used for genotyping. Genomic DNA was prepared using DNA-Releasy (Anachem) and a thermocycler. DNAreleasy was diluted 1:5 with DNAse/RNAse free H2O. 30µl of diluted DNA-Releasy was added to each ear clip. Samples were then placed in a BIO-RAD Tetrad 2 Peltier Thermo cycler as follows:

65^0C for 15 min

96^0C for 2 min

65^0C for 4 min

96^0C for 1 min

65^0C for 1 min

96^0C for 30 sec

4^0C forever

Samples were then centrifuged at 13,000 rpm for 1 minute. Genomic DNA was amplified using Polymerase Chain Reaction (PCR) using the Phusion High Fidelity PCR Master Mix (New England Biolabs). The reaction mix contained Phusion High Fidelity PCR master mix, 0.5µM primers (Listed in Table 2.1) and 2µl DNA template in a 25µl reaction. PCR reactions were carried out in a BIO-RAD Tetrad 2 Peltier Thermo Cycler.

RP2 Genotyping PCR Programme:

Initial Denature 98^0C for 2 min

Denature 98^0C for 10 sec

Extension and Annealing 72^0C for 10 sec 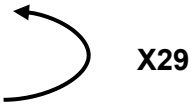 **X29**

Final Extension 72^0C for 10 min

4^0C forever

ARL3 Genotyping Programme:

Initial Denature 98^0C for 2 min

Denature 98^0C for 10 sec

Annealing 66^0C for 30 sec  **X29**

Extension 72^0C for 15 sec

Final Extension 72^0C 10 min

4^0C forever

PCR samples were then analysed by Sanger sequencing. Sanger sequencing was performed by the Institute of Genetic and Molecular Medicine (IGMM) core technical services using a 3730 genetic analyser (Applied Biosystems). The same primers were used for PCR amplification and sequencing of PCR products for genotyping (Listed in Table 2.1).

Table 2. 1 List of Primers and Their Applications

Primer	Sequence 5'-3'	Application	Company
mRP2 F	GGGACCAGTGAAAGGCAGTGTC	RP2 genotyping and sequencing	IDT
mRP2 R	GGCTCCACTTGAGCTCTCCTGAC	RP2 genotyping and sequencing	IDT
mARL3 F	CCGTCTCTTTCAGGGATTAAC	ARL3 genotyping and sequencing	IDT
mARL3 R	CCTGCTCATTCTGAGCAATGT	ARL3 genotyping and sequencing	IDT
ARL3 gRNA	TATGGGACATTGGCGGGCAG	ARL3 CRISPR	IDT
ARL3 Repair Template	GGATTTAACATCAAAAGCGTGCAGTCACAAGGTTTTAAGCTGAATGTATGGGACATTGGCGGGCAGAGGAAAATCAGACCATACTGGAGAAGTTATTTTGAAAATACTGATATTCTCGTAAGTAATCGTGGTGCACTCATC	Introduction of Q71L mutation	IDT
RP2 Repair Template	CACATTGGCTTGCCAGCAATTTCGTGTGAGAGACTGTAGAAAGTTGGAAGTCTTTTTGTGCTGTGCTACTCAACCAATTATTGGATCTTCCACAAACATCAAGTTTGGCTGTTTTCAGTGGTACTACCCTGAATTAGCAGCCCAATTCAAAGATGCAGGCCTCAGTAT	Introduction of E135G mutation	IDT
BIRA* BamH1, EcoR1 F	TTTTGGATCCAAGGACAACACCGTGCC	Generation of BIRA* PCR product containing BamH1 and EcoR1 restriction sites for cloning into PQCXIN	IDT

BIRA* BamHI, EcoR1 R	GGAATTCTCAGAGATCCTCTTCTGAGATGAGTTTTTGTTCCTTCTCTGCGCTTCTCAGGG	Generation of BIRA* PCR product containing BamH1 and EcoR1 restriction sites for cloning into PQCXIN	IDT
RP2 Not1 F	TTTTGCGGCCGCCACCATGGGTGCTTCTTCTCCAAGAGAC	Generation of WT RP2, E135G RP2, R211L RP2 PCR products with Not1 and Pac1 restriction sites	IDT
RP2 Pac1 R	TTTTTTAATTAATATTCCCATCTGTATATCAGCAAAGTTGTAGAAGCT	Generation of WT RP2, E135G RP2, R211L RP2 PCR products with Not1 and Pac1 restriction sites	IDT
RP2 G2A Not1 F	TTTTGCGGCCGCCACCATGGCCTGCTTCTTCCTCCAAGAGAC	Generation of G2A RP2 PCR products with Not1 and Pac1 restriction sites used with RP2 Pac 1 R	IDT
RP2 C3S Not1 F	TTTTGCGGCCGCCACCATGGGCTCCTTCTTCTCCAAGAGAC	Generation of C3S RP2 PCR products with Not1 and Pac1 restriction sites used with RP2 Pac 1 R	IDT

2.1.4 Histology Methods

After euthanasia by cervical dislocation eyes were removed from mice with forceps and washed in PBS before being immersed in Davidson's Fixative (22% v/v 10% neutral formalin in phosphate buffer (40% PFA, 900 ml/L distilled water, 18.6 g/l NaH_2PO_4, 42.2g/l NaOH), 33% v/v 95% ethanol, 11% v/v acetic acid in distilled water). Eyes were fixed at 4°C for 24 hours for paraffin sectioning or 4 hours for cryosectioning.

2.1.4.2 Paraffin Sectioning

After fixation, eyes were stored in 70% ethanol. Dehydration of the tissues and embedding in paraffin took place in the Tissue Tek Tissue VIP5 Jr. embedding console system (Sakura). The procedure included the following steps, each one lasting for 45 minutes:

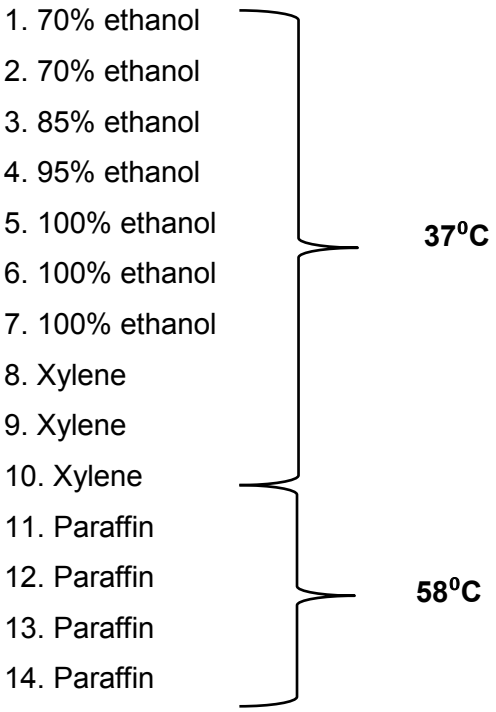

After embedding in molten paraffin, the eyes were transferred into casts where they were orientated according to the plane of sectioning required. Paraffin was then allowed to set completely around the specimen and form a block. A Leica RM2235 microtome was used to obtain 7μm-thick sections of the eyes. Sections were obtained orthogonally to the vertical meridian of the eye. Sections were spread out in a water bath at 47^0C and then collected on the (+) side of Superfrost microscopy slides (Menzer-Gläser, Thermo Fisher Scientific). They were subsequently air-dried for a minimum of one hour and incubated at 55^0C overnight.

2.1.4.3 Cryosectioning

After fixation eyes were washed in PBS and cryoprotected by immersion in sucrose gradients, each eye was moved to the next increment once it had sunk to the bottom.

5% sucrose/PBS

10% sucrose/PBS

15% sucrose/PBS

20% sucrose/PBS (4^0C overnight)

Eyes were then incubated in OCT (VWR International) in vinyl moulds on dry ice. Once the OCT had completely frozen samples were stored at -80^0C. Eyes were sectioned using a Leica 3M3050 S Cryostat. Eyes were allowed to adjust to the chamber temperature (-20^0C) before 10µm sections were cut and collected on Superfrost Plus microscope slides. Sections were then air dried for 1 hour at room temperature then stored at -80^0C.

2.1.4.4 Haematoxylin and eosin (H&E) staining

To prepare for staining, eye sections were first de-waxed by three 5-minute incubations in xylene. Next, they underwent stepwise rehydration; passing through a reverse series of graded ethanol washes (100%, 90%, 70%, 50% and 30%) for two minutes each. Sections were subsequently dipped in haematoxylin for 4 minutes, washed in running tap water, differentiated in 1% HCl in 70% alcohol and washed well in running tap water. Next, the sections were dipped in saturated lithium carbonate solution for a few seconds, washed well in tap water, stained in eosin for 4 minutes, rinsed in water and finally rinsed in 100% ethanol. After staining, the sections were dehydrated again through three 5-minute incubations in 100% ethanol. After passing through three xylene incubations for 5 minutes each, the sections were mounted with 22x 50mm coverslips (VWR International Ltd) and DPX medium (Cell Path). Mounted sections were left to cure overnight.

2.1.4.5 Imaging and analysis

Brightfield microscopy was carried out using the Hamamatsu Nanozoomer XR microscope and the NdpVeiw.2 software used to measure the thickness of each of the retinal layers. This data was then exported to Microsoft Excel for analysis.

2.1.5 Electroretinography in Mice

Mutant and WT control mice were dark adapted overnight prior to electroretinography (ERG) through housing in dark cages. All ERG readings were recorded on a Ocuscience HMsERG Model 2000 Full Field Flash Electroretinography Machine inside a Faraday Cage (Ocuscience). All ERG procedures were carried out in the dark with red safety lights. Immediately prior to the procedure one drop of 1% tropicamide was placed in each eye of the animals in order to dilate the pupils. Anaesthesia was induced with 3% isoflurane in an isoflurane chamber, and after induction of anaesthesia animals were transferred to the ERG apparatus and anaesthesia was maintained at 1.5%-2% isoflurane using a nose cone. The body temperature of the mice was monitored using a rectal probe (Ocuscience, ERGACC5). Reference electrodes were placed sub-dermally in each cheek and a grounding electrode placed sub-dermally at the base of the tail. One drop of methylcellulose was placed on each eye and the eye electrodes placed across the apex of the cornea and secured with a contact lens (Ocuscience). The faraday cage was closed and an earthing cable attached to the cage and the mains electrics supply. An impedance test was run on the electrodes prior to each reading and the experiment only proceeded when the impedance value was below 10,000Ohm. For my studies, the ISCEV (International Society for Clinical Electrophysiology of Vision) protocol was used to investigate the function of both rod and cone photoreceptors (Table 2.2). After recordings, the sub-dermal electrodes were removed and cleaned with 100% ethanol; contact lenses were removed and placed into water to remove any excess methylcellulose. Isoflurane was turned off and animals transferred to a heated recovery chamber (30-34^{0}C) and observed until consciousness was regained.

Table 2. 2 ISCEV Protocol for ERG

	No. 1- ISCEV protocol- Dark adapted Patient. Room Lights are turned off when starting the Session (S0)						
Step	ERG Test **Sessions**	**Flash Intensity** Log	mcd.s/m²	**Number** of Flashes	**Interval** Seconds	**Time Req.** Seconds	**Elapsed Time** Seconds
S0	**Dark Adaptation**	**ISCEV Recommends 20 Minutes**					0
S1	**Rods**	-2.5	10	10	2	18	18
S2	Delay				2	2	20
S3	**Std. Rods & Cones**	0	3000	4	10	30	50
S4	Delay					30	80
S5	**Hi-Int. Rods & Cones**	0.5	10000	4	20	60	140
S6	**BG Adaptation** (Remains ON for remaining testing)	1.0	30000	BG.		600	740
S7	**Cones w/ BG**	0	3000	32	0.5	15.5	755.5
S8	**Delay w/ BG**					2	757.5
S9	**HiCones w/ BG**	0.5	10000	32	0.5	15.5	771
S10	**Delay w/ BG**					2	773
S11	**Std. Flicker w/ BG**	0	3000	128	0.032	4.192	777.2
S12	**Delay w/ BG**					2	779.2
S13	**Hi-Int. Flicker w/ BG**	0.5	10000	128	0.032	4.192	783.4
	Total Elapsed time in Minutes						**13.06**

Table taken from HMsERGLab Manual. Dark Adaptation for my studies was carried out overnight as stated above.

2.1.6 Immunofluorescence Analysis of Retinal Cryosections

Retinal cryosections were post-fixed by immersion in ice cold 100% acetone for 10 minutes at room temperature. After air-drying for 10 minutes and washing 3 times 5 minutes in TBST (0.2% Tx100) or PBS (depending on antibody specifications) sections were blocked in 10% heat inactivated goat serum/TBS (AMS Biotechnology) for 1 hour at room temperature. Primary antibodies were diluted in 1% Goat serum/TBS to the appropriate dilutions (Antibodies listed on Table 2.3) and incubated on sections overnight at 4^0C in a humidified chamber. Slides were washed 3 times for 5 minutes in appropriate wash buffer. Secondary antibodies were diluted in 1% Goat Serum/TBS (Listed Table 2.2) with Dapi (Sigma Aldrich) diluted to 1:10,000 and incubated on sections for 1 hour at room temperature. Slides were then washed 3 times for 5 minutes and mounted with Prolong Gold (Molecular Probes).

2.1.6.1 Imaging and Analysis

Fluorescent images were taken using a Leica SP5 inverted confocal microscope and viewed using LAS AF Lite software where appropriate scale bars were applied. Images were subsequently edited for generation of figures using Adobe Photoshop.

2.1.7 Protein Extraction from Whole Eyes

2.1.7.1 Tissue Lysis

Mice were culled by cervical dislocation and the eyes removed, immediately placed on dry ice then stored at -80^0C. Two eyes per mouse were lysed in either CO-IP lysis buffer or RIPA buffer (supplied by Santa Cruz, sc-24948) (See Table 2.4 for lysis Buffer compositions) supplemented with 1mM PMSF, protease and phosphatase inhibitor cocktails (Sigma- Aldrich) immediately prior to use. Tissues were homogenised using an electric dounce homogeniser. Lysates were then cleared by centrifugation for 20 minutes at 13,000 rpm in a refrigerated centrifuge. Lysates were then transferred to a fresh tube and used immediately or stored at -80^0C.

2.1.7.2 Quantification of Protein Concentration

Protein concentration of lysates made with RIPA buffer was determined using the Biorad DC assay, as per manufacturers' instructions. After mixing well and incubating for 5 minutes at room temperature, colorimetric readings were recorded by measuring absorbance at 750 nm using the BioMate 3 Spectrophotometer (ThermoFisher Scientific). Lysates made using CO-IP lysis buffer or General Triton Lysis buffer were measured using Bradford Reagent (Sigma). 1µl of lysate was added to 1ml of Bradford Reagent, and after mixing and incubating for 15 minutes at room temperature colorimetric readings were recorded by measuring absorbance at 595nm. A BSA (bovine serum albumin) (Sigma) reference curve was used to estimate protein concentration based on the colorimetric readings.

2.1.8 ARL3-GTP Pulldown Assays from Whole Eyes

WT, *Rp2h* and *Arl3* mutant eye lysates, previously lysed in CO-IP lysis buffer and normalised to the same concentration were used for this assay (lysis and protein concentration measurement protocol described above). Ten percent of these lysates were removed for input samples and the remaining lysates were incubated with 15µl glutathione beads +/- 5µl of 1ug/ul GST-RP2 recombinant protein and incubated for 1 hour at 4^0C under continuous rotation. Beads were then washed 3 times by spinning for 2 minutes at 4000rpm and resuspending in lysis buffer. Beads and appropriate volumes of input lysate were then mixed with appropriate volume of sample buffer (1x LDS Sample Buffer (Thermo), 50mM DTT and dH_2O) and incubated at 70^0C for 10 minutes to elute proteins from the beads and to denature proteins in preparation for gel electrophoresis and Western blot analysis. (See 2.3.2 and 2.3.3 for gel electrophoresis and western blot methods).

2.2 Tissue Culture Methods

2.2.1 Cell Culture Techniques

RPE1 cells were cultured with DMEM-F12 medium (Hyclone, Thermo Fisher Scientific) with the addition of 10% v/v foetal calf serum, penicillin/streptomycin cocktail at 1 mg/ml final concentration and hygromycin (10µg/ml final concentration (Gibco)). HEK293T, HEK293-ET and Hela cells were cultured with Dulbecco's

modified Eagle medium (DMEM) with 4.5g/l L/D glucose and pyruvate (Gibco, Life Technologies), with the addition of 10% v/v foetal calf serum and penicillin/streptomycin cocktail at 1 mg/ml final concentration. Cells were regularly split using the TrypLE trypsin substitute (ThermoFisher Scientific). RP2 BIRA and BIRA RP2 null RPE1 cells were cultured in DMEM-F12 medium (Hyclone, Thermo Fisher Scientific) with the addition of 10% v/v foetal calf serum, penicillin/streptomycin cocktail at 1 mg/ml final concentration, hygromycin (10µg/ml final concentration (Gibco) and 500ng/ml G418 (Sigma)).

2.2.2 Transient Transfection and siRNA knockdown

Cells were transiently transfected with 1µg purified plasmid DNA containing the relevant constructs (per $0.2x10^6$ cells) using the nonliposomal reagent Fugene HD (Promega). 1µg of DNA was incubated with the appropriate volume of Opti-Mem serum free media (Thermo Fisher), appropriate volume of Fugene was added (always keeping ratio of 3µl Fugene to 1µg DNA). Reactions were mixed and incubated for 15-20 mins at room temperature. Cells to be transfected were incubated in fresh media and transfection mix was added. After 24 hours cells were incubated in fresh media.

Dish/ Plate Size	**Volume of Opti-Mem (µl)**	**Volume of Media (ml)**	**µg DNA**	**Volume of Fugene (always 3:1 (µg DNA)**
6 well	100	2	1	3
10cm dish	500	10	1-3	9-18

For knockdown experiments, HEK293T or Hela cells were seeded on a six well plate and transfected with 25pmol siRNA per well using Lipofectamine RNAi Max Reagent (Life Technologies). Cells were transfected once they were around 60%-70% confluent. SiRNA (5µm) was added to 75µl of Opti-Mem Reduced Serum Media (Thermo Fisher). 6µl of RNAi Max Reagent (Life Technologies) was added to 75µl of Opti-Mem Reduced Serum Media in a separate tube. The solutions were then mixed and after a 5-minute incubation, 150µl of this mix was added to cells. After 24 hours, this media was removed and replaced with fresh media (as described 2.2.1).

ZDHHC5 siRNA: AGGGATTAGAGTGTGCTCCTA, ACCACCATTGCCAGACTACAA (Qiagen)

CTRL siRNA: SCRAMBLED siRNA (Qiagen)

2.2.3 Generation of RP2 BIRA Cell Lines

2.2.3.1 Generation of RP2 BIRA and BIRA Retroviral Constructs

To generate a BIRA retroviral construct for BIOID assays BIRA (R118G) (BIRA*) was cloned into PQCXIN retroviral plasmid. To insert BIRA* into PQCXIN plasmid a PCR strategy was used to generate a PCR product containing BIRA* and BamHI and EcoR1 restriction sites (Primers listed in Table 2.1). pCDNA3.1 MCS-BirA (R118G)-HA was used as a template for the PCR reaction. A 50µl PCR reaction was set up containing 25µl Phusion High Fidelity PCR Mastermix, 0.5µM F primer, 0.5µM R primer, 19µl dH_2O and 10ng of plasmid template. PCR reactions were carried out on a BIO-RAD Tetrad 2 Peltier Thermo Cycler as before.

BIRA (R118G) BamHI, EcoR1 PCR Programme:

Denature 98^0C 2 min

Denature 98^0C 2 min

Extension and Annealing 72^0C for 20 sec **X34**

Final Extension 72^0C for 10 min

The resulting PCR product was purified using Qiagen PCR purification (Qiagen, 28104) kit as per manufacturer's protocol.

After purification the PCR product was analysed by agarose gel electrophoresis to confirm it was of the expected size (~1kb) (1% agarose gel: 1.5g agarose (Hi pure Low EEO Agarose (Biogene) was added to 150ml 1XTBE and heated in the microwave until agarose had completely dissolved. Agarose was then poured into gel tray and left to set for 30mins before electrophoresis. 5µl of PCR product + 1µl 6X DNA loading dye (New England Biolabs) were loaded onto the gel in lanes adjacent to a lane containing 3µl of 1kb+ DNA ladder (New England Biolabs). Gels were ran in

gel tanks containing 1xTBE at 120V for 40 minutes to allow separation of DNA fragments.

After conformation that the PCR product (BIRA BamHI, EcoR1) was of the correct size, this product and the PQCXIN retroviral plasmid underwent restriction digest with EcoR1 (EcoR1 HF, NEB, R3101S) and BamHI (BamH1 HF, NEB, R3136S) restriction enzymes. 20µl restriction digest was used to digest PQCXIN plasmid. 20µl Restriction digest reaction mix: 3ng plasmid DNA, 2µl 10x cutsmart buffer (NEB, B7204S), 0.5µL BamHI, 0.5µl EcoR1, 12µl dH2O. 100µl restriction digest reaction was used to digest BIRA, BamHI, EcoR1 PCR product. Restriction digest reaction mix: 50µl purified PCR product, 10µl 10x cutsmart buffer,0.5µl BamHI, 0.5µl EcoR1, 39µl dH20. Restriction digests were heated at 37^0C for one hour in a tabletop heat block. After restriction digest the reactions were purified using Qiagen PCR purification kit (as before) and the resulting digested PQCXIN and BIRA PCR product were eluted in 30µl elution buffer (provided in Qiagen PCR purification kit). Digested PQCXIN and digested BIRA PCR products were ligated (as described 2.2.3.1.2) and transformed into competent bacteria (as described 2.2.3.1.3) to generate the PQCXIN-BIRA-Myc plasmid. After transformation and generation of starter cultures and miniprep of plasmid DNA a EcoR1 and BamHI restriction digest (20µl restriction digest as described above) followed by gel electrophoresis (as described above) was used to assess that the PQCXIN plasmid contained the BIRA insert.

In order to generate PQCXIN-BIRA vectors containing RP2 point mutations RP2 pentry plasmids (WT RP2, E135G RP2, R21LL BIRA, G2A BIRA C3S BIRA) were used as templates to generate RP2 PCR products that were cloned into the PQCXIN-BIRA plasmid. To facilitate cloning a PCR strategy was designed to generate RP2 PCR products that contained Not1 and Pac1 restriction sites which are also present on the PQCXIN-BIRA plasmid. Primers used are listed in Table 2.1. 50µl PCR reactions containing (25µl Phusion High Fidelity PCR Mastermix, 0.5µM F primer, 0.5Mm R primer, 10ng plasmid DNA, up to 50µl dH_20). PCR reactions were carried out as described.

RP2 Not1,Pac1 PCR programme:

Denature 98^{0}C 2 min

Denature 98^{0}C 2 min

Extension and Annealing 72^{0}C for 60 sec 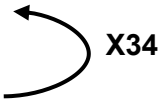

Final Extension 72^{0}C for 10 min

PCR products were then purified using Qiagen PCR purification kit (as described). PCR products and PQCXIN-BIRA (vector) then underwent restriction digest with Not1 (Not1 HF,NEB, R3189S) and Pac1 (Pac1, NEB, R0547S) restriction enzymes. PQCXIN-BIRA 20µl restriction digest reaction mix (3ng plasmid DNA, 0.5µl Not1,0.5 µl Pac1, 10x cutsmart buffer, up to 20µl dH_2O), RP2 PCR product 100µl restriction digest reaction mix (50µl purified PCR product, 10x cutsmart buffer, 1µl Not1, 1µl Pac1, up to 100µl dH_2O). After digestion and purification RP2 PCR products were ligated together (as described 2.2.3.1.2) followed by transformation into competent bacteria (2.2.3.1.4). Miniprepped DNA followed by restriction digest and gel electrophoresis was used to confirm correct incorporation of inserts (as described above) and plasmids from cultures which contained the correct insert were subcultured for midipreps as described (2.2.3.1.3) to extract high purity, high concentration DNA for retroviral transfection.

2.2.3.1.2 Ligation Reactions

All ligation reactions were set up at a 1:3 vector to insert ratio using the NEB quick ligation protocol. 20µl ligation reaction was set up on ice: 50ng vector DNA, 37.5ng insert DNA (~1kb), 10µl 2x Quick Ligase Reaction Buffer (provided in NEB Quick Ligation Kit, M2200S), 1µl Quick Ligase (provided in NEB Quick Ligation Kit, M2200S), dH2O up to 20µl. Ligation reactions were mixed and incubated at room temperature for 5 mins. Ligation reactions were then immediately used for transformation of competent bacteria or stored at -20^{0}C.

2.2.3.1.3 Transformation of Competent Bacteria

Ligation reactions were transformed into DH5α competent bacteria (NEB, C2987I). Vials of competent cells were thawed on ice and 25µl of competent cells were mixed with 1µl of ligation reaction and mixed. This mixture was then incubated on ice for 30

mins then heat shocked by incubation in a 42^{0}C water bath for 30 seconds immediately followed by incubation in ice for 2 minutes. 375µl SOC media (ThermoFisher) was then added to each reaction and reactions were then shaken in a 37^{0}C incubator for 1 hour. 100µl of this transformation mix was plated onto ampicillin agar plates (provided by HGU technical services), as PQCXIN carries an ampicillin resistance gene, and incubated in a 37^{0}C incubator overnight. Single colonies produced were then picked using sterile pipette tips and placed immediately into 15mls of L-Broth containing 100µg/ml Carbenicillin (ampicillin analogue) (L-Broth provided by HGU technical services, Carbenicillin, Sigma) and shaken at 37^{0}C overnight. DNA from starter cultures was extracted using Qiaprep miniprep kit (Qiagen, 27104) per manufacturer's protocol. In order to extract and purify higher concentrations of plasmid DNA for transfections 500µl of starter cultures were added to 50ml L-Broth containing 100µg/ml Carbenicillin and shaken overnight at 37^{0}C. 50ml cultures were then midiprepped using Qiagen plasmid midi kit (Qiagen, 12143) as per manufactures protocol.

2.2.3.1.4 Retroviral Transfection of RP2 null RPE1 cells

HEK293 ET cells were used to generate viral particles containing the RP2 BIRA or BIRA only constructs. HEK293-ET cells were seeded on 6-well plates at a density so they were 70% confluent the next day. These cells were transfected with 1µg of PVSV, 1µg GAG/POL vectors and 1µg each PQXCIN RP2-BIRA vector using Fugene HF reagent (see 2.2.2 for detailed protocol). Cells were then moved to the designated retroviral incubator at 37^{0}C overnight. RP2 null RPE1 cells were seeded so they were 60% confluent the next day. Polybrene (Sigma) was added to 15ml of DMEM-F12 G418 containing media and media from HEK293-ET cells (containing the newly synthesised retrovirus) was filtered through a 0.2µm filter in a 5ml syringe into the polybrene and G418 media mix. RP2 null RPE cells were then incubated in this media and placed in the retroviral incubator overnight at 37^{0}C. Infected RP2 null RPE cells were incubated in fresh media every day for 2 days and then transferred by trypsin detachment, spinning and resuspension in fresh media into a T.75 flask. RP2 null RP2 BIRA RPE cell lines were not transferred to normal incubator until 4 more media changes were performed.

2.2.4 Immunofluorescence of Cultured Cells

Cells were grown on sterile coverslips previously treated with HCl to create a rough surface for the adherent cells (12 hours at 55^0C). Cells were fixed in 4% paraformaldehyde (PFA) in PBS for 10 minutes at room temperature, washed 2 times for 10 minutes in PBS to remove PFA and then permeabilised in 0.2% Triton X100 in PBS for 10 minutes. Cells were blocked in 10% Goat Serum in PBS for one hour at room temperature. Primary antibodies were diluted in 1% Goat serum in PBS to appropriate concentrations (See Table 2.3) and incubated on cells for one hour at room temperature. Cells were then washed 3 times in PBS and incubated with secondary antibodies (Listed in Table 2.3) diluted in 1% Goat Serum in PBS for one hour at room temperature. After three further washes in PBS cells were then mounted with Prolong Gold (Molecular Probes).

2.3 Protein and Proteomics Methods

2.3.1 Protein Extraction from Cells

Cells were plated on either 10cm dishes or 6 well plates and allowed to become fully confluent before lysis. Cells were incubated on ice and washed twice with ice cold PBS, then lysed in appropriate volumes of lysis buffers (Listed Table 2.4) supplemented with 1mM PMSF, protease and phosphatase inhibitor cocktails (Sigma) for 20 minutes on ice. Lysates were then cleared by centrifugation for 10 minutes at 13,00rpm at 4^0C. Lysates were then transferred to a fresh tube and used immediately or stored at -80^0C. Protein concentration of lysates were calculated as described 2.1.7.2 Quantification of Protein Concentration.

2.3.2 Protein Separation by Gel Electrophoresis

Proteins were separated by their molecular weight by SDS-polyacrylamide gel electrophoresis (PAGE) on 4-12% Bis-tris gels (NuPage, Life Technologies), which were inserted in an XCell SureLock electrophoresis chamber (Life Technologies). Before loading on the gel, protein samples were reduced and denatured by the addition of sample buffer (4x LDS Sample buffer, NuPage, 1M DTT and dH_2O), and subsequent heating at 70^0C for 10 minutes. As a molecular weight marker, 5µl of Broad Range Colour Protein Standard (New England Biolabs) was loaded alongside

the protein samples. After sample loading, gels were run in MOPS running buffer with 500µl of antioxidant (Life Technologies) added to the middle chamber immediately before electrophoresis. Gels were run at 180V for one hour until proteins were fully separated.

2.3.3 Western Blotting

Proteins separated by SDS-PAGE were then transferred onto polyvinylidene fluoride (PVDF) or nitrocellulose membranes (0.45 µm pores, Amersham GE Healthcare) by semi-dry transfer. Transfer was carried out in Towbin transfer buffer (0.25 M Tris base, 1.92 M glycine, 20% methanol, pH was fixed to 8.1-8.5). For semi-dry transfer, the gel containing the resolved proteins was "sandwiched" with the activated and equilibrated wet membrane between two stacks of three pieces of wet paper and inserted into the BioRad Trans-Blot Turbo Transfer system. Transfers were run at 25V for 30 minutes. After transfer, transfer membranes were checked by staining the membrane with Ponceau S (Sigma-Aldrich). Ponceau S was removed by TBS washes, and membranes were blocked for either one hour at room temperature or overnight at 4^0C. Membranes were blocked in either 5% Milk in TBS-0.05% Tween (TBST) or 5% BSA (Sigma) in TBST. After blocking Membranes were incubated with primary antibodies for either one-hour at room temperature or overnight at 4^0C. Primary antibodies were diluted to the appropriate dilution in blocking buffer (Listed Table 2.3). After incubation with primary antibodies membranes were washed in TBST 3 times for 5 minutes and incubated with horseradish peroxidase (HRP)-conjugated secondary antibodies (Table 2.3) for one hour at room temperature. Membranes were then washed in TBST 3 times for 5 minutes and protein band detection was achieved by incubating the membrane in Chemiluminescence reagent for Horseradish Peroxidase (Serva) supplemented with hydrogen peroxide solution (Sigma) at a 1:1000 dilution or Clarity Western ECL substrate (BIO-RAD) for low abundance signals. The membrane was then inserted in a darkroom cassette and exposed onto a photographic film (Amersham Hyper film ECL by GE Healthcare) which was then developed in a medical film processor (SRX 101A, Konica) to visualize the bands.

2.3.4 Membrane Stripping

In order to re-probe membranes for a loading control (β-actin), primary and secondary antibodies were removed by incubating the membrane in a mild stripping buffer (0.2M glycine, 0.1% SDS, 0.1% Tween20, pH adjusted to 2.2), twice for 5 minutes. The membrane was then washed twice with PBS (5 minutes each) and twice with TBST (5 minutes each) before proceeding to the blocking stage.

Table 2. 3 List of Antibodies or Conjugates

Primary Antibody or Conjugate	Supplier	Catalogue Number	Lot	Dilution WB	Dilution IF
Streptavidin-HRP Conjugate	Cell Signalling	3999S	7	1:5000	
Mouse anti MycTag Clone A46	Millipore	05-724	2919011	1:1000	
Mouse anti Actin	Sigma	A5441	014M4759	1:10000	
Rabbit anti ZDHHC5	Abcam	Ab200572		1:1000	
Mouse anti HA-Probe F7	Santa Cruz	Sc-7392	L1115	1:2000	1:1000
Mouse anti V5	Invitrogen	46-0705	1805125	1:5000	
Rabbit anti Myc	Cell Signalling	2272S	6		1:1000
Streptavidin-Alexa Flour 594 Conjugate	Life Technologies	S11227	1587669		1:10000
Rabbit anti V5	Bethyl	A190-120A	6		1:1000

Mouse anti Acetylated Tubulin (611-B-1)	Santa Cruz	sc-239050	J2315		1:4000
Rabbit anti ARL13b	Proteintech	17-11-1-AP			1:400
Mouse anti Rhodopsin	Santa Cruz	Sc-57432	E1316		1:500
Rabbit anti M/L Opsin	Millipore	AB5405	3011830		1:500
Goat anti S opsin	Insight	sc-14363			1:500
Rabbit anti GFAP	DAKO	Z0034			1:500
Rabbit anti GRK1	Abcam	Ab2775	GR191822	1:1000	1:100
Mouse anti STAT3 (124H6)	Cell Signalling	9139S	10/2016	1:1000	
Mouse anti pSTAT3 (Y705) (M9C6)	Cell Signalling	4113S	11/2016	1:1000	
Rabbit anti pSTAT3 (S727) (P8C2Z)	Cell Signalling	94994S	11/2016	1:1000	
Secondary Antibody	**Supplier**	**Catalogue Number**	**Lot**	**Dilution WB**	**Dilution IF**
Anti mouse IGg HRP linked	Cell Signalling	706S	32	1:2000	
Anti Rabbit IGg HRP linked	Cell Signalling	704S	36	1:2000	
Goat Anti Rabbit-Alexa Flour 488	Life Technologies	R37116	1884984		1 drop/ml
Goat anti Mouse - Alexa Flour 594	Life Technologies	R32121	1756600		1 drop/ml

Goat Anti Mouse - Alexa Flour 680	Invitrogen	A21058	982289		1:1000
Goat Anti Rabbit – Alexa Flour 594	Life Technologies	R37117	1780825		1 drop/ml
Goat Anti Mouse- Alexa Flour 488	Invitrogen	A28175	RE238148		1:1000

Table 2. 4 List of Buffers used for Protein Extraction

Lysis Buffer	Contents	Application
RIPA	Commercially Available from Santa Cruz (sc-24948)	Lysis of eyes for western blot Lysis of cells for western blot Lysis of RPE1 RP2BIRA and BIRA cells for streptavidin pulldown assays Lysis of cells for Click Chemistry IP assays
Co-IP Lysis Buffer	50mM Tris-HCl pH 7.5, 150mM NaCl, 0.1mM EGTA, 2mM MgCl2, 1% Triton X-100, 10% Glycerol	Lysis of eyes for ARL3-GTP pulldown assays
Triton Lysis Buffer	50mM Tris-HCl pH 7.5, 150 mM NaCl, 1% Triton x100	Lysis of cells for V5-IP assays

2.3.5 BIO-ID Assay

RPE1 RP2 Null RP2-BIRA and RPE1 RP2 Null BIRA cells were seeded on 10 cm dishes and once confluent incubated in DMEM-F12 medium (as above) supplemented with or without 50µm biotin for 24 hours. After two washes with ice cold PBS, cells were lysed in 500µl RIPA lysis buffer (Santa Cruz, sc24928) and PMSF, protease and phosphatase inhibitor cocktails (Sigma) as described above. Streptavidin pulldowns were performed on Kingfisher duo automated IP machine using magnetic streptavidin Dynabeads (Thermo). Plates for processing in Kingfisher duo were set up as follows:

Row	Solution	Composition	Volume
A	Trypsin Working reagent	2M urea + 100 mM tris + 1 mM DTT + 5ug/mL trypsin	100 uL
B	TBS	50 mM tris, 150 mM NaCl, pH 7.4	300 uL
C	TBS	50 mM tris, 150 mM NaCl, pH 7.4	300 uL
D	TBS	50 mM tris, 150 mM NaCl, pH 7.4	300 uL
E	RIPA	Santa Cruz (sc-24948)	300 uL
F	RIPA	Santa Cruz (sc-24948)	300 uL
G	Lysate	RP2-BIRA/ BIRA only Lysate	500 uL
H	Beads	MyOneStreptavidin dynabeads, in RIPA buffer	4uL beads 100 uL

Samples were processed on the 1hr-IP-Digest protocol which performs an 1hr IP followed by an overnight trypsin digestion at 37^0C to elute and digest proteins from beads in preparation for mass spectrometry analysis.

2.3.6 Mass Spectrometry Analysis

2.3.6.1 Peptide Clean-up

Prior to mass spectrometry analysis samples were loaded onto tips containing C18 material (Sigma), proteins were stored at -20^{0}C on the C18 material in the tips before loading onto the mass spectrometry machine. Firstly, samples were acidified by addition of 0.5% TFA and the pH checked by pH paper. After C18 material was loaded onto tips 20µl of MS-grade Methanol was added to each tip to activate the C18 material and pushed through using a syringe. Tips were then equilibrated by addition of 0.1%TFA and the sample then loaded onto the tips. The tips were then washed by a final addition of 0.1%TFA and stored at -20^{0}C.

2.3.6.2 Mass Spectrometry

Samples were processed on a Thermo Scientific 3000 RSLC Nano liquid Chromatography system coupled to QExactive Plus mass spectrometer by Dr Jimi Wills and Dr Alex von Kreigheim at the IGMM Mass Spectrometry Facility. Samples were analysed in three technical repeats. Results were searched, filtered and statistically analysed, any hits that were enriched in experimental samples 5 fold more than in control were considered valid hits and these proteins were then organised by statistical significance.

2.3.7 Streptavidin Pulldown Assay

RP2 BIRA and BIRA cells were plated on 10cm dishes and once confluent supplemented with or without 50µm biotin for 6 hours. Cells were lysed in RIPA lysis buffer (Santa Cruz) with PMSF, protease and phosphatase inhibitor cocktails (Sigma) (As described 2.3.1). Ten percent of the lysates were removed for inputs and the remaining lysate was incubated with 25µl dynobeads (MyOne Streptavidin C1, Invitrogen) for 1 hour at 4^{0}C with continuous rotation. Beads were then washed 3 times with PBS and biotin labelled proteins eluted off the beads by adding Sample Buffer (4x LDS buffer, NuPage and 1MDTT) and subjected to SDS-PAGE and western blotting.

2.3.8 Click Chemistry Immunoprecipitation Assay

HEK293T cells were seeded on six well plates and transiently transfected with RP2-V5 and ZDHHC5-HA. For knockdown experiments, cells were transfected with ZDHHC5 siRNA and CTRL siRNA 48hrs prior to transient transfection with RP2-V5 and ZDHHC5-HA (see 2.2.2). Twenty-four hours after transfection, cells were serum starved in DMEM supplemented with 1% fatty acid free BSA (Sigma) for 30 minutes. After washing in PBS cells were incubated with DMEM/1% fatty acid free BSA supplemented with 100μM ODYA (Caymen Chemicals) overnight to facilitate labelling of palmitolyated proteins. Cells were lysed in Triton lysis buffer (50mM Tris pH7.5, 150mM NaCl, 1% Triton x100) with 1x PMSF, protease and phosphatase Inhibitors (Sigma) (as described 2.3.1). Ten percent of the lysate was removed for input sample. Lysates were incubated with 10μl V5 beads (mouse anti V5 Agarose Affinity gel antibody, Sigma) for 1 hour at 4^0C to immunopercipitate RP2-V5. After 3 washes in triton lysis buffer click chemistry reaction mix (IRdye 800CW,Licor, CuSO4 40mM, TBTA 100mM, Sigma and dH20) was added to each lysate followed by 40mM Ascorbic Acid (Sigma). Reactions were mixed in a table top Thermomixer C (Eppendorf) at 1300rpm 1 hour at room temperature. Samples were then prepared for electrophoresis and Western blot by addition of sample buffer as described above. After electrophoresis and transfer, (see 2.3.3) membranes were blocked in 50% Odyssey Blocking Buffer/PBS (Licor) for 1 hour at room temperature. V5 primary and Alexa- Flour 680 goat anti mouse secondary (Invitrogen) were diluted in the same buffer and incubated on membranes for 1 hour at room temperature. Membranes were imaged on Odyssey FC imaging system (LICOR). Remaining input samples were immunoblotted for HA and Actin expression.

Chapter 3

Phenotype Analysis of Rp2h DEL26/Y and Rp2h E135G/Y Mice

Chapter 3: Phenotype Analysis of *Rp2h* DEL26/Y and *Rp2h* E135G/Y Mice

3.1 Introduction

In order to gain a better understanding of the role of RP2 in the retina and to therefore better understand the mechanism causing photoreceptor death in patients with *RP2* mutations, two *Rp2h* knock out mouse models have previously been generated (L. Li et al. 2013; Houbin Zhang et al. 2015). A gene trap cassette targeting the first intron of the *Rp2h* gene was used to generate *Rp2h* -/- mice (Houbin Zhang et al. 2015). These mice presented with a progressive rod-cone dystrophy with vision loss evident from one month of age. The retinal pathology of these mice was studied up to two years of age with little difference in the thickness of the outer nuclear layer (ONL) detected even at late stages of the disease. However, mislocalisation of the prenylated proteins rod and cone Phosphodiesterase 6 (PDE6) and G- coupled receptor kinase 1 (GRK1) were detected in these mice (Houbin Zhang et al. 2015). This is similar to the findings in zebrafish in which the absence of RP2 results in mislocalisation of PDE6, GRK1 and transducin α (F. Liu et al. 2015). These findings collectively provide strong evidence in support of a mechanism of disease progression caused by mistrafficking of prenylated proteins attributed to excessive levels of ARL3-GTP due to the absence of RP2. However, transducin α appeared to be localised normally in *Rp2h* -/- mice despite it being a known RP2-ARL3 target, highlighting the possibility that *in vivo*, compensatory mechanisms exist.

A second *Rp2h* knockout mouse, $Rp2^{null}$, was generated by flanking exon 2 of the *Rp2h* gene with lox p sites and crossing into a cre line (L. Li et al. 2013). The cre line used expressed the cre transgene under control of the cytomegalovirus immediate early enhancer chicken β-actin hybrid (CAG) promoter. Cre expression in this line is activated before the two cell stage of embryonic development which facilitates deletion of genes from the very early stages of development (Sakai and Miyazaki 1997). $Rp2^{null}$ mice presented with a progressive rod-cone dystrophy with deterioration of photoreceptor function detected as early as one month of age. This model showed no significant decrease in ONL thickness at 1 month however, a significant decrease in ONL thickness was detected at both 5 months and 9 months of age. Immunofluorescence analysis of the retinas revealed normal localisation of

transducin β subunit 1 (Gβ1) and nephrocystin 3 (NPHP3) even in older mice where retinal degeneration was severe. These mice however, did present with early M/L opsin mislocalisation evident from one month of age, which occurred prior to photoreceptor cell death (L. Li et al. 2013). This model demonstrated that in the absence of RP2, prenylated proteins can still be trafficked correctly within the retina and therefore a dysfunction of ARL3 may not be the major factor causing retinal degeneration in this case. This model suggests a novel function for RP2 in cone opsin trafficking, a mechanism which appears to be independent of ARL3 activity.

A review of the clinical symptoms of Retinitis Pigmentosa patients revealed patients with RP2 mutations tend to have early cone deterioration prior to rod deterioration (Jayasundera et.al, 2010) therefore this model may better recapitulate the human phenotype. This is further supported by a study in which RP2 was ablated specifically in rods or cones revealing *Rp2h* knock out in cones leads to an elongated cone OS and phenocopy of the $Rp2^{null}$ mouse, a finding which is not replicated when *Rp2h* is knocked out in rods only (Li et.al, 2015). If *RP2* mutations do cause a cone autonomous effect, which leads to secondary rod cell death it is difficult to explain this defect through a disease mechanism based primarily on ARL3 dysfunction as ARL3 is expressed in the connecting cilia of both rod and cone photoreceptors, consequently a cell autonomous effect would not be expected. Therefore, this suggests RP2 in cones has other functions independent of its GAP activity on ARL3, which when perturbed contribute to retinal degeneration. The differential findings presented in the two *Rp2h* knock out mouse models demonstrate the necessity of establishing whether the major driver of retinal degeneration in cases with *RP2* mutations is attributed solely to defects in ARL3 regulation. Therefore, to address this question, I generated new *Rp2h* knockout and *Rp2h* E135G mouse models using CRISPR genome editing. The mouse E135G mutation is equivalent to the E138G human pathogenic mutation that is predicted to result in a stable RP2 protein, which is unable to interact with ARL3 (Kühnel et.al 2006).This enables the comparison of loss of RP2 GAP activity to complete RP2 knockout, allowing the contribution of ARL3 dysregulation to retinal degeneration to be directly assessed.

3.2 *Rp2h* DEL26/Y and *Rp2h* E135G/Y Mice have Progressive Retinal Degeneration

3.2.1 Validation of *Rp2h* DEL26/Y and *Rp2h* E135G/Y Mice

To generate mice carrying the *Rp2h* E135G mutation paired guide RNAs, cas9 nickase mRNA and a repair template designed to introduce the E135G mutation were injected by cytosolic injection into C57BL6/J single cell embryos (see 2.1.2 for detailed methods and sequences of guide RNAs and the repair template). From this round of injections, a 26bp deletion allele was also introduced which was predicted to result in no protein expression. F0 founder animals carrying both E135G and DEL26 mutations were outbred with C57BL6/J animals to generate F1 mice which were used to establish the line. The line was maintained by crossing *Rp2h* DEL26/+ and *Rp2h* E135G/+ female mice to C57BL6/J control male animals. F2 *Rp2h* DEL26/Y and *Rp2h* E135G/Y were used as experimental animals and *Rp2h* DEL26/+ and *Rp2h* E135G/+ females were continually outbred to C57BL6/J control male animals to generate further generations of experimental male animals and to maintain the line.

In order to confirm that the E135G mutation and the DEL26 mutation introduced by CRISPR genome editing (Figure 3.1 A) generated a stable protein and a null allele respectively, a western blot for RP2 was performed. RP2 expression was detected in WT and *Rp2h* E135G/Y lysates but was absent in *Rp2h* DEL26/Y kidney lysates (Figure 3.1 B). RP2 expression was also detected in WT, *Rp2h* E135G/Y, *Arl3* Q71L/+, *Arl3* Q71L/Q71L eye lysates but not in *Rp2h* DEL26/Y eye lysates (Figure 3.1 C) (*Arl3* Q71L+ and *Arl3* Q71L/Q71L mice discussed in chapter 4). The levels of RP2 E135G were comparable to WT in both kidney and eye lysates demonstrating RP2 E135G is stable and expressed to the same level as WT RP2 (Figure 3.1 A, B).

Figure 3. 1 RP2 DEL26 is a Null Allele and RP2 E135G is Stable

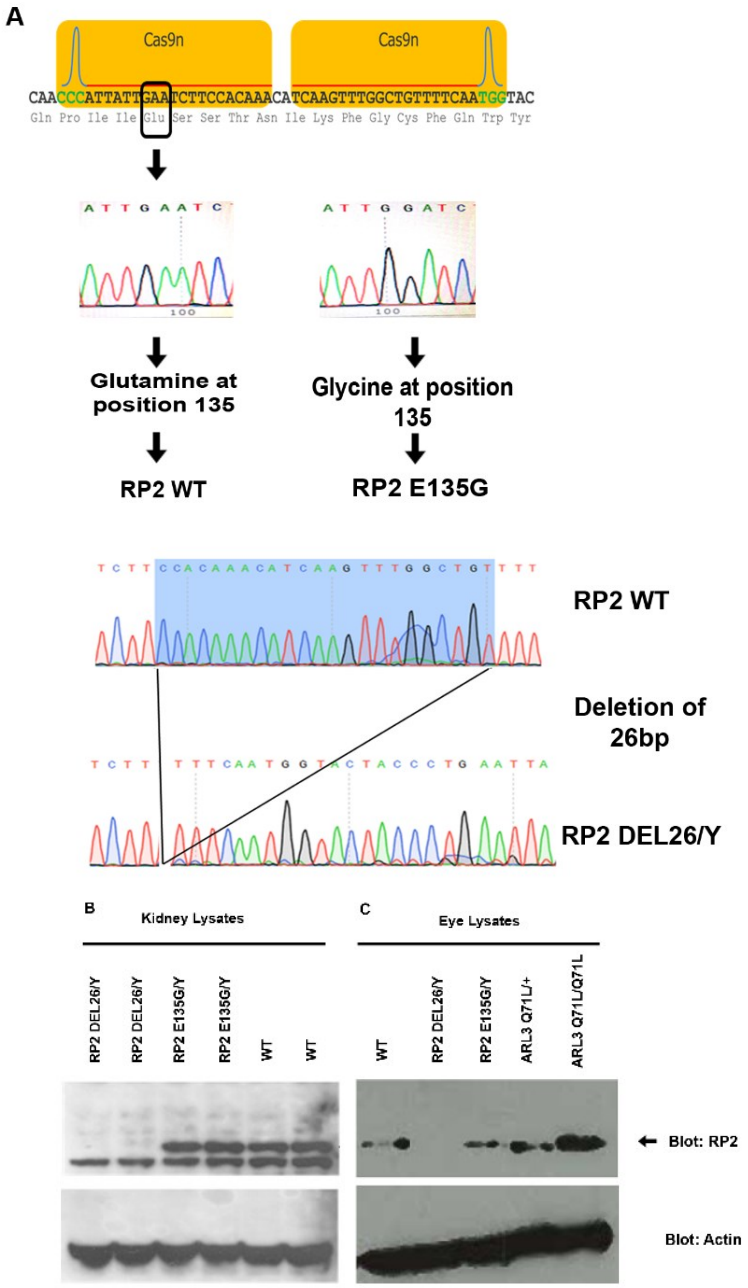

(A) Schematic of the generation of RP2 E135G and RP2 DEL26 mutations by CRISPR genome editing.

(B) Western blot of RP2 expression in *Rp2h* DEL26/Y, *Rp2h* E135G/Y and WT kidney lysates. *Rp2h* DEL26/Y lysates had no RP2 expression. *Rp2h* E135G/Y and WT lysates had RP2 expression.

(C) Western blot of RP2 expression in WT, *Rp2h* DEL26/Y, *Rp2h* E135G/Y, *Arl3* Q71L/+ and *Arl3* Q71L/Q71L whole eye lysates. *Rp2h* DEL26/Y eyes had no RP2 expression. RP2 expression was detected in WT and *Rp2h* E135G/Y eyes.
Arl3 Q71L/+ and Arl3 Q71L/Q71L discussed in chapter 4

3.2.2 Histological Analysis of *Rp2h* DEL26/Y and *Rp2h* E135G/Y Retinas

In order to determine whether *Rp2h* DEL26/Y and *Rp2h* E135G/Y retinas exhibit retinal degeneration, which models the human XLRP phenotype of progressive photoreceptor cell loss, paraffin sections of retinas were stained with haematoxylin and eosin and the histology analysed. Eyes were fixed in Davidson's Fix for 24 hours and processed for wax sectioning (as described 2.1.4), 7μm thick sections were cut from paraffin embedded eyes (as described 2.1.4) and sections which contained the optic nerve (ON) were used for histological analysis. Retina sections were taken from mice aged 1 month, 3 months, 6 months, 9 months and 12 months and the thickness of the ONL measured at specific distance from the ON. The ONL was measured as it contains the nuclei of the photoreceptors therefore thinning of the ONL reflects loss of photoreceptors. To confirm that retinal degeneration was attributed to loss of photoreceptors and not loss of other cells in the retina the inner nuclear layer (INL) thickness was measured as a control as it contains the nuclei of bipolar, horizontal and amacrine cells. *Rp2h* DEL26/Y retinas displayed no difference in ONL thickness at 1 month of age (Figure 3.2 A, Figure 3.3 A (i)). At 3 months of age *Rp2h* DEL26/Y retinas had a significantly thinner ONL at peripheral regions demonstrating loss of photoreceptors (Figure 3.2 B, Figure 3.3 A (ii)). At 6 months of age *Rp2h* DEL26/Y retinas displayed retinal thinning compared to WT and significant reduction in ONL thickness in multiple regions (Figure 3.2 C, Figure 3.3 A (iii)). At 9 months and 12 months of age extensive retinal thinning was observed compared to WT and ONL thickness was significantly reduced at most regions (Figure 3.2 D, E, Figure 3.3 A (iv), (v)). The INL was not significantly thinner than WT at any age (Figure 3.3 C) suggesting that the retinal degeneration was specifically due to loss of photoreceptors.

Rp2h E135G/Y retinas had no significant difference in ONL thickness at 1 month or 3 months of age (Figure 3.2 A, Figure 3.3 A (i), Figure 3.2 B, Figure 3.3 B (ii)). At 6 months of age no retinal thinning was observed in *Rp2h* E135G/Y retinas compared to WT, however ONL thickness was reduced significantly in some regions (Figure 3.2 C, Figure 3.2 A (iii)). At 9 months and 12 months of age, thinning of the retina compared to WT was observed and the ONL was significantly thinner than WT in most regions (Figure 3.2 D, E, Figure 3.3 A (iv), (v)). The INL thickness was not significantly reduced compared to WT at any age demonstrating the retinal degeneration observed

was attributed to loss of photoreceptors (Figure 3.3 B). *Rp2h* E135G/Y retinas were not thin as *Rp2h* DEL26/Y retinas at 9 months or 12 months of age and the ONL thickness of *Rp2h* DEL26/Y retinas was thinner than *Rp2h* E135G/Y from age 3 months demonstrating *Rp2h* knockout results in more severe retinal degeneration than carrying the *Rp2h* E135G mutation.

Figure 3. 2 Histological Analysis of *Rp2h* WT, *Rp2h* DEL26/Y and *Rp2h* E135G/Y Retinas

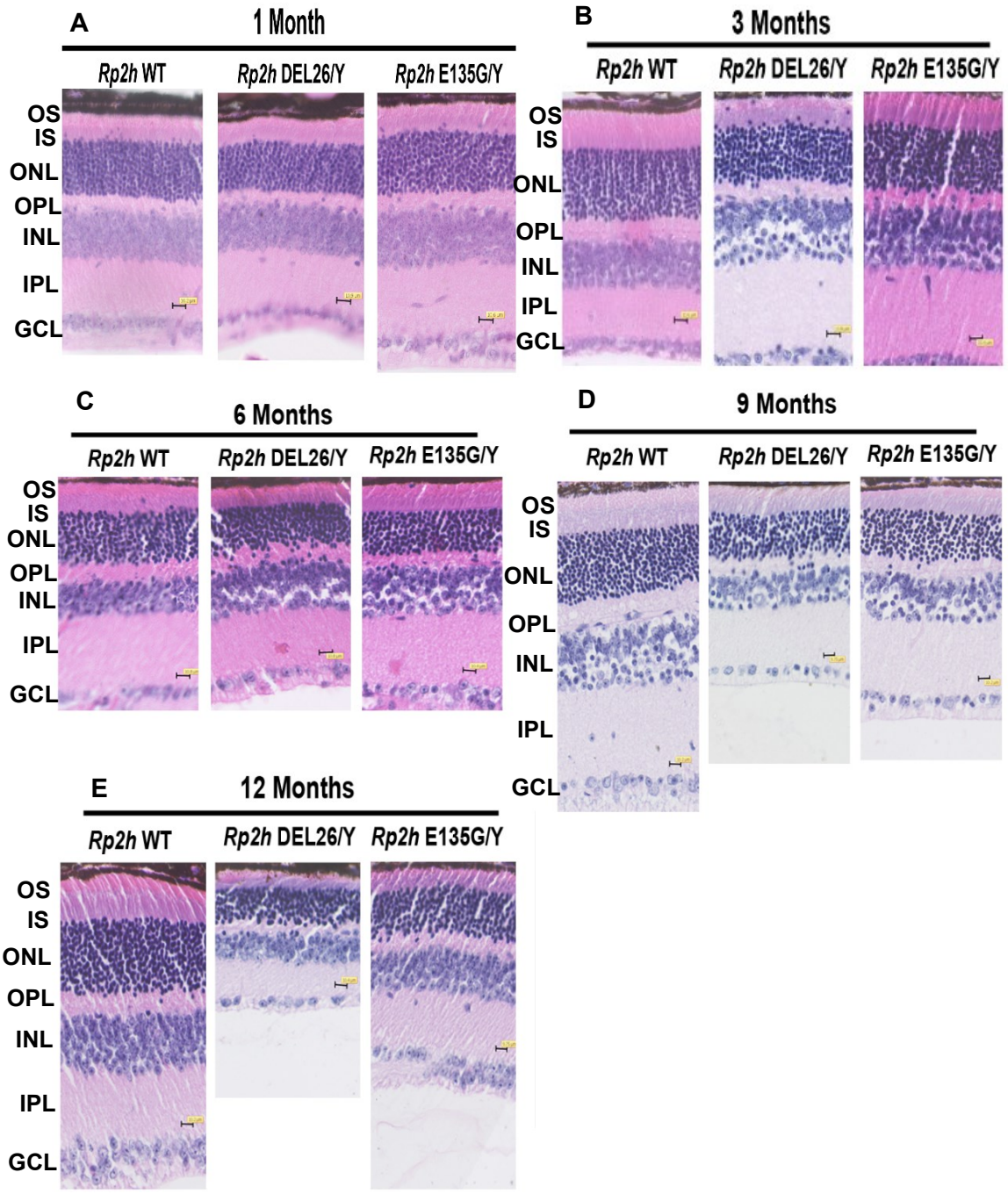

H&E staining of paraffin sections of *Rp2h* WT, *Rp2h* DEL26/Y and *Rp2h* E135G/Y Retinas. Aged 1 month (A), 3 months (B), 6 months (C), 9 months (D) and 12 months (E). Retinal degeneration can be observed from 6 months of age in both *Rp2h* DEL26/Y and 9 months of age in *Rp2h* E135G/Y retinas.

Figure 3. 3 Quantification of ONL and INL Thinning in *Rp2h* DEL26/Y and *Rp2h* E135G/Y Retinas

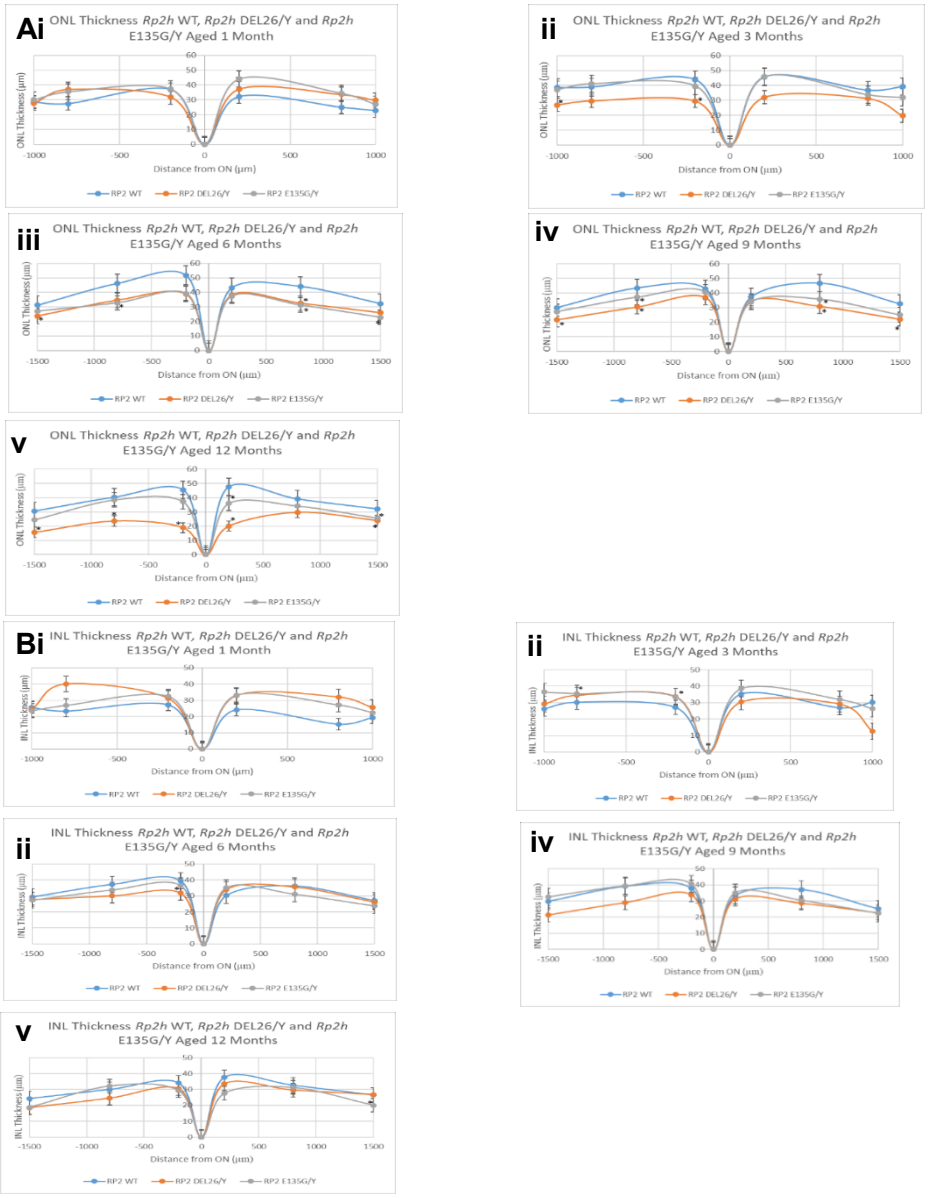

(A) ONL thickness measurements at central, medial and peripheral regions from ON in *Rp2h* WT, *Rp2h* DEL26/Y and *Rp2h* E135G/Y retinas aged 1 month (i), 3 months (ii), 6 months (iii), 9 months (iv) and 12 months (v). Significant reductions in ONL thickness was present in *Rp2h* DEL26/Y retinas from 3 months. Significant reduction in ONL thickness was present in *Rp2h* E135G/Y retinas from 6 months of age.

(B) INL thickness measurements at central, medial and peripheral regions from the ON in *Rp2h* WT, *Rp2h* DEL26/Y and *Rp2h* E135G/Y retinas ages 1 month (i), 3 months (ii), 6 months (iii), 9 months (iv) and 12 months (v). INL thickness is not significantly different from WT for *Rp2h* DEL26/Y and *Rp2h* E135G/Y retinas at any ages examined.

n=3 mice analysed for each genotype at each age. Statistics student's t test. *p<0.05

3.2.3 ERG Analysis of *Rp2h* DEL26/Y and *Rp2h* E135G/Y Retinas

The electroretinogram (ERG) is a test that measures the electrical activity generated by neural and non-neuronal cells in the retina in response to a light stimulus. The electrical response is a result of a retinal potential generated by light-induced changes in the flux of ions during phototransduction (Bach et al. 2013). To perform ERGs on mice, mice were firstly dark adapted to analyse the function of rod photoreceptors and then light adapted to analyse the function of cone photoreceptors. Mice were anaesthetised by inhalation of 1% isoflurane and electrodes were placed over the front of the cornea and secured with a contact lens (see 2.1.5 for detailed methods). ERGs recordings produce wave forms which reflect the activity of photoreceptors. The negative A-wave amplitude reflects the activation of photoreceptors and is used as a read out of photoreceptor function. The positive B-wave amplitude represents activation of the downstream signalling cells such as Muller cells and bipolar cells (Bach et al. 2013).

To examine photoreceptor function in *Rp2h* DEL26/Y and *Rp2h* E135G/Y mice ERG recordings using 3cd flash and 10cd flash were analysed. Firstly, a dark-adapted ERG was recorded using a 3cd flash which can stimulate both rod and cone photoreceptors however, the A-wave amplitude recorded is rod dominated. To examine the function of cone photoreceptors a light adapted ERG was recorded using a 10cd flash. *Rp2h* DEL26/Y mice had no significant difference in 3cd ERG response compared to WT mice aged 3 months (Figure 3.4 A (i), B). From age 6 months a significant reduction in A-wave response was recorded which decreased as the mice aged demonstrating a progressive reduction in photoreceptor function (Figure 3.4 A, B). Similarly, recordings from the 10cd light adapted test demonstrated no significant difference in responses in *Rp2h* DEL26/Y mice aged 3 months but a reduction in A-wave response was detected from age 6 months to12 months (Figure 3.5 A, B). These ERG recordings demonstrate *Rp2h* DEL26/Y mice have progressive reduction in both rod and cone function from age 6 months. *Rp2h* E135G/Y mice had no statistically significant difference in A-wave amplitude detected in the 3cd test, demonstrating no significant reduction in photoreceptor function (Figure 3.4 A, C). Recordings from the 10cd Test revealed a significantly reduced A-wave amplitude in *Rp2h* E135G/Y mice compared to WT at age 9 and 12 months (Figure 3.5 A (iv), (v), C). This demonstrates

Rp2h E135G/Y mice have a reduction in cone photoreceptor function from age 9 months and this occurs prior to any effect on rod photoreceptor function.

Figure 3. 4 ERG Analysis of *Rp2h* DEL26/Y and *Rp2h* E135G/Y Mice 3cd Flash Test

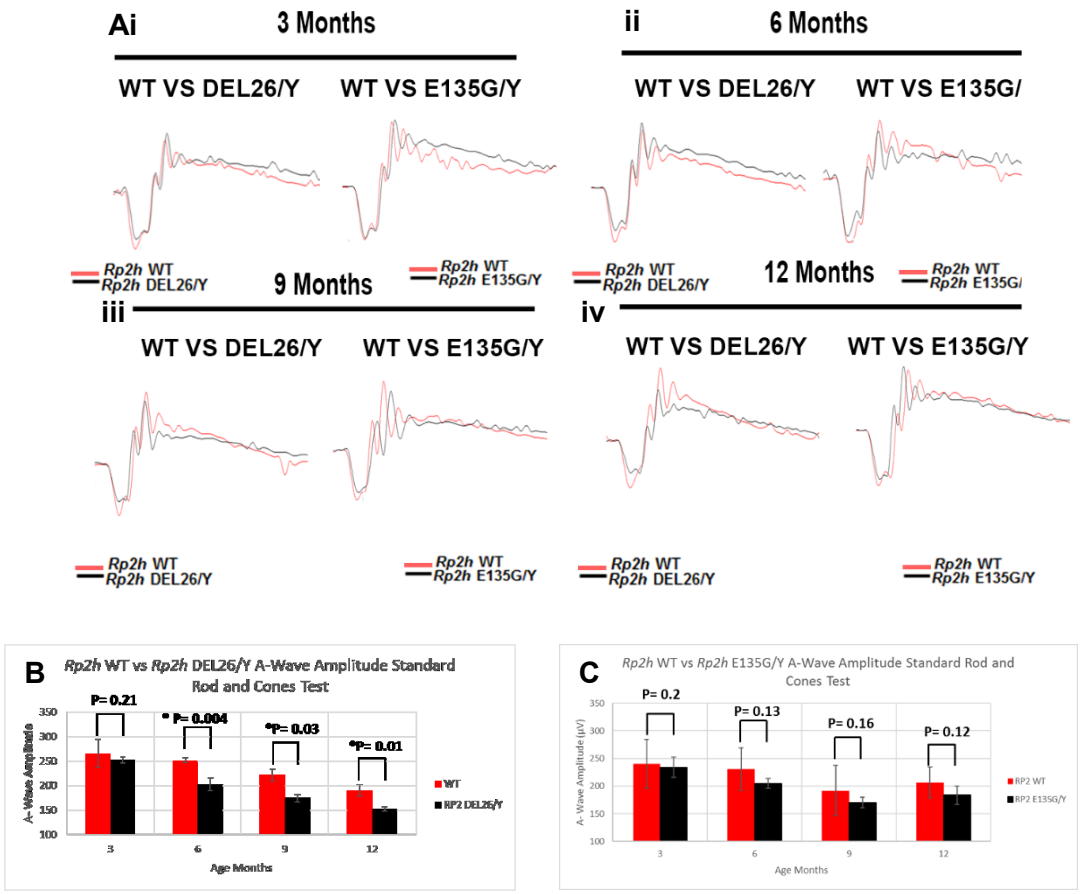

(A) Representative traces from 3cd flash dark adapted ERGs for *Rp2h* DEL26/Y compared to WT and *Rp2h* E135G/Y compared to WT aged 3 months (i), 6 months (ii), 9 months (iii) and 12 months (iv).

(B) Quantification of average A-wave amplitude in *Rp2h* DEL26/Y and WT aged 3, 6, 9 and 12 months. Significant reduction in A-wave amplitude in *Rp2h* DEL26/Y mice detected from age 6 months.

(C) Quantification of average A-wave amplitude in *Rp2h* E135G/Y and WT mice aged 3,6,9 and 12 months. No significant reduction in A-wave amplitude detected at any age.

N=5 for each genotype at each age, statistics calculated by students T.Test. *Rp2h* DEL26/Y and *Rp2h* E135G/Y mice compared to WT CTRL ERGs recorded on the same day.

Figure 3. 5 ERG Analysis of *Rp2h* DEL26/Y and *Rp2h* E135G/Y Mice 10cd Flash Test

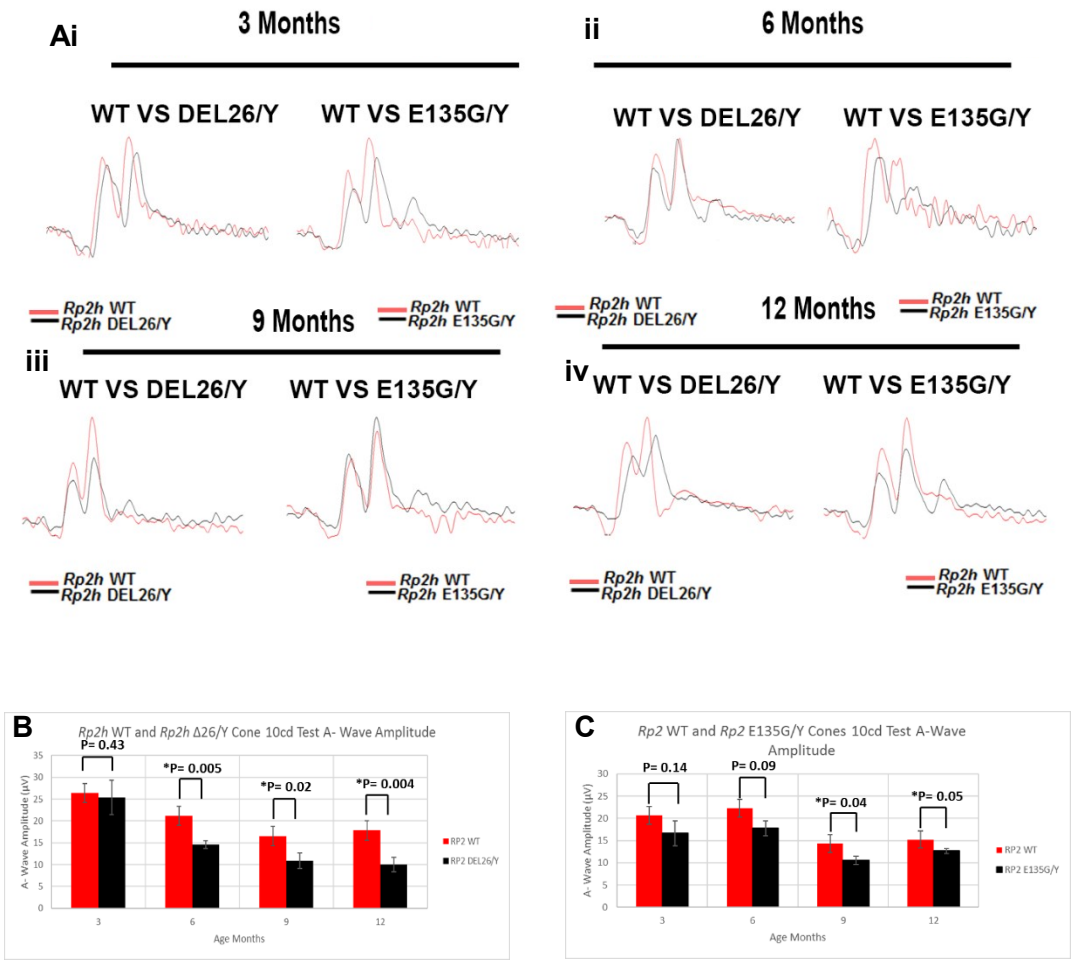

(A) Representative traces from light adapted 10cd Test ERGs for *Rp2h* DEL26/Y compared to WT and *Rp2h* E135G/Y compared to WT aged 3 months (i), 6 months (ii), 9 months (iii) and 12 months (iv).

(B) Quantification of average A-wave amplitude in *Rp2h* DEL26/Y and WT aged 3, 6, 9 and 12 months. Significant reduction in A-wave amplitude in *Rp2h* DEL26/Y mice detected from age 6 months.

(C) Quantification of average A-wave amplitude in *Rp2h* E135G/Y and WT mice aged 3,6,9 and 12 months. Significant reduction in A-wave amplitude detected at 9 and 12 months of age.

N=5 for each genotype at each age, statistics calculated by students T.Test. *Rp2h* DEL26/Y and *Rp2h* E135G/Y mice compared to WT CTRL ERGs recorded on the same day.

3.3 *Rp2h* DEL26/Y and *Rp2h* E135G/Y Retinas exhibit Retinal Stress at 1 month

Given that *Rp2h* DEL26/Y and *Rp2h* E135G/Y mice have a retinal degeneration phenotype apparent from 6 months and 9 months of age respectively by ERG responses, I assessed whether there were any signs of retinal stress prior to photoreceptor loss. Glial fibrillary acidic protein (GFAP) is expressed in astrocytes and Muller cells, however upon retinal stress, these microglial cells become activated forming fibres which spread into other layers of the retina and GFAP expression is increased. Retina sections from *Rp2h* DEL26/Y and *Rp2h* E135G/Y mice aged 1 month were analysed for GFAP expression (Figure 3.6). In WT retinas GFAP staining was confined to the GCL in both central and peripheral regions (Figure 3.6 A, D). In *RP2h* DEL26/Y and *Rp2h* E135G/Y retinas GFAP expression was confined to the GCL in central regions (Figure 3.6 B,C) but was observed in the upper layers of the retina (throughout the ONL, INL, IPL) in peripheral regions (Figure 3.6 E,F). The *Rp2h* DEL26/Y retinas had more gliosis than in *Rp2h* E135G/Y retinas indicating more retinal stress in these mice. As observed at the periphery of the retina, this suggested that peripheral photoreceptors may be more sensitive to *Rp2h* mutation.

Figure 3. 6 GFAP Expression in *Rp2h* DEL26/Y and *Rp2h* E135G/Y Retinas Aged 1 Month

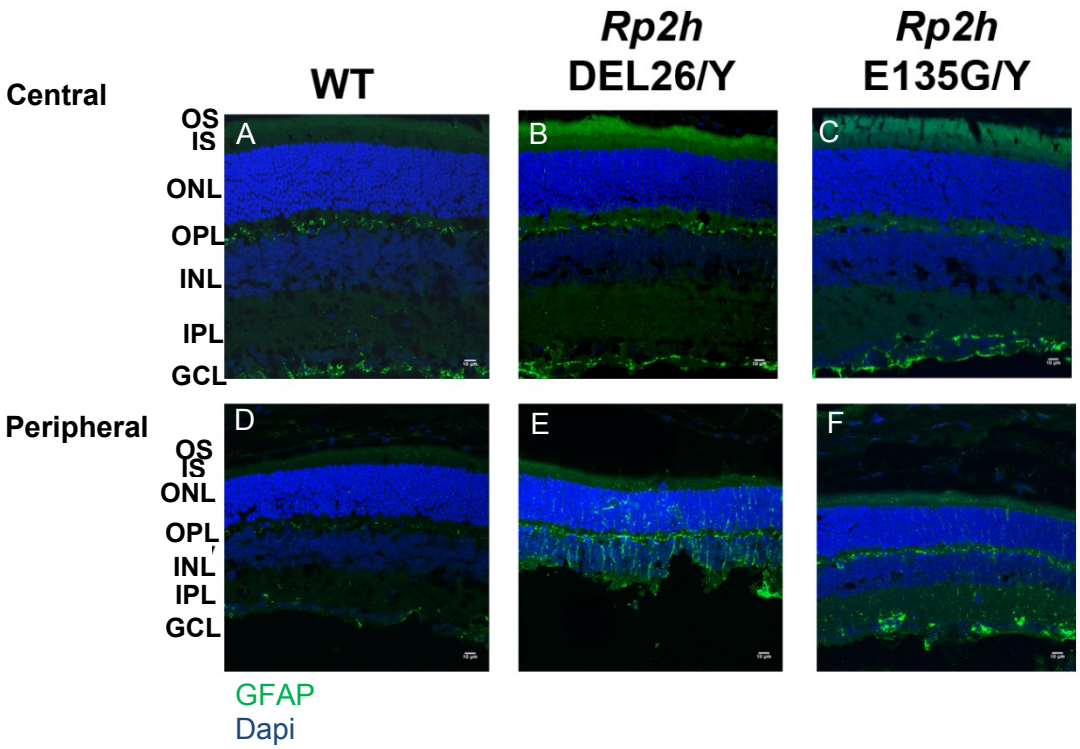

(A) GFAP (green) staining in WT central retina aged 1 month demonstrating GFAP is expressed in ganglion cell layer.

(B) GFAP staining in *Rp2h* DEL26/Y central retina aged 1 month. GFAP staining was present in the ganglion cell layer.

(C) GFAP staining in *Rp2h* E135G/Y central retina aged 1 month. GFAP staining was present in ganglion cell layer.

(D) GFAP staining in WT peripheral retina. GFAP staining was localised to the ganglion cell layer.

(E) GFAP staining in *Rp2h* DEL26/Y peripheral retina. GFAP staining was present within the GCL, INL, OPL and ONL.

(F) GFAP staining in *Rp2h* E135G/Y peripheral retina. Some GFAP staining was present in the IPL and INL.

3.4 M/L Opsin is mislocalised in *Rp2h* DEL26/Y and *Rp2h* E135G/Y Retinas after Onset of Photoreceptor Cell Death

As it has been previously reported that M/L opsin is mislocalised in *Rp2*^{null} mice from one month of age, prior to photoreceptor cell death (L. Li et al. 2013), I analysed M/L opsin localisation in the *Rp2h* DEL26/Y and *Rp2h* E135G/Y mice. *Rp2h* DEL26/Y mice displayed normal M/L opsin localisation to the OS and IS of cone photoreceptors identical to the localisation in WT retinas at ages 1 month and 3 months (Figure 3.7 A). At 6 months of age M/L opsin staining was observed in the IS, ONL and IPL of cone photoreceptors (Figure 3.7 C). At 9 months and 12 months of age a reduction in M/L opsin staining was observed suggesting loss of cone photoreceptors as retinal degeneration progressed. At 6 months of age a reduction in the ERG response of cone photoreceptors and a reduction in ONL thickness (Figure 3.4, Figure 3.2, 3.3) was also observed suggesting that mislocalisation of M/L opsin likely contributes to dysfunction of cones and may cause cone photoreceptor cell death. Significant thinning of the ONL is detected at 3 months of age in peripheral regions when M/L opsin is not mislocalised suggesting that another factor may be driving retinal degeneration at early stages and M/L opsin mislocalisation may be a secondary effect causing dysfunction of cones.

Rp2h E135G/Y retinas had normal M/L opsin localisation in the IS and OS of cone photoreceptors at 1 month, 3 months and 6 months of age (Figure 3.7 A, B, C). At 9 months of age M/L opsin expression was detected in the IS of the cone photoreceptors and not the OS. At 12 months of age the *Rp2h* E135G/Y retinas had reduced M/L opsin immunostaining possibly reflecting loss of cone photoreceptors (Figure 3.7 E). In *Rp2h* E135G/Y mice at 9 months and 12 months of age a significant reduction in cone photoreceptor function was detected by ERG and as M/L opsin mislocalisation was also observed at these ages, this suggests that mislocalisation of M/L opsin contributed to cone dysfunction and cone cell death. Thinning of the ONL in *Rp2h* E135G/Y retinas was first detected at 6 months of age suggesting another factor was driving retinal degeneration and secondary effects on M/L opsin followed this at 9 and 12 months.

A reduction in M/L opsin staining was observed earlier in *Rp2h* DEL26/Y retinas than in *Rp2h* E135G/Y retinas suggesting earlier cone loss in DEL26/Y mutants (Figure 3.7 D). M/L opsin mislocalisation was also detected in *Rp2h* DEL26/Y retinas at earlier

stages than *Rp2h* E135G/Y retinas demonstrating that RP2 E135G expression can facilitate M/L opsin trafficking for some time despite loss of ARL3 GAP activity suggesting that RP2 may interact with other factors along with ARL3 to regulate trafficking of M/L opsin or M/L opsin may be mislocalised as a secondary effect due to disrupted cone function caused by another mechanism which is regulated by RP2.

Figure 3. 7 M/L Opsin Localisation in *Rp2h* DEL26/Y and *Rp2h* E135G/Y Retinas

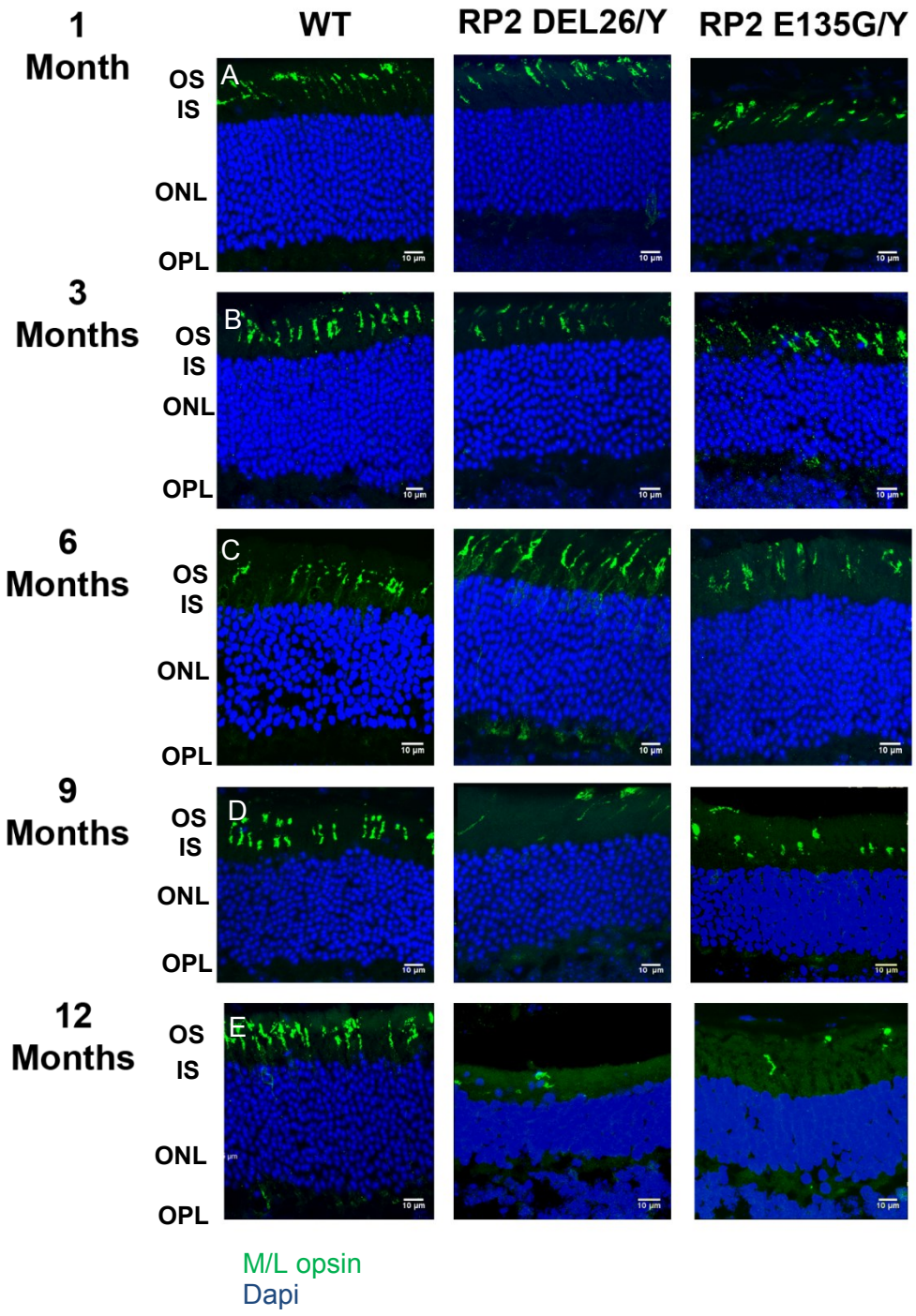

(A) M/L Opsin (green) staining in *Rp2h* WT, *Rp2h* DEL26/Y and *Rp2h* E135G/Y aged 1 month. M/L opsin staining was present in the OS of cone photoreceptors.
(B) M/L opsin staining in *Rp2h* WT, *Rp2h* DEL26/Y and *Rp2h* E135G/Y aged 3 months. M/L opsin staining was present in OS of cone photoreceptors in WT, *Rp2h* DEL26/Y and *Rp2h* E135G/Y retinas.
(C) M/L opsin staining in *Rp2h* WT, *Rp2h* DEL26/Y and *Rp2h* E135G/Y aged 6 months. M/L opsin staining was present in the OS of cone photoreceptors in WT retinas. In *Rp2h* DEL26/Y retinas M/L opsin staining was present in the OS, IS, ONL and OPL of cone photoreceptors. In *Rp2h* E135G/Y retinas M/L opsin staining was detected in the OS of cone photoreceptors similar to WT retinas.
(D) M/L opsin staining in *Rp2h* WT, *Rp2h* DEL26/Y and *Rp2h* E135G/Y retinas aged 9 months. In WT retinas M/L opsin staining was present in the OS of cone photoreceptors. In *Rp2h* DEL26/Y retinas M/L opsin staining was reduced compared to WT. In *Rp2h* E135G/Y retinas M/L opsin staining was present in the IS, ONL and OPL of cones.
(E) M/L opsin staining in *Rp2h* WT, *Rp2h* DEL26/Y and *Rp2h* E135G/Y retinas aged 12 months. In WT retinas M/L opsin staining was present in the OS of cone photoreceptors. In *Rp2h* DEL26/Y and *Rp2h* E135G/Y retinas M/L opsin staining was reduced compared to WT retinas.

3.5 Rhodopsin is mislocalised in *Rp2h* DEL26/Y and *Rp2h* E135G/Y Retinas

As M/L opsin was mislocalised in older *Rp2h* DEL26/Y and *Rp2h* E135G/Y mice I investigated whether the localisation of rhodopsin was affected in these mice. *Rp2h* DEL26/Y mice had normal rhodopsin localisation to the OS of rod photoreceptors identical to WT retinas, at 1 month of age (Figure 3.8 A). At 3 months of age rhodopsin was observed to be mislocalised to the IS of photoreceptors (Figure 3.8 B). At 6 months of age rhodopsin was detected in the OS, IS and OPL. At 9 and 12 months of age rhodopsin was detected throughout the OS, IS, ONL and OPL. In *Rp2h* DEL26/Y retinas significant changes in ONL thickness was observed at 3 months of age in peripheral regions with more widespread changes observed at 6 months of age (Figure 3.3 A (iii)) however, reduction in ERG response was not detected until 6 months of age (Figure 3.4 B). As thinning of the ONL was first detected at the same stage as rhodopsin mislocalisation it is possible that mislocalisation of rhodopsin may be a mechanism driving retinal degeneration in *Rp2h* DEL26/Y mice.

Rp2h E135G/Y mice displayed normal rhodopsin localisation to the OS of rods at 1 month, 3 months and 6 months of age (Figure 3.8 A, B, C). At 9 months of age rhodopsin was detected throughout the photoreceptor layer with signal present in the OS, IS, ONL and OPL (Figure 3.8 C, D). At 12 months of age rhodopsin was again detected in the OS, IS, ONL and OPL (Figure 3.8 E,D). Significant reduction in ONL thickness and ERG response was detected from 6 months however; no significant reduction in rod photoreceptor response was detected even at 12 months of age (Figure 3.3, Figure 3.4 B). As thinning of the ONL was detected prior to rhodopsin mislocalisation it suggests another factor may be driving retinal degeneration in *Rp2h* E135G/Y retinas.

These results demonstrate that mislocalisation of rhodopsin can occur without a significant effect on rod function as no significant difference in rod ERG response was detected in *Rp2h* DEL26/Y mice aged 3 months or in *Rp2h* E135G/Y mice aged 9 months, the ages at which rhodopsin mislocalisation was detected. Rhodopsin mislocalisation was detected at 3 months prior to onset of major photoreceptor cell loss in *Rp2h* DEL26/Y mice suggesting rhodopsin mislocalisation may be a mechanism which drives retinal degeneration in these retinas. In *Rp2h* E135G/Y mice rhodopsin mislocalisation was not observed until age 9 months whereas reduction in ONL thickness was present from age 6 months. This suggests that another

mechanism may drive retinal degeneration in *Rp2h* E135G/Y mice and lead to secondary rhodopsin mislocalisation. This demonstrates that RP2 expression even without GAP activity for ARL3 can partially facilitate proper rhodopsin trafficking but is not sufficient to completely maintain trafficking suggesting that interactors other than ARL3, which can still interact with RP2 E135G may be involved in rhodopsin trafficking. This emphasises that multiple mechanisms may contribute to retinal degeneration in *Rp2h* DEL26/Y mice and may help to explain why they have a more severe phenotype that *Rp2h* E135G/Y mice.

Figure 3. 8 Rhodopsin Localisation in *Rp2h* DEL26/Y and *Rp2h* E135G/Y Retinas

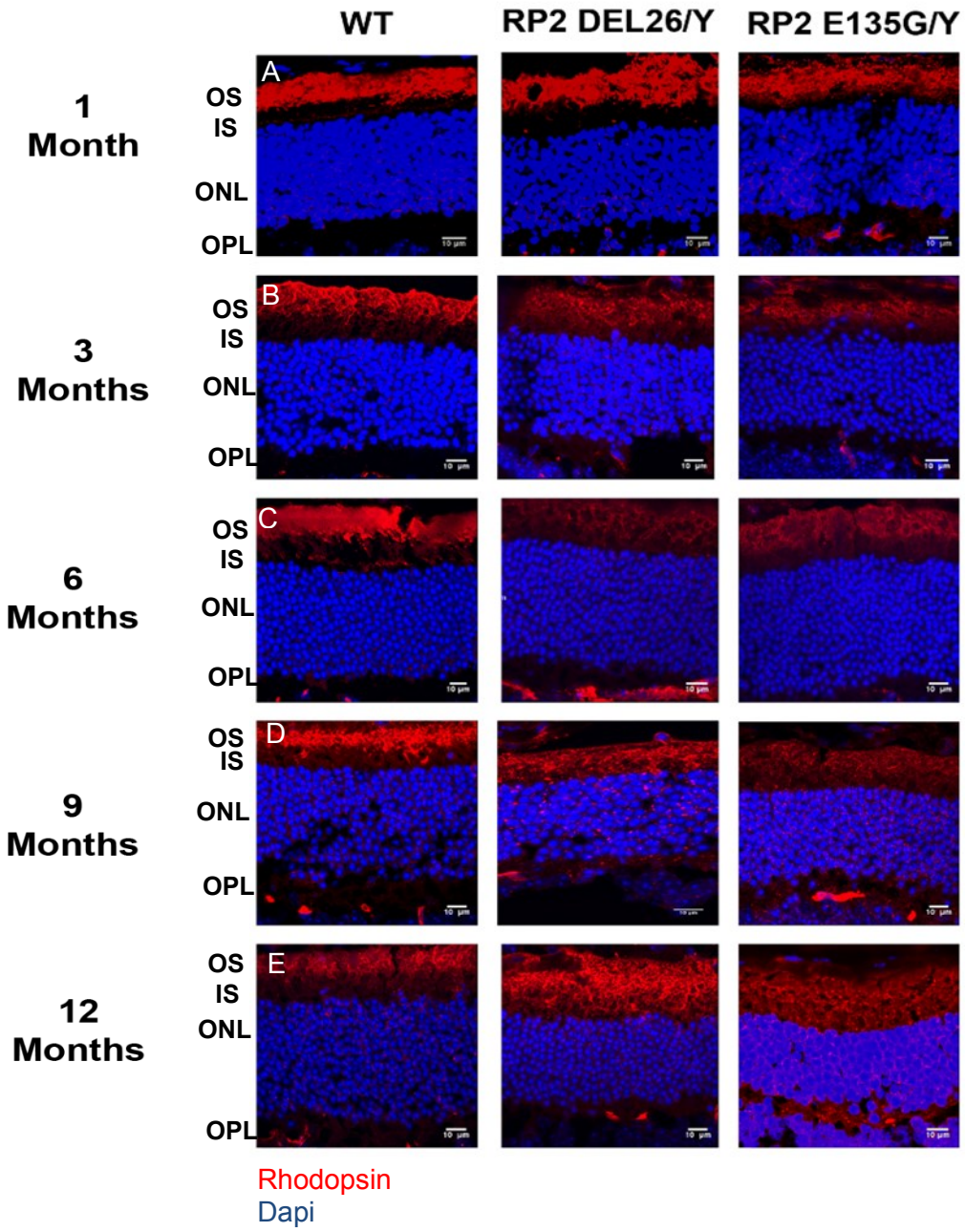

(A) Rhodopsin (red) staining in *Rp2h* WT, *Rp2h* DEL26/Y and *Rp2h* E135G/Y retinas aged 1 month. In WT, *Rp2h* DEL26/Y and *Rp2h* E135G/Y retinas rhodopsin staining was detected in the OS of rod photoreceptors.
(B) Rhodopsin staining in *Rp2h* WT, *Rp2h* DEL26/Y and *Rp2h* E135G/Y retinas aged 3 months. In WT and *Rp2h* E135G/Y retinas rhodopsin was present in the OS of rod photoreceptors. In *Rp2h* DEL26/Y retinas rhodopsin was detected in the OS and IS of rods.
(C) Rhodopsin staining in *Rp2h* WT, *Rp2h* DEL26/Y and *Rp2h* E135G/Y aged 6 months. In WT and *Rp2h* E135G/Y retinas rhodopsin was detected in the OS of rod photoreceptors. In *Rp2h* DEL26/Y retinas rhodopsin was detected in the OS, IS and OPL.
(D) Rhodopsin staining in *Rp2h* WT, *Rp2h* DEL26/Y and *Rp2h* E135G/Y aged 9 months. Rhodopsin was detected in the OS of WT photoreceptors. In *Rp2h* DEL26/Y and *Rp2h* E135G/Y rhodopsin was observed in the OS, IS, ONL and OPL of the photoreceptors.
(E) Rhodopsin staining in *Rp2h* WT, *Rp2h* DEL26/Y and *Rp2h* E135G/Y aged 12 months. In WT retinas rhodopsin was present in the OS of rod photoreceptors. *Rp2h* DEL26/Y and Rp2h E135G/Y retinas had rhodopsin localised throughout the OS, IS, ONL and OPL.

3.6 GRK1 is Mislocalised in *Rp2h* DEL26/Y and *Rp2h* E135G/Y mice

GRK1 is a G- coupled protein receptor essential for recycling rhodopsin during the visual cascade. Following light activation GRK1 phosphorylates activated rhodopsin at multiple sites reducing its activity and facilitating the binding of arrestin which reduces activated rhodopsin's catalytic activity, generating inactive rhodopsin (Yingbin Fu and Yau 2007). Several studies have reported mislocalisation or loss of GRK1 expression when RP2 is mutated (Houbin Zhang et al. 2015; F. Liu et al. 2015). In the *Rp2h -/-* mouse, cone GRK1 was absent from outer segments at 1 month however normal protein levels were detected by western blot (Houbin Zhang et al. 2015). Rp2 null zebrafish displayed mislocalisation of GRK1 to the OPL at 5.5 months old with the protein levels reduced to about ~50% of that in WT (F. Liu et al. 2015). Given these results and that GRK1 has been shown to require RP2, ARL3 and the ARL3 adaptor chaperone PDE6δ for proper trafficking (H Zhang et al. 2007), I investigated GRK1 localisation in *Rp2h* DEL26/Y and *Rp2h* E135G/Y retinas (F. Liu et al. 2015; Houbin Zhang et al. 2015). *Rp2h* DEL26/Y had normal GRK1 localisation in the OS of rod photoreceptors at 1 month of age (Figure 3.9 A). From 3 months of age *Rp2h* DEL26/Y mice had reduced GRK1 immunostaining (Figure 3.9 B, C, D, E) suggesting loss of GRK1 expression. Western blot analysis of whole eye lysates demonstrated that GRK1 was expressed in *Rp2h* DEL26/Y eyes even at 9 months of age (Figure 3.9 G). This suggests that lack of GRK1 immunostaining in the photoreceptor OS was the result of GRK1 mislocalisation, resulting in a diffuse weaker signal.

Rp2h E135G/Y retinas also displayed normal GRK1 localisation aged 1 month (Figure 3.9 A). At 3 months of age mislocalisation of GRK1 to the ONL was observed (Figure 3.9 B). From 6 months of age GRK1 immunostaining was reduced in *Rp2h* E135G/Y retinas (Figure 3.9 C,D,E). Similarly, to the *Rp2h* DEL26/Y mice, western blot analysis of GRK1 expression in whole eye lysates demonstrated GRK1 was still expressed in *Rp2h* E135G/Y mice aged up to 9 months (Figure 3.9 G).

This is similar to the findings in the *Rp2h -/-* mouse in which loss of GRK1 immunostaining from the OS was observed but no reduction in protein levels was detected (Houbin Zhang et al. 2015). In *Rp2h* E135G/Y mice disruptions in GRK1 localisation occurred prior to any defect in photoreceptor function by ERG or change in histology. This suggests that in this mutant mislocalisation of GRK1 and likely other

lipid modified proteins could be a driver mechanism for retinal degeneration. However, in *Rp2h* DEL26/Y mice, loss of GRK1 localisation to the OS occurred age three months, the same stage mislocalisation of rhodopsin and thinning of the ONL was detected. Therefore, it is not possible to conclude which is a driver mechanism in this case and it is likely multiple mechanisms may drive retinal degeneration in *Rp2h* knockout mice.

Figure 3. 9 GRK1 Localisation in WT, *Rp2h* DEL26/Y and *Rp2h* E135G/Y Retinas

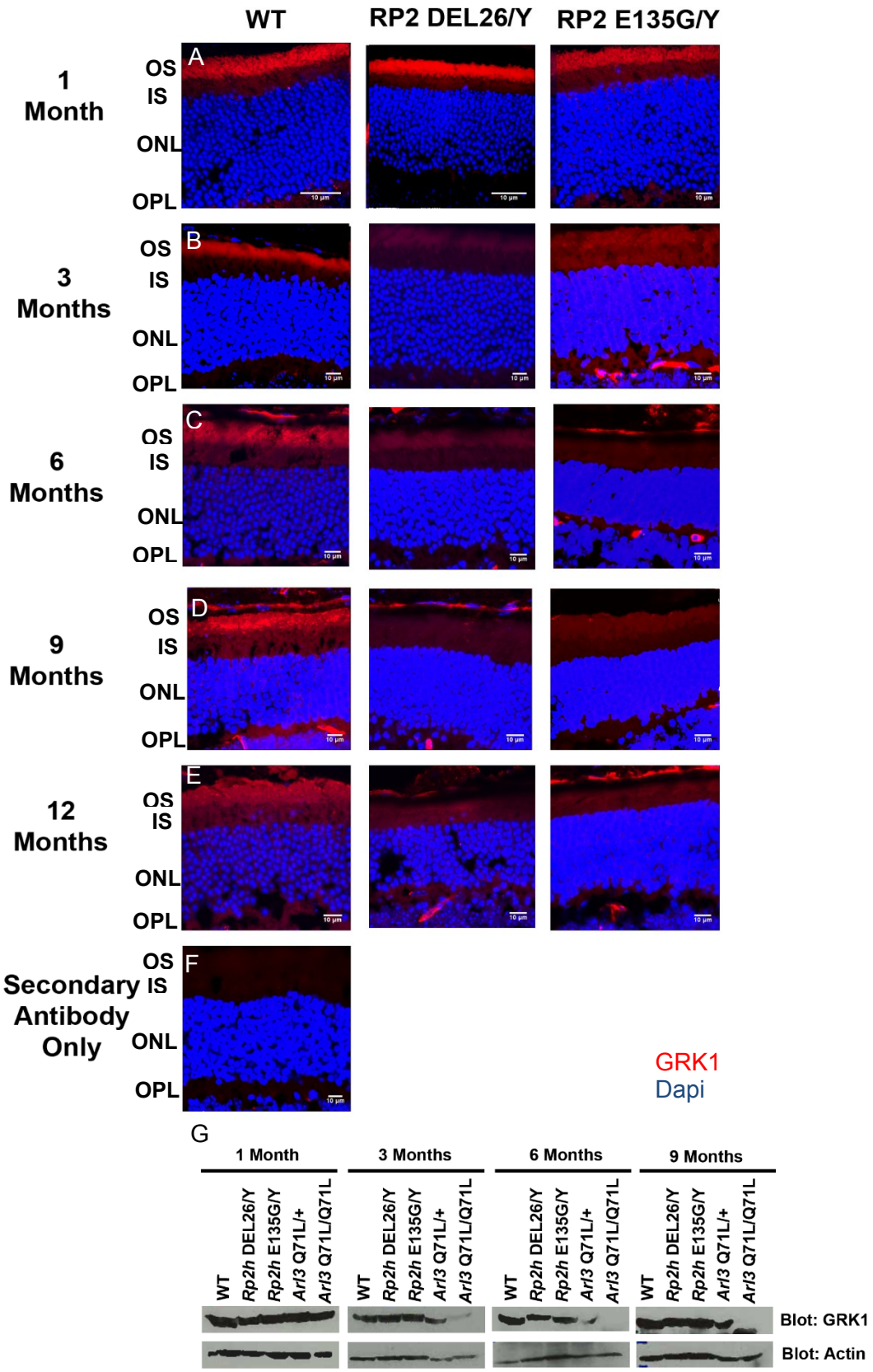

(A) GRK1 (red) staining in *Rp2h* WT, *Rp2h* DEL26/Y and *Rp2h* E135G/Y retinas aged 1 month. GRK1 staining was present in the OS of photoreceptors in WT, *Rp2h* DEL26/Y and *Rp2h* E135G/Y retinas.
(B) GRK1 staining in *Rp2h* WT, *Rp2h* DEL26/Y and *Rp2h* E135G/Y retinas aged 3 months. GRK1 staining was present in the OS of photoreceptors in WT retinas. *Rp2h* DEL26/Y retinas had reduced GRK1 staining compared to WT. *Rp2h* E135G/Y retinas had GRK1 staining present throughout the OS, IS, ONL, OPL of photoreceptors.
(C) GRK1 staining in *Rp2h* WT, *Rp2h* DEL26/Y and *Rp2h* E135G/Y retinas aged 6 months. In WT retinas, GRK1 was present in the OS of photoreceptors. *Rp2h* DEL26/Y and *Rp2h* E135G/Y retinas had reduced GRK1 staining compared to WT.
(D) GRK1 staining in *Rp2h* WT, *Rp2h* DEL26/Y and *Rp2h* E135G/Y retinas aged 9 months. *Rp2h* WT mice had GRK1 staining in the OS of photoreceptors. *Rp2h* DEL26/Y and *Rp2h* E135G/Y had reduced GRK1 staining compared to WT.
(E) GRK1 staining in *Rp2h* WT, *Rp2h* DEL26/Y and *Rp2h* E135G/Y retinas aged 12 months. *Rp2h* WT retinas had GRK1 staining in the OS of photoreceptors. *Rp2h* DEL26/Y and *Rp2h* E135G/Y retinas had reduced GRK1 staining compared to WT.
(F) Secondary antibody only control demonstrating that all samples with reduced GRK1 immunostaining had higher levels than the background staining.
(G) Western blot analysis of GRK1 expression in WT, *Rp2h* DEL26/Y, *Rp2h* E135G/Y, *Arl3* Q71L/+ and *Arl3* Q71L/Q71L aged 1-9 months. GRK1 expression was detected in all lysates aged one month. WT, *Rp2h* DEL26/Y and *Rp2h* E135G/Y lysates had GRK1 expression at all ages and the levels appeared unchanged compared to WT. Actin blots used as loading control.
Arl3 Q71L/+ and Arl3 Q71L/Q71L lysates discussed in Chapter 4

3.7 Discussion

3.7.1 *Rp2h* DEL26/Y and *Rp2h* E135G/Y mice have Progressive Retinal Degeneration

Analysis of histology of *Rp2h* DEL26/Y retinas and *Rp2h* E135G/Y retinas demonstrated differences observed from 3 months and 6 months of age respectively. The thinning of the ONL was not significant in every region measured even at late stages of retinal degeneration. In *Rp2h* DEL26/Y retinas thinning of the retina was firstly observed in peripheral regions in line with increased gliosis observed in peripheral regions at age one month. Rod photoreceptor cell density increases from the periphery of the retina to the centre of the retina however the ratio of photoreceptor to RPE cells is 2 fold higher in the central retina of the mouse than in the periphery (Volland et al. 2015) suggesting that peripheral photoreceptors may be more sensitive as there are less RPE cells present to support their survival. Alternatively, RP2 mutation may affect the function of the RPE cells and therefore effect the photoreceptors they support and peripheral photoreceptors supported by fewer RPE cells would be expected to be the most sensitive. Expression of RP2 was shown not to be photoreceptor specific, as in the aryl hydrocarbon receptor interacting protein like 1 knockout (*Aipl1-/-)* mouse which has no photoreceptors, expression of RP2 was not significantly reduced compared to WT retinas demonstrating RP2 is expressed in other retinal cell types and is not highly enriched in photoreceptors (Murphy et al. 2016). RP2 is also endogenously expressed in cultured human RPE cell lines (Wright et al. 2011). The regions where thinning of the ONL is not significant even at late stages may represent sectioning artefacts and to counteract this the number of nuclei present in the ONL could be calculated at specific distances from the ON and compared between *Rp2h* mutants and WT.

Analysis of ERG responses did not detect significant differences in photoreceptor response in *Rp2h* DEL26/Y mice until 6 months of age. However, differences in histology were detected at 3 months of age. Similarly, no difference in ERG response was detected in *Rp2h* E135G/Y mice aged 6 months despite subtle differences in ONL thickness detected at this age. The ERG responses recorded in mice were quite variable which may have reduced the sensitivity of the assay. The ISCEV (International Society for Clinical Electrophysiology of Vision) protocol runs several

tests to detect changes in rod and cone function however only the 3cd dark adapted ERG test and the 10cd light adapted ERG test gave consistent results in WT mice therefore other tests were not analysed. In order to reduce variability in the ERG response mutants were compared to WT ERGs recorded on the same day however to reduce this variation further and to allow the detection of smaller differences, ERGs could be repeated on more animals. *Rp2h* E135G/Y retinas did not exhibit any significant difference in 3cd ERG response, despite showing significant thinning of ONL and rhodopsin mislocalisation, however a significant reduction in cone A-wave amplitude at 9 months and 12 months of age was observed. Only 3% of all photoreceptors in mice are cones therefore the differences in histology observed are unlikely to be attributed to cone degeneration alone (Carter-Dawson and LaVail 1979). To detect smaller differences in rod responses a scotopic ERG program could be run on these mice which exposes mice to multiple low intensity flashes allowing detection of small defects in rod function. The ERG set up used for my study did not have this programme therefore this analysis was not carried out on *Rp2h* DEL26/Y and *Rp2h* E135G/Y mice.

3.7.2 Mislocalisation of M/L Opsin and Rhodopsin in *Rp2h* DEL26/Y and *Rp2h* E135G/Y Retinas

In the previously described *Rp2*^{null} mouse model mislocalisation of cone opsin was reported at age 1 month. In *Rp2h* DEL26/Y and *Rp2h* E135G/Y mutants no cone opsin mislocalisation was detected until 6 months and 9 months of age respectively. These differences may reflect the differences in the technique used to generate the mice as one was generated using the cre lox system and the other generated using CRISPR genome editing. Reduced M/L opsin staining was observed in *Rp2h* DEL26/Y and *Rp2h* E135G/Y mutants from age 9 months and 12 months of age, which may reflect loss of cone photoreceptors as retinal degeneration progresses however the number of cones was not counted in this experiment and a retinal whole mount section could be used to answer this question directly.

Cone opsin trafficking to the OS is thought to occur through intraflagellar transport (IFT) mediated by the heterotrimeric kinesin II motor complex containing kinesin family member 3a (Kif3a), kinesin family member 3b (Kif3b) or kinesin family member 3c (Kif3c) and kinesin associated protein 3 (KAP3) subunits (Takeda et al. 1999). A cone specific knockout for *Kif3a* demonstrated that cones developed normally however by

p30 no photopic ERG responses were recorded and M/L opsin was absent from the cone OS and mislocalised to the IS, axons and synaptic pedicles (Avasthi et al. 2009). A *Kif17* knockout zebrafish demonstrated that Kif17 was required for OS formation and for cone opsin trafficking as extensive mislocalisation of cone opsin to the cone photoreceptor cell body and synaptic region was detected (Insinna et al. 2008) however a *Kif17* null mouse demonstrated *Kif17* is not required for M/L opsin trafficking (Jiang et al. 2015). Recently it has been shown that RP2 and ARL3 can interact with KIF17 and that knockdown of RP2 or ARL3 disrupted KIF17 localisation in cells (Schwarz et al. 2017) suggesting RP2 and ARL3 could mediate cone opsin trafficking through interaction with KIF17 in cells. Although KIF17 is not thought to be required for the trafficking of M/L opsin in mice (Jiang et al. 2015), the localisation of KIF17 could be tested in *Rp2h* DEL26/Y and *Rp2h* E135G/Y retina sections to determine whether KIF17 is mislocalised and whether this may explain why M/L opsin is mislocalised.

In *Rp2h* DEL26/Y and *Rp2h* E135G/Y mutants rhodopsin was mislocalised throughout the IS, ONL and synaptic layer demonstrating loss of OS targeting as a consequence of RP2 dysfunction. At some stages the levels of rhodopsin appeared reduced in mutant compared to WT however the protein levels of rhodopsin were not examined. The other major gene which causes X-linked Retinitis Pigmentosa (XLRP) is Retinitis Pigmentosa GTPase Regulator (RPGR) and the *Rpgr* knockout mouse demonstrated mislocalisation of cone opsin and reduced rhodopsin expression suggesting that the trafficking of M/L opsin and rhodopsin may be key pathways affected in XLRP (Hong et al. 2000).

Mislocalisation of rhodopsin was not described in either previously published *Rp2h* knockout mouse (Li et al. 2013; Zhang et al. 2015) but mutations in the C-tail of rhodopsin, which control its localisation cause autosomal dominant Retinitis Pigmentosa (ADRP) in humans (Berson et al. 2002). Rhodopsin is trafficked from the Golgi in rhodopsin laden vesicles to the IS (Papermaster et al. 1986). The sorting of rhodopsin into these vesicles has been shown to require the small GTPase ARF4 which interacts specifically with the C-terminal tail of rhodopsin (Deretic et al. 2005). The docking of these vesicles has been shown to involve another small GTPase rab8, demonstrating small GTPases may play an essential role in rhodopsin trafficking (Moritz et al. 2001) however knockout of both *Arf4* and *Rab8* in mice had no effect on rhodopsin localisation (Sato et al. 2014; Pearring et al. 2017) demonstrating the exact

mechanisms which regulate rhodopsin trafficking to the OS *in vivo* are not well understood. After docking at the IS rhodopsin was shown to be trafficked to the OS by IFT, involving the subunit of kinesin 2, KIF3a and intraflagellar transport protein 88 (IFT88), as knockouts of these genes in mice caused mislocalisation of rhodopsin (Jimeno et al. 2006; Pazour et al. 2002). Although no direct interaction between RP2 and IFT88 has been detected it is possible that RP2 could still function in this pathway as it has been reported that a retinal specific knockout of *Arl3* has a similar phenotype to *Kif3a* and *Ift88* knockout mice (Hanke-Gogokhia et al. 2016; Jimeno et al. 2006; Pazour et al. 2002).

3.7.3 Mislocalisation of GRK1 in *Rp2h* DEL26/Y and *Rp2h* E135G/Y Retinas

Mislocalisation of GRK1 was detected in the *Rp2h -/-* mouse however in this mouse mislocalisation of cone GRK1 was observed from one month of age but in *Rp2h* DEL26/Y and *Rp2h* E135G/Y mice changes in GRK1 localisation was not observed until 3 months of age (Zhang et al. 2015). This difference likely reflects differences in the progression of retinal degeneration as in the *Rp2h -/-* mouse differences in ERG response were detected from 1 month of age however differences in ERG response in *Rp2h* DEL26/Y and *Rp2h* E135G/Y mice were only detected in older animals (Houbin Zhang et al. 2015). GRK1 is thought to be trafficked to the photoreceptor OS by the photoreceptor chaperone PDE6δ, RP2 and ARL3 (Zhang et al. 2007; Zhang et al. 2015; F. Liu et al. 2015). Therefore, mislocalisation of GRK1 in *Rp2h* DEL26/Y and *Rp2h* E135G/Y mice suggests that disruption of RP2 function causes an increase in ARL3-GTP levels and aberrant regulation of PDE6δ. In order to confirm that knockout or mutation of RP2 causes mislocalisation of other lipid modified proteins by affecting the function of PDE6δ, through increased levels of ARL3-GTP, the localisation of PDE6 could be examined as it has also been shown to be trafficked to the OS by PDE6δ (Zhang et al. 2007). RP2 and ARL3 have also been shown to interact with the other identified photoreceptor chaperone Uncoordinated 119 (UNC119) which controls the localisation of transducin α and nephrocystin 3 (NPHP3) (Veltel, Kravchenko, et al. 2008; Zhang et al. 2011). Mislocalisation of transducin α or NPHP3 was not detected in either previously published *Rp2h* knockout mouse suggesting compensatory mechanisms may exist to regulate the trafficking of proteins in the absence of RP2 (Li et al. 2013; Zhang et al. 2015). It was suggested that transducin α may still traffic to the OS in the absence of RP2 through rhodopsin transport vesicles

(Zhang et al. 2015), therefore as rhodopsin is mislocalised in *Rp2h* DEL26/Y and *Rp2h* E135G/Y mice it is possible localisation of transducin α is also affected. RP2 and ARL3 have also been shown to regulate the trafficking of the beta subunit of transducin (Gβ1) by controlling loading of Gβ1 to Rab11 vesicles suggesting RP2 and ARL3 may regulate trafficking to the OS through vesicular transport as well as through PDE6δ and UNC119 (Schwarz et al. 2012). If localisation of lipid modified proteins to the OS is exclusively controlled by RP2 and levels of ARL3-GTP then *Rp2h* E135G/Y mice should phenocopy *Rp2h* knockout, however in *Rp2h* E135G/Y retinas GRK1 localisation was affected at a later stage than in the *Rp2h* DEL26/Y suggesting other functions of RP2 independent of ARL3 are also important for proper localisation of GRK1 and potentially other lipid modified proteins or that RP2 E135G may have partial GAP activity for ARL3, and that this may facilitate localisation of GRK1 at the OS temporarily despite the assumed increase in levels of ARL3-GTP.

3.7.4 Effects Independent of ARL3

The RP2 E135G mutation is predicted to reduce RP2's affinity for ARL3 150 fold compared to WT however, another patient pathogenic mutation, R118H, reduces RP2's affinity for ARL3 300 fold (Kühnel et al. 2006). As these predictions have been carried out *in vitro* it is possible that *in vivo* additional mechanisms exist and RP2 E135G could still have partial GAP activity meaning that the E135G mutation is hypomorphic which may explain why *Rp2h* E135G/Y do not have a severe phenotype. Previous studies have demonstrated that RP2 can interact with NSF however RP2 E135G does not interact with NSF (Holopainen et al. 2010). This suggests that the effects observed in my study may not be solely attributed to loss of ARL3-GAP activity and may also be attributed to loss of interaction with NSF. Arrestin-1 has been shown to interact with NSF in the photoreceptor synapse where NSF and the SNARE complex regulate synaptic transmissions (S.P. Huang, Brown, and Craft 2010). Arrestin-1 was shown to increase SNARE complex disassembly by increasing the GTPase activity of NSF, demonstrating NSF plays a functional role in the photoreceptor. Although mutations in *Arr1* have been shown to be causative of a rare form of CSNB (Congenital Stationary Night Blindness), Oguchi disease, and RP (Fuchs et al. 1995; Nakawaza et al. 1997) no direct link between NSF and retinal degeneration has been established.

ARL2 also interacts with PDE6δ and UNC119 and can stimulate cargo release from these proteins however it has been shown that ARL2 can stimulate release of cargo bound with low affinity however only ARL3 can release cargo bound with high affinity (Ismail et al. 2011). Recently a transgenic model was generated which expressed ARL2-Q70L under the rhodopsin promoter, $Rod^{ARL2Q70L}$, this mouse displayed progressive rod degeneration and interestingly unlike the $Rod^{ARL3\text{-}Q71L}$ transgenic model this mouse displayed normal localisation of prenylated OS proteins but had mislocalised rhodopsin (Wright et.al 2018) suggesting ARL2 plays a role in rhodopsin trafficking. The shared phenotype of rhodopsin mistrafficking between $Rod^{ARL2Q70L}$ mice and *Rp2h* DEL26/Y and *Rp2h* E135G/Y mice may suggest RP2 mutation may cause dysregulation of ARL2 leading to rhodopsin mislocalisation, however RP2 has been only been identified as a GAP for ARL3 not ARL2 therefore the potential link RP2 and ARL2 requires further investigation. If mutation of RP2 also disrupted the function of ARL2 causing rhodopsin mistrafficking then mice carrying *Arl3* Q71L would not be expected to display this phenotype however as discussed in chapter 4 *Arl3* Q71L mice do display rhodopsin trafficking defects (see figure 4.9) suggesting mutation of *Rp2h* may cause rhodopsin mistrafficking through increased levels of ARL3-GTP or other mechanisms but this effect is not specific to ARL2.

3.7.5 Discrepancies Between Previously Published *RP2* Knockout Animal Models

The two previously generated *Rp2h* knockout mice have differential phenotypes and suggest different mechanisms that cause retinal degeneration when *RP2* is mutated. The first RP2 knockout mouse was generated by the cre-lox system and displayed early M/L opsin mislocalisation and reduced photopic ERG responses from 1 month of age and reduced scotopic ERG responses at 4 months of age. When analysing which proteins were mislocalised in the $Rp2^{null}$ mice the authors examined localisation of M/L opsin, rhodopsin, transducin subunits and arrestin alongside the localisation of NPHP3 and ARL3 (Li et al. 2013). No mislocalisation of transducin subunits, arrestin or rhodopsin was reported (Li et al. 2013). NPHP3 is reportedly trafficked by RP2, ARL3 and UNC119 however no defect in trafficking NPHP3 was observed suggesting that mislocalisation of M/L opsin was the defect which was causative of retinal degeneration (Li et al. 2013). In this model the localisation of GRK1 and PDE6 which are trafficked by PDE6δ was not investigated therefore these mice could display

mislocalisation of these OS proteins which may also contribute to retinal degeneration. The second *Rp2h* knockout mouse, *Rp2h* -/-, was generated via a gene trap cassette and displayed normal localisation of M/L opsin with mislocalisation of GRK1 and PDE6 (Zhang et al. 2015) a phenotype which was also observed in the *rp2* knockout zebrafish (Liu et al. 2015). As discussed, this suggests a mechanism of retinal degeneration by which increased levels of ARL3-GTP stimulates release of cargo from PDE6 in regions outside the OS. Both models used C57BL6/J as the background strain so the differences are not due to genetic background but they may be due to how the mice were generated. The *Rp2h* -/- mouse was generated by targeting the first intron of the *Rp2h* gene (Zhang et al. 2015) however the *Rp2*^{null} mouse was generated by targeting exon 2 of the *Rp2h* (Li et al. 2013) gene it is possible in this case a small truncated protein may remain which is not detected by the RP2 antibody and this therefore may explain the differences between the previously published models. *Rp2h* DEL26/Y mice were generated using CRIPSR cas9 and gRNA injection into an embryo at the single cell stage therefore in theory every cell in the mouse produced from this procedure should carry the *Rp2h* DEL26 mutation. These mice were also generated on a C57BL6/J background so background strain does not explain the differences in phenotype observed between *Rp2h* DEL26/Y and other published *Rp2h* knockout mice. Mice were outbred for multiple generations and only mice from at least the F2 generation were used as experimental animals to decrease the chance that any phenotypes were attributed to off-target effects and not *Rp2h* deletion. Interestingly *Rp2h* DEL26/Y mice displayed features associated with both the previously generated *Rp2h* knockout mouse models with mislocalisation of GRK1 and M/L opsin suggesting each of these phenotypes does occur as a result of *Rp2h* knockout, therefore differences observed between models may be the result of different techniques used to generate each model.

3.8 Conclusions

In this chapter, I demonstrated that CRISPR genome editing successfully generated a *Rp2h* knockout mouse and a mouse carrying the *Rp2h* E135G/Y mutation. These mice had a late onset progressive retinal degeneration with the *Rp2h* DEL26/Y mouse more severely affected than the *Rp2h* E135G/Y mouse as shown by the increased rate of ONL thinning and reduction of both rod and cone photoreceptor ERG responses. *Rp2h* DEL26/Y mice had mislocalisation of rhodopsin and loss of GRK1

OS localisation aged three months prior to major loss of photoreceptors suggesting both these mechanisms may be driving retinal degeneration in these mice. *Rp2h* E135G/Y mice had mislocalisation of GRK1 at age 3 months and mislocalisation of rhodopsin did not occur until 6 months of age suggesting that in these mice mislocalisation of lipid-modified proteins may be the driver mechanism. Both *Rp2h* DEL26/Y and *Rp2h* E135G/Y mice had mislocalisation of M/L opsin as retinal degeneration progressed suggesting a role for RP2 and ARL3 in the trafficking of M/L opsins. Overall *Rp2h* E135G/Y mice had less severe retinal degeneration and later mislocalisation of OS proteins than *Rp2h* DEL26/Y mice demonstrating that loss of ARL3 GAP activity is not equivalent to loss of RP2 expression suggesting RP2 may have other roles independent of ARL3 which are important for trafficking OS proteins in photoreceptors and may contribute to disease pathogenesis in patients.

Chapter 4

Phenotype Analysis of Arl3 Q71L/+ and Arl3 Q71L/71L Mice

Chapter 4: Phenotype Analysis of *Arl3* Q71L/+ and *Arl3* Q71L/Q71L Mice

4.1 Introduction

Arf-like 3 (ARL3) is a small GTPase that is regulated by its GTPase Activating Protein (GAP) RP2 and its guanine nucleotide exchange factor (GEF) ARL13B. ARL3 is enriched in primary cilia in cell culture systems and is expressed at the connecting cilia (CC) in the human retina (Enjalbert et al. 2006; Avidor-Reiss et al. 2004; Grayson et al. 2002). An *Arl3* -/- mouse was generated and displayed a severe ciliopathy like phenotype further supporting a role for ARL3 in cilia function (Schrick et al. 2006). A role for ARL3 in the trafficking of cilia proteins was elucidating by studying the mechanism by which chaperone proteins phosphodiesterase 6δ (PDE6δ) and uncoordinated 119 (UNC119) traffic proteins from the cytoplasm to the cilia. It was demonstrated that ARL3-GTP localised within the cilia facilitated cargo release from these chaperones. The *Rp2h* -/- mouse displayed mislocalisation of G- coupled receptor kinase 1 (GRK1) and phosphodiesterase 6 (PDE6) and as these proteins are thought to be trafficked to the OS by PDE6δ it was hypothesised that increased levels of ARL3-GTP were present as *Rp2h* was knocked out and therefore this was able to stimulate release of cargo from PDE6δ and UNC119 outside the CC and outer segment (OS) leading to mistrafficking of OS proteins and ultimately cell death. As this is thought to model the disease mechanism which occurs in human X-linked Retinitis Pigmentosa (XLRP) patients with *RP2* mutations an understanding of the consequences of increased levels of ARL3-GTP in the retina is essential for understanding disease pathogenesis in patients.

In order to access the effect of increased levels of ARL3-GTP in photoreceptors a mouse expressing constitutively active ARL3, ARL3 Q71L, under the rhodopsin promoter was generated (Z. C. Wright et al. 2016). ARL3 Q71L was FLAG and HA tagged at it's C-terminus and was overexpressed compared to the WT locus (Z. C. Wright et al. 2016). $Rod^{ARL3Q71L}$ retinas developed normally however subtle defects in the OS were detected at PN20 with severely reduced ERG responses and photoreceptor death evident from PN70. GRK1 was lost from the rod OS, fully assembled PDE6 (PDE6αβγ) and transducin γ accumulated in endosomal structures

within the IS. Retinal lysates from these mice were used to show that ARL3^{Q71L} is able to sequester PDE6δ in vivo demonstrating that proteins are likely mislocalised in these mice due to ARL3-GTP locking PDE6δ in the closed conformation (Z. C. Wright et al. 2016). This phenomenon is thought to be identical to that that which occurs in mice where *Rp2h* expression is knocked out, however Rod^{ARL3Q71L} mice do not phenocopy previously described *Rp2h* knockout mice. *Rp2h* -/- mice generated by a gene trap cassette showed progressive rod/cone dystrophy with little difference in ONL thickness even at 2 years of age (Houbin Zhang et al. 2015). However, similar to Rod^{ARL3Q71L} mice, mislocalisation of GRK1 and PDE6 was detected (Houbin Zhang et al. 2015). The protein levels of GRK1 were not reduced in *Rp2h* -/- mice however a reduction of GRK1 protein levels was reported in Rod^{ARL3Q71L} mice (Zhang et al. 2015; Wright et al. 2016). A second *Rp2h* knockout mouse, *Rp2^{null},* generated using the Cre/lox system also did not phenocopy the Rod^{ARL3Q71L} mouse. The *Rp2^{null}* mouse had thinning of the ONL present from 5 months of age and had early mislocalisation of M/L opsin. No mislocalisation of the lipid modified proteins investigated was reported, suggesting that mislocalisation of lipid modified proteins due to increased levels of ARL3-GTP may not be the only mechanism which drives retinal degeneration in mice deficient of RP2 (Li et al. 2013).

These studies provide evidence for the role of ARL3-GTP in the trafficking of specifically GRK1 and PDE6 to the outer segments of photoreceptors. The differences observed between the *Rp2h*-/- mice and the Rod^{ARL3Q71L} mice may be attributed to the fact that ARL3 Q71L was expressed from the rhodopsin promoter and therefore only expressed in rods and at a level much higher than the endogenous locus (Wright et al. 2016). The expression of ARL3 Q71L appeared 2.5x higher than the endogenous locus by western blot but as the rhodopsin promoter is a very strong promoter it is possible that ARL3 Q71L is expressed much higher and then degraded. Interestingly it appears that RP2 may have specific functions in cones demonstrated by mislocalisation of cone opsins in *Rp2^{null}* mice (Li et al. 2013). Therefore, to address this discrepancy in the field and to establish the effects of ARL3 Q71L in the retina, CRISPR genome editing was used to generate an endogenous knock in of the Q71L gain-of-function mutation into the endogenous *Arl3* gene. This approach was designed to overcome issues associated with overexpression and to provide a more accurate model to compare to RP2 knockout mice in order to establish if increased levels of ARL3-GTP may be the major defect driving retinal degeneration.

4.2 *Arl3* Q71L/+ and *Arl3* Q71L/Q71L mice have Progressive Retinal Degeneration

4.2.1 ARL3 Q71L is Stable and Leads to Increased ARL3-GTP Levels in Tissues

In order to generate mice carrying the *Arl3* Q71L mutation a single guide RNA, conventional cas9 mRNA and a repair template designed to introduce the Q71L mutation were injected by cytosolic injection into C57BL6/J single cell embryos (see 2.1.2 for detailed methods and sequences of guide RNAs and the repair template). F0 founder animals were outbred with C57BL6/J animals to generate F1 Q71L/+ mice which were used to establish the line. The line was maintained by crossing *Arl3* Q71L/+ mice to C57BL6/J control animals. F2 Q71L/+ mice were mated together to generate Q71L/Q71L mice. Q71L/+ x Q71L/+ mating's only involved mice derived from different parents to avoid inbreeding of the colony. In order to ensure any phenotypes detected were attributed to the *Arl3* Q71L mutation and not off target effects from the CRISPR cas9 process only mice derived from at least the F2 generation were used in experiments. Only male *Arl3* Q71L+ and *Arl3* Q71L/Q71L mice were used as experimental animals to enable the most accurate comparison to *Rp2h* DEL26/Y and *Rp2h* E135G/Y mice. The distribution of male and female WT, *Arl3* Q71L/+ and *Arl3* Q71L/Q71L mice that survived to genotyping is shown in Table 4.1. Chi squared analysis demonstrated genotypes were detected at a Mendelian 1:2:1 ratio with no difference in the number of mice born to each genotype in males and females (Table 4.1).

To confirm that the *Arl3* Q71L mutation introduced by CRISPR genome editing (Figure 4.1 A) did not affect ARL3 protein expression, a western blot for ARL3 was performed. ARL3 expression was confirmed in WT, *Arl3* Q71L/+ and *Arl3* Q71L/Q71L kidney lysates. Levels of ARL3 expression were comparable in WT, *Arl3* Q71L/+ and *Arl3* Q71L/Q71L samples demonstrating that ARL3 Q71L was does not affect ARL3 expression (Figure 4.1 B). ARL3 expression was then analysed in whole eye lysates from WT, *Rp2h* DEL26/Y, *Rp2h* E135G/Y, *Arl3* Q71L/+ and *Arl3* Q71L/Q71L mice. ARL3 expression was detected in all lysates at levels comparable to WT confirming that the Q71L mutation does not affect stability of the protein. ARL3 was expressed at low levels in the eye and was only detectable using Femto ECL (Figure 4.1 C).

After establishing, that ARL3 Q71L was expressed and tolerated in tissues an assay was designed to determine whether expression of ARL3 Q71L increased the levels of ARL3-GTP *in vivo*. RP2 only interacts with ARL3 when it is in the GTP bound state, therefore GST-tagged RP2 recombinant protein and glutathione beads were used to isolate ARL3-GTP. Firstly, this assay was performed on kidney lysates as a large quantity of protein can be extracted from kidneys. As expected ARL3-GTP was not detected in WT lysates as at any one time, only a very small percentage of ARL3 in cells is likely in the active GTP-bound state*. Arl3* Q71L/+ and *Arl3* Q71L/Q17L lysates displayed an enrichment of ARL3-GTP in the RP2-GST lanes (+) and not in the lanes where no RP2-GST was added (-) demonstrating increased levels of ARL3-GTP were present in these lysates and that ARL3-GTP specifically interacted with RP2 and not glutathione beads (Figure 4.2 A). After demonstrating that this assay was able to isolate ARL3-GTP, the levels of ARL3-GTP in whole eye lysates from WT, *Rp2h* DEL26/Y, *Rp2h* E135G/Y, *Arl3* Q71L/+ and *Arl3* Q71L/Q71L mice were analysed. In WT lysates, no enrichment of ARL3-GTP was detectable reflecting the low level of ARL3-GTP that exists at any one time in the eye. *Arl3* Q71L/+ and *Arl3* Q71L/Q71L lysates again displayed enrichment of ARL3-GTP in the RP2- GST (+) lanes and not the lanes where no RP2-GST was added (-). *Arl3* Q71L/+ lysates had roughly half the levels of ARL3-GTP than the *Arl3* Q71L/Q71L lysates demonstrating each allele contributed to levels of ARL3-GTP. Interestingly, *Rp2h* DEL26/Y and *Rp2h* E135G/Y did not have any detectable increase in levels of ARL3-GTP compared to WT demonstrating that expression of ARL3 Q71L increases levels of ARL3-GTP substantially more than loss of GAP activity due to knockout or mutation of RP2 (Figure 4.2 B).

Figure 4. 1 ARL3 Q71L is Stable *in vivo*

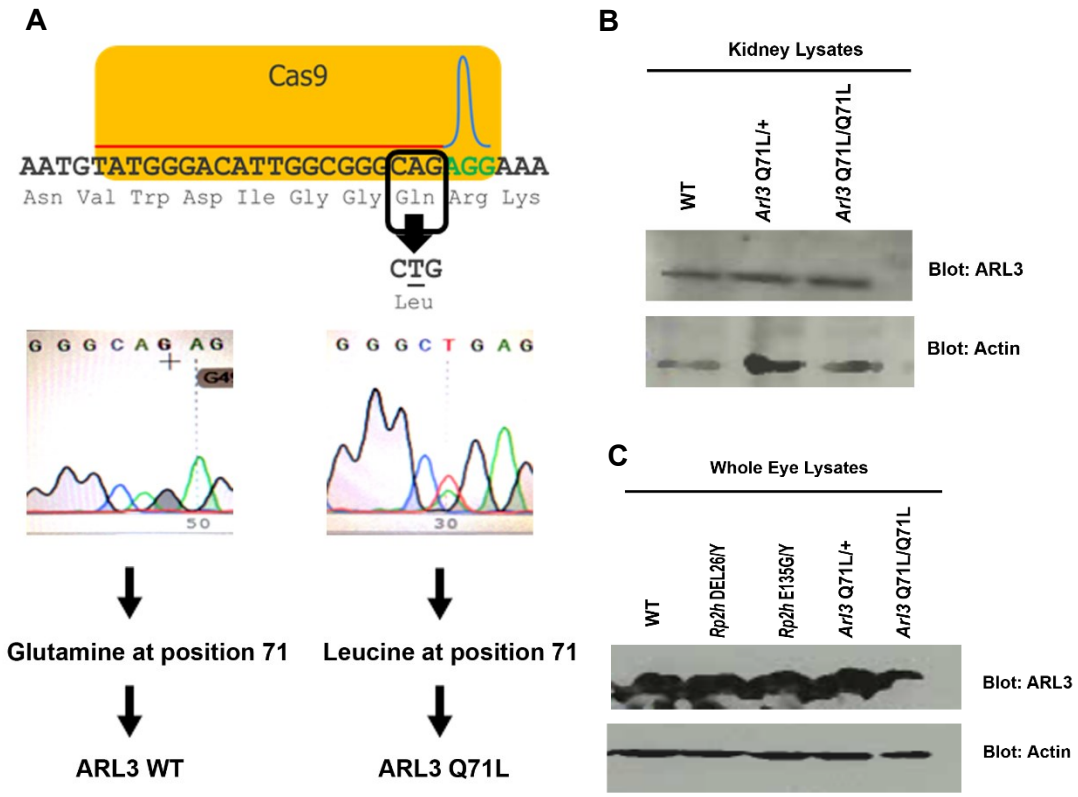

(A) Schematic of ARL3 Q71L mutation introduced by CRISPR genome editing.
(B) Western blot analysis of ARL3 expression in WT, *Arl3* Q71L/+ and *Arl3* Q71L/Q71L kidney lysates. ARL3 expression was detected in WT, *Arl3* Q71L/+ and *Arl3* Q71L/Q71L lysates. Actin blot used as a loading control.
(C) Western blot analysis of ARL3 expression in WT, *Rp2h* DEL26/Y, *Rp2h* E135G/Y, *Arl3* Q71L/+, *Arl3* Q71L/Q71L whole eye lysates. ARL3 expression was detected in all lysates. Expression of ARL3 was only detectable using ECL Femto. Actin used as loading control.

Table 4. 1 Distribution of Arl3 WT, Arl3 Q71L/+ and Arl3 Q71L/Q71L Mice

Sex	WT	Q71L/+	Q71L/Q71L
Male	32	48	27
Female	25	47	16
Male ratio	1.19	1.79	1.01
Female ratio	1.14	2.13	0.73
T.Test Males v Females	0.15	0.46	0.07

Arl3 line sex and allele ratios. χ^2 values: males = 1.59 Females = 2.26 (2 degrees of freedom critical value for significance <0.05 = 5.59 so distribution fits Mendelian 1:2:1 ratio for males and females). No significant difference in the number of male vs female WT, Q71L/+ or Q71L/Q71L animals were born, statistics calculated by students T.Test.

Figure 4. 2 Expression of ARL3-GTP causes Increased Levels of ARL3-GTP *in vivo*

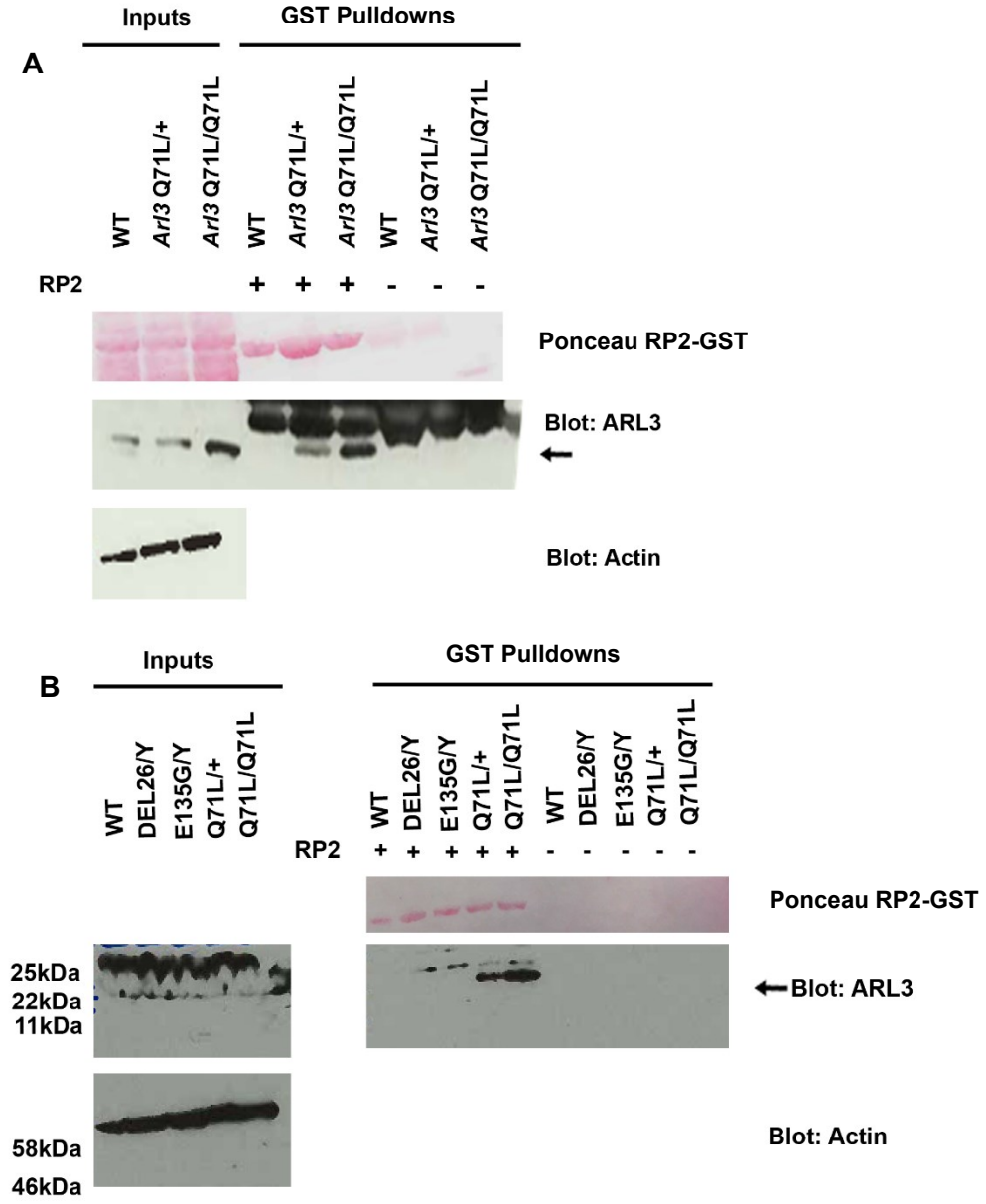

(A) RP2-GST was used to pulldown ARL3-GTP from kidney lysates. ARL3 was detected in only the *Arl3* Q71L/+ and *Arl3* Q71L/Q71L RP2-GST (+) lanes and not the no RP2-GST (-) lanes demonstrating ARL3-GTP specifically interacts with RP2 recombinant protein and not the glutathione beads. No ARL3-GTP was detectable in WT lysates. ARL3 was detected in input samples. Actin used as loading control.

(B) RP2-GST pulldown in WT, *Rp2h* DEL26/Y, *Rp2h* E135G/Y, *Arl3* Q71L/+, *Arl3* Q71L/Q71L whole eye lysates. ARL3-GTP was detected in *Arl3* Q71L/+ and *Arl3* Q71L/Q71L RP2-GST (+) lanes and not in no RP2-GST (-) lanes. No ARL3-GTP was detected in WT, *Rp2h* DEL26/Y and *RP2h* E135G/Y RP2-GST lanes. ARL3 was detected in input samples. Actin used as loading control.

4.2.2 Histological Analysis of *Arl3* Q71L/+ and *Arl3* Q71L/Q71L Retinas

In order to establish whether *Arl3* Q71L/+ and *Arl3* Q71L/Q71L retinas exhibit retinal degeneration paraffin sections were stained with haematoxylin and eosin and the histology analysed. Retinas were prepared in an identical fashion to *Rp2h* retinas (as described (3.2.2), see 2.1.4 for detailed methods). Retina sections were analysed from mice aged 1 month, 3 months, 6 months, 9 months and 12 months as described in 3.2.2. At 1 month and 3 months of age *Arl3* Q71L/+ retinas were comparable to WT retinas and no significant difference in ONL thickness was detected (Figure 4.3 A, B, Figure 4.4 A (i), (ii)). At 6 months of age *Arl3* Q71L/+ had thinning of the ONL in central regions (Figure 4.3 C, Figure 4.4 A (iii)). At 9 months of age *Arl3* Q71L/+ retinas were thinner than WT, and significant thinning of the ONL was measured across the retina (Figure 4.3 D, Figure 4.4 A (iv)). By 12 months of age *Arl3* Q71L/+ retinas were thinner than WT retinas and significant thinning of the ONL was observed in inner, central and peripheral regions (Figure 4.3 E, Figure 4.4. A (v)) demonstrating expression of *Arl3* Q71L acts as dominant allele causing retinal degeneration.

Arl3 Q71L/Q71L retinas were comparable to WT retinas at age 1 month and 3 months however significant thinning of the ONL was detected in peripheral regions (Figure 4.3 A, B Figure 4.4 A (i), (ii)). At 6 months of age *Arl3* Q71L/Q71L retinas did appear thinner than WT and thinning of the ONL was evident in inner, central and peripheral regions (Figure 4.3 C, Figure 4.4 A (iii)). By 9 months and 12 months of age *Arl3* Q71L/Q71L retinas appeared significantly thinner than WT and thinning of the ONL was detected across the retina (Figure 4.3 D, E, Figure 4.4 A (iv), (v)). *Arl3* Q71L/Q71L retinas were thinner than *Arl3* Q71L/+ retinas at age 9 months and 12 months and increased thinning of the ONL was observed (Figure 4.3 D, E, Figure 4.4 A (iv), (v)). The ONL thickness was reduced in some regions at 1 month of age in *Arl3* Q71L/Q71L retinas and was thinner than *Arl3* Q71L/+ retinas at every age examined demonstrating that *Arl3* Q71L/Q71L retinas exhibit more severe degeneration than *Arl3* Q71L/+ retinas, likely due to increased levels of ARL3-GTP (Figure 4.3, Figure 4.4 A). Progressive thinning of the INL was not detected in *Arl3* Q71L/+ or *Arl3* Q71L/Q71L retinas demonstrating retinal degeneration was specific to the photoreceptor layer (Figure 4.4 B (i-v)). However, the INL was found to be thinner in some regions in older *Arl3* Q71L/+ and *Arl3* Q71L/Q71L retinas (Figure 4.4 B (iv), (v)).

This may represent sectioning artefacts or thinning of the entire retina as retinal degeneration becomes more severe in older mice.

Figure 4. 3 Histological Analysis of *Arl3* WT, *Arl3* Q71L/+ and *Arl3* Q71L/Q71L Retinas

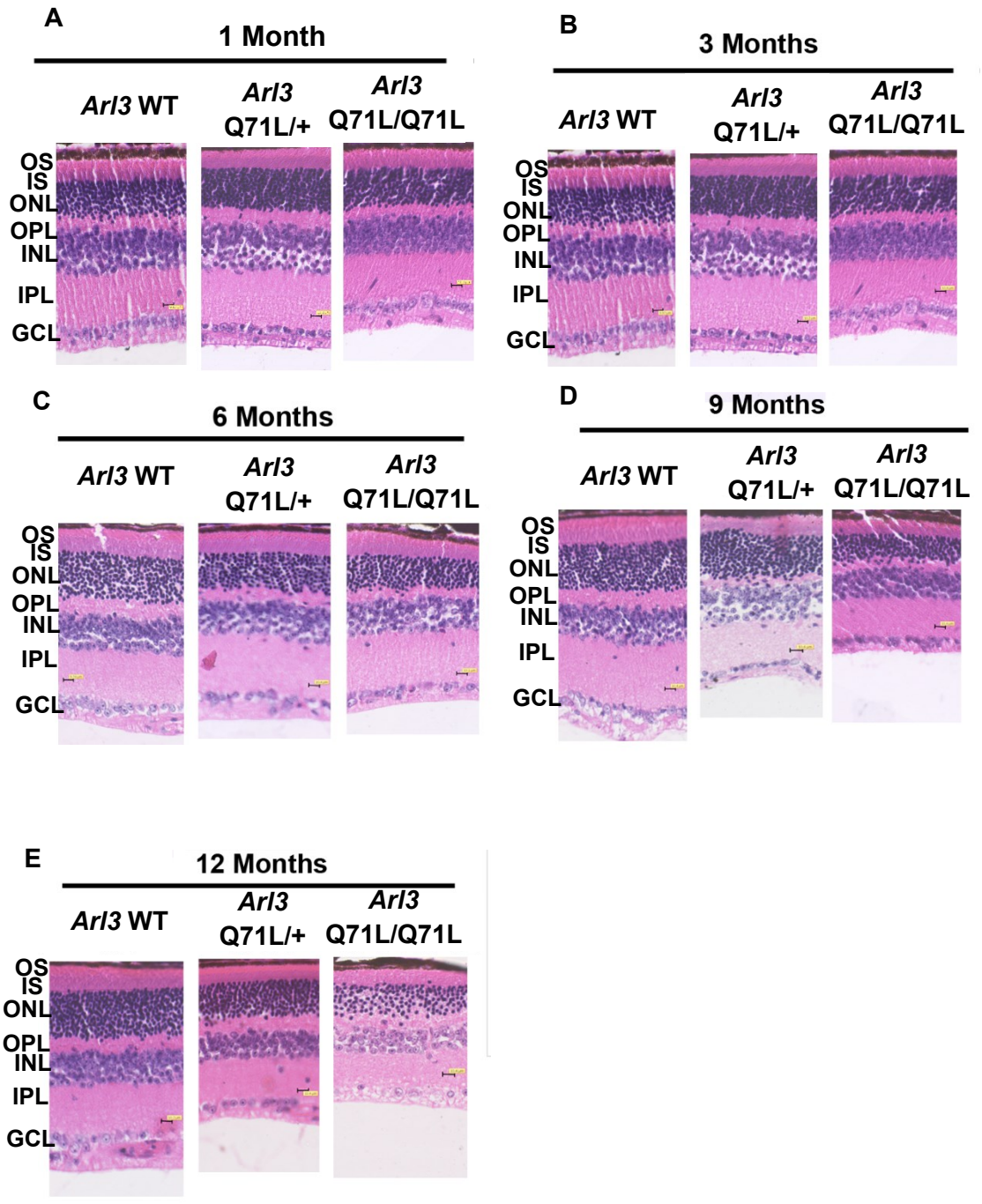

H&E staining of paraffin sections of *Rp2h* WT, *Arl3* Q71L/+ and *Arl3* Q71L/Q71L retinas. Aged 1 month (A), 3 months (B), 6 months (C), 9 months (D) and 12 months (E). Thinning of the retina was apparent from 3 month of age in *Arl3* Q71L/Q71L retinas and 6 months of age in *Arl3* Q71L/+ retinas.

Figure 4. 4 Quantification of ONL and INL in *Arl3* Q71L/+ and *Arl3* Q71L/Q71L Retinas

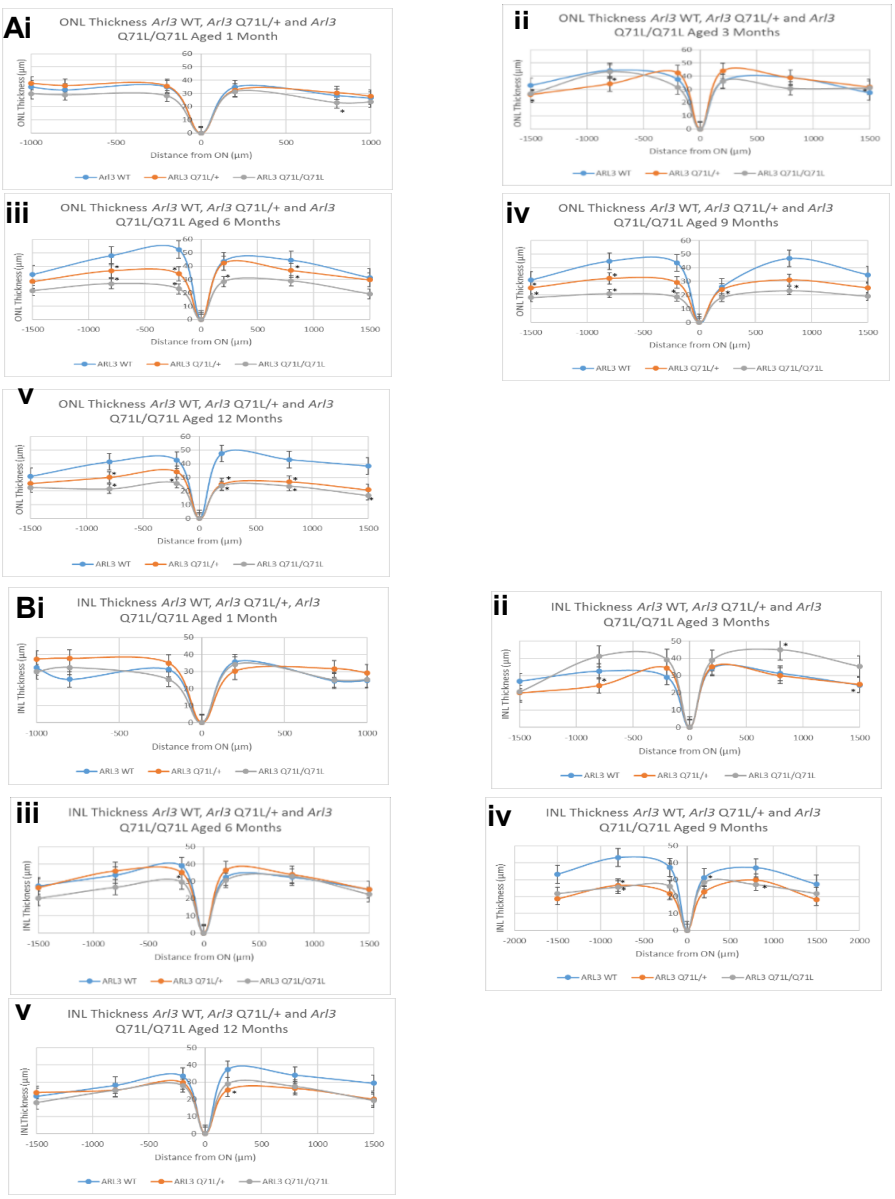

(A) ONL thickness measurements at specific distances from ON in WT, *Arl3* Q71L/+ and *Arl3* Q71L/Q71L retinas aged 1 month (i), 3 months (ii), 6 months (iii), 9 months (iv) and 12 months (v). Significant reductions in ONL thickness was present in *Arl3* Q71L/+ retinas from 6- 12 months. Significant reduction in ONL thickness was present in *Arl3* Q71L/Q71L retinas at 1 month in peripheral regions and 3 -12 months across the retina.

(B) INL thickness measurements at specific distances from the ON in WT, *Arl3* Q71L/+ and *Arl3* Q71L/Q71L retinas ages 1 month (i), 3 months (ii), 6 months (iii), 9 months (iv) and 12 months (v). INL thickness is not significantly different from WT in *Arl3* Q71L/+ and *Arl3* Q71L/Q71L. At 9 months of age some significant differences were observed however these may reflect sectioning artefacts.

n=3 mice analysed for each genotype at each age. Statistics student's t test. *p<0.05

4.2.3 ERG Analysis of *Arl3* Q71L/+ and *Arl3* Q71L/Q71L Mice

To examine the function of rod and cone photoreceptors in *Arl3* Q71L/+ and *Arl3* Q71L/Q71L mice electroretinography (ERG) recordings from a dark-adapted 3cd flash and light adapted 10cd flash ERG were performed and analysed as described in 3.2.3. *Arl3* Q71L/+ had no significant reduction in A-wave amplitude compared to WT at 3 months and 6 months of age however the A-wave amplitude that was recorded appeared reduced but did not reach statistical significance (Figure 4.5 A (i), (ii), B). At 9 months and 12 months of age, a reduction in A-wave amplitude was recorded demonstrating significantly reduced photoreceptor responses (Figure 4.5 A (iii), (v), B). The 10cd flash test which analyses function of cone photoreceptors revealed *Arl3* Q71L/+ mice had a reduction in A-wave amplitude at 3 months of age which was maintained until 12 months of age (Figure 4.6 A, B). This demonstrates that *Arl3* Q71L/+ mice had reduced cone function from 3 months of age and that this occurred prior to defects in rod function. This suggests that these mice suffer from a cone-rod dystrophy and implies that increases in ARL3-GTP levels are more deleterious to cones than rod photoreceptors.

Dark adapted 3cd flash ERG responses from *Arl3* Q71L/Q71L mice revealed these mice had a reduced A-wave amplitude from 3 months to 12 months of age demonstrating reduced photoreceptor responses from age 3 months (Figure 4.5 A (i-v), B). The 10cd light adapted ERG also showed that *Arl3* Q71L/Q71L mice had a reduction in A-wave amplitude from 3 to 12 months of age demonstrating reduced cone photoreceptor responses (Figure 4.6 A (i-v), B). These results reveal that exceptionally high levels of ARL3-GTP is damaging to both rod and cone photoreceptors. In *Arl3* Q71L/+ mice a significant reduction in 3cd A-wave amplitude was not detected until 9 months of age demonstrating that prior to 9 months, despite having increased levels of ARL3-GTP rods are able to survive and function. However, in *Arl3* Q71L/Q71L mice, which have further elevated levels of ARL3-GTP, rod function is reduced from 3 months of age, suggesting that increased levels of ARL3-GTP may be compatible with normal function until a certain level of ARL3-GTP is reached. The 10cd flash ERG revealed that in both *Arl3* Q71L/+ and *Arl3* Q71L/Q71L mice, cone function was significantly reduced from 3 to 12 months of age. The reduction in cone responses from age 3 months in both *Arl3* Q71L/+ and *Arl3* Q71L/Q71L mice demonstrates that cones may be more sensitive to increases in

ARL3-GTP levels than rods, as rod function is maintained until 9 months of age in *Arl3* Q71L/+ mice. As a progressive reduction of cone function was not recorded it suggests that progressive cone cell death may not occur making it possible that less functional cones are able to survive until 12 months of age or before 3 months of age some cone cell death occurred and surviving cones were present until 12 months of age. This suggests the levels of ARL3-GTP may be more tightly regulated in cones compared to rods and differential mechanisms may exist in each cell type to regulate levels of ARL3-GTP.

Figure 4. 5 ERG Analysis of *Arl3* Q71L/+ and *Arl3* Q71L/Q71L Mice 3cd Flash Test

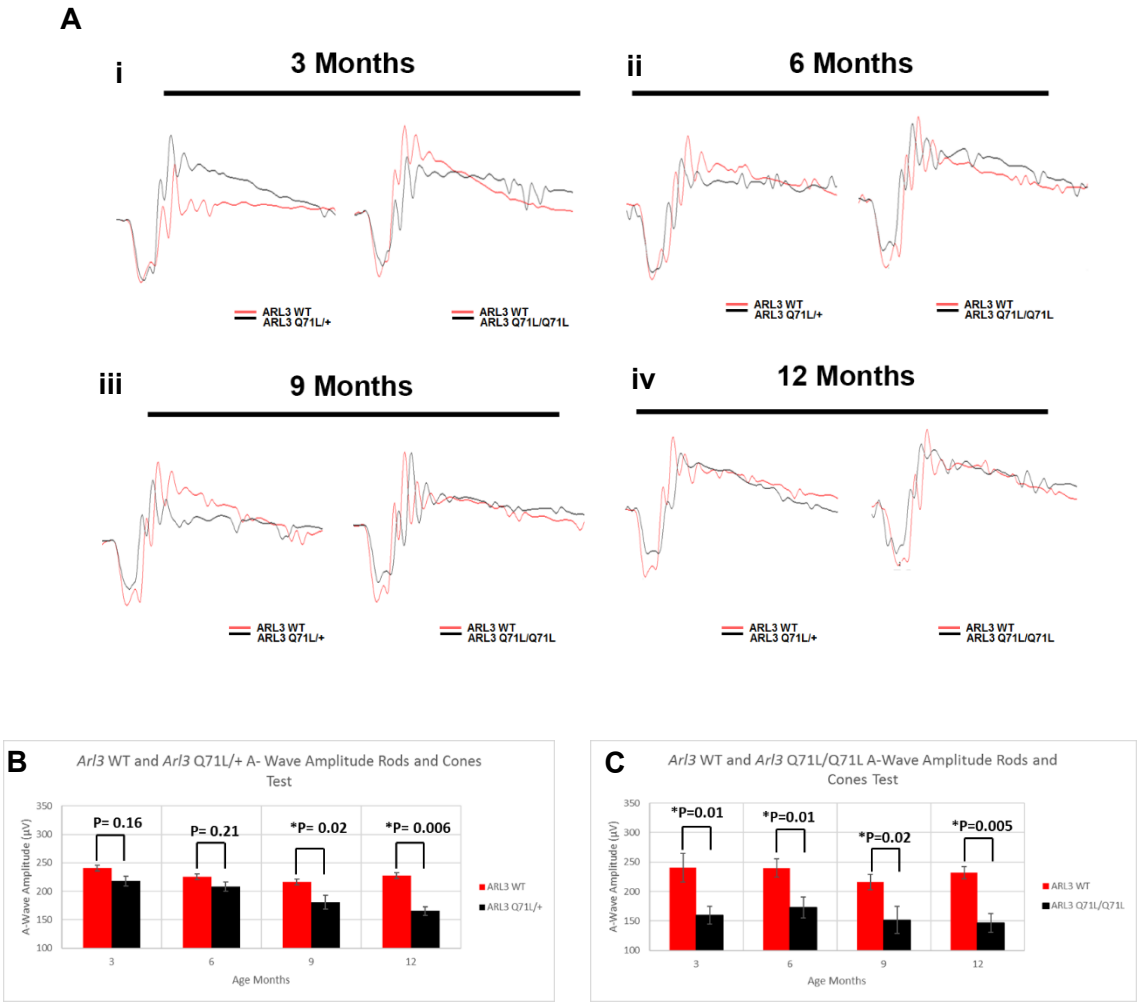

(A) Representative traces from 3cd flash dark adapted ERGs for *Arl3* Q71L/+ compared to WT and *Arl3* Q71L/Q71L compared to WT aged 3 months (i), 6 months (ii), 9 months (iii) and 12 months (iv).

(B) Quantification of average A-wave amplitude in *Arl3* Q71L/+ and WT aged 3, 6, 9 and 12 months. Significant reduction in A-wave amplitude in *Arl3* Q71L/+ mice detected from age 9 months.

(C) Quantification of average A-wave amplitude in *Arl3* Q71L/Q71L and WT mice aged 3,6,9 and 12 months. Significant reduction in A-wave amplitude was detected from 3 months of age.

N=5 for each genotype at each age, statistics calculated by students T.Test. *Arl3* Q71L/+ mice compared to WT CTRL ERGs recorded on the same day.

Figure 4. 6 ERG Analysis of *Arl3* Q71L/+ and *Arl3* Q71L/Q71L Mice 10cd Flash Test

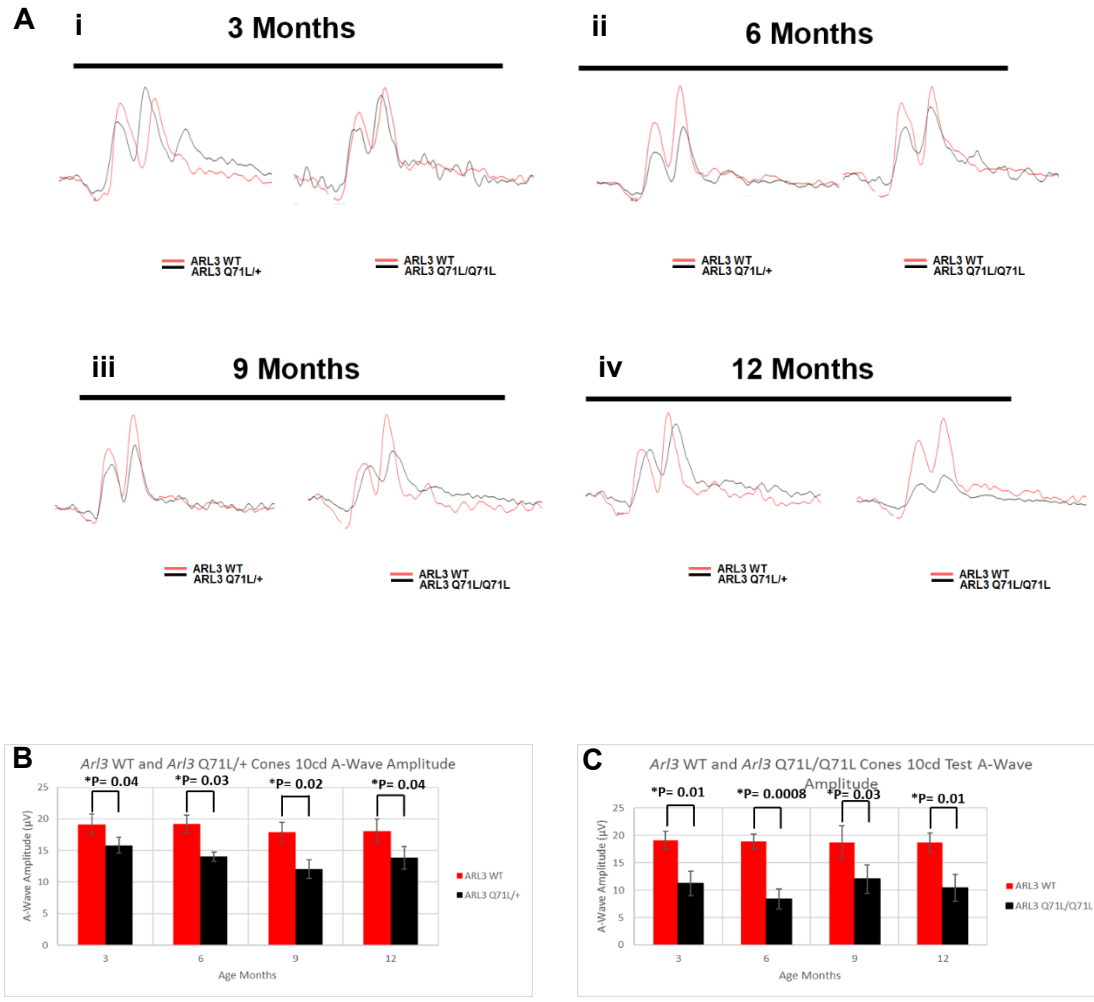

(A) Representative traces from light adapted 10cd Test ERGs for *Arl3* Q71L/+ compared to WT and *Arl3* Q71L/Q71L compared to WT aged 3 months (i), 6 months (ii), 9 months (iii) and 12 months (iv).

(B) Quantification of average A-wave amplitude in *Arl3* Q71L/+ and WT aged 3, 6, 9 and 12 months. Significant reduction in A-wave amplitude in *Arl3* Q71L/+ mice detected from age 3 months.

(C) Quantification of average A-wave amplitude in *Arl3* Q71L/Q71L and WT mice aged 3,6,9 and 12 months. Significant reduction in A-wave amplitude detected at 3 months.

N=5 for each genotype at each age, statistics calculated by students T.Test. *Arl3* Q71L/+ and *Arl3* Q71L/Q71L mice compared to WT CTRL ERGs recorded on the same day.

4.3 *Arl3* Q71L/+ and *Arl3* Q71L/Q71L Retinas Show Retinal Stress at Age 1 month

As the retinas of *Arl3* Q71L/+ and *Arl3* Q71L/Q71L mice aged one month did not exhibit signs of retinal degeneration and given that *Rp2h* DEL26/Y and *Rp2h* E135G/Y retinas showed signs of retinal stress at one month of age (see Figures 3.3, 3.4) I analysed the localisation of glial fibrillary acidic protein (GFAP) in *Arl3* Q71L retinas. As described in 3.5 GFAP expression is present in the ganglion cell layer (GCL) under normal conditions however upon stress GFAP positive retinal stress fibres extend throughout the upper layers of the retina. In central regions WT and *Arl3* Q71L/+ retinas had GFAP staining detected in the GCL however in *Arl3* Q71L/Q71L retinas, reactive gliosis was observed throughout the inner plexiform layer (IPL), inner nuclear layer (INL), outer plexiform layer (OPL) and outer nuclear layer (ONL) demonstrating retinal stress (Figure 4.7 A-C). At peripheral regions in WT retinas GFAP staining was confined to the GCL (Figure 4.7 D). In *Arl3* Q71L/+ and *Arl3* Q71L/Q71L retinas GFAP staining was detected throughout the IPL, INL, OPL and ONL indicative of retinal stress. *Arl3* Q71L/Q71L retinas appeared to have increased gliosis in peripheral regions compared to *Arl3* Q71L/+ retinas, however GFAP intensity levels were not quantified. These results demonstrate that *Arl3* Q71L/Q71L mice had increased retinal stress compared to *Arl3* Q71L/+ mice, establishing very high levels of ARL3-GTP caused retinal stress.

Figure 4. 7 GFAP Expression in *Arl3* Q71L/+ and *Arl3* Q71L/Q71L Retinas Aged 1 Month

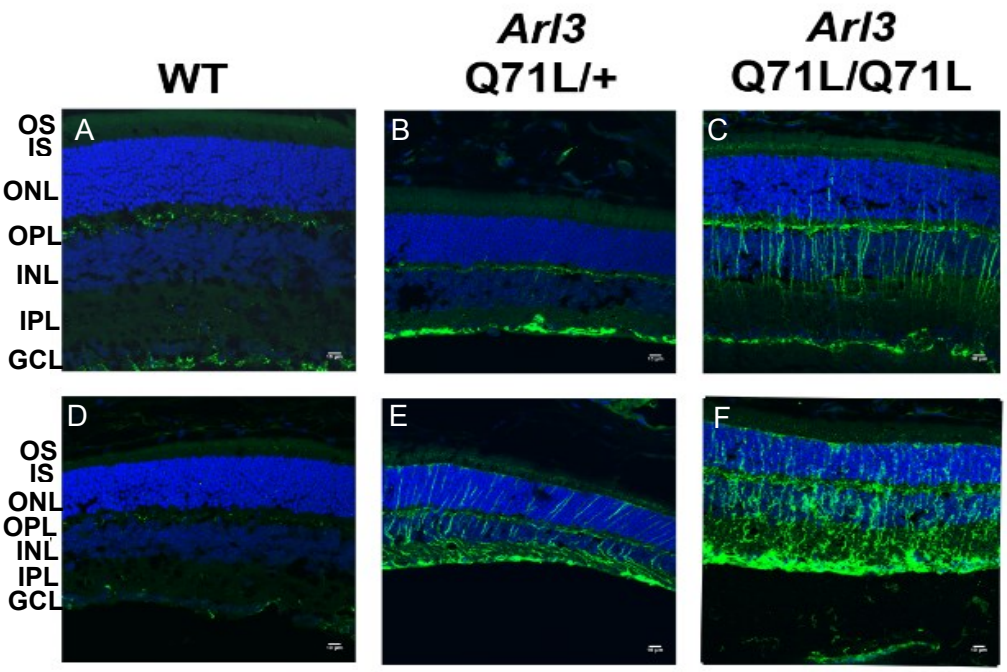

(A) GFAP expression in WT central retina was exclusive to the GCL.
(B) GFAP expression in *Arl3* Q71L/+ central retina. GFAP expression was confined to the GCL.
(C) GFAP expression in *Arl3* Q71L/Q71L central retina. GFAP expression was observed throughout the ONL, OPL, INL, IPL and GCL.
(D) GFAP expression in WT peripheral retina. GFAP expression was detected in the GCL only.
(E) GFAP expression in *Arl3* Q71L/+ peripheral region. GFAP expression was detected throughout the ONL, OPL, INL, IPL and GCL indicating retinal stress.
(F) GFAP expression in *Arl3* Q71L/Q71L peripheral retina. GFAP expression was detected throughout the ONL, OPL, INL, IPL indicating retinal stress.

4.4 M/L Opsin is Mislocalised in *Arl3* Q71L/+ and *Arl3* Q71L/Q71L Retinas After onset of Retinal Degeneration

The role of ARL3 in cones was not addressed in Rod^{Arl3Q71L} mice as ARL3 Q71L expression was driven by the rhodopsin promoter and therefore only expressed in rods. A retina specific knockout of Arl3, ^{ret}*Arl3*-/-, revealed that ARL3 may have a role in the development of the cone OS as these mice developed cones lacking OS's, however in peripheral regions some cones developed OS's and had normal M/L opsin localisation (Hanke-Gogokhia et al. 2016). As discussed in chapter 3, *Rp2h* DEL26/Y and *Rp2h* E135G/Y mice displayed M/L opsin mislocalisation at later stages of retinal degeneration (see 3.4), therefore given this result I analysed the localisation of M/L opsin in *Arl3* Q71L mice. *Arl3* Q71L/+ mice displayed normal M/L opsin localisation, with M/L opsin localised to the OS of cone photoreceptors, at 1 to 6 months of age (Figure 4.8 A-C). At 3 months of age the OS of cones appeared longer than WT, however the length of cone OS was not measured (Figure 4.8 B). At 9 months of age M/L opsin mislocalisation was observed as staining was detected in the OS, IS, Cell body and OPL of cone photoreceptors (Figure 4.8 D). At 12 months of age M/L opsin staining was detected in the IS and cell body of cone photoreceptors however the staining intensity appeared reduced compared to WT retinas (Figure 4.8 E), suggesting loss of cone photoreceptors as retinal degeneration progressed. Thinning of the ONL was first detected in *Arl3* Q71L/+ retinas aged 6 months (Figure 4.3 C, Figure 4.4 A (iii)), as was mislocalised M/L opsin, however cone ERG response was reduced from 3 months of age (Figure 4.6 A,B). This indicates that there may be another mechanism which is contributing to reduced cone function at 3 months of age and suggests that in *Arl3* Q71L/+ mice mislocalisation of M/L opsin is not a mechanism driving cone degeneration.

Arl3 Q71L/Q71L retinas had M/L opsin localised to the OS of cone photoreceptors, similar to WT retinas, at 1 month and 3 months of age (Figure 4.8 A, B). At 3 months of age OS appeared longer than WT however, this was not quantified (Figure 4.8 B). At 6 months of age M/L opsin was not localised to the OS but M/L opsin staining was detected in the cell body and OPL of cone photoreceptors (Figure 4.8 C). At 9 months of age M/L opsin staining was detected in the cell body and OPL of cone photoreceptors however the staining intensity appeared reduced compared to WT (Figure 4.8 D). At age 12 months, M/L opsin staining appeared reduced compared to

WT suggesting loss of cone photoreceptors. Some residual staining was detected in the cell body and OPL (Figure 4.8 E). Thinning of the ONL in *Arl3* Q71L/Q71L retinas was first detected in peripheral regions at 1 month of age with more widespread thinning observed at 3 and 6 months. A reduction in cone photoreceptor function was detected from 3 months of age, when normal M/L opsin localisation was observed. This suggests that another mechanism is driving dysfunction of cones in *Arl3* Q71L/Q71L retinas.

M/L opsin was mislocalised in *Arl3* Q71L/+ and *Arl3* Q71L/Q71L retinas after onset of retinal degeneration suggesting another factor is driving retinal degeneration in *Arl3* Q71L mutant mice. Mislocalisation of M/L opsin was detected at later stages and therefore may contribute to the dysfunction of cones in older *Arl3* Q71L mutant mice. M/L opsin mislocalisation was detected at 6 months in *Arl3* Q71L/Q71L retinas but was not detected until 9 months of age in *Arl3* Q71L/+ retinas demonstrating that levels of ARL3-GTP may affect M/L opsin trafficking. As this was not an early event initiating retinal degeneration it demonstrates that M/L opsin trafficking can be maintained despite high levels of ARL3-GTP however after onset of retinal degeneration high levels of ARL3-GTP may contribute to mislocalisation of M/L opsin.

Figure 4. 8 M/L Opsin Localisation in *Arl3* Q71L/+ and *Arl3* Q71L/Q71L Retinas

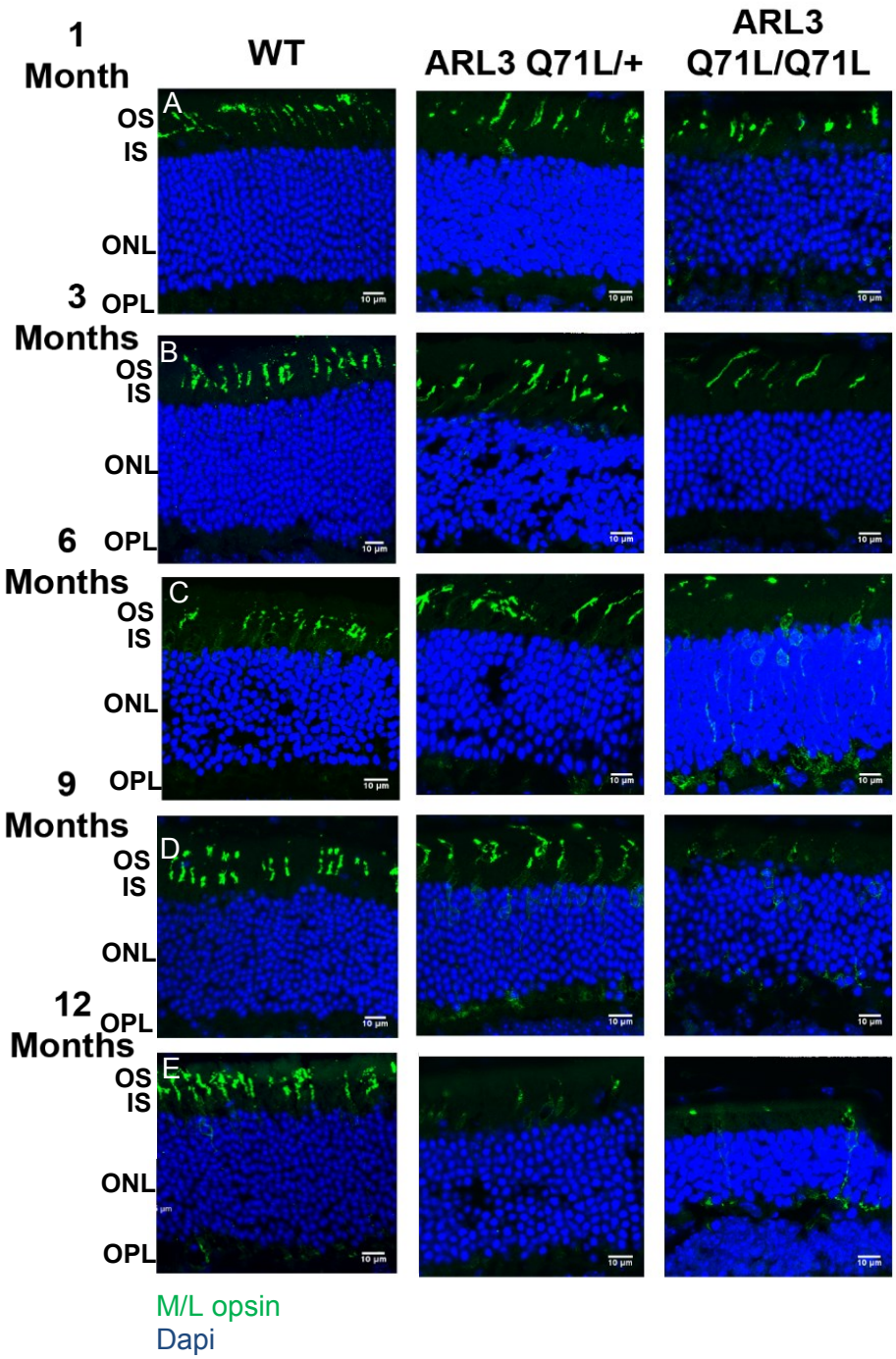

(A) M/L opsin staining in *Arl3* WT, *Arl3* Q71L/+ and *Arl3* Q71L/Q71L retinas aged one month. M/L opsin staining was detected in the OS of cone photoreceptors.
(B) M/L opsin staining in *Arl3* WT, *Arl3* Q71L/+ and *Arl3* Q71L/Q71L retinas age 3 months. M/L opsin was localised to the OS of cone photoreceptors.
(C) M/L opsin staining in *Arl3* WT, *Arl3* Q71L/+ and *Arl3* Q71L/Q71L retinas aged 6 months. In WT and *Arl3* Q71L/+ retinas M/L opsin was localised to the OS of cone photoreceptors. In *Arl3* Q71L/Q71L retinas M/L opsin staining was observed in the cell body and OPL of cone photoreceptors.
(D) M/L opsin staining in *Arl3* WT, *Arl3* Q71L/+ and *Arl3* Q71L/Q71L retinas aged 9 months. In *Arl3* WT retinas M/L opsin staining was detected in the OS of cone photoreceptors. In *Arl3* Q71L/+ retinas M/L opsin staining was detected in the OS, IS, cell body and OPL of cone photoreceptors. In *Arl3* Q71L/Q71L retinas appeared reduced compared to WT with some staining detected throughout the IS, cell body and OPL.
(E) M/L opsin staining in *Arl3* WT, *Arl3* Q71L/+ and *Arl3* Q71L/Q71L retinas aged 12 months. In *Arl3* WT retinas M/L opsin was detected in the OS of cone photoreceptors. In *Arl3* Q71L/+ retinas M/L opsin staining appeared reduced compared to WT with some staining remaining in the IS. In *Arl3* Q71L/Q71L retinas M/L opsin staining appeared reduced compared to WT with some staining remaining in the IS, cell body and OPL.

4.5 Rhodopsin is Mislocalised in *Arl3* Q71L/+ and *Arl3* Q71L/Q71L Mice

Rhodopsin mislocalisation was not detected in rods deficient of ARL3 (^{Rod}*Arl3-/-)* mice despite progressive rod degeneration (Hanke-Gogokhia et al. 2016). ^{Ret}*Arl3-/-* mice demonstrated that ARL3 may have a role in ciliogenesis and OS formation as no connecting cilia or OS's were formed in these mice and therefore rhodopsin was mislocalised throughout the ONL (Hanke-Gogokhia et al. 2016). In Rod^{ARL3Q71L} mice rhodopsin localisation was not examined but the levels of rhodopsin expression were comparable to WT suggestive of normal rhodopsin trafficking. This implies that mutation of ARL3 does not disrupt rhodopsin trafficking. As previously discussed in chapter 3, *Rp2h* DEL26/Y and *Rp2h* E135G/Y mice displayed rhodopsin mislocalisation demonstrating increased levels of ARL3-GTP may affect rhodopsin localisation. Therefore to investigate whether high levels of ARL3-GTP causes mislocalisation of rhodopsin, rhodopsin localisation was examined in *Arl3* Q71L/+ and *Arl3* Q71L/Q71L retinas.

Arl3 Q71L/+ retinas presented with normal rhodopsin localisation to the OS of rods, identical to WT retinas, at 1 month and 3 months of age (Figure 4.9 A, B). At 6 months of age rhodopsin staining was observed in the OS, IS, ONL and OPL of the retina reflecting mislocalised rhodopsin (Figure 4.9 C). At 9 months and 12 months of age rhodopsin staining intensity appeared reduced in *Arl3* Q71L/+ retinas compared to WT (Figure 4.9 D, E) however neither the signal intensity nor the protein levels were quantified. *Arl3* Q71L/Q71L retinas displayed reduced rhodopsin staining compared to WT from age 1 month (Figure 4.9 A-E). The staining that was detected was present throughout the photoreceptor layer (OS, IS, ONL, OPL) (Figure 4.9 A-E). This suggests that elevated levels of ARL3-GTP cause mislocalisation of rhodopsin which then may be degraded.

In *Arl3* Q71L/+ retinas thinning of the ONL was first detected at 6 months with more substantial thinning detected at 9 months of age (Figure 4.4 A (iii), (iv)) along with reduced rod photoreceptor responses (Figure 4.5 A, B). Rhodopsin was mislocalised at 6 months of age prior to the observed reduction in rod photoreceptor function. As rhodopsin is a key component of phototransduction this was unexpected but may imply that some rhodopsin was still localised to the OS and was therefore able to be activated and generate an A-wave response. *Arl3* Q71L/+ mice aged 9 months had reduced rod photoreceptor responses and reduced rhodopsin immunostaining

suggesting that the possible reduction in rhodopsin expression may contribute to the reduction in rod photoreceptor function that was recorded. As thinning of the ONL was observed at the same age as mislocalisation of rhodopsin, this advocates that rhodopsin mislocalisation may contribute to retinal degeneration. In *Arl3* Q71L/Q71L retinas rhodopsin mislocalisation and potential reduction in expression was detected from age one month. Thinning of the ONL was first detected at one month of age in *Arl3* Q71L/Q71L retinas with more substantial thinning observed from age 3 months (Figure 4.3 A, B). ERGs were only performed on mice from age three months and demonstrated reduced rod photoreceptor responses in these mice (Figure 4.5 A, C). This again demonstrates that rhodopsin mislocalisation and reduced expression was likely a mechanism which contributed to reduced photoreceptor responses and photoreceptor cell death in *Arl3* Q71L mice.

This data proposes a role for ARL3-GTP in rhodopsin trafficking. The later mislocalisation of rhodopsin in *Arl3* Q71L/+ mice compared to *Arl3* Q71L/Q71L mice demonstrates that despite elevated levels of ARL3-GTP rhodopsin can be trafficked correctly but rhodopsin trafficking cannot be maintained when high levels of ARL3-GTP persist indicating this could be secondary to mislocalisation of other OS proteins and that multiple mechanisms may regulate rhodopsin trafficking *in vivo.*

Figure 4. 9 Rhodopsin Localisation in *Arl3* Q71L/+ and *Arl3* Q71L/Q71L Retinas

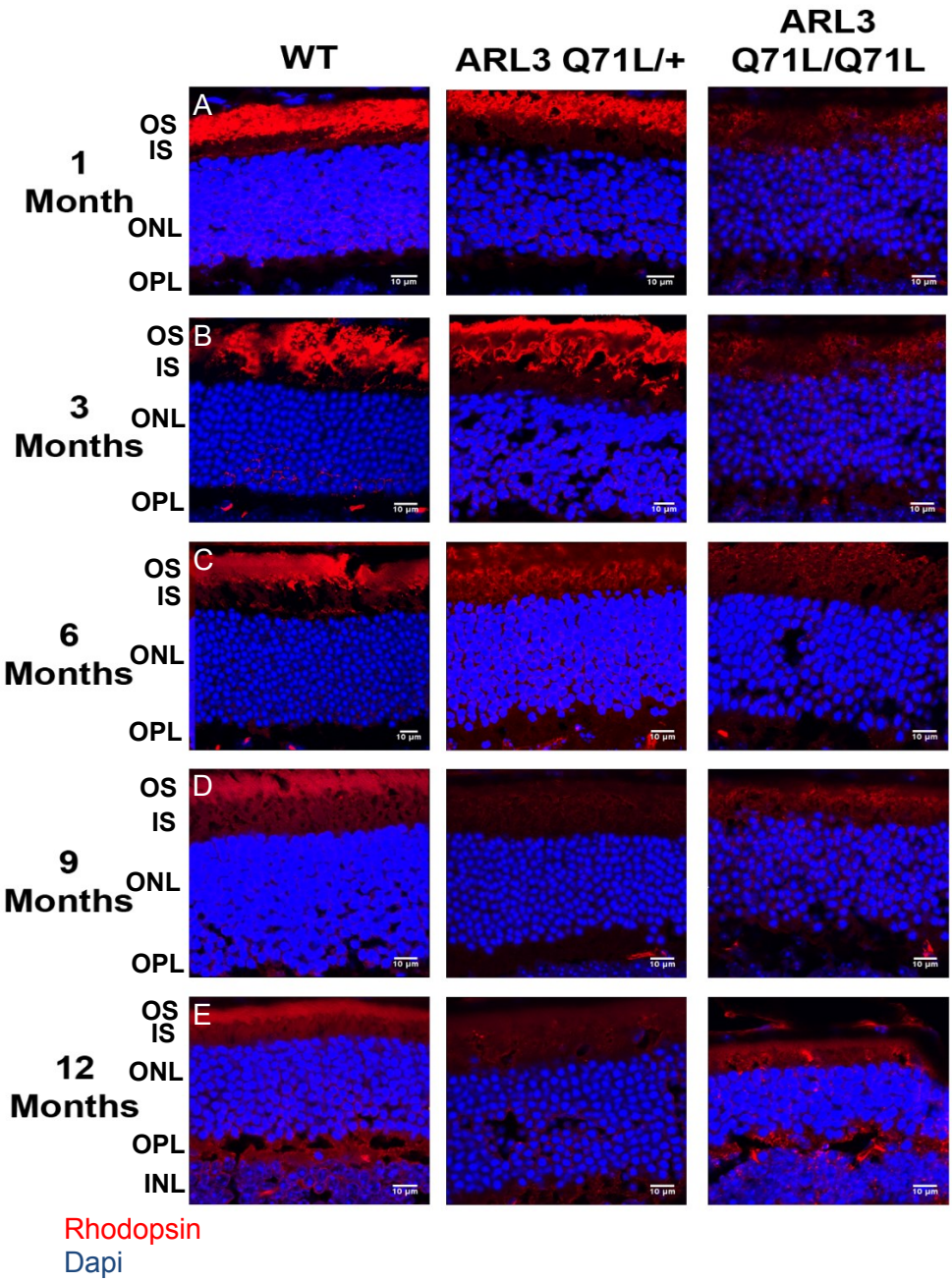

(A) Rhodopsin staining in *Arl3* WT, *Arl3* Q71L/+ and *Arl3* Q71L/Q71L retinas aged 1 month. In WT and *Arl3* Q71L/+ retinas rhodopsin was localised to the OS of rod photoreceptors. In *Arl3* Q71L/Q71L retinas rhodopsin staining was detected throughout the OS, IS, ONL and OPL of photoreceptors. The signal intensity appeared reduced compared to WT and *Arl3* Q71L/+ retinas.

(B) Rhodopsin staining in *Arl3* WT, *Arl3* Q71L/+ and *Arl3* Q71L/Q71L retinas aged 3 months. In WT and *Arl3* Q71L/+ retinas rhodopsin staining was detected in the OS of rod photoreceptors. In *Arl3* Q71L/Q71L retinas rhodopsin staining was detected throughout the OS, IS and ONL of photoreceptors reflecting mislocalised rhodopsin. The staining intensity appeared reduced compared to WT and *Arl3* Q71L/+ retinas.

(C) Rhodopsin staining in *Arl3* WT, *Arl3* Q71L/+ and *Arl3* Q71L/Q71L retinas aged 6 months. In *Arl3* WT retinas rhodopsin was detected in the OS of rod photoreceptors. In *Arl3* Q71L/+ retinas rhodopsin staining was detected in the OS, IS and ONL of photoreceptors. The staining intensity appeared reduced compared to WT. In *Arl3* Q71L/Q71L retinas rhodopsin staining was detected in the OS, IS, ONL and OPL however the staining was markedly reduced compared to WT and *Arl3* Q71L/+ retinas.

(D) Rhodopsin staining in *Arl3* WT, *Arl3* Q71L/+ and *Arl3* Q71L/Q71L retinas aged 9 months. In *Arl3* WT retinas rhodopsin was detected in the OS of rod photoreceptors. In *Arl3* Q71L/+ retinas rhodopsin staining was reduced compared to WT with some staining detected throughout the OS, IS and ONL. In *Arl3* Q71L/Q71L retinas staining intensity was also reduced compared to WT with some staining in the OS, IS and ONL.

(E) Rhodopsin staining in *Arl3* WT, *Arl3* Q71L/+ and *Arl3* Q71L/Q71L retinas aged 12 months. In *Arl3* WT retinas rhodopsin was detected in the OS of rod photoreceptors. In *Arl3* Q71L/+ retinas rhodopsin staining appeared reduced compared to WT with some staining remaining in the OS, IS, ONL. In *Arl3* Q71L/Q71L retinas rhodopsin staining appeared reduced compared to WT with some staining remaining in the OS, IS, ONL and OPL reflecting mislocalised rhodopsin.

4.6 GRK1 Immunostaining is Reduced in *Arl3* Q71L/+ and *Arl3* Q71L/Q71L Retinas

Many studies have implicated ARL3 and levels of ARL3-GTP in the trafficking of GRK1 to the photoreceptor OS (Hanke-Gogokhia et al. 2016; Z. C. Wright et al. 2016; Houbin Zhang et al. 2015). ^{Rod}*Arl3-/-,* ^{Ret}*Arl3-/- and Pde6δ -/-* mice displayed GRK1 mislocalisation suggesting GRK1 is trafficked to the OS by PDE6δ and ARL3. PDE6δ is known to be regulated by ARL3-GTP suggesting that in *Arl3* Q71L retinas this may be disrupted (Hanke-Gogokhia et al. 2016; H Zhang et al. 2007). The phenotype reported in Rod^{ARL3Q71L} mice supports this hypothesis as loss of GRK1 immunostaining in the OS and reduction in GRK1 expression was observed (Wright et al. 2016). As previously discussed in chapter 3 *Rp2h* DEL26/Y and *Rp2h* E135G/Y retinas displayed mislocalisation and reduction of GRK1 immunostaining. Therefore to elucidate whether this was directly attributed to levels of ARL3-GTP, the localisation of GRK1 in *Arl3* Q71L/+ and *Arl3* Q71L/Q71L retinas was analysed.

In WT retinas, GRK1 was localised to OS of photoreceptors at ages 1, 3, 6, 9 and 12 months of age (Figure 4.10 A-E). *Arl3* Q71L/+ and *Arl3* Q71L/Q71L retinas displayed reduced GRK1 immunostaining compared to WT from 1 month to 12 months of age although the levels observed appeared to be higher than background levels demonstrated by the secondary only control (Figure 4.10 A-F). Western blot analysis of whole eye lysates demonstrated that at one month of age WT, *Rp2h* DEL26/Y, *Rp2h* E135G/Y, *Arl3* Q71L/+ and *Arl3* Q71L/Q71L had equivalent levels of GRK1 expression (Figure 4.10 G). At 3, 6 and 9 months of age GRK1 expression was reduced in *Arl3* Q71L/+ and *Arl3* Q71L/Q71L compared to WT, *Rp2h* DEL26/Y and *Rp2h* E135G/Y eyes (Figure 4.10 G). GRK1 expression was not detected in *Arl3* Q71L/Q71L eyes post 3 months of age, however some expression was detected in *Arl3* Q71L/+ eyes up to 9 months of age (Figure 4.10 G). This demonstrates that high levels of ARL3-GTP leads to mislocalisation and eventual degradation of GRK1.

Reduced GRK1 immunostaining was observed in *Arl3* Q71L/+ retinas from age 1 month with reduced protein levels detected from age 3 months (Figure 4.10 A-G). ERG analysis revealed that *Arl3* Q71L/+ retinas had no significant reduction in rod photoreceptor function until age 9 months demonstrating that in young mice reduction of GRK1 expression did not affect activation of photoreceptors. However, in older mice as levels of GRK1 became further reduced this may have contributed to the

reduction in photoreceptor function observed. Thinning of the ONL was first detected in *Arl3* Q71L/+ mice aged 6 months with more substantial thinning of the ONL detected from 9 months, after mislocalisation of GRK1 was observed. This suggests that in *Arl3* Q71L/+ retinas mislocalisation of GRK1 may be a mechanism which drives retinal degeneration despite having a minimal effect on photoreceptor function.

Arl3 Q71L/Q71L mice also displayed reduction in GRK1 immunostaining from 1 month of age and a reduction of GRK1 expression from age 3 months. ERGs were only performed on mice from age 3 months therefore in these mice it is possible that the large reduction in GRK1 expression did contribute to the reduced ERG responses. Thinning of the ONL was detected from 1 month of age with more widespread thinning present from 3 months of age in *Arl3* Q71L/Q71L retinas. As GRK1 mislocalisation was also observed at one month of age it is possible that this is a mechanism that initiated retinal degeneration and functional defects in *Arl3* Q71L/Q71L retinas. This demonstrates that high levels of ARL3-GTP can cause mislocalisation of GRK1, with extremely elevated levels of ARL3-GTP ultimately leading to degradation of GRK1 which may drive retinal degeneration.

Figure 4. 10 GRK1 Localisation in *Arl3* Q71L/+ and *Arl3* Q71L/Q71L Retinas

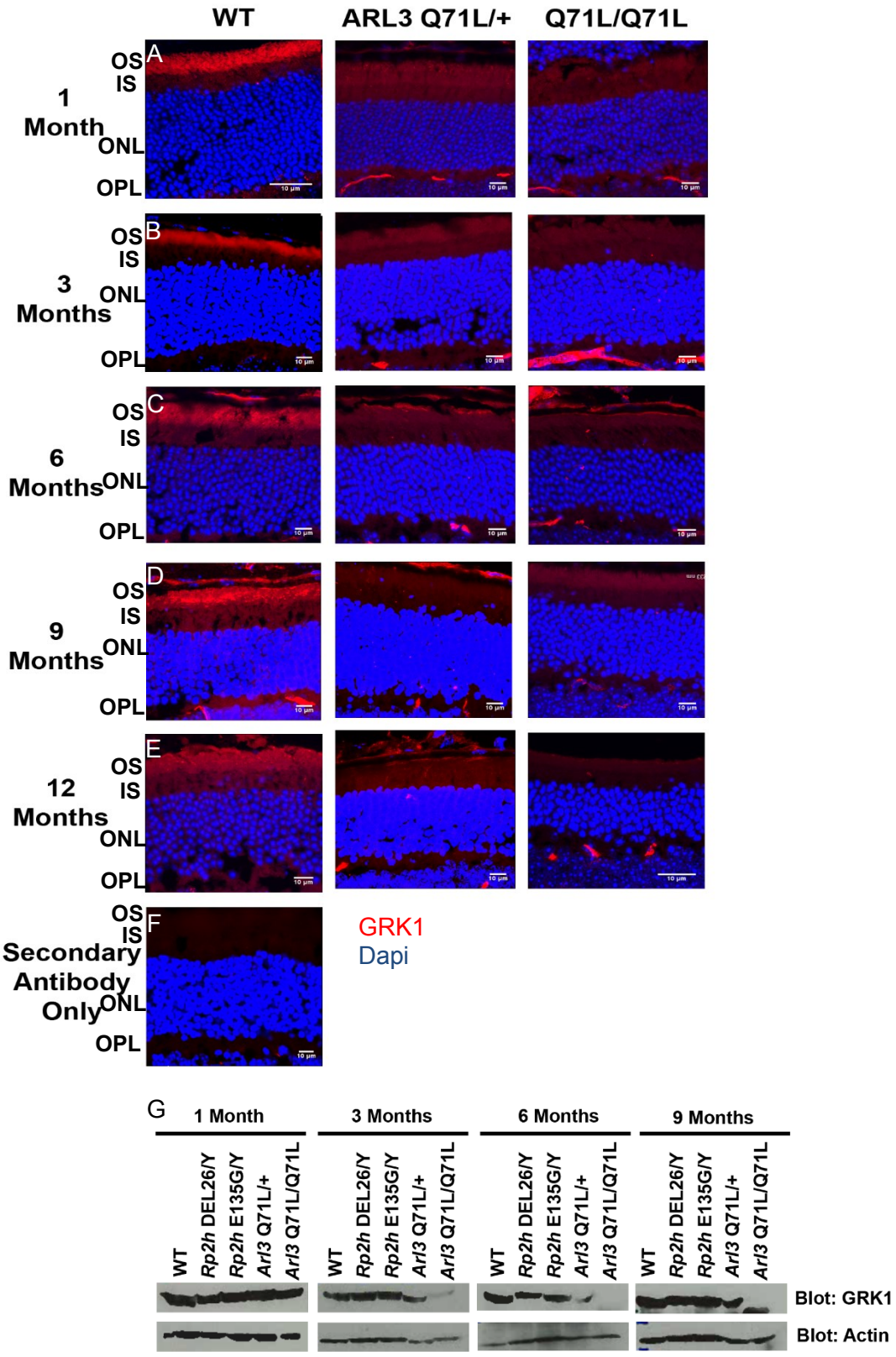

(A-E) GRK1 staining in *Arl3* WT, *Arl3* Q71L/+ and *Arl3* Q71L/Q71L retinas aged 1 month (A), 3 months (B), 6 months (C), 9 months (D) and 12 months (E). In WT retinas GRK1 was detected in the OS of photoreceptors. In *Arl3* Q71L/+ and *Arl3* Q71L/Q71L retinas GRK1 staining was reduced compared to WT with no staining detected in the OS.
(F) Secondary Antibody only control on WT retina section demonstrating background staining from unspecific binding of the secondary antibody. Background levels of staining were lower than those detected in *Arl3* Q71L/+ and *Arl3* Q71L/Q71L retinas suggesting signal in these samples may be attributed to residual GRK1.
(G) Western blot analysis of GRK1 expression in *Arl3* WT, *Rp2h* DEL26/Y, *Rp2h* E135G/Y, *Arl3* Q71L/+ and *Arl3* Q71L/Q71L eyes aged 1 month, 3 months, 6 months and 9 months. GRK1 expression was detected in all samples at equivalent level at 1 month of age. At 3 months of age GRK1 expression was reduced in *Arl3* Q71L/+ lysates compared to WT, *Rp2h* DEL26/Y and *Rp2h* E135G/Y eyes. *Arl3* Q71L/Q71L lysates displayed reduced GRK1 expression compared to all other samples. At 6 months GRK1 staining was detected in WT, *Rp2h* DEL26/Y, *Rp2h* E135G/Y retinas at comparable levels. In *Arl3* Q71L/+ retinas GRK1 expression was detected but was reduced compared to WT, *Rp2h* DEL26/Y and *Rp2h* E135G/Y samples. In *Arl3* Q71L/Q71L eyes GRK1 expression was not detected. At 9 months of age GRK1 expression was detected in WT, *Rp2h* DEL26/Y, *Rp2h* E135G/Y and *Arl3* Q71L/+ eyes with expression reduced in *Arl3* Q71L/+. In *Arl3* Q71L/Q71L eyes GRK1 expression was not detected. Actin used as a loading control.

Rp2h DEL26/Y and Rp2 E135G/Y samples discussed in 3.6, Figure 3.8.

4.7 STAT3 Phosphorylation is Reduced in *Arl3* Q71L/+ and *Arl3* Q71L/Q71L Eyes

STAT3 (signal transducer and activator of transcription 3) is a transcription factor which plays a central role in transmitting signals from the membrane to the nucleus after Interleukin 6 (IL-6) cytokine signalling (Hirano, Ishihara, and Hibi 2000). STAT3 has been shown to regulate cell growth, differentiation, migration, cell survival and the inflammatory response, and as such is found mutated in many malignancies (Pilati et al. 2011; Koskela et al. 2012; H. Yu, Pardoll, and Jove 2009; Hirano, Ishihara, and Hibi 2000). STAT3 signalling is induced by binding of cytokine IL-6 to its receptor on the cell surface which leads to dimerisation of glycoprotein 130 (Gp130). Gp130 is the common subunit of the receptor complexes of the interleukin 6 (IL6) family of cytokines (Hirano, Ishihara, and Hibi 2000) which upon dimerisation results in activation of Gp130 associated Janus associated kinases (JAK1, Jak2, TYK2) (Lutticken et al. 1994; Matsuda, Yamanaka, and Hirano 1994; Stahl et al. 1994). Gp130 is then phosphorylated by the JAK kinases and subsequently recruits signal transducing molecules such as STAT3 (Stahl et al. 1995; T. Fukada et al. 1996). STAT3 then becomes phosphorylated at Tyrosine705 (Y705) and forms a homodimer or a heterodimer with STAT1 (J E Darnell, Kerr, and Stark 1994; James E Darnell 1997). STAT3 nuclear translocation requires a Nuclear Localisation Signal on STAT3's coiled coiled domain and interaction with Importin α3 and α6 (L. Liu, McBride, and Reich 2005). More recently it was revealed that the small GTPase Ran and Importin β1 also regulate STAT3 nuclear localisation (Cimica et al. 2011). Interestingly both of these studies revealed STAT3 nuclear accumulation did not require tyrosine phosphorylation and that unphosphorylated STAT3 also localised to the nucleus, demonstrating tyrosine phosphorylation may not be essential for STAT3 nuclear accumulation (L. Liu, McBride, and Reich 2005; Cimica et al. 2011). Once in the nucleus STAT3 is phosphorylated on Serine 727 (S727) which is required for the activation of STAT3 controlled gene expression (Schindler, Levy, and Decker 2007). Recently it was demonstrated that ARL3 interacts with STAT3 and that upon stimulation by IL-6, ARL3-GTP interacts with phosphorylated STAT3 and increases its nuclear translocation (Togi et al. 2016). Expression of ARL3 Q71L in cells increased STAT3 transactivation while knockdown of ARL3 reduced STAT3 mediated gene expression demonstrating that levels of ARL3-GTP may affect downstream STAT3 signalling (Togi et al. 2016). Therefore given this finding, I investigated the

levels of STAT3 and phosphorylated STAT3 (pY705 and pS727) in WT, *Arl3* Q71L/+, *Arl3* Q71L/Q71L, *Rp2h* DEL26/Y and *Rp2h* E135G/Y mice.

In order to control for photoreceptor number, eyes from *Rp2h* DEL26/Y, *Rp2h* E135G/Y, *Arl3* Q71L/+ and *Arl3* Q71L/Q71L mice aged one month were used, as no retinal degeneration was detected at this stage in any *Rp2h* or *Arl3* mutants. After electrophoresis and transfer, membranes were probed for both total STAT3 and STAT3 with phosphorylated Y705 (pY705) and the same samples run on subsequent blots and probed for STAT3 and STAT3 phosphorylated S727 (pS727) in order to avoid ambiguity associated with membrane stripping and re-probing. Total STAT3 levels were equivalent in each sample (Figure 4.11 A, B) demonstrating mutation of *Rp2h* or expression of ARL3 Q71L did not disrupt STAT3 expression or stability. Analysis of STAT3 pY705 revealed that in WT, *Rp2h* DEL26/Y and *Rp2h* E135G/Y eyes STAT3 was phosphorylated however in *Arl3* Q71L/+ and *Arl3* Q71L/Q71L lysates reduced STAT3 phosphorylation was observed (Figure 4.11 A). This suggests that increased levels of ARL3-GTP decreased STAT3 phosphorylation in eyes. Similarly analysis of STAT3 pS727 demonstrated that reduced levels were present in *Arl3* Q71L/+ and *Arl3* Q71L/Q71L eyes compared to WT, *Rp2h* DEL26/Y and *Rp2h* E135G/Y eyes. These results suggest that increased levels of ARL3-GTP lead to decreased levels of active STAT3 *in vivo*. As no difference in STAT3 pY705 or pS727 phosphorylation was detected in *Rp2h* DEL26/Y or *Rp2h* E135G/Y mutants this demonstrated a specific effect stemming from mutation of ARL3 and may highlight a mechanism contributing to retinal degeneration that is specific to ARL3 mutation.

Figure 4. 11 STAT3 Phosphorylation is Reduced in *Arl3* Q71L/+ and *Arl3* Q71L/Q71L Eyes Aged 1 Month

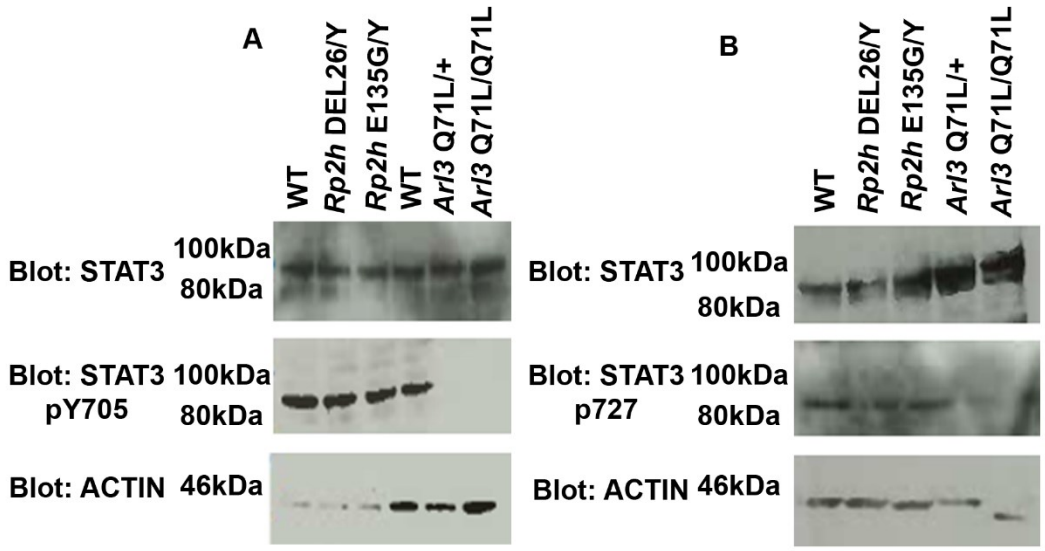

(A) STAT3 protein expression and pSTAT3 Y705 levels In WT, *Rp2h* DEL26/Y, *Rp2h* E135G/Y, *Arl3* Q71L/+ and *Arl3* Q71L/Q71L eye lysates aged 1 month. In WT, *Rp2h* DEL26/Y, *Rp2h* E135G/Y, *Arl3* Q71L/+ and *Arl3* Q71L/Q71L eyes STAT3 is expressed at the same level as WT. STAT3 pY705 was detected in WT, *Rp2h* DEL26/Y and *Rp2h* E135G/Y at levels equivalent to WT but was not detected in *Arl3* Q71L/+ and *Arl3* Q71L/Q71L mice.

(B) STAT3 and pS727 protein expression in WT, *Rp2h* DEL26/Y, *Rp2h* E135G/Y, *Arl3* Q71L/+ and *Arl3* Q71L/Q71L eyes aged 1 month. STAT3 expression was detected in every sample however STAT3 pS727 was detected in WT, *Rp2h* DEL26/Y and *Rp2h* E135G/Y lysates but not in *Arl3* Q71L/+ and *Arl3* Q71L/Q71L lysates.
Actin used as loading control

4.8 Discussion

4.8.1 *Arl3* Q71L/+ and *Arl3* Q71L/Q71L have Progressive Retinal Degeneration

In order to assess whether increased levels of ARL3-GTP were present in *Arl3* Q71L mutant mice an assay was designed using RP2 recombinant protein to isolate ARL3-GTP. This assay revealed that *Arl3* Q71L expressing lysates have substantially higher levels of ARL3-GTP than WT, *Rp2h* DEL26/Y and *Rp2h* E135G/Y lysates (Figure 4.2). As ARL3 Q71L was expressed at the same level as ARL3 WT and as RP2 is the only known GAP for ARL3 the levels of ARL3-GTP were expected to be equivalent in *Arl3* Q71L/Q71L, *Rp2h* DEL26/Y and *Rp2h* E135G/Y lysates, therefore as this was not observed, this could suggest that in tissues lacking RP2 another GAP exists which regulates the levels of ARL3-GTP. It is also possible that in lysates with RP2 function disrupted levels of ARL3-GTP are regulated through the GEF, ARL13b, such that the activity of ARL13b may be reduced in order to prevent increases in levels of ARL3-GTP. In this assay no ARL3-GTP was detected in WT lysates despite the fact some must be present in vivo therefore it is possible that in *Rp2h* DEL26/Y and *Rp2h* E135G/Y lysates levels of ARL3-GTP are increased compared to WT but are not high enough to be detected by this assay.

In *Arl3* Q71L/+ retinas thinning of the ONL was detected at 6 months of age but was not established in most regions until 9 to 12 months of age (Figure 4.3, 4.4). ERG results demonstrated a reduction in cone function from age 3 months and no reduction in rod photoreceptor function until 9 months of age (Figure 4.5, 4.6). This suggests that the retinal degeneration detected by ONL thinning prior to 9 months is due to loss of cone photoreceptors only. As discussed in chapter 3, ERG experiments were quite variable therefore ERGs could be repeated in more animals from each genotype. ERGs could be performed on younger mice to establish if normal cone function is present.

In *Arl3* Q71L/Q71L retinas, thinning of the ONL was first detected at 1 month and was widespread from 6 months of age (Figure 4.3, 4.4). ERG results demonstrated a significant reduction in rod and cone function from 3 months of age (Figure 4.5, 4.6). Although some thinning of the ONL was detected at 1 month and 3 months in these mice, severe retinal degeneration was not observed demonstrating that high levels of

ARL3-GTP adversely affects photoreceptor function without promoting massive photoreceptor cell death. The Rod^{ARL3Q71L} mouse exhibited severe retinal degeneration by PN70 with only one nuclei left in the ONL (Wright et al. 2016) however in *Arl3* Q71L/Q71L mice aged 3 months (PN90) retinas did not appear significantly thinner than WT. This highlights the potential issues created by use of the rhodopsin promoter to express ARL3 Q71L, as it is possible that massive overexpression of this protein triggered ER stress and ultimately photoreceptor cell death, rather than expression of ARL3 Q71L itself. For instance to detect ARL3 in eye lysates on western blot ECL Femto was used demonstrating endogenous ARL3 is not highly expressed in the eye.

Overall, this data demonstrates that expression of ARL3-GTP in the retina increases levels of ARL3-GTP hundreds of fold higher than WT and that this is relatively well tolerated as some photoreceptors survived up to 12 months of age. These mice demonstrate that increased levels of ARL3-GTP cause defects in both rod and cone photoreceptors and that cone photoreceptors may be more sensitive than rods. This agrees with a review of XLRP patient phenotypes, where patients with RP2 mutations had a severe cone phenotype (Jayasundera et al. 2010).

4.8.2 Mislocalisation of M/L Opsin and Rhodopsin in *Arl3* Q71L/+ and *Arl3* Q71L/Q71L Retinas

In *Arl3* Q71L/+ and *Arl3* Q71L/Q71L retinas mislocalisation of M/L opsin was observed at 9 months and 6 months of age respectively (Figure 4.8). ERG results demonstrated reduced cone function from 3 months signifying that mislocalisation of M/L opsin is not causative of the reduced cone function, however it may contribute to reduced cone function in older *Arl3* Q71L mice (Figure 4.6). Prior to mislocalisation of M/L opsin the length of the cone OS appeared longer in *Arl3* Q71L mutants compared to WT however, this was not quantified (Figure 4.8 B,C). Previously it has been shown that knockout of *Rp2h* in cones resulted in increased cone OS length, suggesting ARL3-GTP may be involved in this process (L. Li et al. 2015). As discussed in chapter 3, RP2 and ARL3 regulate the trafficking of KIF17, a homomeric kinesin which is required for M/L opsin trafficking to the cone OS indicating this could be a mechanism by which ARL3-GTP regulates M/L opsin localisation (Schwarz et al. 2017; Insinna et al. 2008). KIF17 has been shown to play a role in disc shedding in zebrafish cones, with loss of KIF17 reducing disc shedding in cones (Lewis et al. 2018), therefore RP2

and ARL3 may also influence disc shedding through KIF17 as disc shedding is required for normal photoreceptor function this may be linked to the photoreceptor degeneration phenotype (Kevany and Palczewski 2010). In older *Arl3* Q71L mice loss of M/L opsin staining was detected as photoreceptor degeneration progressed suggesting loss of cones (Figure 4.8). However, ERG results demonstrated that cone function is reduced from 3 months of age and this reduction in function is maintained until 12 months of age as the A-wave amplitude recorded at 12 months of age is not substantially reduced compared to 3 months of age, arguing against progressive cell death (Figure 4.6). Therefore, it is possible that less functional cones can survive in these mice, thus retinal whole mounts with PNA staining could be used to quantify the number of cones present in these mice and address whether cone photoreceptor cell death occurs over time.

In *Arl3* Q71L/+ and *Arl3* Q71L/Q71L mice rhodopsin mislocalisation was detected from 6 months and 1 month of age prior to reduced rod photoreceptor function and retinal degeneration suggesting this may be an early event which initiates retinal degeneration (Figure 4.9). In rod^{ARL3Q71L} mice mislocalisation of prenylated proteins was detected but no mislocalisation of rhodopsin was shown (Wright et al. 2016). In ^{rod}*Arl3-/-* mice rhodopsin was mislocalised throughout the IS and ONL of rod photoreceptors suggesting ARL3 may play a role in rhodopsin trafficking (Hanke-Gogokhia et al. 2016). After loading into vesicles rhodopsin is trafficked to the base of the connecting cilia via microtubules and the dynein motor (Pearring et al. 2013). Recently it was shown that ARL3 interacts with the p150Glu domain of the dynein motor and this interaction disrupts the dynein- dynactin complex and leads to release of cargo during vesicular trafficking (Jin et al. 2014). Furthermore pulldowns using ARL3 Q71L revealed that GTP bound ARL3 facilitates this function (Jin et al. 2014) suggesting increased levels of ARL3-GTP may cause disruptions in vesicular trafficking in vivo.

IFT occurs in photoreceptors and has important roles in the morphogenesis and maintenance of the OS (Marszalek et al. 2000; Pazour et al. 2002). Rhodopsin trafficking involves IFT as retinal knockouts of *Kif3a*, *Ift88* and *Ift20* result in rhodopsin mislocalisation. Interestingly it has also been shown that rhodopsin directly interacts with intraflagellar transport protein 20 (IFT20) (Keady, Le, and Pazour 2011; Marszalek et al. 2000; Pazour et al. 2002). Furthermore it has been demonstrated in cells, that depletion of RP2, ARL3 or Kif3a cause Golgi fragmentation and dispersion

of IFT20, interestingly this result was also observed when ARL3 Q71L was expressed in cells (Evans et al. 2010), suggesting in *Arl3* Q71L mice IFT20 may be mislocalised and this may result in rhodopsin mislocalisation. In *Ift20-/-* cones M/L opsin was also mislocalised suggesting that expression of *Arl3* Q71L could also cause M/L opsin mislocalisation through this mechanism (Keady, Le, and Pazour 2011). It has been demonstrated in C.elegans Arl-13 and ARL3 regulate IFT and ciliogenesis by regulating the interaction between IFTA and IFTB (Yujie Li et al. 2010). Arl-13 is a homologue of human *ARL13B* a gene which when mutated causes Joubert Syndrome (Cantagrel et al. 2008) and it has been established that ARL13B has GEF activity for ARL3 *in vitro* (Gotthardt et al. 2015), implying levels of ARL3-GTP may regulate this process. In order to generate further evidence that IFT may be disrupted in *Arl3* Q71L mice the localisation of Guanyl Cyclase 1 (GC1) could also be investigated as it has also been shown to require IFT for trafficking to the OS (Insinna and Besharse 2008). Interestingly *Arl3* Q71L mice did not display any other obvious defects as they survived until 12 months of age and were indistinguishable from WT mice however the motors and proteins which regulate IFT are expressed in all ciliated cells demonstrating that in other cilia mechanisms exist which maintain IFT regulation despite high levels of ARL3-GTP.

4.8.3 GRK1 Immunostaining is Reduced in *Arl3* Q71L/+ and *Arl3* Q71L/Q71L Retinas

GRK1 immunostaining was reduced compared to WT in *Arl3* Q71L/+ and *Arl3* Q71L/Q71L retinas from age 1 month however no reduction in GRK1 protein level was detected at this age (Figure 4.10). This is similar to the results discussed in chapter 3, where in *Rp2h* DEL26/Y and *Rp2h* E135G/Y retinas GRK1 immunostaining was reduced but protein levels were not and suggests mislocalisation of GRK1. From 3 months of age the protein levels of GRK1 were reduced in *Arl3* Q71L/+ and *Arl3* Q71L/Q71L retinas suggesting degradation of mislocalised GRK1 (Figure 4.9 G). In *Arl3* Q71L/Q71L retinas the protein levels of GRK1 were reduced compared to *Arl3* Q71L/+ and WT at all the ages examined demonstrating levels of ARL3-GTP were directly related to rate of GRK1 loss (Figure 4.10 G). This result is similar to that reported in $Rod^{ARL3Q71L}$ mice in which GRK1 protein levels were reduced ~40% compared to WT (Wright et al. 2016). In this model levels of PDE6 and Transducin γ (Tγ) were also reduced compared to WT retinas (Wright et al. 2016) however I was

unable to investigate these proteins in the *Arl3* Q71L mice. In ^{Rod}*Arl3-/-* retinas GRK1, PDE6, Tα and Tγ were all mislocalised to the IS, ONL and synaptic layer of the retina however a reduction in protein levels was not reported.

GRK1 is also expressed in cone photoreceptors, in *Arl3* Q71L/+ and *Arl3* Q71L/Q71L mice the loss of GRK1 immunostaining was consistent across the retina suggesting GRK1 expression was also lost in cones. In order to confirm GRK1 expression was reduced in cones as well as rods co-staining with PNA could be used to label the cone photoreceptors. It was established that cone GRK1 was mislocalised in *Rp2h* -/- mice (Houbin Zhang et al. 2015) and that rod and cone GRK1 localisation was disrupted in the *PDE6δ* -/- knockout mouse (H Zhang et al. 2007) implying that when RP2 is absent and ARL3-GTP levels increased PDE6δ function was compromised in cones. In a double knockout *Pde6δ-/- Unc119-/-* localisation of cone GRK1 was partially rescued (Houbin Zhang, Frederick, and Baehr 2014) suggesting GRK1 in rods and cones may be differentially regulated. Given that cone photoreceptor function is disrupted from 3 months of age in *Arl3* Q71L retinas this could be an interesting lane for further investigation as it is possible localisation and expression of cone GRK1 may be affected prior to rod GRK1. Interestingly in ^{Rod}*Arl3-/-* retinas GRK1, PDE6, Tα and Tγ were still partially localised to the OS as well as the IS and ONL suggesting that in the absence of ARL3 compensatory mechanisms may exist to maintain trafficking of proteins to the OS (Hanke-Gogokhia et al. 2016).

Reduced GRK1 expression would be expected to directly affect levels of rhodopsin phosphorylation and therefore result in changes in photoreceptor responses. ERG results demonstrated that in *Arl3* Q71L/+ mice 3cd A-wave amplitudes were not reduced compared to WT until 9 months of age, however a reduction in GRK1 immunostaining was observed from 1 month and reduced protein levels were observed from 3 months demonstrating that in younger *Arl3* Q71L/+ mice GRK1 reduction does not affect A-wave amplitude (Figure 4.5, Figure 4.10). However as GRK1 is involved in rhodopsin recycling during phototransduction it would be expected that reduced GRK1 expression would result in decreased rate of recovery of photoresponses after phototransduction. This effect was detected in both the Rod^{ARL3Q71L} mice and *Rp2h -/-* mice where GRK1 expression and localisation was disrupted (Wright et al. 2016; Zhang et al. 2015). In order to test whether the observed reduction in GRK1 expression has a functional consequence on phototransduction, scotopic ERG recovery could be measured using two low intensity flashes with

varying delays between and the time required for the A-wave amplitude to recover recorded in *Arl3* Q71L mutants compared to WT.

It has been shown that GRK1 can be trafficked to the OS by PDE6δ and that cargo release from PDE6δ can be stimulated by ARL3-GTP and not ARL3-GDP (Linari, Hanzal-Bayer, and Becker 1999; H Zhang et al. 2007). ARL13B, the GEF for ARL3, is localised to primary cilia (Gotthardt et al. 2015; Cantagrel et al. 2008) and RP2 also localises to primary cilia in cultured cells (T. W. Hurd, Fan, and Margolis 2011). Therefore as the OS is a modified cilium (Besharse and Horst 1990) this suggests that in WT retinas ARL3-GTP is restricted to the OS and CC ensuring release of cargo from PDE6δ can only occur in this region. In *Arl3* Q71L retinas, where ARL3 is constitutively GTP bound, cargo may be released from PDE6δ in all regions of the photoreceptor cell leading to cell stress and ultimately photoreceptor cell death.

4.8.4 STAT3 phosphorylation is Reduced in *Arl3* Q71L/+ and *Arl3* Q71L/Q71L Eyes Aged 1 month

STAT3 expression and phosphorylation status was examined in eyes aged 1 month as no reduction in photoreceptor number or changes in retinal morphology were present at this age in either *Rp2h* DEL26/Y, *Rp2h* E135G/Y, *Arl3* Q71L/+ and *Arl3* Q71L/Q71L retinas. As retinal degeneration progresses microglial activation occurs and triggers an inflammatory response which is thought to contribute to photoreceptor cell death (Langmann 2007; Zeng et al. 2005; Hollyfield et al. 2008). Therefore as STAT3 is involved in inflammatory signalling only mice aged one month were analysed to prevent detection of changes in STAT3 activation associated with increased inflammation (Heinrech *et al.*, 1998; Hirano, Ishihara and Hibi, 2000; Yu, Pardoll and Jove, 2009; Pilati *et al.*, 2011). Togi et.al demonstrated that ARL3 interacts with STAT3 and that ARL3-GTP interacts with STAT3 phosphorylated at Y705 resulting in increased STAT3 nuclear accumulation and STAT3 mediated gene expression in HeLa cells (Togi et al. 2016). In *Arl3* Q71L/+ and *Arl3* Q71L/Q71L mice, which have highly elevated levels of ARL3-GTP (Figure 4.2), levels of STAT3 phosphorylation at Y705 and S727 were reduced (Figure 4.11). As Y705 phosphorylation is thought to be required for dimerisation and nuclear translocation and phosphorylation of S727 is thought to be required for activation of STAT3 mediated gene expression, reduced phosphorylation of these residues would be predicted to result in reduced STAT3 activity *in vivo* (Z. Wen, Zhong, and Darnell

1995). This result contrasts the results described by Togi et.al in which ARL3-GTP increased phosphorylation of STAT3 and increased its nuclear accumulation, leading to increased STAT3 mediated gene expression (Togi et al. 2016). The reasons for this difference could be that to detect the ARL3 and STAT3 interaction and increased STAT3 phosphorylation in HeLa cells leukaemia inhibitory factor (LIF) stimulation was required and the interaction was undetectable in the absence of LIF (Togi et al. 2016). In 1 month old eyes without retinal degeneration IL6 receptors may not be stimulated and this may explain the differences in findings between this work and my study. Importantly, HeLa cells are an immortalised human cancer cell line and as STAT3 expression has been shown to be upregulated in many malignancies these cells may not accurately reflect STAT3 interactions under normal physiological conditions (H. Yu, Pardoll, and Jove 2009). In the retina STAT3 signalling can also be stimulated by ciliary neurotrophic factor (CNTF), another member of the IL6 family of cytokines, which is upregulated through retinal stress (Stahl et al. 1994; R. Wen et al. 1995; Cao et al. 1997; Rose-John 2018). CNTF binds its receptor CNTFα which binds Gp130 and leukaemia inhibitory factor receptor (LIFR) and stimulates phosphorylation of Y705 on STAT3 (Stahl et al. 1994) .Multiple studies have demonstrated that expression of CNTF in the retina is protective in models of inherited retinal degeneration (Cayouette and Gravel 1997; Tao et al. 2002; Chong et al. 1999) and CNTF expression may be particularly beneficial for cone survival making it an attractive avenue for therapeutic treatment in patients (Yiwen Li et al. 2010). In transgenic rats carrying the rhodopsin S334ter-3 mutation, which generates a truncated rhodopsin which is not trafficked to the OS (Martinez-Navarrete et al. 2011), CNTF expression rescued secondary degeneration of cones (Yiwen Li et al. 2010). Transplantation of a microdevice which secretes CNTF at PN20 rescued cone OS degeneration and treated eyes at PN160 had increased cone ERG responses compared to untreated eyes (Yiwen Li et al. 2010). A phase 1 clinical trial demonstrated that expression of CNTF via an ocular implant is safe for patients and although clinical efficacy was not assessed in this trail 7 of the patients treated did display a 2-3 line improvement in vision after treatment (Sieving et al. 2006).

In *Arl3* Q71L eyes phosphorylation of STAT3 was reduced this could result from reduced CNTFα or IL6 receptor activation or it may be that receptors are activated but downstream signalling prevented. In order to test whether CNTF or IL6 expression is affected in *Arl3* Q71L/+ and *Arl3* Q71L/Q71L retinas western blots for CNTF or IL6 could be performed or their expression could be analysed by RNA sequencing of

whole retinas. Expression of CNTF is increased with GFAP expression in neuronal cells (Cao et al. 1997) and if this occurs in the retina then it may be that CNTF expression is increased in *Arl3* Q71L/Q71L mice as these retinas had the highest levels of GFAP expression, and subsequently ARL3 Q71L expression prevents STAT3 phosphorylation by an undetermined mechanism. Expression of ARL3 Q71L lead to accumulation of STAT3 in the nucleus even in the absence of LIF stimulation in HeLa cells (Togi et al. 2016), therefore it could be that in the retina ARL3-GTP shuttles STAT3 into the nucleus in the absence of phosphorylation resulting in STAT3 no longer being able to interact with the membrane localised Gp130. This hypothesis could be tested by analysing the localisation of STAT3 in WT and *Arl3* Q71L/+ and *Arl3* Q71L/Q71L retinas.

In this experiment whole eye lysates were used therefore these results do not specifically reflect the levels of STAT3 in photoreceptors. Multiple studies have demonstrated a role for STAT3 in rod photoreceptor development (S. S.-M. Zhang et al. 2005; Ozawa et al. 2004; S. S. M. Zhang et al. 2004) and it has been suggested that STAT3 is expressed in the nuclei of Muller cells, ganglion cells and astrocytes with some expression in the IS of photoreceptors (Samardzija et al. 2006; Peterson et al. 2000). It has been shown in zebrafish that high levels of STAT3 are expressed in the eye and that when photoreceptors are exposed to high levels of light, levels of total and activated STAT3 are increased in microglial and photoreceptor cells (Oates et al. 1999; Kassen et al. 2007). In order to establish where STAT3 is expressed in the mouse retina immunofluorescence experiments were attempted on retinal sections with STAT3, STAT3 pY705 and STAT3 pS727 antibodies, however these were unsuccessful. In order to improve specificity of this experiment retinas could be dissociated from whole eyes and levels of STAT3 expression and activation examined. STAT3 expression in the retina could also be confirmed by RNA sequencing and to specifically identify expression in photoreceptors single cell RNA sequencing techniques could be used to separate the transcriptome of specific retinal cell types. RNA sequencing could also be used to examine the expression of STAT3 target genes in photoreceptors in order to demonstrate if decreased STAT3 phosphorylation effects downstream signalling in *Arl3* Q71L/+ and *Arl3* Q71L/Q71L photoreceptors. Any downstream targets could be further investigated in order to determine whether they may affect function of photoreceptors and whether they may contribute to photoreceptor cell death.

Knockout of endogenous *Lif* expression in mouse retina revealed that LIF protects against light induced photoreceptor cell death (Bürgi, Samardzija, and Grimm 2009). LIF is member of the IL6 family of cytokines which is expressed in Muller cells and expression of endogenous LIF has been shown to increase with retinal stress (Bürgi, Samardzija, and Grimm 2009; Rose-John 2018). *VPP* mice contain a transgene encoding mutant rhodopsin (V20G, P23H, P27L), after which they are named, that causes rapid rod degeneration followed by secondary cone cell death which models Autosomal Dominant Retinitis Pigmentosa (ADRP) (Naash et al. 1993; Qtaishat et al. 1999). In *Vpp* mice which had endogenous LIF expression knocked out, *Vpp Lif -/-*, it was shown that LIF is protective against photoreceptor cell death as *Vpp Lif -/-* mice had more rapid retinal degeneration than mice expressing the VPP transgene only (Joly et al. 2008). The effect of STAT3 expression on photoreceptor survival was assessed in a transgenic model expressing mutant rhodopsin (RHO P347S) and in a peripherin knockout mouse, Prph2/$^{rds+}$. Overexpression of STAT3 by insertion of a transgene expressing either STAT3^{WT} constitutively active STAT3, STAT3^{C} or dominant negative STAT3 Y705F demonstrated expression of WT and STAT3^{C} improved photoreceptor cell survival. STAT3^{C} has higher DNA binding efficiency than STAT3^{WT} due stabilisation of the active tyrosine phosphorylated homodimer on DNA, cysteine residues introduced at 662 and 664 reduce the efficiency of dephosphorylation of tyrosine 705. The highest improvement in cell survival was detected in mice expressing STAT3^{C} and no effect was observed when the STAT3 Y705F mutant was expressed demonstrating that Y705 phosphorylated STAT3 has a pro survival effect in vivo (K. Jiang et al. 2014). Together this suggests that loss of STAT3 activation may contribute to retinal degeneration due to loss of pro survival signalling. In models of light induced and inherited retinal degeneration it was demonstrated that STAT3 signalling was stimulated upon photoreceptor cell death however the downstream signalling targets were different. The model of light induced retinal degeneration was the BALB/c mouse which is an albino mouse that develops rapid photoreceptor degeneration when exposed to bright light (LaVail and Gorrin 1987), the models of inherited retinal degeneration were the *rd1* mouse which contains a null allele for the β subunit of PDE6 (Bowes et al. 1990) and the *VPP* mouse (Samardzija et al. 2006). In the model of light induced degeneration JAK2, STAT3 and extracellular- signal related kinase 1/2 (ERK1/2) phosphorylation was induced after initiation of photoreceptor degeneration however in the model of inherited retinal degeneration phosphorylation of JAK2 was only mildly induced but

phosphorylation of cellular homolog of murine thymoma virus akt8 oncogene (Akt) was increased (Samardzija et al. 2006). Inhibition of JAK2 in an induced model of retinal degeneration increased photoreceptor survival but no benefit was observed in the inherited model (Samardzija et al. 2006). Furthermore, expression of CTCF is upregulated in mouse models of light induced retinal degeneration and in the *rd1* mouse but is not induced in the *VPP* mouse. Fibroblast growth factor 2 (FGF-2) is induced in the *VPP* mouse but not in the *rd1* mouse (Samardzija et al. 2006). This validates that mutations in different genes which cause retinal degeneration, can perturb the same pathways in different ways that can influence disease progression. Consequently this finding has important implications for disease mechanism in patients which have RP2 mutations, as it provides evidence that *Rp2h* mutation and increased levels of ARL3-GTP may not drive retinal degeneration through identical pathogenic mechanisms. This also has significant consequences in terms of potential treatment options as treatments designed to increase STAT3 signalling in the retina may prove ineffective in patients with *RP2* mutations if levels of STAT3 expression and activation are not affected.

4.9 Conclusions

In this chapter, I demonstrated that CRISPR mediated knock in of ARL3 Q71L in the endogenous locus in mice resulted in high levels of ARL3-GTP in tissues and caused a progressive retinal degeneration with no other adverse phenotypes. *Arl3* Q71L retinas displayed early mislocalisation of GRK1, a farnesylated protein trafficked to the OS by PDE6δ, which is regulated by ARL3-GTP suggesting that increased levels of ARL3-GTP cause disruption of PDE6δ, leading to mistrafficking of GRK1 and potentially other OS proteins. *Arl3* Q71L mice also displayed mislocalisation of rhodopsin prior to reduced photoreceptor function and photoreceptor degeneration demonstrating that increased levels of ARL3-GTP also effect trafficking of rhodopsin. Interestingly *Arl3* Q71L mice displayed reduced cone function from 3 months of age signifying cones may be more sensitive than rods to increased levels of ARL3-GTP. Mislocalisation of M/L opsin was not detected until later stages demonstrating this was not the initial functional defect in cones and another mechanism may cause early defects in cone function. I also demonstrated that *Arl3* Q71L/+ and *Arl3* Q71L/Q71L eyes had reduced STAT3 activation prior to retinal degeneration and this effect was not detected in *Rp2h* DEL26/Y and *Rp2h* E135G/Y mice revealing a pathway, which

may drive retinal degeneration, that is specifically regulated by levels of ARL3-GTP. Taken together this data suggests a role for ARL3-GTP in the trafficking of lipid-modified proteins to the OS, and in opsin trafficking and that *Rp2h* mutants and *Arl3* mutants may drive retinal degeneration through multiple mechanisms that are not necessarily identical, implying increased levels of ARL3-GTP in patients with *RP2* mutations may not fully explain the downstream phenotype. Never the less these mice demonstrate that increased levels of ARL3-GTP is a driver for retinal degeneration and they facilitate direct comparison to other *Rp2h* mouse models providing insights into disease mechanism in RP patients with *RP2* mutations.

Chapter 5

Characterisation of ZDHHC5 as a New Interactor of RP2

Chapter 5: Characterisation of ZDHHC5 as a new Interactor of RP2

5.1 Introduction

Protein complexes can be very dynamic *in vivo* with alterations in post translational modifications and activity of the proteins involved altering the stability and conformation of the complex (Wang et.al 2017). Identification of protein-protein interactions *in vitro* is commonly carried out using Yeast 2 Hybrid (Y2H) or co-immunoprecipitation assays. Y2H studies utilise the DNA binding domain (BD) and the activating domain (AD) of a transcription factor which activates expression of a reporter gene. The BD is fused to the protein of interest (the bait) and the AD is fused to the potentially interacting protein (the pray). Expression of the transgene is activated if the bait and pray proteins interact (Brückner et.al 2009). The advantage of Y2H is that it identifies direct protein interactions, but the major caveat with these assays is that they rely on the interactions taking place in the unnatural environment of a yeast cell. Immunoprecipitation assays often involve overexpressed or tagged proteins, which do not always replicate the localisation of the endogenous proteins, followed by pulldown to identify interactors. The major issue with immunoprecipitation assays is difficulty in solubilising proteins and the resulting loss of transient or weak interactions as the conditions required to solubilise proteins may not be compatible with maintaining these weak interactions (Roux et.al 2012).

RP2 likely functions in many transient interactions, which cannot always be detected by traditional immunoprecipitation assays, therefore it is likely that many of the proteins RP2 interacts with in cells remain unknown. In order to identify proteins with which RP2 interacts and to overcome the limitations of traditional IP approaches, a strategy was designed based on the BIO-ID method (Roux et.al 2012). Using this assay, zinc finger DHHC-Type containing 5 (ZDHHC5) was identified as a novel potential interactor of RP2. ZDHHC5 is one of the 23 human palmitoyltransferases (PATs) and as RP2 is itself palmitoylated, this was believed to be an interesting hit to investigate further.

BIO-ID is a recently developed technique, which utilises a promiscuous prokaryotic biotin ligase to label proximal and interacting proteins of a protein of interest in

mammalian cells. This assay involves the fusion of a mutant BIRA, BIRA R118G, a promiscuous biotin ligase known as BIRA*, to the protein of interest and expression of this fusion protein in cells. BIRA* biotinylates proteins by the generation of biotinoyl-5-AMP from biotin and ATP (Roux et al. 2012). This activated biotin radical biotinylates peptides by reacting with lysine residues. Upon addition of biotin to the cell culture media the BIRA* promiscuously biotinylates proteins interacting and proximal to the protein of interest. Cells are then lysed and biotinylated proteins purified using streptavidin beads and identified via mass spectrometry (Roux et.al, 2012) (Figure 5.1).

Protein fatty acid acylations are a group of dynamic post translational modifications which affect protein stability, trafficking and interaction with the plasma membrane (Hannoush 2015). Palmitoylation acts as an anchor for proteins to attach to the plasma membrane as well as a plasma membrane trafficking signal, as many membrane associated proteins are palmitoylated at the Golgi then trafficked to the plasma membrane (Rocks et al. 2010). The two most common fatty acid modifications are S-Palmitoylation and N-myristoylation. S-Palmitoylation is the attachment of a 16 carbon fatty acid chain onto a free cysteine residue (by a thioester bond) while N-myristoylation involves the addition of a 14 carbon fatty acid chain (Hannoush 2015) to the N terminal glycine (Farazi, Waksman, and Gordon 2001). The 23-palmitoyltransferase (PAT) enzymes in humans catalyse protein palmitoylation of cytoplasmic and membrane bound proteins. The second family of PAT's, the membrane bound O-acyl transferase (MBOAT) family catalyse the addition of palmitate and other fatty acids to lipid and protein substrates (C. C. Y. Chang, Sun, and Chang 2011). The MBOAT family members Hhat, Porcupine, and ghrelin O-acyltransferase (GOAT) are responsible for fatty acylation of secreted proteins (Buglino and Resh 2008). Hhat is required for palmitoylation of sonic hedgehog which is essential for its signalling function (Buglino and Resh 2008) and porcupine palmitoylates members of the Wnt signalling pathway which is again essential for their function as a knockout of *Porcn* in mice causes embryonic lethality due to absence of Wnt signalling (Galli et.al 2007; Gao & Hannoush, 2014).

PAT proteins all contain the catalytic zinc finger cysteine rich Asp-His-His-Cys (DHHC) domain and four transmembrane domains (Mitchell et.al 2006). Most human PAT enzymes are localised to the ER and Golgi however ZDHHC5, 2, 20, 23 and 24 are plasma membrane localised (Korycka et al. 2012). All of the PATs that have been

identified are themselves palmitoylated and it is thought that this plays a role in regulating enzyme activity and/or substrate specificity (Greaves et.al 2011; Yang et.al 2010). Recent co-expression and co- repression studies have demonstrated that most ZDHHCs can palmitoylate a broad range of substrates with a few showing more specificity. For example depletion of ZDHHC3 or ZDHHC17 was required to reduce palmitoylation of synaptosomal-associated protein of 25kDa (SNAP25) however co-repression of ZDHHC3, 5, 9 and 17 was required to reduce palmitoylation of the STREX domain of BK potassium transport channel in HEK293 cells (Huang et al., 2009; Tian, et.al 2010). These studies demonstrate that in cell types that express multiple ZDHHCs it is possible for functional redundancy to exist and that a regulated array of multiple ZDHHCs are likely required for proper regulation of protein palmitoylation in cells.

ZDHHC5 is ubiquitously expressed across multiple tissues with high expression observed in testes, brain and lung (Human Protein Atlas, https://www.proteinatlas.org/ENSG00000156599-ZDHHC5/tissue). ZDHHC5 has been shown to be enriched in the brain and to localise to synaptic membranes. Multiple neuronal substrates have been identified including Flotillin2, glutamate receptor interacting protein 1 (GRIP1), postsynaptic density 95kDa (PSD-95) and δ-catenin and mice homozygous for a hypomorphic null *ZDHHC5* allele have defects associated with hippocampal learning, supporting the view that *ZDHHC5* has an important role in neurons (Brigidi et al., 2014; Li et al., 2010; Li, Martin et.al 2012; Thomas et.al 2012). Photoreceptor enriched expression of *ZDHHC5* has been recently demonstrated by comparison of the gene expression profiles from WT and aryl hydrocarbon receptor interacting protein like 1 *(Aipl1)* knockout mice. *Aipl1* knockout mice develop a retina devoid of photoreceptors, *ZDHHC5* expression was reduced > four fold in these mice compared to WT (Murphy et.al 2016).

The mechanism by which ZDHHC5 recognises substrates is not well understood but has been shown to involve both the PDZ binding domain and the disorganised C-tail region. Palmitoylation of PSD-95 by ZDHHC5 was shown to be dependent on ZDHHC5's PDZ domain however pulldown experiments using ZDHHC5 truncations demonstrated that the C-terminal tail only was required for recognition of PLM and for palmitoylation of Flotillin 2 (Howie et al. 2014; Yi Li et al. 2010). A recent study in hippocampal neuron cells demonstrated that upon neuronal stimulation ZDHHC5 is dynamically trafficked within the cell. Brigidi et.al demonstrated that under non-

stimulated conditions ZDHHC5 is anchored at the postsynaptic membrane through interaction with PSD-95, Fyn and adaptor complex 2 (AP2) (a protein that inhibits endocytosis). Upon neuronal stimulation Fyn phosphorylates ZDHHC5 reducing its affinity for AP2 leading to dissociation, which causes endocytosis of ZDHHC5 and trafficking to dendritic shafts allowing it to come into close contact with its substrate δ- catenin. ZDHHC5 palmitoylates δ-catenin and traffics with it to the synaptic membrane. This activity-regulated trafficking of ZDHHC5 demonstrates that the localisation of ZDHHC5 and its substrates are tightly regulated and can be co-dependant (Brigidi et.al 2015) eluding to the possibility ZDHHC5 may have roles in trafficking substrates as well as palmitoylating them.

RP2 localisation in cells is controlled by the addition of two post translational acylations, myristoylation at Glycine 2 (G2) and palmitoylation at Cysteine 3 (C3) (Chapple et al. 2000). WT RP2 localises to the plasma membrane of cells, however, mutation of C3 prevents palmitoylation therefore RP2 cannot anchor to the cell membrane and becomes localised within the cytoplasm on intracellular membranes (Chapple et al. 2000). Mutation of G2 results in RP2 failing to be myristoylated or palmitoylated and results in nuclear and cytoplasmic localisation of RP2, (Chapple et al. 2000) thought to be due to the presence of a NLS-like signal on RP2's N terminus (Hurd et.al, 2011). Mutations of both C3 and G2 have been identified in patients (Jayasundera et al. 2010) confirming that these post translational modifications are essential for normal RP2 function and that the mechanisms which regulate RP2 post translational modifications are relevant to disease pathology.

Figure 5. 1 Application of BIO-ID Method to the study of RP2 *in vitro*

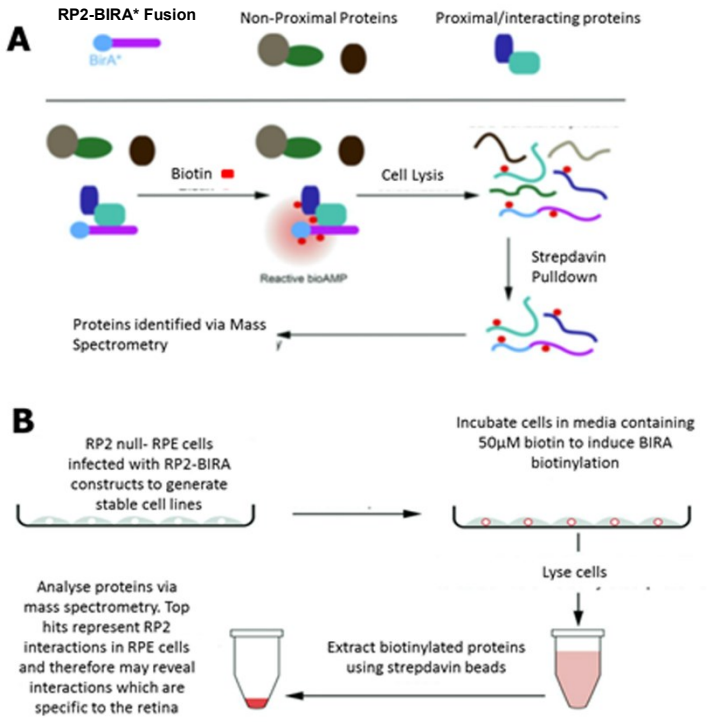

(A) Model of BIO-ID method using RP2-BIRA fusion protein. RP2-BIRA and BIRA only control constructs were transfected into cells. Upon addition of biotin to the cell culture media BIRA biotinylated interacting and proximal proteins.

(B) BIO-ID method workflow. RP2 null RPE1 cells were infected with RP2-BIRA retroviral constructs to generate stable cell lines. Cells were then incubated in media containing 50µM biotin to induce BIRA biotinylation. Proteins were then isolated by lysis and pulldown with streptavidin beads and identified by mass spectrometry.

Figure adapted from Roux et.al 2012

5.2 Identification and Conformation of Interaction between ZDHHC5 and RP2

5.2.1 Generation and Validation of RP2-BIRA and BIRA RPE1 RP2 Null Cell Lines

A BIO-ID assay was initially designed to identify interactors of RP2 WT as well as interactors of RP2 proteins carrying the human pathogenic mutations RP2 E135G, RP2 R211L, RP2 C3S and RP2 G2A in the hopes of identifying novel interactors which are relevant to disease pathogenesis. To generate RP2 BIRA cell lines for the BIO-ID assay RP2-BIRA retroviral constructs were firstly prepared. The initial step involved the generation of a retroviral construct carrying the BIRA (R118G) mutation. PCR amplification was used to generate a PCR product which contained BIRA (R118G) with a Myc tag, to enable easy detection of expression via western blot and immunofluorescence, and BamH1 and EcoR1 restriction sites. This product was ligated into the PQCXIN plasmid via the BamH1 and EcoR1 restriction sites. PQCXIN is a retroviral construct that carries a neomycin selection marker (G418), allowing infected cells to be cultured in G418 containing media to select for cells expressing the construct. RP2 pEntry plasmids containing RP2 WT and RP2 point mutations, RP2 E135G, RP2 R211L, RP2 C3S, RP2 G2A were used as templates and a PCR strategy was used to produce products containing each RP2 sequence and Not1 and Pac1 restriction sites. As the PQCXIN- BIRA (R118G)- Myc plasmid also contained Not1 and Pac1 restriction sites, digestion then ligation of sticky ended products produced PQCXIN- BIRA (RG118)-Myc constructs containing RP2 WT, RP2 E135G, RP2 R211L, RP2 C3S and RP2 G2A sequences. These constructs were transfected into HEK293- ET cells to generate virus which was used to infect RP2 null RPE cells which produced the RP2 BIRA cell lines used in this assay.

As it is not possible to culture photoreceptor cells *in vitro* RPE cells were used. The RPE is the single layer of cells which function to convert retinyl esters to 11-cis retinal and to engulf the OS of photoreceptors during daily photoreceptor disc renewal (Moiseyev et.al 2005; Redmond. et al., 1998). Some inherited retinal degenerations are caused by mutations in genes exclusively expressed in the RPE such as *RPE65* mutations which cause Leber Congenital Amaurosis (LCA). As RP2 is expressed in the RPE it is possible that in XLRP attributed to RP2 mutation some component of pathogenesis may be related to dysfunction of RP2 in the RPE, therefore interactors identified in these cells may be relevant to disease pathogenesis. RP2 null RPE cells

were used in order to avoid any contamination from endogenous RP2. RP2 null RPE cells were made as described ((Lyraki et al. 2018).

To confirm that RP2 WT-BIRA, RP2 E135G-BIRA, RP2 R211L-BIRA, RP2 G2A-BIRA, RP2 C3S-BIRA and BIRA RP2 Null Cell lines could be used to identify potential interactors of RP2 via BIO-ID, I first assessed whether RP2-BIRA fusion constructs and BIRA were expressed and whether they were capable of biotinylating proteins (Figure 5.2 A, B). RP2 WT-BIRA, RP2 E135G-BIRA, RP2 R211L- BIRA, RP2 G2A – BIRA, RP2 C3S-BIRA and BIRA only RP2 null RPE1 cells were grown to confluence then treated with or without 50μM biotin for 24 hours. These cells were then lysed and immunoblotted for Myc tag to confirm expression of the BIRA constructs (Figure 5.2 A). Streptavidin HRP was used to visualise the presence of biotinylated proteins (Figure 5.2 A). These blots demonstrated that the RP2-BIRA fusion proteins and BIRA were expressed and the proteins were of the expected size (Figure 5.2 A). Streptavidin-HRP blotting demonstrated that the RP2-BIRAs and BIRA biotinylated proteins in the presence of 50μM biotin and not when biotin was absent from the media (Figure 5.2 A). Stronger streptavidin HRP signal was present in the BIRA only cells compared to the RP2-BIRA fusion construct expressing cells, suggesting the RP2-BIRA fusions were only biotinylating a subset of proteins in the cell. Encouragingly, there was also a distinct streptavidin- HRP band at ~70kDa in all the RP2-BIRA lysates; this is the same molecular weight as the RP2-BIRA fusions suggesting that the RP2-BIRAs were biotinylating themselves, which was expected as BIRA can only biotinylate proteins within a 10nm radius (Figure 5.2 A).

In order to confirm that the RP2-BIRA fusion was localised to the same regions in the cell as endogenous RP2, RP2 WT-BIRA, RP2 E135G- BIRA, RP2 R211L-BIRA, RP2 G2A-BIRA, RP2 C3S-BIRA and BIRA only RPE1 cells were treated with or without 50μM biotin (as above), fixed and stained with anti-Myc, to visualise the localisation of BIRA fusions, and streptavidin -Alexa 594 to visualise the localisation of biotinylated proteins (Figure 5.2 B). Immunofluorescence for the Myc tag demonstrated that RP2 WT-BIRA, RP2 E135G-BIRA and RP2 R211L-BIRA were localised at the plasma membrane, as is RP2 WT (Chapple et al. 2000). RP2 C3S-BIRA and RP2-G2A BIRA were localised to the ER and internal membranes and nucleus in line with the previously described localisation of these mutants (Chapple et al. 2000). Localisation of constructs was unchanged upon addition of biotin and BIRA was diffusely localised throughout the cell in the presence and absence of 50μM biotin. The streptavidin-HRP

conjugate again confirms the presence of biotinylated proteins only upon the addition of biotin to the cell culture media. The co-localisation between the Myc tag and streptavidin-594 confirmed that biotinylated proteins were present where the RP2-BIRA fusion constructs and BIRA were expressed (Figure 5.2 B).

Figure 5. 2 Validation of RP2 WT- BIRA, RP2 E135G-BIRA, RP2 R211L- BIRA, RP2 G2A-BIRA, RP2 C3S-BIRA and BIRA Only RP2 null RPE Cells

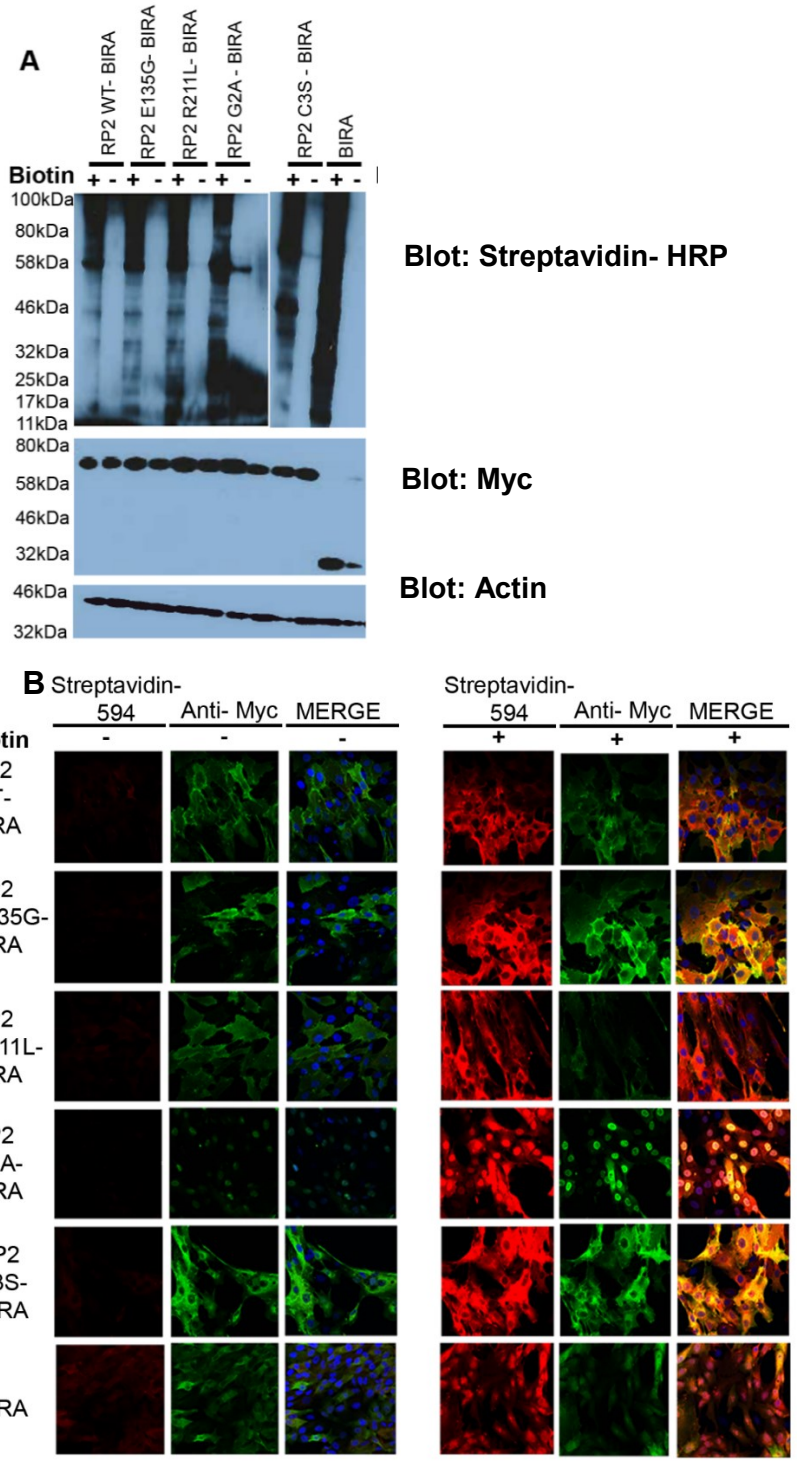

(A) RP2 WT- BIRA, RP2 E135G-BIRA, RP2 R211L- BIRA, RP2 G2A-BIRA, RP2 C3S –BIRA and BIRA only RP2 null RPE cells were grown to confluence and treated with (+) or without (-) 50μM biotin for 24 hours prior to lysis. Cell lysates were analysed for the presence of biotinylated proteins by immunoblotting with streptavidin-HRP. Biotinylated proteins were detected in the biotin treated lysates and minimally in the untreated lysates. The presence of some bands in the RP2 G2A and RP2 C3S (–) biotin samples represents background levels of activity in BIRA*. Lysates were immunoblotted with anti-Myc antibody to analyse expression of RP2-BIRA and BIRA only. All the RP2-BIRA lysates had a band correlating to the molecular weight of RP2-BIRA fusion ~70kDa and the BIRA only lysates had a band ~30kDa correlating with the molecular weight of BIRA.

(B) Representative images of RP2 WT- BIRA, RP2 E135G-BIRA, RP2 R211L-BIRA, RP2 G2A-BIRA, RP2 C3S–BIRA and BIRA immunofluorescence analysis for the presence of biotinylated proteins and expression of RP2-BIRA or BIRA. Cells were cultured to confluence and treated with (+) or without (-) 50μM biotin 24 hours prior to fixation. The presence of biotinylated proteins was visualised using streptavidin- 594 conjugate. In the absence of biotin no streptavidin-594 staining was observed in any cell line. Cells treated with biotin had streptavidin -594 staining showing the presence of biotinylated proteins. Anti-Myc was used to visualise localisation of RP2-BIRA fusion construct and BIRA. RP2 WT-BIRA, RP2 E135G-BIRA and RP2 R211L- BIRA localised to the plasma membrane with some signal in the cytoplasm. RP2 G2A –BIRA localised to the nucleus. RP2 C3S-BIRA localised within the cytoplasm. BIRA had a diffuse localisation throughout the cell. Merge images show that green and red channels overlap demonstrating that biotinylated proteins are present in regions of the cell where RP2-BIRA fusions and BIRA are expressed.

5.2.2 BIO-ID Assay and Conformation of ZDHHC5-RP2 Interaction

After generation of RP2 WT-BIRA, RP2 E135G-BIRA, RP2 R211L-BIRA, RP2 G2A-BIRA and RP2 C3S-BIRA RP2 null RPE cell lines, to ease identification of novel potential interactors, that interact specifically with RP2 and not with BIRA, the BIO-ID assay was performed in only RP2 WT–BIRA (from here on RP2-BIRA), BIRA and RP2 null RPE cells (Figure 5.3). Conformation of expression and function of RP2-BIRA fusion construct and BIRA only was confirmed by western blot for streptavidin-HRP and the Myc Tag (as before) (Figure 5.3 B). Expression and function of RP2-BIRA and BIRA was confirmed by immunofluorescence analysis of streptavidin- Alexa 594 and the Myc Tag (as before) (Figure 5.3 C).

The BIO-ID assay was performed in triplicate and involved treating confluent RP2-BIRA, BIRA and RP2 null RPE cells with 50μM biotin 24 hours prior to lysis. Cells were lysed in RIPA buffer to solubilise all proteins in the cell. Lysates were then incubated with streptavidin beads for 1 hour to isolate biotinylated proteins. Biotinylated proteins were identified by mass spectrometry. To establish potential candidate RP2 interactors over proteins non-specifically biotinylated by BIRA*, proteins were sorted such that any hit that was ≥ 5-fold enriched in the RP2-BIRA lysates compared to the BIRA only lysate and absent in the parental control cell line was considered. This provided a list of ~60 proteins the top 15 of which are listed in Table 5.1. As expected RP2 was the top hit with known interactor ARL3 also detected as one of the top hits. ZDHHC5 was detected only in the RP2-BIRA lysates and not in the BIRA or the RP2 null RPE1 parental cell line control (Table 5.1). ZDHHC5 is a PAT which is localised to the plasma membrane in cells (Korycka et al. 2012). RP2 is known to be palmitoylated and this is thought to be essential for its function and as the mechanisms which regulate RP2 palmitoylation are yet to be identified I decided to investigate this hit further.

In order to confirm RP2-ZDHHC5 interaction in cells RP2-BIRA and BIRA only cells were treated with 50μM biotin to facilitate biotinylation of proteins. Streptavidin beads were used to isolate biotinylated proteins and lysates were immunoblotted for ZDHHC5 (Figure 5.3 D). ZDHHC5 was detected only in the RP2-BIRA lysate and not in the BIRA only lysate confirming ZDHHC5 was interacting specifically with RP2 and not the BIRA. The localisation of RP2 and ZDHHC5 was analysed in HeLa cells transfected with V5 tagged RP2 and HA tagged ZDHHC5. Immunofluorescence of

the V5 and HA tags demonstrated that ZDHHC5 and RP2 are localised to the plasma membrane in HeLa cells, strong co-localisation of the V5 and HA signals was detected at the plasma membrane (Figure 5.3. E).

Figure 5. 3 Conformation of RP2-ZDHHC5 Interaction

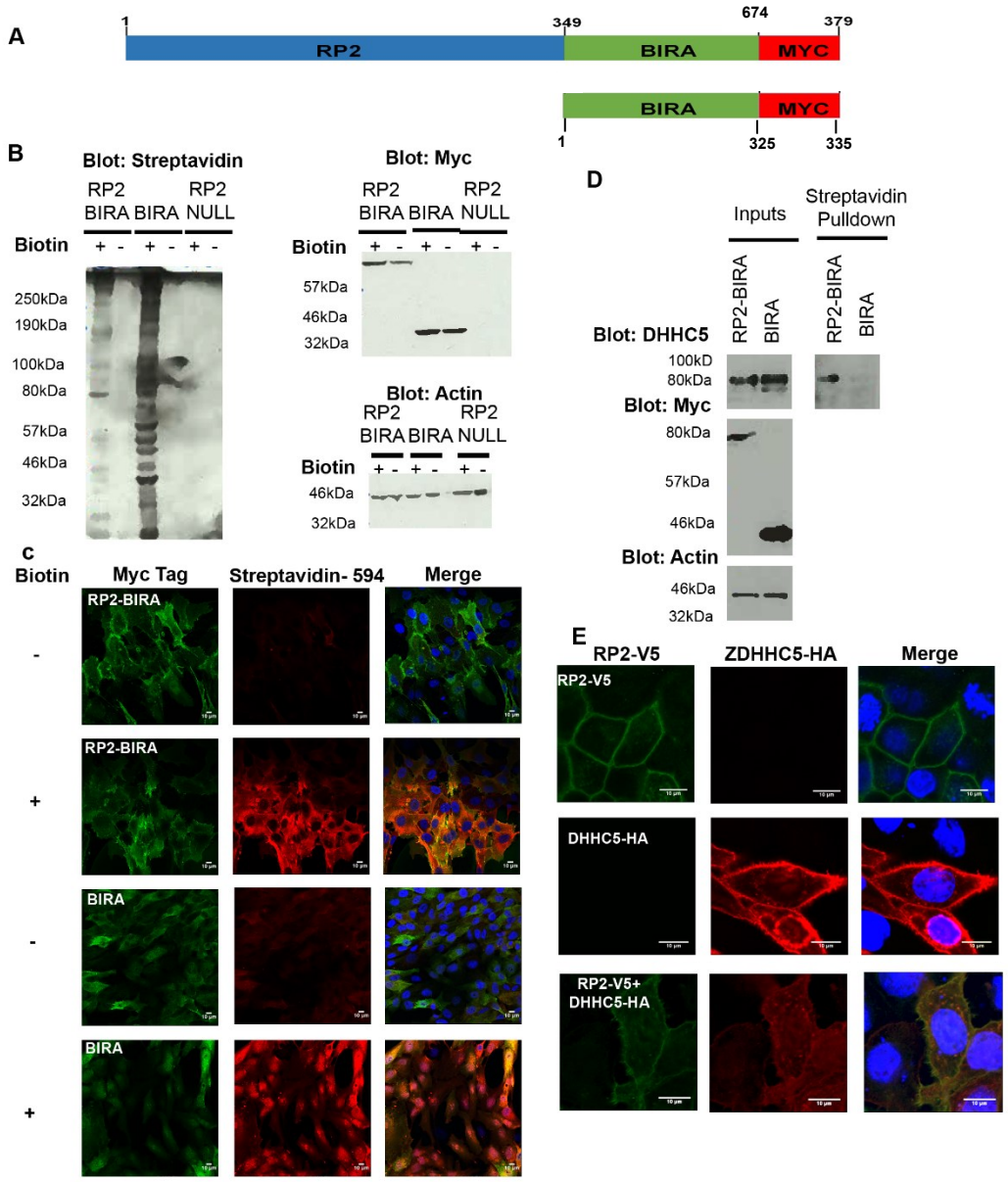

(A) Schematic of RP2-BIRA and BIRA constructs. Stable cell lines were generated using retroviral transfection of these constructs into RP2 Null RPE1 cells.

(B) Validation of RP2-BIRA and BIRA Cell Lines. RP2-BIRA, BIRA and parental RP2 Null RPE1 cells were treated with 5µm biotin (+) or without (-) for 24 hours. After lysis and electrophoresis, membranes were blotted with Streptavidin HRP to visualise the presence of biotinylated proteins. Biotinylated proteins were detected in the RP2-BIRA and BIRA (+) lanes and not the RP2-BIRA, BIRA (-) lanes or in the parental RPE1 RP2 Null cell line. Lysates were also immunoblotted for the presence of Myc tag.

(C) Immunofluorescence images of RP2-BIRA and BIRA cell lines. Cells were cultured in + or – biotin conditions for 24hrs prior to fixation. Myc Tag immunofluorescence (green channel) shows the localisation of the RP2-BIRA and BIRA constructs in cells. Streptavidin- 594 conjugate was used to visualise the presence of biotinylated proteins. Cells cultured with biotin have intense streptavidin 594 staining demonstrating the presence of biotinylated proteins. Co-localisation of red and green channels was observed indicating biotinylation of proteins is specific to regions where the BIRA constructs are localised.

(D) Streptavidin pulldown of RP2-BIRA RPE1 cells. RP2-BIRA and BIRA RPE1 cells were treated with Biotin for 5hrs to allow biotinylation of proteins. Lysates were incubated with streptavidin beads for 1 hour and immunoblotted for ZDHHC5. ZDHHC5 was biotinylated in the RP2-BIRA sample not the BIRA sample, demonstrating ZDHHC5 was specifically interacting with RP2-BIRA not BIRA alone.

(E) RP2-V5 and ZDHHC5-HA colocalisation in HeLa cells. Representative immunofluorescence images of V5 and HA staining show RP2-V5 and ZDHHC5-HA colocalised at the plasma membrane of HeLa cells.

Table 5. 1 BIO-D Assay Top Candidate RP2 Interactors

Protein Name	Protein ID	Q Value	Score	Control LFQ Intensity	BirA Only LFQ Intensity	RP2-BirA LFQ Intensity	RP2-BirA/Control Ratio	RP2-BirA/BirA Ratio
RP2	O75695	0	80.338	0.00E+00	4.73E+06	6.89E+08	-	145.75
PLCB1	Q9NQ66	0	50.835	0.00E+00	0.00E+00	5.00E+07	-	-
FERMT2	Q96AC1	0	36.639	0.00E+00	6.44E+05	4.75E+07	-	73.68
ITGB1	P05556	0	35.236	0.00E+00	6.32E+06	1.01E+08	-	15.97
ARL3	P36405	0	28.114	0.00E+00	0.00E+00	7.21E+06	-	-
EPB41L5	Q9HCM4	0	23.983	0.00E+00	0.00E+00	2.07E+07	-	-
TMEM237	Q96Q45	0	22.999	0.00E+00	3.26E+06	4.58E+07	-	14.07
GBE1	Q04446	0	15.957	0.00E+00	0.00E+00	4.40E+07	-	-
SNAP23	O00161	0	11.853	0.00E+00	8.47E+05	1.39E+07	-	16.37
CIRBP	Q14011	0	6.504	0.00E+00	0.00E+00	3.38E+06	-	-
RASA3	Q14644	0	6.2244	0.00E+00	6.48E+05	1.39E+07	-	21.47
STK10	O94804	0	5.458	0.00E+00	0.00E+00	7.15E+06	-	-
FABP5	Q01469	0	4.7829	0.00E+00	0.00E+00	7.08E+06	-	-
ZDHHC5	Q9C0B5	0	4.7191	0.00E+00	0.00E+00	3.63E+06	-	-

Top hits were calculated as any protein more that 5-fold enriched over the BIRA sample and not present in the RP2 null RPE parental cell line control. RP2 was the top hit as expected. ZDHHC5 was absent in both the BIRA only and parental cell line controls demonstrating it was specifically interacting with RP2 not BIRA.

5.3 ZDHHC5 is not required for RP2 Palmitoylation

As RP2 is palmitoylated and ZDHHC5 is a palmitoyltransferase, I decided to investigate whether ZDHHC5 is required for RP2 palmitoylation. To analyse the palmitoylation of RP2, the incorporation of 17-ODYA (a palmitate analogue) was analysed. HeLa cells were transiently transfected with RP2-V5. Twenty-four hours post transfection cells were incubated in fresh media supplemented with 1% fatty acid free BSA containing 100mM 17-ODYA. 17-ODYA was diluted in serum free media supplemented with 1% fatty acid free BSA so that no other fatty acids present in the media could be incorporated by proteins and therefore reduce the signal from 17-ODYA incorporation. Cells were cultured with 17-ODYA for 24 hours allowing any proteins that were palmitoylated in this time to incorporate 17-ODYA. Cells were then lysed and a V5 IP performed to isolate RP2-V5. 17-ODYA incorporation was assayed via a click chemistry reaction in which 17-ODYA was labelled with an Infrared azide dye that fluoresces in the 800nm channel. To visualise 17-ODYA incorporation these IP reactions were analysed by immunoblotting and imaged using the LICOR system. To image immunoblots on the LICOR florescent imaging system, Alexa dye conjugated secondary antibodies were used. For this assay, RP2-V5 was detected using an anti V5 primary antibody and an anti-mouse Alexa 680 secondary antibody allowing RP2-V5 to be visualised in the 700nm channel. 17-ODYA incorporation was quantified as a ratio of 800nm (green) signal/ 700nm (red) signal to normalise to the amount of RP2-V5 isolated by V5-IP. Each experiment was repeated 3 times and an average 800nm/700nm ratio was calculated for each condition.

In order to analyse whether co-expression of ZDHHC5 and RP2 increases RP2's 17-ODYA incorporation, HeLa cells were transfected with RP2-V5, ZDHHC5-HA or co-transfected with both RP2-V5 and ZDHHC5-HA and then incubated with media supplemented with 100mM 17-ODYA. When RP2- V5 and ZDHHC5- HA were co-transfected in HeLa cells no significant difference in RP2 palmitoylation was observed compared to cells where only RP2 was transfected (Figure 5.4 A, B). As HeLa cells express endogenous ZDHHC5 it is possible that this endogenous expression was enough to palmitoylate RP2 therefore to observe if reduction of ZDHHC5 perturbed RP2 palmitoylation HeLa cells were treated with siRNAs for ZDHHC5 to knockdown endogenous ZDHHC5 expression (Figure 5.4 C). Upon knockdown of ZDHHC5, no significant reduction in 17-ODYA incorporation by RP2 was observed compared to

control siRNA treated cells (Figure 5.4 C, D). These results together suggest that ZDHHC5 is not required for RP2 palmitoylation.

Figure 5. 4 Analysis of RP2 Palmitoylation

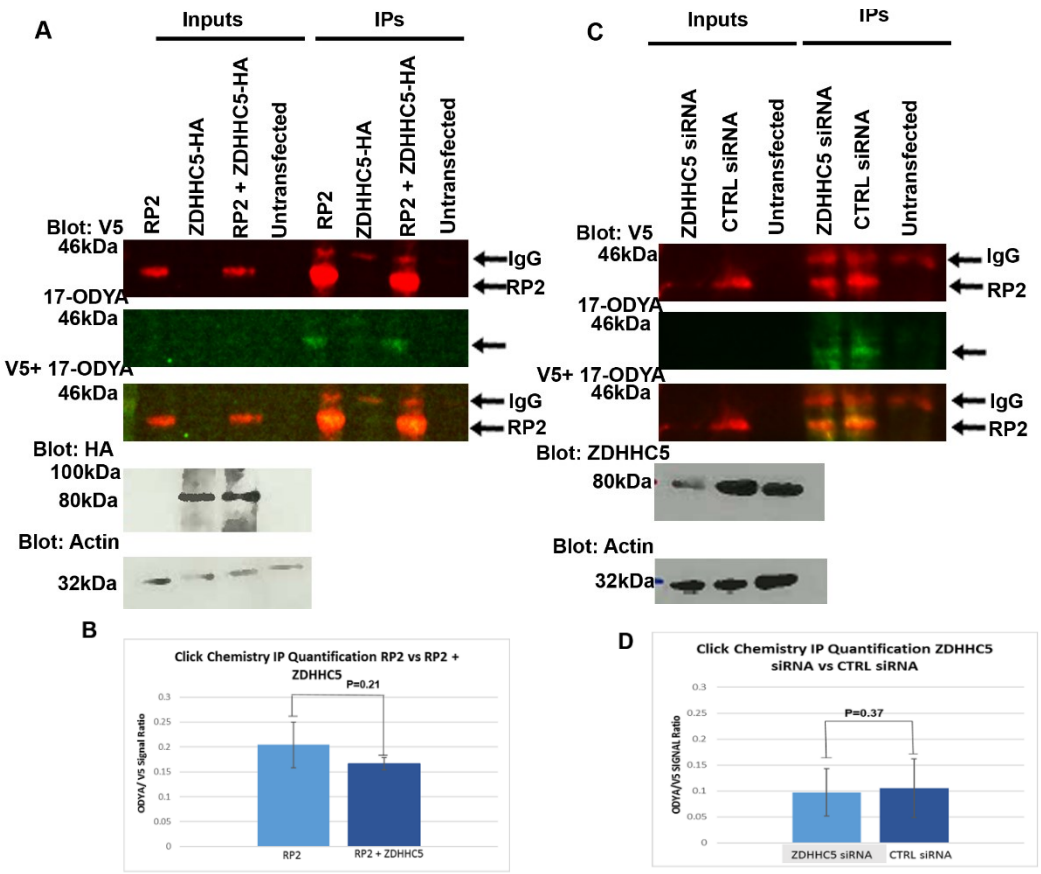

(A) HeLa Cells transiently transfected with RP2-V5 and ZDHHC5-HA were incubated with 17- ODYA overnight. Cells were lysed and a V5 COIP used to immunoprecipitate RP2 V5. A Click Chemistry reaction was used to label ODYA with an Azide dye, which fluoresces in the 800W channel to allow visualisation of RP2 palmitoylation. After electrophoresis, membranes were immunoblotted for V5 and imaged using the LICOR system. Red channel shows RP2-V5 expression, Green channel shows 17- ODYA incorporation. Input samples were immunoblotted for HA and Actin.

(B) Quantification of 17- ODYA signal in RP2 and RP2 +ZDHHC5 IP lanes. The RP2 V5 IP lane and the RP2 +ZDHHC5 COIP lane show no significant differences in 17- ODYA incorporation suggesting ZDHHC5 is not directly responsible for palmitoylation of RP2. 17- ODYA signal was normalised to V5 signal, statistical significance analysed by students T.Test n=3.

(C) HeLa cells were transfected with ZDHHC5 siRNA and CTRL siRNA to knockdown endogenous ZDHHC5. RP2-V5 was transiently transfected into these cells and analysis of palmitoylation carried out as in (A).

(D) Quantification of 17- ODYA signal in ZDHHC5 siRNA and CTRL siRNA IP lanes. No significant difference in RP2 17- ODYA incorporation was detected in the ZDHHC5 siRNA treated lane suggesting ZDHHC5 is not directly responsible for palmitoylation of RP2. Analysis and Statistics as in (B).

5.4 ZDHHC5 is required for RP2 Plasma Membrane Localisation

5.4.1 RP2 C3S and RP2 G2A Localisation with ZDHHC5 Overexpression

As ZDHHC5 was not required for RP2 palmitoylation but did interact and co-localise with RP2, ZDHHC5 and non-palmitoylated RP2 mutants, RP2 C3S and RP2 G2A, were transfected into Hela cells to establish whether they co-localised. To assess co-localisation, HeLa cells were transfected with WT RP2-V5, C3S RP2-V5, G2A RP2-V5 alone or in conjunction with ZDHHC5-HA. Cells transfected with WT RP2-V5 or ZDHHC5-HA only again confirmed WT RP2-V5 and ZDHHC5-HA were localised to the plasma membrane in HeLa cells (Figure 5.5 A, B). C3S RP2-V5 and G2A RP2-V5 localised to the cytoplasm on intracellular membranes and nucleus respectively (as previously described (Chapple et al. 2000)), when transfected alone. However, co-transfection with ZDHHC5-HA revealed RP2 C3S was present at the plasma membrane, resembling RP2 WT (Figure 5.5 A,C,D). Co-transfection of G2A RP2-V5 and ZDHHC5-HA revealed a significant reduction in cells with RP2 G2A –V5 nuclear localisation compared to G2A RP2-V5 only transfected cells, with G2A RP2-V5 localisation detected at the plasma membrane and cytoplasm (Figure 5.5 E, F, and G). To quantify the change in localisation observed in between G2A RP2-V5 only transfected cells and cells transfected with G2A RP2-V5 and ZDHHC5-HA the number of cells with purely nuclear V5 staining was counted for each condition. One hundred cells were counted in each of 3 technical replicates, and an average percentage of cells with V5 nuclear staining when G2A RP2-V5 was transfected alone or with ZDHHC5 was calculated (Figure 5.5 G) and a significant reduction was detected. This demonstrated that ZDHHC5 overexpression rescued the mistrafficking of RP2 mutants associated with loss of palmitoylation or myristoylation.

Figure 5. 5 Localisation of RP2 C3S and RP2 G2A with ZDHHC5 Overexpression

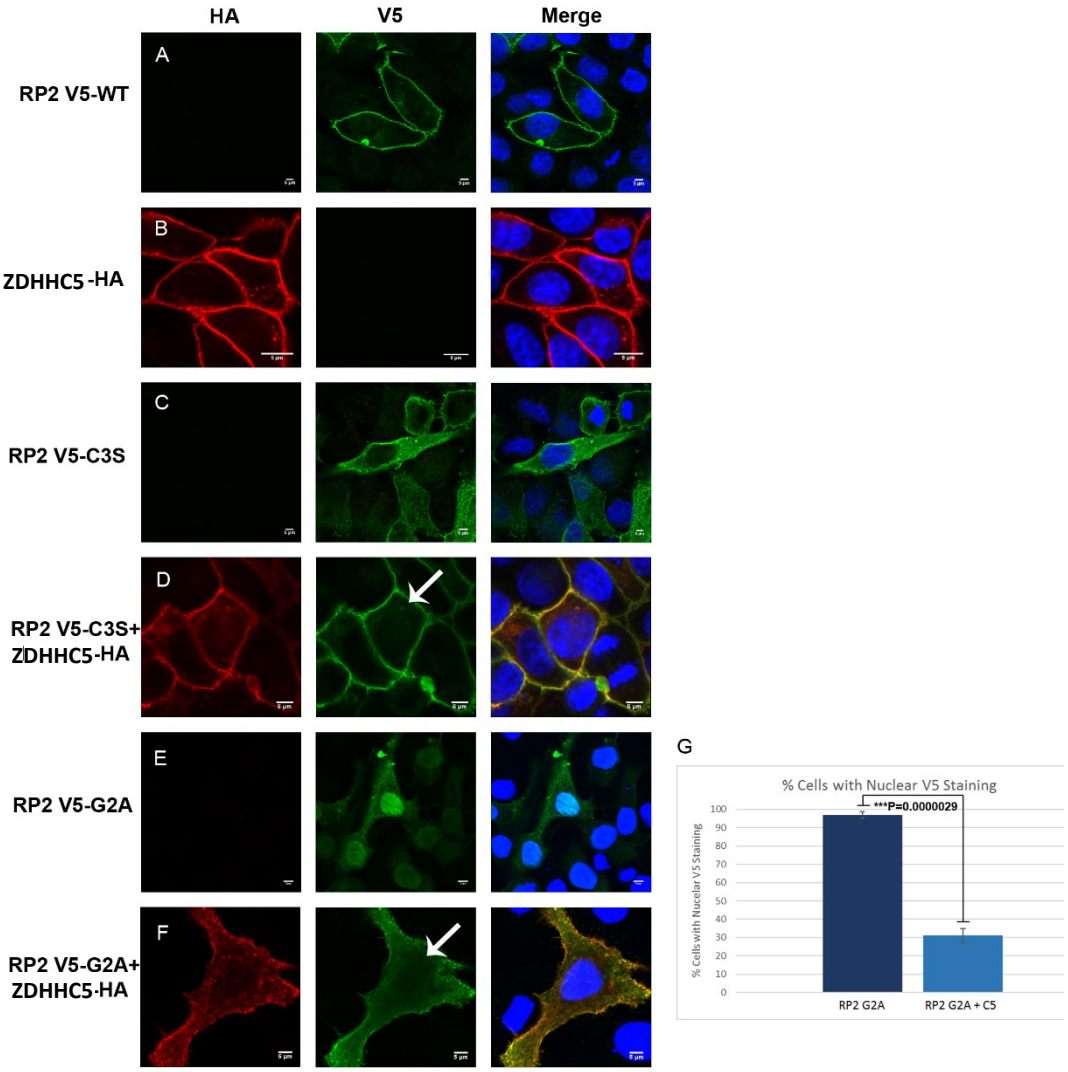

(A) WT RP2-V5 is localised to the plasma membrane of HeLa cells.
(B) ZDHHC5-HA is localised to the plasma membrane of HeLa Cells.
(C) C3S RP2-V5 is localised in the cytoplasm of HeLa cells.
(D) Co-expression of C3S RP2-V5 (green) and ZDHHC5-HA (Red) rescues the localisation of C3S RP2-V5 back to the plasma membrane.
(E) G2A RP2- V5 is localised within the nucleus of HeLa cells.
(F) Co-expression of G2A RP2-V5 (green) and ZDHHC5-HA (red) leads to loss of nuclear localisation of RP2 G2A and an enrichment at the plasma membrane.
(G) Quantification of nuclear localisation in G2A RP2- V5 and ZDHHC5-HA co-transfected cells. Cells co-expressing G2A RP2- V5 and ZDHHC5-HA have significantly less cells with V5 nuclear immunostaining than G2A RP2-V5 only cells. Statistical analysis by students 100 cells counted for each condition over 3 repeats T.Test *P ≤0.05, **P ≤0.01, ***P ≤ 0.001.

5.4.2 Rescue of Mistrafficking does not Requires ZDHHC5 Catalytic Activity

In order to assess whether the ability of ZDHHC5 to rescue mistrafficking of RP2 C3S and RP2 G2A required ZDHHC5 catalytic activity, I transfected HeLa cells with C3S RP2-V5, G2A RP2-V5 only or with catalytically dead ZDHHC5 (ZDHHS5-HA) and the localisation of C3S RP2- V5 and G2A RP2- V5 was analysed. The DHHC domain is required for the catalytic activity of ZDHHC's as it is thought to be directly involved in the palmitoyl transfer reaction. Therefore mutation of the catalytic cysteine residue to a serine generates a catalytically dead ZDHHC (Mitchell et al. 2006). Transfection of ZDHHS5-HA only revealed ZDHHS5-HA was also localised to the plasma membrane in HeLa cells similar to the wild type (Figure 5.6 A). Co-transfection of C3S RP2-V5 and ZDHHS5-HA displayed C3S RP2-V5 localised to the plasma membrane, demonstrating ZDHHC5 catalytic activity is not required for rescue of mistrafficking (Figure 5.5 C). Similarly, co-transfection of G2A RP2-V5 and ZDHHS5-HA revealed significantly less cells with G2A RP2-V5 nuclear staining compared to G2A RP2-V5 only transfected cells, with G2A RP2-V5 localised to the plasma membrane and cytoplasm (Figure 5.6 D, E,F). To quantify rescue of mistrafficking the percentage of cells containing V5 nuclear only staining was counted when G2A RP2-V5 was transfected alone and when G2A RP2-V5 and ZDHHC5 were co-transfected. This assay was repeated 3 times and 100 cells per replicate were counted after which an average percentage of cells with V5 nuclear staining in each case was calculated (Figure 5.6 G). This data showed that catalytic activity of ZDHHC5 is not required for RP2 trafficking.

Figure 5. 6 Localisation of RP2 C3S and RP2 G2A with ZDHHS5 Overexpression

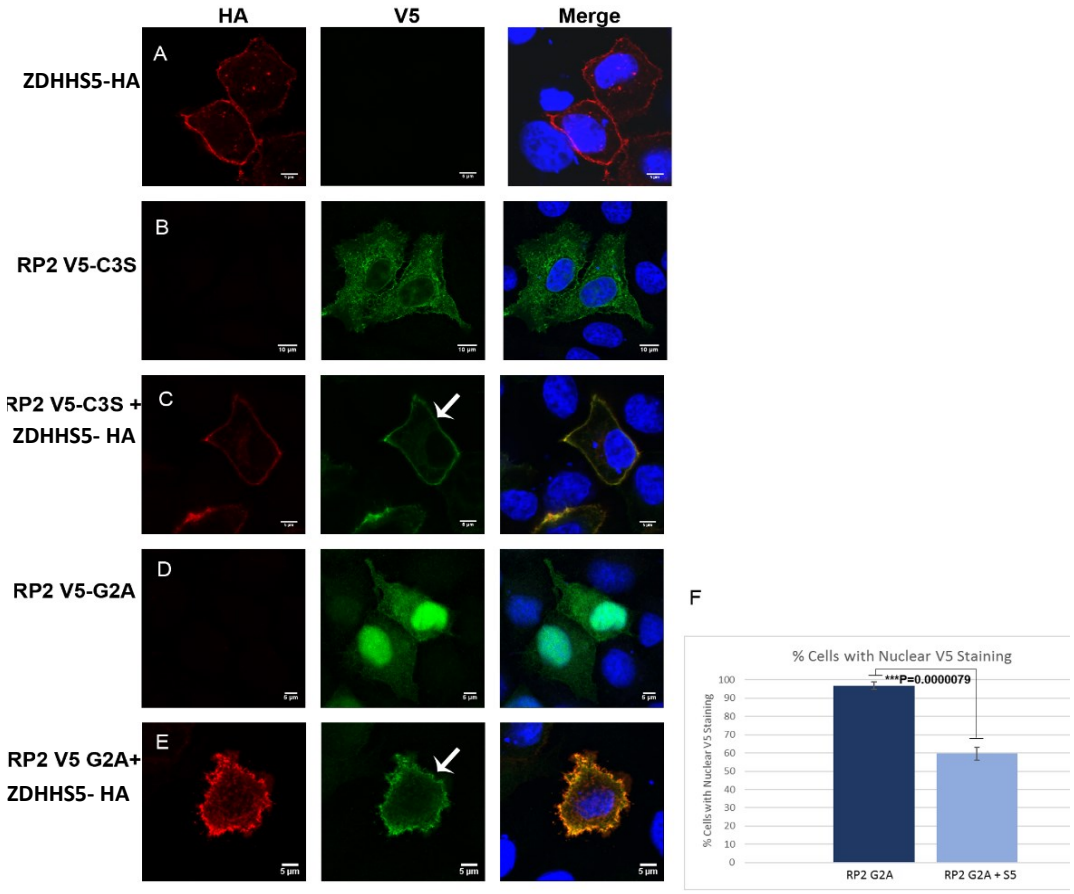

(A) ZDHHS5-HA is localised to the plasma membrane of HeLa Cells.
(B) RP2-C3S- V5 is localised in the cytoplasm of HeLa cells.
(C) Co-expression of C3S RP2-V5 (green) and ZDHHS5-HA (Red) rescues the localisation of RP2-C3S back to the plasma membrane.
(D) G2A RP2- V5 is localised within the nucleus of HeLa cells.
(E) Co-expression of G2A RP2-V5 (green) and ZDHHS5-HA (red) leads to loss of nuclear localisation of RP2 G2A and an enrichment at the plasma membrane.
(F) Quantification of nuclear localisation in G2A RP2- V5 and ZDHHS5-HA co-transfected cells. Cells co-expressing G2A RP2-V5 and ZDHHS5-HA have significantly less cells with V5 nuclear immunostaining than G2A RP2- V5 only cells. Statistical analysis by students T.Test 100 cells counted for each condition per replicate *P ≤0.05, **P ≤0.01, ***P ≤ 0.001.

5.4.3 ZDHHC5 Knockdown Changes RP2 Localisation in Cells

After establishing ZDHHC5 could rescue mistrafficking of RP2 C3S and RP2 G2A the effect of ZDHHC5 expression on RP2 WT localisation was examined. To ascertain if ZDHHC5 has a role in trafficking RP2 to the plasma membrane, I knocked down expression of endogenous ZDHHC5 in HeLa cells using siRNAs and the localisation of WT RP2-V5 was observed. HeLa cells were transfected with siRNAs targeting ZDHHC5 or control scrambled siRNAs and successful knockdown was confirmed by immunoblot for ZDHHC5 (Figure 5.7 B), 48 hours post knockdown cells were transiently transfected with WT RP2-V5. Immunofluorescence of V5 revealed that in cells treated with CTRL siRNA, WT RP2-V5 localised exclusively to the plasma membrane, however, in cells treated with ZDHHC5 siRNAs WT RP2-V5 had a more cytoplasmic localisation (Figure 5.7 A, C). Quantification of the percentage of cells that had exclusive WT RP2-V5 membrane localisation when transfected with CTRL siRNA vs ZDHHC5 siRNA confirmed knockdown of ZDHHC5 reduces WT RP2-V5 membrane localisation (Figure 5.7 C). This suggests that ZDHHC5 could play a role in trafficking RP2 to the cell membrane. In the human retina RP2 has been reported to localise to the plasma membrane of rods and cones (Grayson et al. 2002) therefore as ZDHHC5 is also expressed in photoreceptors (Murphy et al., 2016) it is possible that ZDHHC5 may play a role in trafficking RP2 *in vivo*.

Figure 5. 7 ZDHHC5 Knockdown Effects WT RP2-V5 Localisation in HeLa Cells

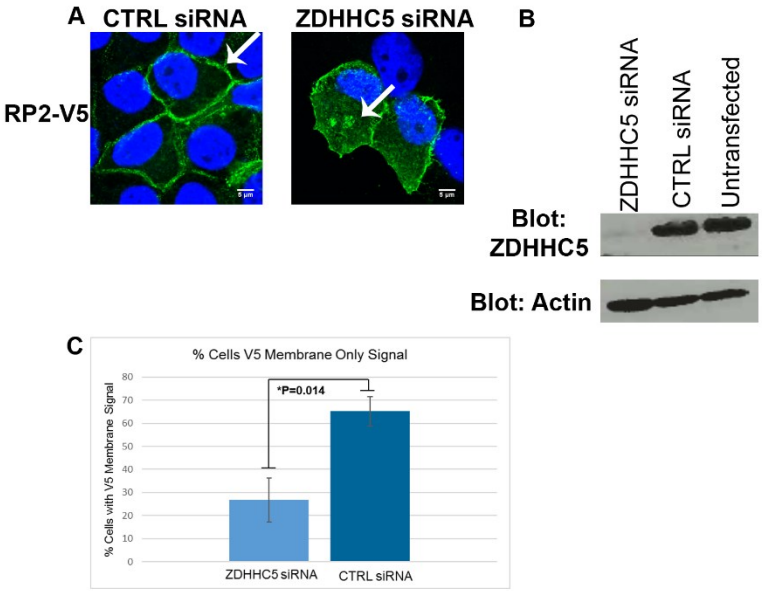

(A) Representative images of V5 immunostaining in ZDHHC5 siRNA treated and CTRL siRNA treated HeLa cells. Knockdown of ZDHHC5 leads to increased intracellular localisation of RP2-V5.

(B) Immunoblot of ZDHHC5 siRNA and CTRL siRNA treated lysates for ZDHHC5 expression. ZDHHC5 expression is absent in the ZDHHC5 siRNA treated lysates demonstrating efficient knockdown of endogenous ZDHHC5.

(C) Quantification of RP2-V5 localisation in ZDHHC5 siRNA treated cells and CTRL siRNA treated cells. Cells treated with ZDHHC5 siRNA have significantly less cells with RP2-V5 membrane localisation. Statistical analysis by students T.Test 100 cells counted for each condition per replicate *P ≤0.05, **P ≤0.01, ***P ≤ 0.001.

5.5 ZDHHC5 Knockdown Reduces Ciliogenesis in RPE1 Cells

Given that ZDHHC5 had a role in regulating RP2 localisation I investigated whether knockdown of ZDHHC5 influenced other palmitoylated proteins. It has been calculated that a large proportion of cilia proteins are palmitoylated. Roy et.al used Swisspalm, a database of palmitoylated proteins, and found that 35% of high confidence (Tier 1) cilia proteins are palmitoylated and 32% of Tier 2 cilia proteins were also found to be palmitoylated (Roy et al. 2017). Therefore, to establish if ZDHHC5 has a role related to cilia proteins, ZDHHC5 was knocked down using siRNAs in RPE cells and the effect on ciliogenesis was analysed. WT RPE1 cells were used for these assays as they undergo efficient ciliogenesis when serum starved. These cells were transfected with either ZDHHC5 siRNAs to knockdown endogenous ZDHHC5 or CTRL scrambled siRNAs. 48 hours post transfection cells were either lysed and analysed for ZDHHC5 expression by western blot to confirm knockdown (Figure 5.8 B) or incubated in serum free media to induce ciliogenesis. After growth in serum free media for 24 hours, cells were fixed and stained for the cilia markers acetylated tubulin and ARL13b. Cells transfected with ZDHHC5 siRNA produced significantly less cilia than cells treated with CTRL siRNA (Figure 5.8, C). The length of the cilia that was produced in ZDHHC5 knockdown cells was measured and was found to be equivalent in length to those produced by CTRL siRNA treated cells (Figure 5.8, D).

Figure 5. 8 ZDHHC5 Reduces Ciliogenesis in RPE1 Cells

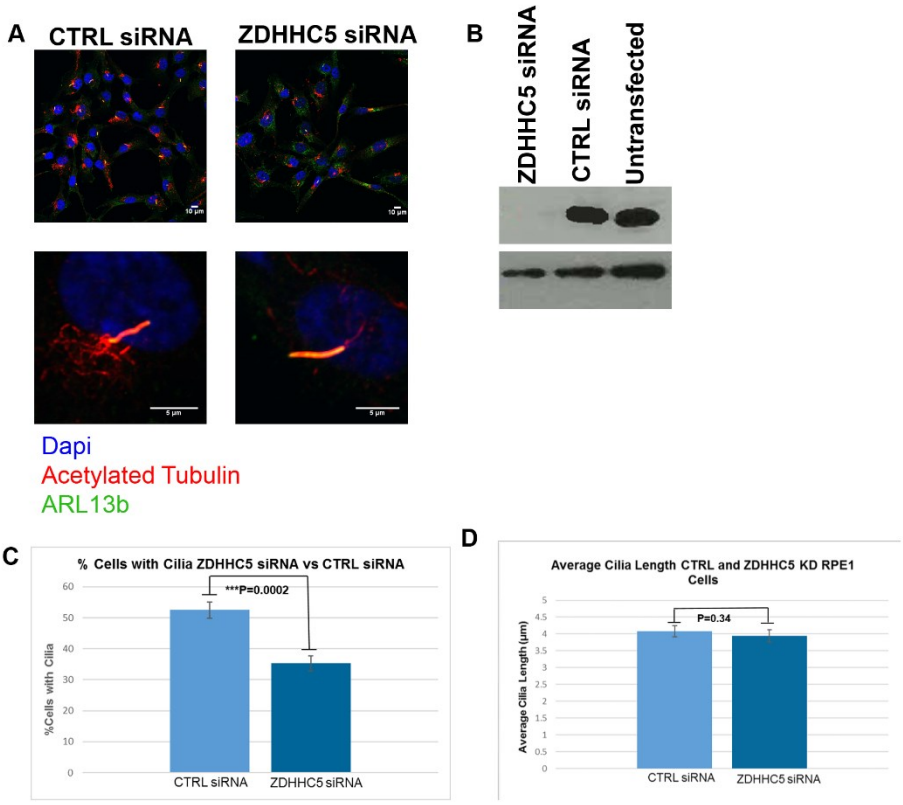

(A) Representative images of acetylated tubulin and ARL13b immunostaining in CTRL and ZDHHC5 siRNA treated RPE1 cells. Knockdown of ZDHHC5 does not prevent ciliogenesis.

(B) Immunoblot of ZDHHC5 siRNA and CTRL siRNA treated lysates. ZDHHC5 is absent in the ZDHHC5 siRNA treated sample demonstrating efficient knockdown of endogenous ZDHHC5.

(C) Quantification of percentage of cells with cilia in ZDHHC5 siRNA and CTRL siRNA treated cells. ZDHHC5 knockdown resulted in significantly reduced cilia compared to CTRL. 100 cells counted for each condition per replicate, statistical analysis by students T.Test *P ≤0.05, **P ≤0.01, ***P ≤ 0.001.

(D) Quantification of cilia length in ZDHHC5 siRNA and CTRL siRNA treated cells. Knockdown of ZDHHC5 does not result in a change in cilia length in RPE1 cells. 100 cilia measured for each condition over 3 repeats, statistical analysis by students T.Test *P ≤0.05, **P ≤0.01, ***P ≤ 0.001.

5.5.1 ZDHHC5 does not Localise to Cilla

As knockdown of ZDHHC5 reduced ciliogenesis in RPE1 cells I tested if ZDHHC5 itself was localised to cilia. RPE1 cells were transiently transfected with ZDHHC5-HA and then serum starved for 24 hours to induce ciliogenesis. After fixation cells were stained with ARL13b to mark cilia and ZDHHC5 localisation was detected by anti-HA antibody staining. ZDHHC5 was localised more intracellularly in RPE1 cells compared to HeLa cells (Figure 5.9, Figure 5.3 E). HA immunostaining did not co-localise with ARL13b demonstrating ZDHHC5 did not localise to cilia in RPE1 cells (Figure 5.9).

Figure 5. 9 ZDHHC5 does not Localise to Cilia in RPE1 Cells

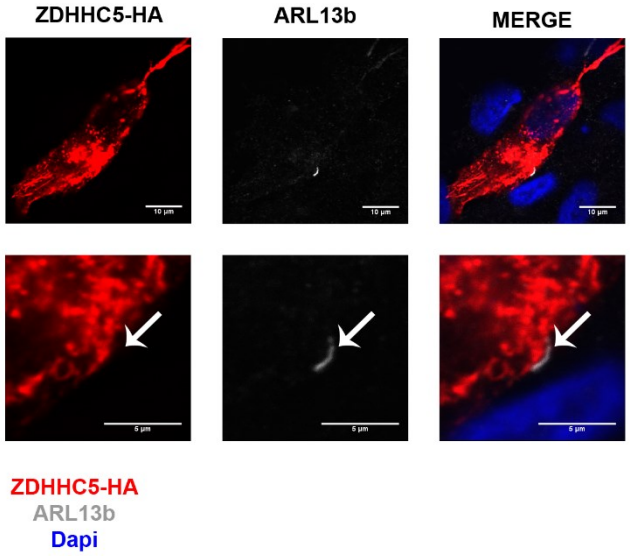

Representative immunofluorescence images of ZDHHC5-HA and ARL13b staining in RPE1 cells. Cells were serum starved to induce ciliogenesis and immunostained with anti ARL13b, to mark cilia, and anti HA. No colocalisation between ARL13b and HA was observed.

5.6 ARL3 is Palmitoylated in HeLa Cells

The regulators of ARL3, ARL13B and RP2 are palmitoylated and membrane associated (Chapple et al. 2000; Roy et al. 2017). ARL3 has been reported to be localised to Golgi membranes therefore the palmitoylation status of ARL3 was assessed (Zhou et al. 2006; Roy et al. 2017; Chapple et al. 2000). To ascertain whether ARL3 was palmitoylated HeLa cells were transiently transfected with WT ARL3-GFP. Twenty-four hours post transfection cells were incubated in media containing 100mM 17-ODYA (as before). Cells were then lysed and lysates were incubated with anti-GFP beads to isolate ARL3-GFP. After immunoprecipitation these IP's were subject to click chemistry labelling of 17-ODYA with an Infrared Azide dye (as before). After electrophoresis and transfer membranes were probed with a rabbit anti-ARL3 antibody and a rabbit –Alexa 680 secondary antibody. 17-ODYA incorporation and ARL3 expression were visualised on the LICOR imaging system (as before). 17-ODYA incorporation was quantified as before as a ratio of 800nm signal/700nm signal (Figure 5.10). WT ARL3-GFP incorporated 17-ODYA demonstrating ARL3 can be palmitoylated *in vitro*.

After establishing ARL3 was palmitoylated the residues on ARL3 which were required for palmitoylation were investigated. ARL3 only contains 3 cysteine residues, the residue that is palmitoylated, so these were individually mutated to serine residues (constructs designed and generated by Isobel Robb, an honours student in the lab) and tagged with GFP. These constructs were transiently transfected into HeLa cells and 24 hours after transfection, these cells were incubated with media containing 100mM 17-ODYA and lysates were subject to GFP IP followed by click chemistry (as above). ARL3 immunoblotting revealed each ARL3 cysteine mutant was stably expressed and successfully immunoprecipitated (Figure 5.10 A). Analysis of 17-ODYA incorporation demonstrated that C158, C118 and C174 may be palmitoylated *in vitro* as mutation of each of these residues reduced the 17-ODYA incorporation by ARL3 (Figure 5.10 B). Each ARL3 C>S mutation construct incorporated some 17-ODYA demonstrating one single residue may not responsible for ARL3 palmitoylation and that ARL3 could be palmitoylated on several residues. The average 800nm/700nm signal from 3 assays is shown in Figure 5.10 B, even though this assay was repeated several times the levels of 17-ODYA incorporation in the ARL3 WT lane was variable suggesting that ARL3 may be dynamically palmitoylated.

As expression of each mutant ARL3-GFP construct consistently appeared to be less that WT ARL3-GFP and consequently GFP IP of WT ARL3- GFP was more efficient than C158S ARL3- GFP, C118S ARL3 GFP and C174S ARL3 GFP (Figure 5.10 A) the effect each of these mutations had on the structure of ARL3 was assessed. The effect of each mutation on the structure of ARL3 was modelled by Joe Marsh and all the mutations were predicted to be non-destabilising (Table 5.2) suggesting that the differences in palmitoylation might regulate ARL3 stability rather than the cysteine to serine mutation itself (Table 5.2). For example in yeast palmitoylation of Tlg1, a member of the yeast SNARE complex, prevents degradation by the proteasome maintaining stability of the complex (Valdez-Taubas and Pelham 2005).

Figure 5. 10 ARL3 is Palmitoylated in HeLa Cells

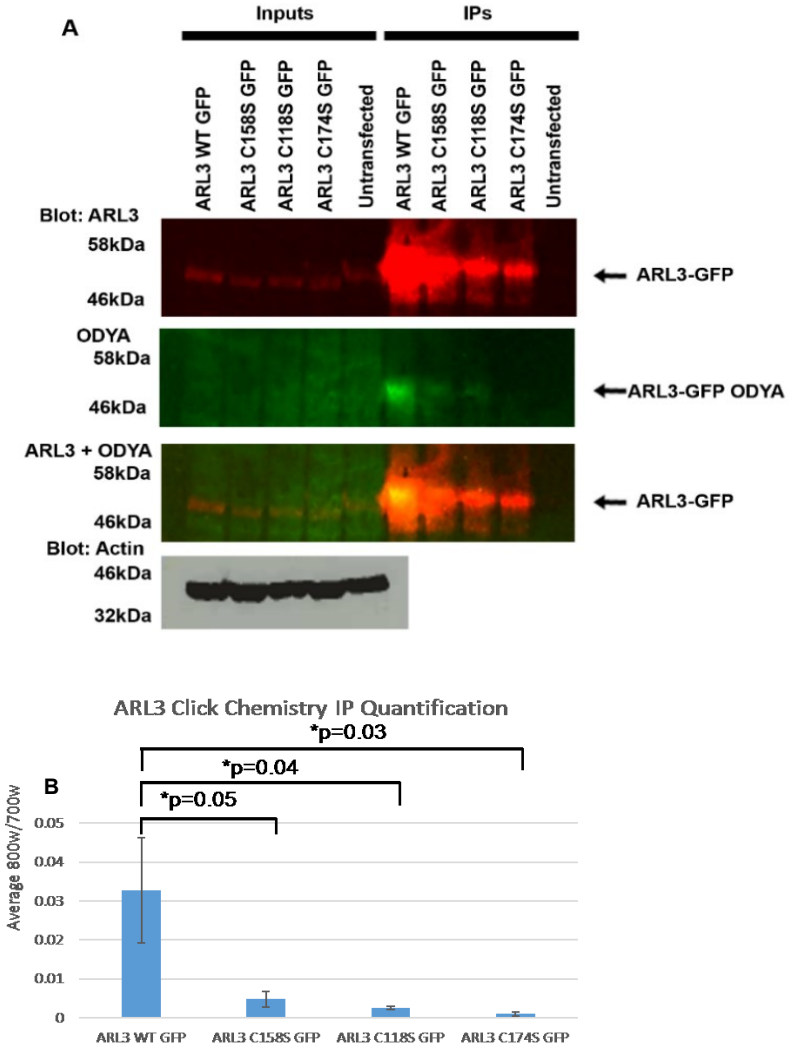

(A) HeLa cells transiently transfected with ARL3 WT-GFP, ARL3 C158S-GFP, ARL3 C118S-GFP or ARL3 C174S-GFP were incubated with 17-ODYA overnight. Cells were lysed and GFP COIP used to immunoprecipitate ARL3-GFP. A click chemistry reaction was used to label 17-ODYA with an Azide dye that fluoresces in the 800W channel to allow visualisation of ARL3 palmitoylation. After electrophoresis, membranes were immunoblotted for ARL3 and imaged using the LICOR system. Red channel shows ARL3 WT, C158S, C118S and C174S expression, Green channel shows 17-ODYA incorporation. Input samples were immunoblotted for Actin.

(B) Quantification of 17- ODYA incorporation in ARL3 WT, C158S, C118S and C174S- GFP IP lanes. Average ODYA signal was normalised to levels of immunoprecipitated ARL3 in each lane. These values were then compared to ARL3 WT-GFP values. Mutation of C158, C118 and C174 leads to reduction of ARL3 ODYA incorporation. Statistical significance analysed by students T-Test n=3.

Table 5. 2 ARL3 Cysteine Mutation Stability Prediction

ARL3 Mutation	ΔG (kcal/mol)
C158S	0.13
C118S	0.80
C174S	0.41

The effect of C158S, C118S and C174S mutation on the structure of ARL3 was predicted. All mutations had a ΔG score of >1 kcal/mol therefore were predicted to be non-destabilising.

5.7 Discussion

5.7.1 Identification and Characterisation of RP2-ZDHHC5 Interaction

The BIO-ID method was to identify new potential interactors of RP2. This assay proved an effective method at identifying RP2 interactors as known interactor ARL3 was detected as a top hit, whereas previously in our lab we have struggled to detect this interaction using traditional IP-mass spectrometry approaches, likely due to its transient nature. ZDHHC5 was identified as a novel interactor of RP2 that had not been previously identified using traditional IP/mass spec. ZDHHC5 is a multi-pass transmembrane protein which may explain why this interaction has failed to be detected using other approaches. Transmembrane proteins are highly hydrophobic and therefore hard to extract from cells therefore strong detergent buffers such as RIPA must be used to solubilise proteins, however these buffers due to their high SDS content are not compatible with IP. The BIO-ID assay therefore facilitates the identification of these interactions as interacting proteins are labelled with biotin and isolated using streptavidin beads and as the streptavidin-biotin interaction is a very strong covalent interaction high SDS content lysis buffers can be used to extract highly hydrophobic proteins. Many transmembrane proteins rely on lipid groups within the membrane for their stability and these can be lost during extraction from cells leading to destabilisation of the protein however as the BIO-ID technique labels interacting proteins in their natural environment interactions are not lost during extraction as in traditional IP/Mass spec approaches.

This assay facilitated the identification of other novel potential interactors of RP2 which were not investigated further (Table 5.1). Many of these interactions may be relevant to further understanding the function of RP2 in the retina, for example phospholipase C β1 (PLCβ1) has been shown to effect the expression of splicing factors in cells (Bavelloni et al. 2006) and mutations in genes which encode for splicing factors such as pre-mRNA-processing-splicing factor 8, 3 and 31 (*PRPF8*, *PRPF3*, *PRPF31)* and pim-1-associated protein *(PAP-1)* have been identified in patients with dominantly inherited Retinitis Pigmentosa (Vithana et al. 2001; McKie et al. 2001; Maita et al. 2004). Splicing of pre-mRNAs is catalysed by a large ribonucleoprotein complex known as the spliceosome. The spliceosome contains many small nuclear ribonuclear proteins (snRNPs) and splicing factors. Splicing of most introns involves five snRNPs U1, U2, U3, U4 and U5. U1 and U2 firstly bind the

pre- mRNA which is followed by binding of the U4/U6+U5 trimer to form the spliceosome (Will and Lührmann 2001). PRP31 is thought to function to bring together U5 and U4/U6 to form the trimer (Teigelkamp et al. 1998). PRP3 is associated with U4/U6 and PRP8 is thought to be a core component of U5 (Chakarova et al. 2002; McKie et al. 2001). Analysis of the effect of two human pathogenic mutations on PRP31 function demonstrated that neither mutation abolished the splicing function of PRP31 as no defect in splicing efficiency was detected. Both mutations did reduce the proteins ability to shuttle to the nucleus (Deery et al. 2002). It is hypothesised that mutations of these genes cause an eye specific phenotype as photoreceptors shed and renew their OS discs daily therefore the demand for newly synthesised proteins is exceptionally high meaning small defects in splicing efficiency are amplified (Deery et al. 2002). If RP2 has a role in regulating splicing or in regulating the function of proteins that regulate splicing this could be relevant to disease pathogenesis. It has been previously demonstrated that RP2 can shuttle to the nucleus after DNA damage and may have a role in the DNA damage response (Yoon et al. 2006), therefore this pathway in combination with splicing defects could explain why photoreceptors die when RP2 is mutated and could reveal a new avenue for the development of treatments for patients.

Fermitin Family Member 2 (FERMT2) (also known as Kindlin 2) has been shown to be essential for the formation of cell-cell contacts in epithelial cells and to regulate podocyte formation (He et.al 2011; Yasuda-Yamahara et al., 2018). As RP2 can interact with microtubules (Bartolini et al. 2002) this could imply that Kindlin 2 and RP2 may have a role in regulating microtubule dynamics in photoreceptors. FERMT2 has also been identified as a susceptibility locus for late onset Alzheimer's disease therefore it's functions may be required for the survival of neuronal cells with aging (Chapuis et al. 2017).

Transmembrane protein 237 (TMEM 237) is a ciliary transition zone protein found to be mutated in families with the embryonic lethal Joubert Syndrome related disorder, Meckel Syndrome (Huang et al., 2011). Meckel syndrome is a rare lethal ciliopathy manifesting in renal cystic dysplasia and central nervous system defects (Leightner and Harris 2013). TMEM 237 localises to the transition zone of cilia and is essential for ciliogenesis in mammalian cells (L. Huang et al. 2011). TMEM 237 requires RPGR interacting protein 1 like (RPGRIP1L) for localisation to the transition zone in C.elegans (Huang et al., 2011). RPGR interacting protein 1 (RPGRIP1) is also

required for localisation of retinitis pigmentosa GTPase regulator (RPGR) to the connecting cilia of photoreceptors (Zhao et al. 2003). Interaction between RP2 and TMEM 237 implies a role for RP2 at the ciliary transition zone, where proteins are sorted for entry into the cilia, and in photoreceptors where the CC acts as a transition zone for regulating entry of proteins to the OS (Elliott and Brugmann 2018). This suggests that *in vivo* this interaction may play a role in sorting proteins to the OS which may be relevant to disease pathogenesis *in vivo*.

To confirm the interaction between ZDHHC5 and RP2 an IP approach using transiently transfected RP2-V5 was attempted. Immunoprecipitation of V5 was followed by immunoblotting for endogenous ZDHHC5 in HeLa cells and in RPE1 cells, however these approaches failed to detect the interaction. This is likely due to ZDHHC5 lipid modifications and membrane association making extraction of the protein during cell lysis difficult as well as the potential transient nature of the interaction. As ZDHHC5 is a multi-pass transmembrane protein extracting this protein from the cell whilst maintaining its structure is difficult due to the need to use high SDS content lysis buffers. RP2 BIRA RP2 null RPE1 and BIRA RP2 null RPE1 biotin treated cells were used to confirm this interaction as the biotin label was maintained even when cells were lysed with RIPA buffer however, as BIRA biotinylates proteins that are within a 10nm radius this does not confirm a direct interaction between ZDHHC5 and RP2 and it is possible that the two proteins come into close proximity transiently in a non-stable complex. To confirm a direct interaction a Y2H assay could be designed however the yeast cell may not facilitate proper folding or localisation of ZDHHC5 and as the ZDHHC5-RP2 interaction may be transient it is possible that this interaction may not be stable enough to facilitate BD and AD interaction and thus activation of reporter gene expression. A pulldown assay using RP2 recombinant protein and glutathione beads to extract ZDHHC5 from WT RPE cell lysates could be attempted as an alternative approach to detect a direct interaction. However, for this approach to be successful the same issues associated with conventional IP approaches would have to be overcome. An alternative approach that could be used to overcome some of these issues is a crosslinking immunoprecipitation mass spectrometry assay. The crosslinking step should preserve the interaction so that a stronger lysis buffer could be used to extract ZDHHC5 from cells and immunoprecipitation with anti V5 beads could be used to demonstrate a direct interaction between RP2 and ZDHHC5.

5.7.2 ZDHHC5 is not required for RP2 Palmitoylation

In order to assay RP2 palmitoylation a click chemistry based assay which measured 17-ODYA incorporation was performed. Similar assays have been published in multiple studies where the palmitoylation status of proteins have been examined (J. Murphy and Kolandaivelu 2016; Howie et al. 2014; Yi Li et al. 2012). Another assay commonly used to analyse the palmitoylation status of proteins is the acyl-Rac assay. Acyl- Rac involves the detection of palmitoylated proteins using a thiol-reactive sepharose resin. After cell lysis free thiols (which contain free unpalmitoylated cysteine residues) are blocked with MMTS (S-methylmethanethiosulfonate). Thioesters are then cleaved with neutral hydroxylamine (NH2OH), and the newly liberated thiols are captured with thiol-reactive sepharose resin. After washing, captured proteins are eluted and analysed by SDS-PAGE and western blotting (Forrester et al. 2011). These techniques are largely comparable however, one benefit of 17-ODYA incorporation is that it allows for pulse-chase experiments to investigate palmitoylation dynamics. If the enzyme responsible for RP2 palmitoylation was identified then this assay could be used to analyse the dynamics of RP2 palmitoylation to establish whether RP2 is dynamically or stably palmitoylated.

Co-expression of RP2-V5 and ZDHCC5-HA should increase levels of RP2 palmitoylation if ZDHHC5 is responsible for palmitoylation of RP2, however this does not exclude the possibility that the level of endogenous ZDHHC5 in HeLa cells was sufficient to palmitoylate overexpressed RP2 WT-V5. To address this issue, knockdown experiments were carried out using ZDHHC5 siRNAs. If ZDHHC5 is solely responsible for palmitoylation of RP2, then a reduction in RP2 palmitoylation would be expected upon ZDHHC5 knockdown. As no significant difference in RP2 palmitoylation was detected in ZDHHC5 siRNA treated cells compared to CTRL siRNA treated cells this signified ZDHHC5 was not responsible for RP2 palmitoylation. This does not exclude the possibility that in the absence of ZDHHC5 there is compensation by another ZDHHC which maintains RP2 palmitoylation.

Previously in *Aipl1* -/- mice which have a retina devoid of photoreceptors, expression of ZDHHC5 was > 4-fold reduced compared to WT, demonstrating it is expressed in photoreceptors. However, the expression of the closely related membrane associated Palmitoyltransferase ZDHHC2 was reduced >8 fold compared to WT suggesting this protein is highly expressed in photoreceptors (Murphy et al., 2016). Therefore, it is possible that ZDHHC2 also plays a role in palmitoylation of RP2. As HeLa cells

express endogenous ZDHHC2 this could be investigated via knockdown of ZDHHC2 and analysis of RP2's 17-ODYA incorporation. As multiple ZDHHC enzymes have been shown to be able to palmitoylate the same substrates (K. Huang et al. 2009; Tian et al. 2010) it may be that ZDHHC2, ZDHHC5 and potentially other ZDHHC's are responsible for RP2 palmitoylation *in vivo*. This could be tested by knockdown of each of the 23 ZDHHC's in cells followed by assay of RP2's palmitoylation status. Alternatively, this experiment could be repeated in RPE cells and the ZDHHC's which are expressed in RPE cells knocked down and the palmitoylation status of RP2 examined in order to identify ZDHHC's which are responsible for RP2 palmitoylation in a disease relevant cell type.

5.7.3 ZDHHC5 is required for RP2 Membrane Localisation

The observation that ZDHHC5 is able to rescue mistrafficking of RP2 C3S and RP2 G2A in cells is striking as these are human pathogenic mutations hypothesised to be mislocalised *in vivo* (Chapple et al. 2000). The caveat to this experiment is that this finding is based on over expression therefore does not directly represent the *in vivo* situation. HeLa cells used in this assay express endogenous ZDHHC5 however transient transfection with only C3S RP2-V5 or G2A RP2-V5 in HeLa cells demonstrated C3S RP2-V5 and G2A RP2-V5 were mislocalised signifying endogenous levels of ZDHHC5 are not sufficient to rescue mistrafficking (Figure 5.4 C,E). However, knockdown of endogenous ZDHHC5 is enough to cause mislocalisation of RP2 WT-V5 demonstrating that ZDHHC5 may well have a role in trafficking RP2 to the membrane. To further investigate the mechanism by which ZDHHC5 may traffic RP2 to the cell membrane imaging approaches could be used. Cells expressing RP2-V5 and ZDHHC5-HA could be analysed by imaging with markers for particular types of vesicles. ZDHHC5- HA and WT RP2-V5 could be imaged alongside a marker for post Golgi vesicles such as Rab11 (Takahashi et al. 2012). This could demonstrate if RP2 and ZDHHC5 are trafficked in the same vesicles to the membrane. To determine whether RP2 and ZDHHC5 interact before vesicle sorting occurs co-staining with Golgi markers such as Giantin and TGN38 (Linstedt and Hauri 1993; Luzio et al. 1990) could be performed. To determine whether ZDHHC5 and RP2 may require actin for trafficking, cells could be co-stained with a dye that allows visualisation of the actin cytoskeleton such as rhodamine phalloidin and ZDHHC5-HA and RP2-V5. Live cell imaging could be used to track RP2-V5 and

ZDHHC5-HA as they move through the cell in order to observe where they interact and whether they traffic to the cell membrane together.

5.7.4 Knockdown of ZDHHC5 Reduces Ciliogenesis in RPE1 Cells

Ciliogenesis was not absent in cells treated with ZDHHC5 siRNAs as about 30% of cells were still formed cilia (Figure 5.8 C). To assess if these cilia were equivalent to WT cilia the length of cilia was measured and was shown to be equivalent to that in CTRL siRNA treated cells (Figure 5.8 D). This suggests that ZDHHC5 is required for ciliogenesis and that it may be required for palmitoylation and/ or trafficking of cilia proteins *in vivo*. Multiple proteins involved in cilia are palmitoylated and palmitoylation may be essential for protein function for example palmitoylation of ARL13B is required for protein stability and cilia localisation (Roy et al. 2017). ARL13B C8S/C9S is not palmitoylated, does not localise to cilia and is unable to activate ARL3 (Roy et al. 2017). As knockdown of only ZDHHC5 caused ciliogenesis defects this implies that other ZDHHC's in RPE cells cannot compensate for the function of ZDHHC5 suggesting that it may have specific cilia substrates. Swisspalm is an online database of palmitoylated proteins therefore proteins essential for ciliogenesis could be checked as to whether they are predicted to be palmitoylated and the effect on ZDHHC5 knockdown on their palmitoylation status analysed. For example, CEP290 regulates ciliogenesis and is predicted to be palmitoylated on at least one of its 7 cysteine residues. As ZDHHC5 is not itself localised to cilia it is possible that it has a role in trafficking proteins to the base of the cilia as well as palmitoylating them which is required for attachment to the cilia membrane. Therefore, the effect of ZDHHC5 knockdown on the localisation of proteins required for ciliogenesis could be analysed.

ARL13B was used as a marker for cilia in my assays and in the 30% of ZDHHC5 siRNA treated cells, which still developed cilia possibly as a result of inefficient knockdown of ZDHHC5, ARL13B localised normally to the cilia. In ZDHHC5 siRNA treated cells which did not develop cilia ARL13B localisation appeared to be diffused throughout the cell. This could be a direct result of no cilia formation therefore ARL13B was unable to localise there or it may be that ZDHHC5 is required to palmitoylate ARL13B and as this has been previously shown to be essential for cilia formation (Roy et al. 2017) this may be the reason why cells with ZDHHC5 knocked down failed to ciliate. This hypothesis could be tested by transiently transfecting cells with ARL13B tagged with GFP or V5 and using a 17-ODYA incorporation assay as described above. ARL13B 17-ODYA incorporation could be assayed in cells with ZDHHC5

overexpression and with ZDHHC5 knocked down, to assess whether ZDHHC5 may be required for ARL13B palmitoylation.

5.7.5 ZDHHC5 is not localised to Cilia

ZDHHC5 did not localised to cilia in RPE1 cells (Figure 5.9) however it was localised within the cell rather than exclusively at the cell membrane as in HeLa cells (Figure 5.9, Figure 5.5 B). This may suggest that ZDHHC5 has differential roles in RPE1 cells and HeLa cells. It is possible that in RPE1 cells ZDHHC5 is located within intracellular membranes where it functions to regulate the palmitoylation and or trafficking of proteins destined for the plasma membrane, in theory ZDHHC5 could traffic with them in intracellular vesicles to the cell membrane analogous to the mechanism proposed for δ-catenin and ZDHHC5 trafficking in synaptic neurons (Brigidi et al. 2015).

5.7.6 ARL3 is Palmitoylated in HeLa Cells

Palmitoylation status of ARL3 was assessed using the 17-ODYA click chemistry assay, after confirming that ARL3 was palmitoylated, the cysteine residues on ARL3's surface were mutated to serine's to test which cysteine residues are required for palmitoylation. This assay revealed that mutation of C158S, C174 and C118 reduced ARL3's 17-ODYA incorporation compared to WT suggesting these residues are palmitoylated *in vivo*. This suggests that ARL3 is likely dynamically palmitoylated on multiple residues this hypothesis was supported by the data from ARL3 WT which was quite variable further suggesting that palmitoylation of ARL3 may be dynamic. It has been previously shown in drosophila that ARL3 is N-terminally acylated and in yeast this acylation was shown to be essential for Arl3p localisation to vesicles. Furthermore, human ARL8 is acylated at its N-terminus which is essential for its localisation to lysosomes (Hofmann 2006).

If ARL3 is dynamically acylated this could be investigated using a pulse chase 17-ODYA assay. Hela cells could be transfected with WT ARL3-GFP and treated with 100mM 17-ODYA. Rather than waiting for 24 hours cells could be lysed at various times after treatment to observe if 17-ODYA incorporation varies overtime. Whether palmitoylation of ARL3 varies under other conditions could also be tested with this assay for example whether palmitoylation of ARL3 increases with overexpression of ARL13B or RP2 may imply whether palmitoylation is required for ARL3's activity. The known regulators of ARL3, RP2 and ARL13B, are both palmitoylated and membrane

associated (Roy et al. 2017; Chapple et al. 2000) therefore palmitoylation of ARL3 likely facilitates membrane associations which may be required for interaction with RP2 and ARL13B. Dynamic acylation of ARL3 may also serve as a means of regulating the activity of ARL3 *in vivo*, as if palmitoylation is required for ARL3 to associate with membranes and thus RP2 and ARL13B this infers that palmitoylation is required for its activity *in vivo*. My data also suggests that palmitoylation of ARL3 may effect stability of ARL3, suggesting another mechanism by which palmitoylation of ARL3 may affect its activity *in vivo*.

The PAT or PATs which are responsible for palmitoylation of ARL3 could be investigated through knockdown of ZDHHC's and analysis of ARL3 palmitoylation through 17-ODYA incorporation. Whether ZDHHC5 also interacts with ARL3 could be investigated in cells expressing ARL3-GFP by GFP pulldown and blotting for ZDHHC5. The localisation of ARL3 in cells could be analysed when ZDHHC5 is knocked down to establish if like RP2 its localisation is regulated by ZDHHC5. If ARL3's localisation is regulated by ZDHHC5 it may suggest that RP2 and ARL3 may traffic to the cell membrane together in vesicles, a hypothesis which could be further investigated using live cell imaging to visualise the two proteins interacting in cells. This experiment would demonstrate whether they are trafficked together in vesicles and whether their interaction only occurs once both proteins are membrane localised providing insights into the dynamics of ARL3 regulation in cells.

5.8 Conclusions

In this chapter, I utilised the BIO-ID method to identify ZDHHC5 as a novel interactor of RP2. I characterised this interaction demonstrating that surprisingly ZDHHC5 is not required for RP2 palmitoylation but is required for its membrane association. This suggests that ZDHHC5 may play a role in trafficking RP2 to the cell membrane. I also demonstrated that overexpression of ZDHHC5 is capable of rescuing mistrafficking of RP2 mutants, RP2 C3S and RP2 G2A, which are not post translationally palmitoylated or myristoylated respectively. These are human pathogenic mutations which are hypothesised to cause mislocalisation of RP2 *in vivo* (Chapple et al. 2000). I then demonstrated that knockdown of ZDHHC5 reduces ciliogenesis in RPE1 cells, this suggests that ZDHHC5 may have roles in palmitoylation and or trafficking of proteins required for ciliogenesis and that other ZDHHCs in the cell cannot compensate for this function. I then established that known interactor of RP2, ARL3 is also

palmitoylated potentially at multiple cysteine residues. Together this data suggests a role for ZDHHC5 in the trafficking of lipid-modified proteins. As it is well established that mistrafficking of lipid-modified proteins is a potential mechanism underlying photoreceptor cell death in Retinitis Pigmentosa, further understanding of the role ZDHHC5 plays in the eye may have important implications for the understanding of disease pathogenesis in patients.

Chapter 6

Discussion

Chapter 6: Discussion

6.1 Introduction

The overarching aim of my PhD project was to assess whether the pathogenesis of X-linked Retinitis Pigmentosa (XLRP) caused by mutation of *RP2* can be solely attributed to dysfunction of ARL3. I also aimed to address how RP2 itself is regulated by identification of novel interactors via a BIO-ID analysis. In order to address these aims new mouse models were generated using CRISPR- mediated genome editing. *Rp2h* DEL26/Y is a RP2 null mouse, *Rp2h* E135G/Y expresses a mutant RP2 which is unable to interact with ARL3, *Arl3* Q71L/+ and *Arl3* Q71L/Q71L mice express constitutively active ARL3. By comparing the phenotypes of these mice, the contribution of increased levels of ARL3-GTP to retinal degeneration was addressed. I observed that *Arl3* Q71L/Q71L retinas had the most severe retinal degeneration of all the mouse models and the highest levels of ARL3-GTP demonstrating that increased levels of ARL3-GTP can drive retinal degeneration in mice. I designed an assay to detect increased levels of ARL3-GTP in mouse tissues that revealed that increased levels of ARL3-GTP were not detectable in *Rp2h* WT, *Rp2h* DEL26/Y and *Rp2h* E135G/Y tissues suggesting that other mechanisms may exist to regulate levels of ARL3-GTP in the absence of RP2 GAP activity. I demonstrated that all mice displayed mistrafficking of OS proteins rhodopsin, M/L opsin and G- coupled receptor kinase 1 (GRK1) which may contribute to retinal degeneration. In addition, I observed that signal transducer and activator of transcription 3 (STAT3) activation is lost in *Arl3* Q71L/+ and *Arl3* Q71L/Q71L eyes but not *Rp2h* DEL26/Y or *Rp2h* E135G/Y eyes. This may represent a mechanism which drives retinal degeneration when levels of ARL3-GTP are high but not when RP2 function is disrupted, suggesting that expression of ARL3 Q71L may drive retinal degeneration through different mechanisms than loss of RP2 function.

6.2 *Rp2h* DEL26/Y and *Rp2h* E135G/Y Mice

As discussed in chapter 3, *Rp2h* DEL26/Y and *Rp2h* E135G/Y mice have progressive retinal degeneration as shown by decreased thickness of the ONL and decreased photoreceptor response measured by electroretinography (ERG). These mice

displayed mislocalisation of GRK1, rhodopsin and M/L opsin and consistently *Rp2h* DEL26/Y mice had a more severe phenotype than *Rp2h* E135G/Y. As the DEL26 mutation results in no RP2 protein expression but the E135G mutation produces a RP2 protein that does not have GAP activity for ARL3 it suggests that the more severe phenotype observed in the RP2 DEL26/Y mutant may be due to functions of RP2 which are independent of ARL3. Other studies have demonstrated that RP2 may have other roles in the cells independent to its roles in protein trafficking. RP2 has homology with tubulin specific chaperone C (TBCC) and RP2 can stimulate the intrinsic GTPase activity of tubulin but is unable to facilitate heterodimerisation of newly folded tubulin subunits (Bartolini et al. 2002). Furthermore, a study in Trypanosama Brucei demonstrated that RP2 is localised to the basal body of the flagellum, and that knockdown of RP2 resulted in flagellum defects (Andre et al. 2014). Mutation of Arg248 in the TBCC domain abolished RP2's function in tubulin processing resulting in lengthened flagella. Additionally, knockdown of RP2 resulted in failure of the transition zone proteins Meckel syndrome type 1 (MKS1) and Meckel syndrome type 6 MKS6 to localise to the basal body of flagella (Andre et al. 2014). This suggests a role for RP2 in the regulation of microtubules which is essential for cilia formation and function. However studies in human MDCK cells have demonstrated that siRNA knockdown of RP2 does not affect cilia formation (T. Hurd et al. 2010). Retinitis Pigmentosa 1 (*RP1)*, a cause of ADRP is a microtubule associated protein which localises to the tip of the CC, at the base of the OS, in photoreceptors (Q. Liu, Zuo, and Pierce 2004). RP1 interacts with microtubules and regulates the length and stability of the photoreceptor axoneme suggesting RP in this case may be caused by microtubule defects (Q. Liu, Zuo, and Pierce 2004). As other RP associated genes such as *RPGR*, *RP2* and Family With Sequence Similarity 161 Member A *(FAM161A)* have been shown to associate with microtubules this suggests that microtubule organisation defects may be a common feature that is disrupted in RP (Grayson et al. 2002; Khanna et al. 2005; Shu et al. 2005; Zach et al. 2012), although further research is required to assess whether microtubule defects contribute to the pathogenesis of RP.

ARL3 has also been shown to have a role in microtubule regulation through its interaction with HDAC6. In *C.elegans* it was shown that ARL3 regulated ciliogenesis via a HDAC6 dependant pathway (Yujie Li et al. 2010). It has been reported that knockdown of ARL3 in mammalian cells leads to an increase in the levels of acetylated tubulin and that ARL3 colocalises with acetylated tubulin at the mitotic

spindle and in the cilia (Enjalbert et al. 2006). In RPE-1 cells it has been shown that HDAC6 localises to the primary cilia and that activation of HDAC6 is required for ciliary disassembly during the cell cycle (Pugacheva et al. 2007). Overexpression of WT HDAC6 in NIH3T3 cells increased cell migration (Valenzuela-Fernández et al. 2008), likely through increased deactylation of microtubules which decreases microtubule stability and increases cell motility (Wadsworth 1999). Additionally cells lacking ARL13b have been shown to have a defect in cell migration and have increased levels of stable microtubules (Pruski et al. 2016). These studies demonstrate that ARL3 as well as RP2 may have roles in regulating microtubules in vivo.

The nucleoside diphosphate kinase-like domain (NDKL) domain of RP2 was shown to have exonuclease activity and to translocate to the nucleus in response to DNA damage (Yoon et al. 2006). It was demonstrated that RP2 can most efficiently translocate to the nucleus under oxidative stress and increased oxidative stress has been suggested to drive cell death in Retinitis Pigmentosa (Campochiaro and Mir 2018; Mendes et al. 2005; Yoon et al. 2006). Furthermore a patient pathogenic mutation, L253R, in this domain has reduced exonuclease activity (Yoon et al. 2006). Although this mutation has since been shown to destabilise RP2 protein expression suggesting the reduced exonuclease activity is due to reduced protein expression rather than disruption of exonuclease catalytic activity (F. Liu et al. 2017). Nevertheless, this suggests that RP2 may play a role in repairing oxidative stress induced DNA damage and may explain why *Rp2h* DEL26/Y mice have a more severe phenotype than *Rp2h* E135G/Y mice as knockout of RP2 may ablate RP2's role in DNA damage as well as ARL3 GAP activity. In order to test this hypothesis, levels of DNA damage associated proteins, such as oxoguanine glycosylase (OGG) or γH2ax, could be examined in the retinas of *Rp2h* DEL26/Y and *Rp2h* E135G/Y retinas. This could be tested *in vitro* by assessing survival of WT, RP2 null RPE cells and RP2 E135G RPE cells after oxidative stress induced DNA damage.

The other explanation as to why *Rp2h* E135G/Y mice have a less severe phenotype than *Rp2h* DEL26/Y may be because RP2 E135G still has residual GAP activity. The RP2 E135G mutation is predicted to reduce RP2's affinity for ARL3 150 fold compared to WT however, another patient pathogenic mutation, R118H, reduces RP2's affinity for ARL3 over 800 fold (Kühnel et al. 2006). As these predictions have been carried out *in vitro* it is possible that *in vivo* additional mechanisms exist and RP2 E135G could still have partial GAP activity meaning that the E135G mutation is hypomorphic.

In order to test this hypothesis, a mouse expressing RP2 R118H could be generated and its phenotype compared to that of *Rp2h* E135G/Y. In order to assess whether mutation of both residues is required to ablate GAP activity female compound heterozygous mice (*Rp2h* E135G/R118H) could be generated and the phenotype compared to female homozygous single mutants, *Rp2h* DEL26/DEL26 and female WT mice.

6.3 *Rp2h* DEL26/Y, *Rp2h* E135G/Y, *Arl3* Q71L/+ and *Arl3* Q71L/71L Mice

6.3.1 Elevated Levels of ARL3-GTP

In chapter 4, a pulldown assay using RP2 recombinant protein was used to isolate ARL3-GTP, demonstrating that in *Arl3* Q71L/+ and *Arl3* Q71L/Q71L tissue extremely elevated levels of ARL3-GTP were present compared to WT and *Rp2h* DEL26/Y and *Rp2h* E135G/Y tissues. In *Rp2h* DEL26/Y and *Rp2h* E135G/Y tissues, levels of ARL3-GTP were indistinguishable from WT. This result suggests that in tissues deficient in RP2 another GAP may exist which is able to regulate the levels of ARL3-GTP or levels of ARL3-GTP are regulated via another mechanism e.g. guanine nucleotide exchange factor (GEF) activity. Throughout my analysis I observed similar defects in protein trafficking between *Rp2h* DEL26/Y, *Rp2h* E135G/Y, *Arl3* Q71L/+ and *Arl3* Q71L/Q17L retinas with M/L opsin, rhodopsin and GRK1 all mislocalised although specific differences in age of onset was observed. Overall, this suggests that the same trafficking pathways may be disrupted in each case implying that in *Rp2h* DEL26/Y and *Rp2h* E135G/Y eyes levels of ARL3-GTP may be increased slightly compared to WT but were not high enough to be detected in my assay. This infers that *in vivo* only a small increase in ARL3-GTP levels may be required to cause issues with protein trafficking. It also implies that mechanisms exist which prevent a huge increase in ARL3-GTP levels in tissues that lack RP2, this could be another GTPase activating protein (GAP) for ARL3 or regulation of GEF activity so that less ARL3-GTP is produced. GEF's for other small GTPase families have been shown to have domains which autoregulate their activity (Cherfils and Zeghouf 2013) so it is possible that GEF activity of ARL13B could be subject to autoregulation and it's activity may be reduced when high levels of ARL3-GTP are present.

As the mice generated in my study were created using CRISPR genome editing of single cell embryo, the mutations introduced should be present in every tissue in the

resulting mouse and as both RP2 and ARL3 are ubiquitously expressed, the resulting eye specific phenotype for *Arl3* Q71L mice was unexpected. Mice from both the *Rp2h* and *Arl3* lines displayed only retinal degeneration with no other adverse phenotypes as they survived until 12 months of age and were indistinguishable from WT mice apart from retinal degeneration. In both previously published *Rp2h* knockout mice only retinal degeneration is observed with no other adverse phenotypes (Houbin Zhang et al. 2015; L. Li et al. 2013) suggesting that in other ciliated tissues another GAP for ARL3 exists which compensates for RP2 function. In chapter 4, pulldown with RP2 recombinant protein demonstrated that increased levels of ARL3-GTP were present in *Arl3* Q71L kidney lysates with no obvious kidney phenotype detected. However, *Arl3* -/- mice have a severe ciliopathy like phenotype and do not develop photoreceptor outer segments, have pancreatic lesions and cystic kidneys resulting in death by p21, knockout of *Arl3* has also reported to be lethal on C57BL/J background strain (Schrick et al. 2006; Hanke-Gogokhia et al. 2016). This contrasting phenotype is attributed to the fact *Arl3* -/- mice have defects in ciliogenesis but in *Arl3* Q71L mice photoreceptor outer segments develop normally and no lethality occurs suggesting ciliogenesis occurs normally potentially as ARL3-GTP is still present. In order to assess if ARL3-GTP is required for ciliogenesis the phenotype of an *Arl3* T31N mouse could be analysed as this mutation would generate an ARL3 which is constitutively bound to GDP (Linari, Hanzal-Bayer, and Becker 1999). Increased levels of ARL3-GTP would be expected to cause mistrafficking of proteins trafficked to the cilia by RP2-ARL3-PDE6δ such as INP55E however some evidence exists demonstrating other ARL's can compensate for the function of ARL3 (Humbert et al. 2012; Fansa et al. 2016). Therefore, in other ciliated tissues trafficking pathways may be able to compensate for the mistrafficking caused by increased levels of ARL3-GTP. Humbert et.al demonstrated that ARL13b also regulates cilia localisation of INPP5E (Humbert et al., 2012). After knockdown of ARL3 in renal epithelial cells INPP5E is still partially localised within cilia (Fansa et al. 2016) however knockdown of ARL13b leads to loss of INP55E cilia localisation (Humbert et al. 2012). Mutation of ARL13B and ARL6 cause Joubert syndrome and Bardet Bidel syndrome respectively (Cantagrel et al. 2008; Khan et al. 2013), which are syndromic conditions affecting multiple ciliated tissues however the only reported human pathogenic mutation in ARL3, results in dominantly inherited Retinitis Pigmentosa (Strom et al. 2016). This mutation is predicted to result in a ARL3 protein unable to interact with RP2 or UNC119 (Strom et al. 2016). This suggests that non- ocular tissues can

tolerate loss or mutation of ARL3 but this is not the case for other small GTPases such as ARL13B or ARL6. In the eye the heavy burden on protein trafficking resulting from daily renewal of OS discs may result in a small trafficking defect that is tolerable in other tissues being amplified resulting in a phenotype, analogous to the mechanism which is proposed to underlie Retinitis Pigmentosa in cases where splicing factors are mutated (Deery et al. 2002). Alternatively, ARL3 may have evolved specific functions trafficking OS proteins in the eye therefore other GTPases are unable to compensate for this function and eye specific phenotypes arise from both *RP2* and *ARL3* mutation.

6.3.2 Cones are More Sensitive to Increases in ARL3-GTP

In chapter 4, I demonstrated through 10cd flash ERGs that cone photoreceptor function was more sensitive than rods to elevated levels of ARL3-GTP. The reduction in cone function was detected prior to M/L opsin mislocalisation, this was also observed in *Rp2h* DEL26/Y and *Rp2h* E135G/Y mice demonstrating that mislocalisation of M/L opsin was not likely the cause of the functional defect detected. A reduction in photoreceptor function suggests that proteins that are involved in phototransduction such as PDE6, GRK1 and transducin may be defective. As these proteins are trafficked to the OS by PDE6δ in rods as well as cones, a cone autonomous effect would not be expected (H Zhang et al. 2007). However, previous studies have suggested that the trafficking of these proteins may be differentially regulated in cones and rods. For example it has been demonstrated that cone outer segment proteins PDE6, GRK1, cone transducin subunit α and GC1 are not trafficked to the OS in the absence of 11-cis retinal but rod OS proteins are unaffected (Houbin Zhang et al. 2008). Also knockout of GC1 (*Guca2e* -/-) in mice results in mislocalisation of cone OS membrane proteins with no effect on rod OS proteins however when a double knockout of GC1 and GC2 (*Guca2e* -/-, *Guca2f* -/-) was generated both rod and cone OS membrane proteins were affected (Karan et al. 2008). Furthermore in the P*de6δ* -/- mouse mislocalisation of GRK1 and PDE6 is observed in rods and cones however in the *Pde6δ* -/-, *Unc119* -/- double knockout mouse cone GRK1 localisation to the OS is rescued demonstrating distinct mechanisms may exist which regulate the trafficking of cone OS proteins (H Zhang et al. 2007; Houbin Zhang, Frederick, and Baehr 2014). In order to test whether the increased levels of ARL3-GTP present in *Arl3* Q71L mice causes mistrafficking of cone OS proteins the localisation of cone specific isoforms could be assessed by

specific antibodies or co-staining with PNA could be used to aid identification of cones. Furthermore, *Rp2h* DEL26/Y, *Rp2h* E135G/Y or *Arl3* Q71L/+ mice could be crossed onto a *Nrl* -/- background to generate a mouse with a retina that contained only cones expressing RP2 DEL26, RP2 E135G or ARL3 Q71L (Mears et al. 2001).

6.3.3 Rhodopsin Is Mislocalised in *Rp2h* DEL26/Y, *Rp2h* E135G/Y, *Arl3* Q71L/+ and *Arl3* Q71L/Q71L Retinas

In chapter 3, I demonstrated that rhodopsin is mislocalised in *Rp2h* DEL26/Y and *Rp2h* E135G/Y retinas. In chapter 4, I also observed that *Arl3* Q71L/+ retinas have mislocalised rhodopsin followed by reduced rhodopsin immunostaining and that *Arl3* Q71L/Q71L retinas have reduced rhodopsin immunostaining from 1 month of age. Presuming that reduced immunostaining equates to reduced expression (although this was not confirmed in my analysis) this suggests that mutation of RP2 and elevated levels of ARL3-GTP do not necessarily cause the same phenotype in terms of rhodopsin mislocalisation. As discussed previously it has been shown that the C terminus of rhodopsin interacts with IFT20 and that in cells when RP2 is knocked down IFT20 becomes dispersed and the Golgi becomes fragmented (Evans et al. 2010; Keady, Le, and Pazour 2011). When ARL3-Q71L is expressed in cells, this phenotype is also observed (Evans et al. 2010), implying that *RP2* mutation may cause Golgi fragmentation through increased levels of ARL3-GTP and consequently mis-sorting of OS destined proteins such as IFT20 and rhodopsin. In *Arl3* Q71L/Q71L, mice where levels of ARL3-GTP are elevated hundreds of times more than in *Rp2h* DEL26/Y and *Rp2h* E135G/Y other mechanisms may contribute to rhodopsin mislocalisation. The trafficking of rhodopsin is regulated by many small GTPases (Moritz et al. 2001; Deretic et al. 2005) therefore it may be that another aspect of rhodopsin trafficking is also affected when levels of ARL3-GTP are hugely increased. For example rhodopsin docking at the connecting cilia is regulated by the small GTPase Rab8 (Moritz et al. 2001). If this were disrupted, rhodopsin would be unable to localise to the OS. Elevated levels of ARL3-GTP may disrupt kinesin motor transport of rhodopsin (Insinna et al. 2008; Schwarz et al. 2017) resulting in rhodopsin accumulation that stimulates ER stress and protein degradation. To investigate whether kinesin motor subunit function is disrupted in *Arl3* Q71L mice the localisation of other proteins trafficked by this mechanism such as IFT proteins IFT88, IFT52 and IFT57 (Insinna and Besharse 2008) could be examined in these retinas. An interesting

further experiment would be to age *Rp2h* DEL26/Y and *Rp2h* E135G/Y mice longer to see if they ever display reduced rhodopsin immunostaining to the same extent as *Arl3* Q71L/Q71L mice.

6.3.4 GRK1 is mislocalised in *Rp2h* DEL26/Y and *Rp2h* E135G/Y mice but is degraded in *Arl3* Q71L/+ and *Arl3* Q71L/Q71L mice

In chapter 3, I demonstrated that in *Rp2h* DEL26/Y and *Rp2h* E135G/Y retinas GRK1 immunostaining is lost from the photoreceptor OS but protein expression is unaffected. In chapter 4, I revealed that in *Arl3* Q71L/+ and *Arl3* Q71L/Q71L retinas GRK1 immunostaining was absent from the photoreceptor OS and the protein expression decreased with age. *Rp2h* mutants had mislocalised GRK1 and in *Arl3* Q71L mice GRK1 was degraded signifying that the mechanisms involved in mislocalisation or the mechanisms which are activated to combat accumulation of mislocalised proteins are not identical in each case. A study in the *Lcat*-/- mouse, which is a model of Leber Congenital Amaurosis (LCA), showed that in cones although both M/L and S opsin were mislocalised only S opsin was degraded and M/L opsin was resistant to degradation. This study showed that M/L opsin aggregates were resistant to proteasomal degradation whilst S opsin was labelled with ubiquitin and degraded. Accumulation of M/L opsin aggregates caused ER stress, activated the unfolded protein response (UPR), and ultimately caused rapid photoreceptor degeneration. In cells where S opsin was degraded, the burden on the cell was relieved and less ER stress was present. Cells with degraded S opsin did still degenerate but at a slower rate than cells with M/L opsin aggregates (T. Zhang et al. 2011). This study demonstrated that mislocalised proteins can be managed by different mechanisms *in vivo* which influences cell survival. This proposes that in *Rp2h* retinas where GRK1 is not degraded the UPR is activated and may contribute to cell death but in *Arl3* Q71L retinas where GRK1 is degraded less ER stress is present and apoptosis does not occur. However, consistently throughout my analysis *Arl3* Q71L/Q71L retinas had the most severe phenotype in terms of age of onset of photoreceptor functional defects and rate of ONL thinning suggesting degradation of GRK1 does not protect against cell death. This could be attributed to the fact that reduced GRK1 expression may cause increased levels of R* that may cause hyper-activation of the phototransduction cascade, which could stimulate apoptosis. Alternatively, other mechanisms may drive retinal degeneration in *Arl3* Q71L/+ and

Arl3 Q71L/Q71L mice. The UPR is activated by three ER transmembrane proteins inositol requiring 1 (IRE1), PKR-like ER kinase (PERK), and activating transcription factor 6 (ATF6), in order to detect if the UPR is activated in *Rp2h* DEL26/Y, *Rp2h* E135G/Y, *Arl3* Q71L/+ and *Arl3* Q71L/Q71L the levels of IRE1 and PERK1 phosphorylation or levels of ATF6α cleavage could be examined by western blot in retinal lysates (Oslowski and Urano 2013).

6.3.5 STAT3 Activation is Reduced in *Arl3* Q71L/+ and *Arl3* Q71L/Q71L Eyes but not in *Rp2h* DEL26/Y and *Rp2h* E135G/Y Eyes

The protein mislocalisation that was observed *Rp2h* DEL26/Y, *Rp2h* E135G/Y, *Arl3* Q71L/+ and *Arl3* Q71L/Q71L mice suggest that ER stress may contribute to retinal degeneration however differences in whether mislocalised proteins were degraded infers that other mechanisms may also contribute to photoreceptor cell death. In chapter 4, I demonstrated that phosphorylation of tyrosine 705 (Y705) and serine 727 (S727) on STAT3 was reduced in *Arl3* Q71L/+ and *Arl3* Q71L/Q71L eyes but not in *Rp2h* DEL26/Y and *Rp2h* E135G/Y eyes. These residues are thought to be required for STAT3 dimerisation, nuclear accumulation and activation of STAT3 gene expression respectively (J E Darnell, Kerr, and Stark 1994; James E Darnell 1997; Schindler, Levy, and Decker 2007). This result suggested that in *Arl3* Q71L/+ and *Arl3* Q71L/Q71L retinas cell death may be driven by loss of STAT3 signalling which is not the case in *Rp2h* DEL26/Y and *Rp2h* E135G/Y eyes, suggesting that increased levels of ARL3-GTP and mutation of RP2 may drive retinal degeneration through differential mechanisms.

STAT3 does not only regulate cell survival signalling but also regulates cell migration and proliferation (Hirano, Ishihara, and Hibi 2000). Interestingly some evidence exists to suggest that levels of ARL3-GTP may also regulate cell migration. Togi et.al demonstrated that siRNA knockdown of ARL3 reduced levels of STAT3 gene expression which reduced the migration capacity of cells (Togi et al. 2016). $Rod^{ARL3Q71L}$ mice were reported to have defects in cell migration such that some rod photoreceptor nuclei were present in the INL and OPL (Z. C. Wright et al. 2016). This phenotype has not been reported in any previously generated *Rp2h* knockout mouse (L. Li et al. 2013; Houbin Zhang et al. 2015) therefore this may be another mechanism by which high levels of ARL3-GTP affect cell function independently of RP2 (Houbin Zhang et al. 2015; L. Li et al. 2013). In some cell types the microtubule organising

centre and the Golgi apparatus are positioned at the leading edge of the cell in order to ensure directed molecule and vesicular transport which is essential for migration (Watanabe, Noritake, and Kaibuchi 2005). The dynein-dynactin motor complex involved in vesicular trafficking is also located at the leading edge of cells (Hubbert et al. 2002). HDAC6 has been shown to colocalise with the P150Glued domain of dynactin (Hubbert et al. 2002) and recently it was discovered that ARL3 directly interacts with p150Glued domain and that this interaction dissociates the dynein-dynactin complex and leads to cargo unloading during vesicular trafficking (Jin et al. 2014). Overexpression of WT HDAC6 in NIH3T3 cells increased cell migration (Valenzuela-Fernández et al. 2008), likely through increased deactylation of microtubules which decreases microtubule stability and increases cell motility (Wadsworth 1999). Additionally cells lacking ARL13B have been shown to have a defect in cell migration and have increased levels of stable microtubules (Pruski et al. 2016). Therefore, a mechanism by which ARL3 activates HDAC6 and regulates release of cargo from vesicles at the leading edge of cells could contribute to cellular migration *in vivo*. Nevertheless, it should be noted that the migration phenotype reported in $Rod^{ARL3Q71L}$ mice was variable between founder lines and the level of the migration defect correlated with level of transgene expression (Z. C. Wright et al. 2016) and the *Arl3* -/- had no reported cell migration phenotype (Schick et al., 2006). In *Arl3* Q71L/+ and *Arl3* Q71L/Q71L retinas no obvious cell migration defect was detected suggesting that the cell migration phenotype reported in $Rod^{ARL3Q71L}$ mice may be attributed to overexpression or tagging of ARL3 Q71L rather than increased levels of ARL3-GTP. Examination of younger retinas may be required to observe whether some photoreceptors have migration defects. Still this serves as an example of another mechanism which may be regulated only by ARL3 and not RP2.

Another interesting comparison highlighting differential mechanisms which may be regulated by RP2 and ARL3 is the comparison of the *Arl3* -/- mouse and the previously published *Rp2h* knockout mice. *Arl3* -/- mice have a severe ciliopathy like phenotype with pancreatic lesions, failure of OS development and death by P.21 due to kidney disease (Schrick et al. 2006). Other groups have reported *Arl3* -/- mice to be an embryonic lethal (Hanke-Gogokhia et al. 2016) and in my CRISPR screen no *Arl3* null mice survived to genotyping. *Rp2h* knockout mice on the other hand have normal retina development followed by retinal degeneration with no other adverse phenotypes (L. Li et al. 2013; Houbin Zhang et al. 2015). This demonstrates that complimentary mechanisms must exist to compensate for loss of RP2 function in non-

ocular tissues. As ARL3 has been shown to regulate the activity of STAT3 in vivo ARL3 may also have roles in regulating other transcription factors which control cell survival. This could further explain the differences in phenotype which were observed between *Rp2h* DEL26/Y, *Rp2h* E135G/Y and *Arl3* Q71L/+ and *Arl3* Q71L/Q71L and may reveal other mechanisms which may contribute to cell death in vivo.

This result also has significant consequences in terms of potential treatment options as reintroduction of STAT3 signalling was shown to be protective against photoreceptor cell death in a model of inherited retinal degeneration (K. Jiang et al. 2014). Therefore, treatments designed to increase STAT3 signalling in the retina may prove ineffective in patients with *RP2* mutations if levels of STAT3 expression and activation are not affected. In order to confirm if loss of STAT3 signalling causes photoreceptor cell death *in vivo* WT mice would be treated with STAT3 inhibitors and examined for development of retinal degeneration. *Rp2h* DEL26/Y or *Rp2h* E135G/Y could also be treated with STAT3 inhibitors and examined to determine whether their retinal degeneration becomes much more severe.

6.4 OS Sink Hole Hypothesis

A common feature in animal models and human patients with RP is normal photoreceptor function at birth and progressive reduction in function over time followed by photoreceptor cell death. In *Rp2h* DEL26/Y and *Rp2h* E135G/Y retinas M/L opsin, rhodopsin and GRK1 were initially localised normally. *Rp2h* -/- mice have a similar phenotype with mislocalisation of PDE6 observed at 1 month of age however, the majority of PDE6 is localised to the OS with a minor fraction localised to the IS (Houbin Zhang et al. 2015). This data demonstrates that despite the hypothesis that RP2 is required for the trafficking of these proteins mechanisms exist which can facilitate trafficking to the OS in the absence of RP2. Even in the *Pde6δ* knockout mouse (*Pde6δ* -/-) proteins trafficked by PDE6δ are still initially localised to the OS but become mislocalised overtime (H Zhang et al. 2007) demonstrating another mechanism must exist which enables trafficking in the absence of the RP2-ARL3-PDE6δ pathway.

A study by Baker et.al demonstrated that the outer segment is the default destination for transmembrane proteins in the photoreceptor (Baker et al. 2008). Using R9AP as an example of an OS localised protein and syntaxin 3 as an example of an IS localised

protein they demonstrated that only syntaxin 3 had a sequence specific targeting motif that facilitated exclusion from the OS. No sequence specific moiety required for OS localisation was detected and the only requirement for OS targeting was a transmembrane domain of sufficient length (Baker et al. 2008). This finding may help to explain why in *Rp2h* DEL26/Y, *Rp2h* E135G/Y, *Arl3* Q71L/+, *Arl3* Q71L/Q71L and in published models some proteins are localised normally to the OS before they become mislocalised.

In mice the OS discs first develop at p10 and are fully developed by p14 (Salinas et al. 2017) whereas pups do not open their eyes until roughly p17, therefore there are a few days after OS development before OS function is required. During this time proteins could be expressed and localised to the OS by this default mechanism. Perhaps after eyes open the functional demand on OS proteins, specifically those involved in phototransduction, cannot be maintained by this default trafficking pathway thus alternative trafficking mechanisms have evolved. This hypothesis may help to explain why in *Rp2h* deficient mice and in XLRP patients with *RP2* mutations proteins are initially localised normally but become mislocalised over time. For example, the default trafficking pathway is able to maintain trafficking of OS proteins enough initially facilitate function, however, over time other trafficking mechanisms such as the RP2-ARL3-PDE6δ pathway are required for maintenance of OS protein load. In the absence of this pathway proteins gradually become mislocalised, photoreceptor function declines and ultimately photoreceptors die.

This “OS sink hole” hypothesis suggests that proteins may be able to freely diffuse to the OS providing an attractive mechanism to explain how proteins can still be trafficked to the OS despite loss of the trafficking pathway that shuttles them there. Knockout of *RP2* is hypothesised to lead to increased levels of ARL3-GTP and aberrant release of cargo from PDE6δ, and if proteins are able to freely diffuse into the OS these proteins could end up in the OS regardless. However, this is not what is observed as GRK1 was lost from the OS in *Rp2h* DEL26/Y, *Rp2h* E135G/Y, *Arl3* Q71L/+, *Arl3* Q71L/Q71L and in *Rp2h* -/- mice (Houbin Zhang et al. 2015). Also PDE6 was observed in punctate structures in the IS in *Rp2h* -/- mice (Houbin Zhang et al. 2015). This may be explained by considering that the OS is a modified cilia and proteins cannot freely diffuse into the cilia due to the presence of the cilia diffusion barrier (Q. Hu and Nelson 2011). The ciliary diffusion barrier is localised to the transition zone and consists of the ciliary necklace (two rows of particles which are

connected to the basal body by appendages), the Y-link that connects the ciliary necklace to the microtubules, a septin cytoskeleton and multiple protein complexes (Q. Hu and Nelson 2011). Photoreceptor OS are separated from the IS via the CC which contains transition zone proteins implying proteins cannot freely diffuse to the OS (Besharse et.al1999).

If proteins can be trafficked to the OS without any sequence specific targeting information but cannot arrive there by diffusion, these proteins may co-opt vesicles which contain proteins which do have sequence specific targeting information. For example, rhodopsin and cone opsins contain the (Valine X Proline X) VXPX ciliary targeting sequence which is required for OS targeting. Rhodopsin mutants lacking the VXPX sequence are mislocalised and human mutations in rhodopsin's C-terminus which contains this sequence cause autosomal dominant Retinitis Pigmentosa (ADRP) (Deretic et al. 2005). However when rhodopsin lacking the VXPX targeting sequence was expressed with WT rhodopsin the majority of rhodopsin molecules were localised to the OS with only a small fraction observed in the ER and other cellular compartments (Sung et al. 1994; T. Li et al. 1996; Green et al. 2000). This suggests that rhodopsin lacking VXPX may still able to traffic to the OS in vesicles containing rhodopsin with the VXPX domain.

If this model is applied to a situation where RP2 is absent it may explain why an accumulation of mislocalised proteins is observed in the IS and ONL of photoreceptors. Using GRK1 as an example, it can be hypothesized that in WT photoreceptors during development proteins are trafficked to the OS in vesicles containing proteins with sequence specific OS targeting motifs- default trafficking pathway. After eyes open and photoreceptor function is required the default pathway cannot maintain sufficient levels of GRK1 in the OS so PDE6δ is then required to extract GRK1 from the ER and traffic it to the OS. When RP2 is mutated and levels of ARL3-GTP increased, GRK1 is still extracted from the ER by PDE6δ, therefore can no longer co-opt vesicles destined to the OS. PDE6δ is converted to the closed conformation by ARL3-GTP releasing GRK1 into the cytoplasm which ultimately leads to photoreceptor cell stress and apoptosis.

This model can also be applied to *Arl3* Q71L/+ and *Arl3* Q71L/Q71L mice where M/L opsin is localised normally at one month but becomes mislocalised with aging. In *Arl3* Q71L/+ rhodopsin is initially localised normally but becomes mislocalised over time however in *Arl3* Q71L/Q71L mice rhodopsin is mislocalised from one month of age.

As 1 month of age was the youngest age I examined it is not possible to conclude whether *Arl3* Q71L/Q71L mice ever have normally localised rhodopsin. Similarly GRK1 is mislocalised in *Arl3* Q71L/+ and *Arl3* Q71L/Q71L retinas at 1 month of age so it is not possible to conclude whether *Arl3* Q71L mice have normally localised GRK1 at birth. In order to assess whether GRK1 is localised normally earlier ages could be analysed. If GRK1 or rhodopsin is never localised normally in *Arl3* Q71L mice, but it is initially localised normally in *Rp2h* DEL26/Y and *Rp2h* E135G/Y retinas, it would demonstrate that the extremely elevated levels of ARL3-GTP in *Arl3* Q71L mice is capable of disrupting the pathway that traffics GRK1 to the OS in the absence of RP2.

6.5 Implications for Therapeutic Approaches for X-linked Retinitis Pigmentosa

Retinitis Pigmentosa is not a disease attributed to defects in the visual cycle as patients can see throughout their early lives, the key pathogenic defect is onset of photoreceptor cell death (Travis 1998). *Rp2h* DEL26/Y and *Rp2h* E135G/Y mice model this aspect of the disease as photoreceptors remain functional for some time before photoreceptor cell death occurs. The hypothesis that *RP2* mutations cause increased levels of ARL3-GTP and therefore mislocalisation of OS proteins trafficked by PDE6δ and UNC119 and activation of apoptosis through ER stress is somewhat supported by my data however my results suggest that increased levels of ARL3-GTP may not fully explain the cell death phenotype which occurs in these mice. Increased levels of ARL3-GTP were undetectable in *Rp2h* DEL26/Y and *Rp2h* E135G/Y tissues compared to WT demonstrating that if levels of ARL3-GTP are increased it is not substantially greater than WT. As *Rp2h* DEL26/Y retinas have a more severe retinal degeneration than *Rp2h* E135G/Y retinas this suggests that functions of RP2 independent of ARL3 contribute to photoreceptor cell death. Furthermore *Arl3* Q71L/+ and *Arl3* Q71L/Q71L not *Rp2h* DEL26/Y or *Rp2h* E135G/Y eyes had reduced STAT3 activation which may contribute to cell death providing evidence that photoreceptor apoptosis may not be driven by the same mechanisms *in vivo*. Overall, my results indicate that targeting levels of ARL3-GTP may not be the best approach to treat XLRP patients with *RP2* mutations, as although trafficking defects may be alleviated the as yet unknown functions of RP2 which are independent of ARL3 would not be addressed and therefore cell death may still occur. Ultimately, further research is

required into the alternative roles of RP2 in the retina and how these contribute to photoreceptor survival so that effective treatment strategies can be developed.

Although my study suggests that ARL3 may not be an ideal drug target for the treatment of XLRP patients it suggests that targeting of RP2 itself may be the most effective strategy. Gene therapy is an attractive therapeutic option for diseases of inherited retinal degeneration. The eye is an attractive tissue for the application and validation of gene therapy based approaches as it is an encapsulated organ so the risk of systemic exposure of the transgene to the rest of the body is reduced and in the event of an adverse outcome, such as cancer development, eyes can be treated or ultimately removed from patients without risk to life (Whiting et al. 2015). Effectiveness of therapy is easily assessed by non-invasive approaches which measure increased visual acuity and the patients untreated eye serves as an ideal control to assay treatment effectiveness (Whiting et al. 2015).

In October 2017 the first gene therapy to treat inherited retinal degeneration achieved FDA approval. Luxturna, the commercial name for the therapy, is a drug that reintroduces RPE65 into patients who suffer from Leber Congenial Amaurosis (LCA) caused by mutation in *RPE65*. Previous clinical trials have demonstrated that reintroduction of RPE65 into young patients improved visual acuity however after 3 years of follow up despite improved vision retinal degeneration still persisted in patients (Cideciyan et al. 2013). This example highlights the issues associated with timing and efficacy of therapies as if a therapy is administered after initiation of photoreceptor degeneration restoration of gene function may not prevent cell death, as loss of some photoreceptors can trigger secondary death in others due to changes in oxygen tension (Campochiaro and Mir 2018). Similarly if only a small percentage of photoreceptors express the re-introduced gene, cell death may still occur secondary to death of other non- transgene expressing photoreceptors. The mechanisms which drive photoreceptor degeneration in LCA patients treated with *RPE65* gene therapy are currently unknown therefore further investigation is required so that innovative treatments such as this can provide maximum benefit to patients.

Despite the issues associated with *RPE65* gene therapy, its success in restoring vison has spurred on the development of gene therapies for other inherited retinal degenerations. Gene therapy approaches for XLRP caused by *RPGR* mutations are under development. A recent update of this approach in X-linked Progressive Retinal Atrophy 2 (XLPRA2) dogs, which contain a naturally occurring frameshift mutation in

RPGR^{ORF15}, demonstrated that treatment with human codon optimised RPGR^{ORF15} driven by the GRK1 promotor restored vision and protected against retinal degeneration 2 years post treatment (Beltran et al. 2012). A phase 1 trial for AAV administered RPGR in XLRP is due to be completed in 2020 (https://clinicaltrials.gov/ct2/show/study/NCT03252847).

The development of gene therapy approaches for RP2 patients has also begun, AAV administration of RP2 to the *Rp2*^{null} mouse rescued the M/L opsin mislocalisation phenotype, improved ERG response of cone photoreceptors and protected against cone degeneration suggesting this could be a therapeutic option for patients in the future (Mookherjee et al. 2015). Patients which contain nonsense mutations may also be applicable for treatment with translational read through drugs to reintroduce expression of the full-length protein in cells. Administration of translational read through drugs in RPE cells derived from patient derived iPSCs (induced pluripotent stem cells) restored sufficient RP2 expression to reduce the cellular phenotypes of Golgi fragmentation and IFT20 dispersion associated with *RP2* mutation (Schwarz et al. 2015). Recently antisense oligonucleotides have been used to correct the splicing defect which results from human the c.2991+1655A>G intronic mutation in *CEP290* which causes Leber Congenital Amaurosis (LCA). QR-110 (the antisense oligonucleotide) restored full length CEP290 expression in patient derived iPSC retinal organoids and when injected into the eyes of mice and rabbits QR-110 localised to all retinal layers. Antisense oligonucleotide approaches are an attractive option for patients with splice site mutations and a major benefit from this approach is that the final result is restoration of WT protein levels avoiding overexpression of proteins, the effect of which for many genes including RP2 is unknown (Dulla et al. 2018).

Gene therapy approaches are promising for RP2 patients which harbour null, nonsense or missense mutations which lead to an unstable protein product but for patients that harbour RP2 point mutations such as RP2 E135G, RP2 R118H, RP2 R211L, which affect a specific aspect of RP2 function, gene replacement therapies may be ineffective. In these cases cell based therapies may be a viable option. Cell therapies involve the introduction of a healthy stem cell population to the retina in the hopes they will differentiate to healthy photoreceptors or RPE cells to replace those lost in disease. A study in patients with Macular Degeneration (MD) and Stargardt's disease demonstrated that transplantation of human ESCs (Embryonic Stem Cells)

was safe and potentially affective (Schwartz et al. 2015) however the use of human embryos to derive human ESCs is controversial and holds the possibility of the recipient rejecting the donor tissue. An alternative approach involves using the patient's own fibroblasts to generate iPSCs which could be transplanted into the eye with no fear of rejection. Patients own fibroblasts will contain pathogenic mutations that would first have to be corrected before cells could be used for therapeutic purposes. The advent of CRISPR technology facilitates the correction of human pathogenic point mutations. A proof of principal study demonstrated that correction of a pathogenic point mutation in RPGR is possible by CRISPR editing of patient derived iPSC (Bassuk et al. 2016). An issue with cell therapies is the difficulty in encouraging stem cell populations to differentiate into photoreceptor cells, therefore restoration of damaged RPE cells by stem cell therapies to promote photoreceptor survival is a strategy which could benefit patients with RP. In the rhodopsin knockout (*rho* -/-) mouse transplantation of bone marrow derived stem cells into the retina resulted in preservation of photoreceptors by restoring healthy RPE at the transplant site (Arnhold et al. 2007). For patients with MD which is caused by defects in the RPE, cell based therapy may be widely available in the future as remarkable sight restoration has been achieved in a patient with Wet MD after treatment with RPE cells engineered from stem cells (Da Cruz et al. 2018). Recently differentiation of rod photoreceptors was achieved through a two-step reprogramming of Muller glia cells. The resulting rods have functional outer segments with disc structures and expression of rhodopsin and other outer segment proteins and were capable of generating a calcium gradient upon light stimulation (Yao et al. 2018). Although this achievement is no doubt exciting if this method was to be applied in a therapeutic context, a mechanism to repair the pathogenic mutation in patient cells would be required, otherwise rods generated from patient Muller glial cells would still containing the pathogenic mutation and would degenerate once again.

6.6 ZDHHC5 Traffics RP2 to the Cell Membrane in Vitro

ZDHHC5 was identified as a novel interactor of RP2 in my BIO ID analysis. Using 17-ODYA incorporation as a measure of RP2 palmitoylation I demonstrated that ZDHHC5 is likely not soley responsible for RP2 palmitoylation *in vitro*. Overexpression of ZDHHC5 was able to rescue the mistrafficking of RP2 mutants, RP2 C3S and RP2 G2A, independently of its catalytic activity suggesting that ZDHHC5 may have a role

in trafficking RP2. Knockdown of endogenous ZDHHC5 in HeLa cells caused RP2-V5 to be mislocalised from the plasma membrane to intracellular membranes suggesting that it may be required for trafficking of WT RP2 *in vivo* and this may could play a role in trafficking of lipid modified OS proteins in photoreceptors. I also tested whether ARL3 is palmitolyated and demonstrated that ARL3 is palmitolyated and mutation of C158, C118 and C174 reduced palmitoylation of ARL3 in cells, suggesting ARL3 is palmitolyated at multiple residues to facilitate membrane associations which may be required for interaction with its regulator proteins RP2 and ARL13B.

ZDHHC5 overexpression was able to rescue the mistrafficking of RP2 C3S and G2A which are not palmitolyated or myristolated respectively (Chapple et al. 2000). These mutations are human pathogenic mutations which are presumed to be mislocalised *in vivo* this finding suggests that the pathogenesis of these mutants may not be purely due to mislocalisation as ZDHHC5 is expressed in photoreceptors (D. Murphy et al. 2016). It is possible that other interactions of RP2 are perturbed when palmitoylation or myristolation is blocked as it has been demonstrated that palmitoylation can regulate protein -protein interactions for example palmitoylation of cysteine residues on tetraspanin is essential for its interaction with integrins which is essential for function (X. Yang et al. 2004). As overexpression of ZDHHC5 was required for rescue of mistrafficking it may be that *in vivo* endogenous levels of ZDHHC5 are not sufficient to rescue trafficking of RP2 C3S and RP2 G2A thus these mutants are mislocalised. Increased ZDHHC5 expression in the photoreceptor could be an interesting avenue for therapeutic intervention in patients with RP2 C3 and RP2 G2 mutations as this may be able to rescue the trafficking defect.

Knockdown of ZDHHC5 by siRNAs demonstrated that ZDHHC5 expression was required for RP2-V5 localisation to the plasma membrane. This finding suggests that ZDHHC5 may be involved in trafficking RP2 to the membrane *in vivo* independently of its catalytic activity (Figure 6.1). As ARL3 was identified as being palmitolyated in HeLa cells the effect of ZDHHC5 overexpression on ARL3 palmitoylation or localisation could be investigated this would provide more information into the regulation of RP2 and ARL3 and whether they share common mechanisms of regulation. As RP2 and ARL3 are involved in the trafficking of lipid modified proteins it suggests ZDHHC5 may be another player in this pathway, which may have a dual role in trafficking and palmitoylation of OS proteins in the photoreceptor. ZDHHC5 and ZDHHC2 are enriched in photoreceptors compared to other ZDHHC's suggesting

they may have specific roles in photoreceptors which other ZDHHC's cannot compensate for (D. Murphy et al. 2016). Furthermore, as mislocalisation of lipid modified proteins is a phenomenon common to X-linked Retinitis Pigmentosa, demonstrated through the study of *Rp2h* and *Rpgr* knockout mice (L. Li et al. 2013; F. Liu et al. 2015; Hong et al. 2000), further study of this protein may be relevant do disease pathogenesis.

Figure 6. 1 ZDHHC5 Traffics RP2 to the Cell Membrane but does not Palmitoylate RP2

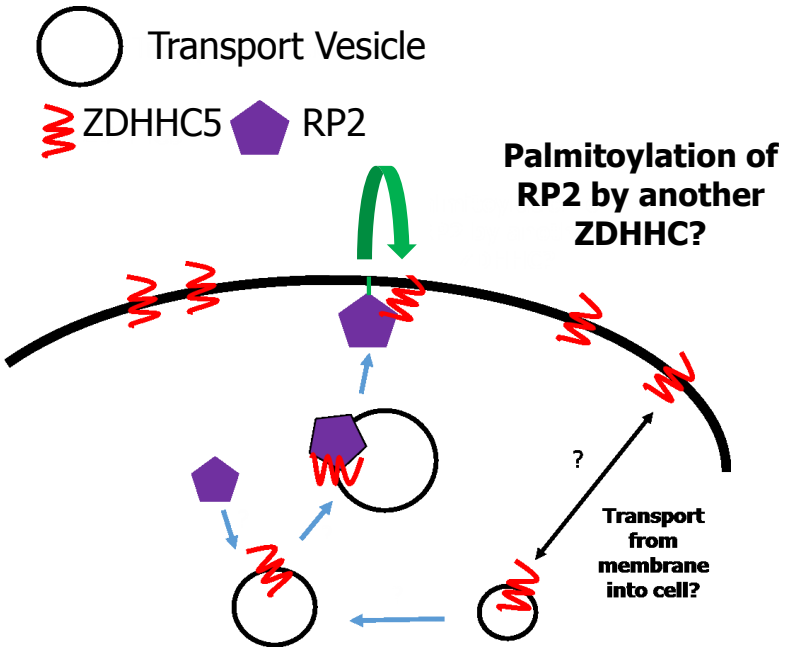

Schematic of ZDHHC5 and RP2 trafficking to the plasma membrane. RP2 may be trafficked from the plasma membrane into membrane bound vesicles by an unknown mechanism or newly synthesised RP2 is packaged into vesicles destined for the plasma membrane. RP2 and ZDHCC5 interact in membrane bound vesicles and are trafficked to the plasma membrane where RP2 is palmitolyated by an as yet unidentified palmitolyltransferase and anchors to the plasma membrane.

6.7 Future Work

By studying the phenotype of *Rp2h* DEL26/Y, *Rp2h* E135G/Y, *Arl3* Q71L/+ and *Arl3* Q71L/Q71L mice I demonstrated that high levels of ARL3-GTP is a driver of retinal degeneration in mice and that mutation of *Rp2h* and increased levels of ARL3-GTP cause mistrafficking of GRK1 likely through misregulation of the PDE6δ. *Rp2h*

DEL26/Y, *Rp2h* E135G/Y, *Arl3* Q71L/+ and *Arl3* Q71L/Q71L retinas all displayed defects in rhodopsin trafficking which indicates a novel role for RP2 and ARL3 in the trafficking of opsins *in vivo*. I demonstrated that RP2 might have functions that are important in the retina which are not related to GAP activity on ARL3 as *Rp2h* DEL26/Y mice have a more severe retinal degeneration than *Rp2h* E135G/Y mice. I demonstrated that *Arl3* Q71L/+ and *Arl3* Q71L/Q71L mice have substantially increased levels of ARL3-GTP compared to WT, *Rp2h* DEL26/Y and *Rp2h* E135G/Y demonstrating that mechanisms exist which regulate the levels of ARL3-GTP in the eye in the absence of RP2. Finally I showed that only *Arl3* Q71L/+ and *Arl3* Q71L/Q71L eyes and not *Rp2h* DEL26/Y or *Rp2h* E135G/Y eyes had reduced STAT3 activation at one month of age which may contribute to retinal degeneration. This finding suggests that mutations of *RP2* and increased levels of ARL3-GTP may not promote retinal degeneration by the same mechanisms.

Along with the further experiments discussed throughout this chapter and my results chapters the key questions which remain unanswered from this study and that require further investigation are:

6.7.1 How are levels of ARL3-GTP regulated in the absence of RP2?

In order to address this question and search for an alternative GAP for ARL3, novel interactors of ARL3 could be examined through an Immunoprecipitation and Mass spectrometry (IP/Mass Spec) approach in RPE cells. Alternatively, a BIO-ID assay for ARL3 could be utilised as this may better facilitate the capture of transient interactions in RPE cells. This assay could also be carried out in RP2 null RPE cells in order to identify interactors that interact with ARL3 in the absence of RP2. In order to identify a retina specific GAP IP/Mass spec proteomics from the retinas of ARL3 Q71L/Q71L retinas could be attempted, since GAPs should preferentially bind to the GTP bound form this approach would enrich for potential gaps for ARL3. Attempting to identify GAPs from eye tissue might identify a second retina specific GAP not found in other tissues and hence not previously identified as all other studies have been carried out in cell culture systems. In order to assess whether levels of ARL3-GTP may be regulated by the GEF ARL13B the level of expression of ARL13B could be assessed in WT, *Rp2h* DEL26/Y and *Rp2h* E135G/Y eyes. The GEF activity of ARL13B for ARL3 could be measured, by measuring the presence of ARL3-GTP in cells using an

antibody specific for ARL3-GTP, in WT RPE cells and in RP2 null RPE cells in order to establish if GEF activity is affected by the absence of RP2.

6.7.2 What functions does RP2 have that are Independent of ARL3?

In order to address RP2 functions which are independent of ARL3, that are relevant to disease pathogenesis *in vivo*, a BIO-ID assay on WT RP2 and RP2 E135G expressing RPE cells could be performed to identify interactors which are present when interaction with ARL3 is lost. In order to infer whether these interactors are important to disease pathogenesis the findings could be compared to BIO-ID analysis of other non-destabilising pathogenic point mutations, such as R211L, to assess whether they may represent molecular mechanisms which could underlie disease pathogenesis in these cases. After identification of interesting hits, the relevance of these hits *in vivo* could be assessed in *Rp2h* DEL26/Y and *Rp2h* E135G/Y mice.

6.7.3 How does mutation of *RP2* stimulate Photoreceptor Cell Death?

There are likely multiple mechanisms that drive photoreceptor cell death in *Rp2h* mutant mice. As *Rp2h* mutants have mislocalised OS proteins it is possible that accumulation of mislocalised proteins causes ER stress which leads to apoptosis. In order to evaluate whether *Rp2h* DEL26/Y and *Rp2h* E135G/Y mice have increased ER stress, RNA sequencing of retinas could be analysed and analysis of expression levels of genes associated with ER stress and UPR could be compared to WT retinas. This experiment could also be performed in *Arl3* Q71L/+ and *Arl3* Q71L/Q71L mice in order to ascertain whether these retinas also suffer from ER stress. As it was established that GRK1 is degraded it may be that degradation of mislocalised proteins protects against ER stress. As some evidence exists, which suggests RP2 may have a role in the DNA damage response (Yoon et al. 2006) and as other models of inherited retinal degeneration have been shown to have increased levels of oxidative stress induced DNA damage (Ahuja-Jensen et al. 2007) this hypothesis could be investigated further. Whether RP2 has roles in the DNA damage response could be addressed through *in vitro* assays in RP2 null RPE cells. WT and RP2 null RPE cells could be treated with hydrogen peroxide or UV to induce DNA damage and the survival of RP2 knockout cells assessed. It would be expected that if RP2 had a role in DNA damage response then RP2 null RPE cells would be unable to repair their DNA efficiently and may undergo growth arrest or apoptosis as a result. In order to

identify which proteins RP2 interacts with post-DNA damage a time course IP/Mass spec experiment could be performed in which WT RPE cells and RP2 null RPE cells are exposed to a DNA damaging agent and cells lysed at various times after DNA damage. Alternatively, this same approach could be combined with the BIO-ID system such that RP2 null RP2 BIRA RPE cells are treated with a DNA damaging agent and biotin to facilitate labelling of proximal proteins, cells could be lysed at different times after exposure to the DNA damaging agent to examine RP2's interactors during DNA repair. Any interesting interactors identified could be validated *in vivo* in *Rp2h* DEL26/Y and *Rp2h* E135G/Y mice.

6.7.4 How is RP2 Palmitoylation Regulated *in Vivo* and does ZDHHC5 have an Important Function in the Eye?

In order to examine whether multiple ZDHHC's are required for palmitoylation of RP2 *in vivo* knockdown of multiple ZDHHC's in cells followed by an assessment of RP2's 17-ODYA incorporation could be undertaken. In order to assess whether the RP2-ZDHHC5 interaction has an important function *in vivo* the residues which are required for this interaction could first be investigated through targeted deletions of RP2 and assay of ZDHHC5 interaction. Once the residues required for this interaction were established mutations of these residues could be introduced into mice via CRISPR genome editing. Whether these mice have retinal degeneration could be confirmed by histology and ERG analysis. An interesting observation may be whether these mice have mislocalisation of proteins known to be trafficked by RP2 and ARL3 which would infer that the RP2-ZDHHC5 interaction has a functional role *in vivo*. Generation of a ZDHHC5 null mouse could also be invaluable in assessing the role of ZDHHC5 in the eye. The previously published DHHC5 *gt/gt* mouse carried a hypomorphic null allele (Yi Li et al. 2010) therefore in order to cleanly assess the role of ZDHHC5 in the retina a new model could be generated by CRISPR cas9. The localisation of RP2 could be investigated in these mice to establish whether ZDHHC5 is required for RP2 localisation *in vivo*. As knockdown of ZDHHC5 caused ciliogenesis defects in RPE cells the development of the photoreceptor CC and OS could be investigated in order to determine whether ZDHHC5 plays a role in photoreceptor ciliogenesis *in vivo*. Overall, further work in *in vivo* models is required in order to determine whether ZDHHC5 is involved in photoreceptor function and whether this is relevant to pathogenesis of XLRP caused by *RP2* mutations.

6.8 Concluding Remarks

Retinitis Pigmentosa is the leading cause of inherited blindness worldwide and currently limited treatment options and no cures are available. 15% -20% of cases of XLRP are caused by mutations in *RP2* a gene that's function is still not well understood. As RP2 is known to have GAP activity for ARL3 it is hypothesised that mutation of RP2 causes increased levels of ARL3-GTP which leads to mislocalisation of OS proteins in photoreceptors leading to cell death. My PhD research aimed to ascertain whether the pathogenesis of XLRP in cases of *RP2* mutation is attributed solely to dysregulation of ARL3. In order to do this new mouse models were generated by CRISPR including a new RP2 null model, *Rp2h* DEL26/Y and a mouse with GAP activity deficient RP2, *Rp2h* E135G/Y. The phenotype of these mice was compared to mice harbouring a constitutively activating mutation in ARL3, *Arl3* Q71L/+ and *Arl3* Q71L/Q71L. Discrepancies in the phenotypes of these mice imply that pathogenesis of XLRP caused by *RP2* mutation cannot be fully explained by increased levels of ARL3-GTP. My results validated a role for RP2 and ARL3 in protein trafficking but highlighted that cell death may not be activated by the same mechanisms in *Rp2h* mutants and *Arl3* Q71L mice. As blindness in RP results from cell death of photoreceptors this is an important finding which sheds new light on disease pathogenesis in patients. This finding highlights the need for further research into mechanisms which stimulate photoreceptor cell death *in vivo* so that effective therapies can be developed for patients.

Reference List

Adamian, Michael, Basil S. Pawlyk, Dong Hyun Hong, and Eliot L. Berson. 2006. "Rod and Cone Opsin Mislocalization in an Autopsy Eye From a Carrier of X-Linked Retinitis Pigmentosa With a Gly436Asp Mutation in the RPGR Gene." *American Journal of Ophthalmology*. https://doi.org/10.1016/j.ajo.2006.03.061.

Adler, Ruben, and M. Valeria Canto-Soler. 2007. "Molecular Mechanisms of Optic Vesicle Development: Complexities, Ambiguities and Controversies." *Developmental Biology*. https://doi.org/10.1016/j.ydbio.2007.01.045.

Ahuja-Jensen, Poonam, Siv Johnsen-Soriano, Satpal Ahuja, Francisco Bosch-Morell, María Sancho-Tello, Francisco Javier Romero, Magnus Abrahamson, and Theo Van Veen. 2007. "Low Glutathione Peroxidase in Rd1 Mouse Retina Increases Oxidative Stress and Proteases." *NeuroReport*. https://doi.org/10.1097/WNR.0b013e3280c1e344.

Ahuja, P., A. R. Caffé, S. Ahuja, P. Ekström, and T. Van Veen. 2005. "Decreased Glutathione Transferase Levels in Rd1/Rd1 Mouse Retina: Replenishment Protects Photoreceptors in Retinal Explants." *Neuroscience*. https://doi.org/10.1016/j.neuroscience.2004.11.012.

Alfinito, Peter D, and Ellen Townes-Anderson. 2002. "Activation of Mislocalized Opsin Kills Rod Cells: A Novel Mechanism for Rod Cell Death in Retinal Disease." *Proceedings of the National Academy of Sciences of the United States of America* 99 (8): 5655–60. https://doi.org/10.1073/pnas.072557799.

Andre, Jane, Louise Kerry, Xin Qi, Erica Hawkins, Kristina Drižyte, Michael L. Ginger, and Paul G. McKean. 2014. "An Alternative Model for the Role of RP2 Protein in Flagellum Assembly in the African Trypanosome." *Journal of Biological Chemistry* 289 (1): 464–75. https://doi.org/10.1074/jbc.M113.509521.

Angleson, J. K., and T. G. Wensel. 1994. "Enhancement of Rod Outer Segment GTPase Accelerating Protein Activity by the Inhibitory Subunit of CGMP Phosphodiesterase." *Journal of Biological Chemistry*.

Applebury, M. L., M. P. Antoch, L. C. Baxter, L. L.Y. Chun, J. D. Falk, F. Farhangfar, K. Kage, M. G. Krzystolik, L. A. Lyass, and J. T. Robbins. 2000. "The Murine

Cone Photoreceptor: A Single Cone Type Expresses Both S and M Opsins with Retinal Spatial Patterning." *Neuron*. https://doi.org/10.1016/S0896-6273(00)00062-3.

Arnhold, Stefan, Y. Absenger, H. Klein, K. Addicks, and U. Schraermeyer. 2007. "Transplantation of Bone Marrow-Derived Mesenchymal Stem Cells Rescue Photoreceptor Cells in the Dystrophic Retina of the Rhodopsin Knockout Mouse." *Graefe's Archive for Clinical and Experimental Ophthalmology*. https://doi.org/10.1007/s00417-006-0382-7.

Avasthi, P., C. B. Watt, D. S. Williams, Y. Z. Le, S. Li, C.-K. Chen, R. E. Marc, J. M. Frederick, and W. Baehr. 2009. "Trafficking of Membrane Proteins to Cone But Not Rod Outer Segments Is Dependent on Heterotrimeric Kinesin-II." *Journal of Neuroscience*. https://doi.org/10.1523/JNEUROSCI.3976-09.2009.

Avidor-Reiss, Tomer, Andreia M. Maer, Edmund Koundakjian, Andrey Polyanovsky, Thomas Keil, Shankar Subramaniam, and Charles S. Zuker. 2004. "Decoding Cilia Function: Defining Specialized Genes Required for Compartmentalized Cilia Biogenesis." *Cell* 117 (4): 527–39. https://doi.org/10.1016/S0092-8674(04)00412-X.

Bach, Michael, Mitchell G. Brigell, Marko Hawlina, Graham E. Holder, Mary A. Johnson, Daphne L. McCulloch, Thomas Meigen, and Suresh Viswanathan. 2013. "ISCEV Standard for Clinical Pattern Electroretinography (PERG): 2012 Update." *Documenta Ophthalmologica*. https://doi.org/10.1007/s10633-012-9353-y.

Baker, Sheila A., Katie Freeman, Katherine Luby-Phelps, Gregory J. Pazour, and Joseph C. Besharse. 2003. "IFT20 Links Kinesin II with a Mammalian Intraflagellar Transport Complex That Is Conserved in Motile Flagella and Sensory Cilia." *Journal of Biological Chemistry*. https://doi.org/10.1074/jbc.M300156200.

Baker, Sheila A., Mohammad Haeri, Peter Yoo, Sidney M. Gospe, Nikolai P. Skiba, Barry E. Knox, and Vadim Y. Arshavsky. 2008. "The Outer Segment Serves as a Default Destination for the Traffi Cking of Membrane Proteins in Photoreceptors." *Journal of Cell Biology*. https://doi.org/10.1083/jcb.200806009.

Bartolini, Francesca, Arunashree Bhamidipati, Scott Thomas, Uwe Schwahn, Sally A. Lewis, and Nicholas J. Cowan. 2002. “Functional Overlap between Retinitis Pigmentosa 2 Protein and the Tubulin-Specific Chaperone Cofactor C.” *Journal of Biological Chemistry* 277 (17): 14629–34. https://doi.org/10.1074/jbc.M200128200.

Bassuk, Alexander G., Andrew Zheng, Yao Li, Stephen H. Tsang, and Vinit B. Mahajan. 2016. “Precision Medicine: Genetic Repair of Retinitis Pigmentosa in Patient-Derived Stem Cells.” *Scientific Reports*. https://doi.org/10.1038/srep19969.

Bavelloni, Alberto, Irene Faenza, Gabriella Cioffi, Manuela Piazzi, Daniela Parisi, Ivan Matic, Nadir M. Maraldi, and Lucio Cocco. 2006. “Proteomic-Based Analysis of Nuclear Signaling: PLCβ1affects the Expression of the Splicing Factor SRp20 in Friend Erythroleukemia Cells.” *Proteomics*. https://doi.org/10.1002/pmic.200600318.

Beltran, W. A., A. V. Cideciyan, A. S. Lewin, S. Iwabe, H. Khanna, A. Sumaroka, V. A. Chiodo, et al. 2012. “Gene Therapy Rescues Photoreceptor Blindness in Dogs and Paves the Way for Treating Human X-Linked Retinitis Pigmentosa.” *Proceedings of the National Academy of Sciences*. https://doi.org/10.1073/pnas.1118847109.

Berson, Eliot L, Bernard Rosner, Carol Weigel-DiFranco, Thaddeus P Dryja, and Michael a Sandberg. 2002. “Disease Progression in Patients with Dominant Retinitis Pigmentosa and Rhodopsin Mutations.” *Investigative Ophthalmology & Visual Science*.

Besharse, Joseph C, Sheila A Baker, Katherine Luby-Phelps, and Gregory J Pazour. 2003. “Photoreceptor Intersegmental Transport and Retinal Degeneration.” In *Retinal Degenerations*, edited by Matthew M LaVail, Joe G Hollyfield, and Robert E Anderson, 157–64. Boston, MA: Springer US.

Besharse, Joseph C, and Cynthia J Horst. 1990. “The Photoreceptor Connecting Cilium A Model for the Transition Zone.” In *Ciliary and Flagellar Membranes*, edited by Robert A Bloodgood, 389–417. Boston, MA: Springer US. https://doi.org/10.1007/978-1-4613-0515-6_15.

Bhowmick, Reshma, Mei Li, Jun Sun, Sheila A. Baker, Christine Insinna, and

Joseph C. Besharse. 2009. “Photoreceptor IFT Complexes Containing Chaperones, Guanylyl Cyclase 1 and Rhodopsin.” *Traffic*. https://doi.org/10.1111/j.1600-0854.2009.00896.x.

Biel, M, M Seeliger, a Pfeifer, K Kohler, a Gerstner, a Ludwig, G Jaissle, S Fauser, E Zrenner, and F Hofmann. 1999. “Selective Loss of Cone Function in Mice Lacking the Cyclic Nucleotide-Gated Channel CNG3.” *Proceedings of the National Academy of Sciences of the United States of America*. https://doi.org/10.1073/pnas.96.13.7553.

Bonifaci, N, J Moroianu, A Radu, and G Blobel. 1997. “Karyopherin Beta2 Mediates Nuclear Import of a MRNA Binding Protein.” *Proceedings of the National Academy of Sciences of the United States of America*. https://doi.org/10.1073/pnas.94.10.5055.

Boughman, J. A., M. Vernon, and K. A. Shaver. 1983. “Usher Syndrome: Definition and Estimate of Prevalence from Two High-Risk Populations.” *Journal of Chronic Diseases*. https://doi.org/10.1016/0021-9681(83)90147-9.

Bowes, Cathy, Tiansen Li, Michael Danciger, Leslie C. Baxter, Meredithe L. Applebury, and Debora B. Farber. 1990. “Retinal Degeneration in the Rd Mouse Is Caused by a Defect in the β Subunit of Rod CGMP-Phosphodiesterase.” *Nature*. https://doi.org/10.1038/347677a0.

Boylan, J P, and A F Wright. 2000. “Identification of a Novel Protein Interacting with RPGR.” *Human Molecular Genetics*. https://doi.org/10.1093/hmg/9.14.2085.

Brann, Mark R., and Leslie V. Cohen. 1987. “Diurnal Expression of Transducin MRNA and Translocation of Transducin in Rods of Rat Retina.” *Science*. https://doi.org/10.1126/science.3101175.

Bravo, Roberto, Valentina Parra, Damián Gatica, Andrea E. Rodriguez, Natalia Torrealba, Felipe Paredes, Zhao V. Wang, et al. 2013. “Endoplasmic Reticulum and the Unfolded Protein Response. Dynamics and Metabolic Integration.” *International Review of Cell and Molecular Biology*. https://doi.org/10.1016/B978-0-12-407704-1.00005-1.

Brigidi, G. Stefano, Brendan Santyr, Jordan Shimell, Blair Jovellar, and Shernaz X. Bamji. 2015. “Activity-Regulated Trafficking of the Palmitoyl-Acyl Transferase

DHHC5.” *Nature Communications*. https://doi.org/10.1038/ncomms9200.

Brigidi, G. Stefano, Yu Sun, Dayne Beccano-Kelly, Kimberley Pitman, Mahsan Mobasser, Stephanie L. Borgland, Austen J. Milnerwood, and Shernaz X. Bamji. 2014. “Palmitoylation of δ-Catenin by DHHC5 Mediates Activity-Induced Synapse Plasticity.” *Nature Neuroscience*. https://doi.org/10.1038/nn.3657.

Brückner, Anna, Cécile Polge, Nicolas Lentze, Daniel Auerbach, and Uwe Schlattner. 2009. “Yeast Two-Hybrid, a Powerful Tool for Systems Biology.” *International Journal of Molecular Sciences*. https://doi.org/10.3390/ijms10062763.

Buglino, John A., and Marilyn D. Resh. 2008. “Hhat Is a Palmitoylacyltransferase with Specificity for N-Palmitoylation of Sonic Hedgehog.” *Journal of Biological Chemistry*. https://doi.org/10.1074/jbc.M803901200.

Bürgi, Sandra, Marijana Samardzija, and Christian Grimm. 2009. “Endogenous Leukemia Inhibitory Factor Protects Photoreceptor Cells against Light-Induced Degeneration.” *Molecular Vision*.

Burns, M. E. 2006. “Deactivation of Phosphorylated and Nonphosphorylated Rhodopsin by Arrestin Splice Variants.” *Journal of Neuroscience*. https://doi.org/10.1523/JNEUROSCI.3301-05.2006.

Burns, Marie E., Ana Mendez, Jeannie Chen, and Denis A. Baylor. 2002. “Dynamics of Cyclic GMP Synthesis in Retinal Rods.” *Neuron*. https://doi.org/10.1016/S0896-6273(02)00911-X.

Calvert, P. D., V. A. Klenchin, and M. D. Bownds. 1995. “Rhodopsin Kinase Inhibition by Recoverin. Function of Recoverin Myristoylation.” *Journal of Biological Chemistry*. https://doi.org/10.1074/jbc.270.41.24127.

Calvert, P. D., N. V. Krasnoperova, A. L. Lyubarsky, T. Isayama, M. Nicolo, B. Kosaras, G. Wong, et al. 2000. “Phototransduction in Transgenic Mice after Targeted Deletion of the Rod Transducin Alpha -Subunit.” *Proceedings of the National Academy of Sciences*. https://doi.org/10.1073/pnas.250478897.

Campochiaro, Peter A., and Tahreem A. Mir. 2018. “The Mechanism of Cone Cell Death in Retinitis Pigmentosa.” *Progress in Retinal and Eye Research*.

https://doi.org/10.1016/j.preteyeres.2017.08.004.

Campochiaro, Peter A., Rupert W. Strauss, Lili Lu, Gulnar Hafiz, Yulia Wolfson, Syed M. Shah, Raafay Sophie, Tahreem A. Mir, and Hendrik P. Scholl. 2015. “Is There Excess Oxidative Stress and Damage in Eyes of Patients with Retinitis Pigmentosa?” *Antioxidants & Redox Signaling*. https://doi.org/10.1089/ars.2015.6327.

Cantagrel, Vincent, Jennifer L. Silhavy, Stephanie L. Bielas, Dominika Swistun, Sarah E. Marsh, Julien Y. Bertrand, Sophie Audollent, et al. 2008. “Mutations in the Cilia Gene ARL13B Lead to the Classical Form of Joubert Syndrome.” *American Journal of Human Genetics* 83 (2): 170–79. https://doi.org/10.1016/j.ajhg.2008.06.023.

Cao, Wei, Rong Wen, Feng Li, Matthew M. Lavail, and Roy H. Steinberg. 1997. “Mechanical Injury Increases BFGF and CNTF MRNA Expression in the Mouse Retina.” *Experimental Eye Research*. https://doi.org/10.1006/exer.1997.0328.

Carter-Dawson, L D, and M M LaVail. 1979. “Rods and Cones in the Mouse Retina. I. Structural Analysis Using Light and Electron Microscopy.” *The Journal of Comparative Neurology*. https://doi.org/10.1002/cne.901880204.

Cayouette, Michel, and Claude Gravel. 1997. “Adenovirus-Mediated Gene Transfer of Ciliary Neurotrophic Factor Can Prevent Photoreceptor Degeneration in the Retinal Degeneration (Rd) Mouse.” *Human Gene Therapy* 8 (4): 423–30. https://doi.org/10.1089/hum.1997.8.4-423.

Chakarova, Christina F, Matthew M Hims, Hanno Bolz, Leen Abu-Safieh, Reshma J Patel, Myrto G Papaioannou, Chris F Inglehearn, et al. 2002. “Mutations in HPRP3, a Third Member Ofpre-MRNA Splicing Factor Genes, Implicated in Autosomal Dominant Retinitis Pigmentosa.” *Human Molecular Genetics* 11 (1): 87–92.

Chang, B., N. L. Hawes, R. E. Hurd, M. T. Davisson, S. Nusinowitz, and J. R. Heckenlively. 2002. “Retinal Degeneration Mutants in the Mouse.” *Vision Research*. https://doi.org/10.1016/S0042-6989(01)00146-8.

Chang, Catherine C. Y., Jie Sun, and Ta-Yuan Chang. 2011. “Membrane-Bound O-Acyltransferases (MBOATs).” *Frontiers in Biology*.

https://doi.org/10.1007/s11515-011-1149-z.

Chang, Guo Qing, Ying Hao, and Fulton Wong. 1993. “Apoptosis: Final Common Pathway of Photoreceptor Death in Rd, Rds, and Mutant Mice.” *Neuron*. https://doi.org/10.1016/0896-6273(93)90072-Y.

Chapple, J. Paul, Alison J. Hardcastle, Celene Grayson, Keith R. Willison, and Michael E. Cheetham. 2002. “Delineation of the Plasma Membrane Targeting Domain of the X-Linked Retinitis Pigmentosa Protein RP2.” *Investigative Ophthalmology and Visual Science*.

Chapple, J Paul, Alison J Hardcastle, Celene Grayson, L A Spackman, Keith R Willison, and Michael E Cheetham. 2000. “Mutations in the N-Terminus of the X-Linked Retinitis Pigmentosa Protein RP2 Interfere with the Normal Targeting of the Protein to the Plasma Membrane.” *Human Molecular Genetics*. https://doi.org/10.1093/hmg/9.13.1919.

Chapuis, Julien, Amandine Flaig, Benjamin Grenier-Boley, Fanny Eysert, Virginie Pottiez, Gaspard Deloison, Alexandre Vandeputte, et al. 2017. “Genome-Wide, High-Content SiRNA Screening Identifies the Alzheimer’s Genetic Risk Factor FERMT2 as a Major Modulator of APP Metabolism.” *Acta Neuropathologica*. https://doi.org/10.1007/s00401-016-1652-z.

Chen, C K, M E Burns, M Spencer, G A Niemi, J Chen, J B Hurley, D A Baylor, and M I Simon. 1999. “Abnormal Photoresponses and Light-Induced Apoptosis in Rods Lacking Rhodopsin Kinase.” *Proceedings of the National Academy of Sciences of the United States of America*. https://doi.org/10.1073/pnas.96.7.3718.

Chen, Ching-Kang, Pamela Eversole-Cire, Haikun Zhang, Valeria Mancino, Yu-Jiun Chen, Wei He, Theodore G Wensel, and Melvin I Simon. 2003. “Instability of GGL Domain-Containing RGS Proteins in Mice Lacking the G Protein Beta-Subunit Gbeta5.” *Proceedings of the National Academy of Sciences of the United States of America*. https://doi.org/10.1073/pnas.0631825100.

Chen, Ching Kang, Marie E. Burns, Wel He, Theodorø G. Wensel, Denis A. Baylor, and Melvin I. Simon. 2000. “Slowed Recovery of Rod Photoresponse in Mice Lacking the GTPase Accelerating Protein RGS9-1.” *Nature*. https://doi.org/10.1038/35000601.

Cherfils, J., and M. Zeghouf. 2013. “Regulation of Small GTPases by GEFs, GAPs, and GDIs.” *Physiological Reviews*. https://doi.org/10.1152/physrev.00003.2012.

Chiang, Chin, Ying Litingtung, Eric Lee, Keith E. Young, Jeffrey L. Corden, Heiner Westphal, and Philip A. Beachy. 1996. “Cyclopia and Defective Axial Patterning in Mice Lacking Sonic Hedgehog Gene Function.” *Nature*. https://doi.org/10.1038/383407a0.

Chong, N H, R A Alexander, L Waters, K C Barnett, A C Bird, and P J Luthert. 1999. “Repeated Injections of a Ciliary Neurotrophic Factor Analogue Leading to Long-Term Photoreceptor Survival in Hereditary Retinal Degeneration.” *Investigative Ophthalmology & Visual Science* 40 (6): 1298–1305.

Cideciyan, A. V., S. G. Jacobson, W. A. Beltran, A. Sumaroka, M. Swider, S. Iwabe, A. J. Roman, et al. 2013. “Human Retinal Gene Therapy for Leber Congenital Amaurosis Shows Advancing Retinal Degeneration despite Enduring Visual Improvement.” *Proceedings of the National Academy of Sciences*. https://doi.org/10.1073/pnas.1218933110.

Cimica, Velasco, Hui Chen Chen, Janaki K. Iyer, and Nancy C. Reich. 2011. “Dynamics of the STAT3 Transcription Factor: Nuclear Import Dependent on Ran and Importin-B1.” *PLoS ONE*. https://doi.org/10.1371/journal.pone.0020188.

Craft, C M, B Brown, K Wu, L Rife, and X Zhu. 2006. “Cone Arrestin Knockout: Structure and Potential Function in Cone Photoreceptors .” *Investigative Ophthalmology & Visual Science* 47 (13): 4315.

Craft, Cheryl M., and Donald H. Whitmore. 1995. “The Arrestin Superfamily: Cone Arrestins Are a Fourth Family.” *FEBS Letters*. https://doi.org/10.1016/0014-5793(95)00213-S.

Cruz, Lyndon Da, Kate Fynes, Odysseas Georgiadis, Julie Kerby, Yvonne H. Luo, Ahmad Ahmado, Amanda Vernon, et al. 2018. “Phase 1 Clinical Study of an Embryonic Stem Cell-Derived Retinal Pigment Epithelium Patch in Age-Related Macular Degeneration.” *Nature Biotechnology*. https://doi.org/10.1038/nbt.4114.

Cuenca, N, S Lopez, K Howes, and H Kolb. 1998. “The Localization of Guanylyl

Cyclase-Activating Proteins in the Mammalian Retina." *Investigative Ophthalmology & Visual Science*.

Curcio, Christine A., Kenneth R. Sloan, Robert E. Kalina, and Anita E. Hendrickson. 1990. "Human Photoreceptor Topography." *Journal of Comparative Neurology*. https://doi.org/10.1002/cne.902920402.

D'Cruz, P M, D Yasumura, J Weir, M T Matthes, H Abderrahim, M M LaVail, and D Vollrath. 2000. "Mutation of the Receptor Tyrosine Kinase Gene Mertk in the Retinal Dystrophic RCS Rat." *Human Molecular Genetics*. https://doi.org/ddd061 [pii].

Daemen, Frans J.M. 1973. "Vertebrate Rod Outer Segment Membranes." *BBA - Reviews on Biomembranes*. https://doi.org/10.1016/0304-4157(73)90006-3.

Daiger, S. P., L. S. Sullivan, and S. J. Bowne. 2013. "Genes and Mutations Causing Retinitis Pigmentosa." *Clinical Genetics*. https://doi.org/10.1111/cge.12203.

Darnell, J E, I M Kerr, and G R Stark. 1994. "Jak-STAT Pathways and Transcriptional Activation in Response to IFNs and Other Extracellular Signaling Proteins." *Science* 264 (5164): 1415–21. https://doi.org/10.1126/science.8197455.

Darnell, James E. 1997. "STATs and Gene Regulation." *Science* 277 (5332): 1630–35. https://doi.org/10.1126/science.277.5332.1630.

Deery, Evelyne C, Eranga N Vithana, Richard J Newbold, Victoria A Gallon, Shomi S Bhattacharya, Martin J Warren, David M Hunt, and Susan E Wilkie. 2002. "Disease Mechanism for Retinitis Pigmentosa (RP11) Caused by Mutations in the Splicing Factor Gene PRPF31." *Human Molecular Genetics*. https://doi.org/10.1093/hmg/11.25.3209.

Deguchi, J, a Yamamoto, T Yoshimori, K Sugasawa, Y Moriyama, M Futai, T Suzuki, K Kato, M Uyama, and Y Tashiro. 1994. "Acidification of Phagosomes and Degradation of Rod Outer Segments in Rat Retinal Pigment Epithelium." *Investigative Ophthalmology & Visual Science*.

Deng, W.-T., K. Sakurai, S. Kolandaivelu, A. V. Kolesnikov, A. Dinculescu, J. Li, P. Zhu, et al. 2013. "Cone Phosphodiesterase-6 ' Restores Rod Function and

Confers Distinct Physiological Properties in the Rod Phosphodiesterase-6 - Deficient Rd10 Mouse." *Journal of Neuroscience*. https://doi.org/10.1523/JNEUROSCI.1536-13.2013.

Deretic, Dusanka, Andrew H Williams, Nancy Ransom, Valerie Morel, Paul A Hargrave, and Anatol Arendt. 2005. "Rhodopsin C Terminus, the Site of Mutations Causing Retinal Disease, Regulates Trafficking by Binding to ADP-Ribosylation Factor 4 (ARF4)." *Proceedings of the National Academy of Sciences of the United States of America*. https://doi.org/10.1073/pnas.0500095102.

Desvignes, Thomas, Thaovi Nguyen, Franck Chesnel, Aurélien Bouleau, Christian Fauvel, and Julien Bobe. 2015. "X-Linked Retinitis Pigmentosa 2 Is a Novel Maternal-Effect Gene Required for Left-Right Asymmetry in Zebrafish." *Biology of Reproduction*. https://doi.org/10.1095/biolreprod.115.130575.

Ding, Jin Dong, Raquel Y. Salinas, and Vadim Y. Arshavsky. 2015. "Discs of Mammalian Rod Photoreceptors Form through the Membrane Evagination Mechanism." *Journal of Cell Biology*. https://doi.org/10.1083/jcb.201508093.

Doan, Thuy, Ana Mendez, Peter B. Detwiler, Jeannie Chen, and Fred Rieke. 2006. "Multiple Phosphorylation Sites Confer Reproducibility of the Rod's Single-Photon Responses." *Science*. https://doi.org/10.1126/science.1126612.

Dryja, T P, J T Finn, Y W Peng, T L McGee, E L Berson, and K W Yau. 1995. "Mutations in the Gene Encoding the Alpha Subunit of the Rod CGMP-Gated Channel in Autosomal Recessive Retinitis Pigmentosa." *Proc Natl Acad Sci U S A.* https://doi.org/10.1073/pnas.92.22.10177.

Du, Lina, Xiaopeng Zhang, Yong Y. Han, Nancy A. Burke, Patrick M. Kochanek, Simon C. Watkins, Steven H. Graham, Joseph A. Carcillo, Csaba Szabó, and Robert S B Clark. 2003. "Intra-Mitochondrial Poly(ADP-Ribosylation) Contributes to NAD+ Depletion and Cell Death Induced by Oxidative Stress." *Journal of Biological Chemistry*. https://doi.org/10.1074/jbc.M301295200.

Dulla, Kalyan, Monica Aguila, Amelia Lane, Katarina Jovanovic, David A. Parfitt, Iris Schulkens, Hee Lam Chan, et al. 2018. "Splice-Modulating Oligonucleotide QR-110 Restores CEP290 MRNA and Function in Human c.2991+1655A>G LCA10 Models." *Molecular Therapy - Nucleic Acids*.

https://doi.org/10.1016/j.omtn.2018.07.010.

Eferl, Robert, and Erwin F. Wagner. 2003. “AP-1: A Double-Edged Sword in Tumorigenesis.” *Nature Reviews Cancer*. https://doi.org/10.1038/nrc1209.

Elias, Rajesh V, Steven S Sezate, Wei Cao, and James F McGinnis. 2004. “Temporal Kinetics of the Light/Dark Translocation and Compartmentation of Arrestin and Alpha-Transducin in Mouse Photoreceptor Cells.” *Molecular Vision*. https://doi.org/v10/a81 [pii] ET - 2004/10/07.

Elliott, Kelsey H., and Samantha A. Brugmann. 2018. “Sending Mixed Signals: Cilia-Dependent Signaling during Development and Disease.” *Developmental Biology*, 2018. https://doi.org/10.1016/j.ydbio.2018.03.007.

Enjalbert, Brice, Deborah a Smith, Michael J Cornell, Intikhab Alam, Susan Nicholls, Alistair J P Brown, and Janet Quinn. 2006. “Arl2 and Arl3 Regulate Different Microtubule-Dependent Processes.” *Molecular Biology of the Cell* 17 (2): 1018–32. https://doi.org/10.1091/mbc.E05.

Evans, R. Jane, Nele Schwarz, Kerstin Nagel-Wolfrum, Uwe Wolfrum, Alison J. Hardcastle, and Michael E. Cheetham. 2010. “The Retinitis Pigmentosa Protein RP2 Links Pericentriolar Vesicle Transport between the Golgi and the Primary Cilium.” *Human Molecular Genetics* 19 (7): 1358–67. https://doi.org/10.1093/hmg/ddq012.

Fain, G. L., H. R. Matthews, and M. C. Cornwall. 1996. “Dark Adaptation in Vertebrate Photoreceptors.” *Trends in Neurosciences*. https://doi.org/10.1016/S0166-2236(96)10056-4.

Fansa, Eyad Kalawy, Stefanie Kristine Kösling, Eldar Zent, Alfred Wittinghofer, and Shehab Ismail. 2016. “PDE6δ-Mediated Sorting of INPP5E into the Cilium Is Determined by Cargo-Carrier Affinity.” *Nature Communications* 7: 11366. https://doi.org/10.1038/ncomms11366.

Farazi, T. A., G. Waksman, and J. I. Gordon. 2001. “The Biology and Enzymology of ProteinN-Myristoylation.” *Journal of Biological Chemistry*. https://doi.org/10.1074/jbc.R100042200.

Farber, Debora B., and R. N. Lolley. 1977. “LIGHT- INDUCED REDUCTION IN

CYCLIC GMP OF RETINAL PHOTORECEPTOR CELLS IN VIVO: ABNORMALITIES IN THE DEGENERATIVE DISEASES OF RCS RATS AND Rd MICE." *Journal of Neurochemistry*. https://doi.org/10.1111/j.1471-4159.1977.tb10673.x.

Farjo, Rafal, Jeff S. Skaggs, Barbara A. Nagel, Alexander B. Quiambao, Zack A. Nash, Steven J. Fliesler, and Muna I. Naash. 2006. "Retention of Function without Normal Disc Morphogenesis Occurs in Cone but Not Rod Photoreceptors." *Journal of Cell Biology*. https://doi.org/10.1083/jcb.200509036.

Feng, Wei, Douglas Yasumura, Michael T. Matthes, Matthew M. Lavail, and Douglas Vollrath. 2002. "Mertk Triggers Uptake of Photoreceptor Outer Segments during Phagocytosis by Cultured Retinal Pigment Epithelial Cells." *Journal of Biological Chemistry*. https://doi.org/10.1074/jbc.M107876200.

Ferrari, Stefano, Enzo Di Iorio, Vanessa Barbaro, Diego Ponzin, Francesco S. Sorrentino, and Francesco Parmeggiani. 2011. "Retinitis Pigmentosa: Genes and Disease Mechanisms." *Current Genomics* 12 (4): 238–49. https://doi.org/10.2174/138920211795860107.

Finnemann, S C, and R L Silverstein. 2001. "Differential Roles of CD36 and Alphavbeta5 Integrin in Photoreceptor Phagocytosis by the Retinal Pigment Epithelium." *The Journal of Experimental Medicine*. https://doi.org/10.1084/jem.194.9.1289.

Finnemann, Silvia C. 2003. "Focal Adhesion Kinase Signaling Promotes Phagocytosis of Integrin-Bound Photoreceptors." *The EMBO Journal*. https://doi.org/10.1093/emboj/cdg416.

Finnemann, Silvia C, Vera L Bonilha, Alan D Marmorstein, Enrique Rodriguez-Boulan, and Margaret M Dyson. 1997. "Phagocytosis of Rod Outer Segments by Retinal Pigment Epithelial Cells Requires ␣v␣5 Integrin for Binding but Not for Internalization." *Cell Biology Communicated by Torsten N. Wiesel*. https://doi.org/10.1073/pnas.94.24.12932.

Flaxel, Christina J., Marcelle Jay, Dawn L. Thiselton, Mani Nayudu, Alison J. Hardcastle, Alan Wright, and Alan C. Bird. 1999. "Difference between RP2 and RP3 Phenotypes in X Linked Retinitis Pigmentosa." *British Journal of*

Ophthalmology. https://doi.org/10.1136/bjo.83.10.1144.

Fliegauf, M. 2006. “Nephrocystin Specifically Localizes to the Transition Zone of Renal and Respiratory Cilia and Photoreceptor Connecting Cilia.” *Journal of the American Society of Nephrology*. https://doi.org/10.1681/ASN.2005121351.

Forrester, M T, D T Hess, J W Thompson, R C Hultman, M A Moseley, J S Stamler, and P J Casey. 2011. “Site-Specific Analysis of Protein S-Acylation by Resin-Assisted Capture (Acyl-RAC).” *J Lipid Res*. https://doi.org/10.1194/jlr.D011106.

Forsythe, Elizabeth, and Philip L Beales. 2013. “Bardet-Biedl Syndrome.” *European Journal of Human Genetics : EJHG*. https://doi.org/10.1038/ejhg.2012.115.

Fu, Y., H. Zhong, M.-H. H. Wang, D.-G. Luo, H.-W. Liao, H. Maeda, S. Hattar, L. J. Frishman, and K.-W. Yau. 2005. “Intrinsically Photosensitive Retinal Ganglion Cells Detect Light with a Vitamin A-Based Photopigment, Melanopsin.” *Proceedings of the National Academy of Sciences*. https://doi.org/10.1073/pnas.0501866102.

Fu, Yingbin, and King Wai Yau. 2007. “Phototransduction in Mouse Rods and Cones.” *Pflugers Archiv European Journal of Physiology* 454 (5): 805–19. https://doi.org/10.1007/s00424-006-0194-y.

Fuchs, Sigrid, Mitsuru Nakazawa, Marion Maw, Makoto Tamai, Yoshihisa Oguchi, and Andreas Gal. 1995. “A Homozygous 1–base Pair Deletion in the Arrestin Gene Is a Frequent Cause of Oguchi Disease in Japanese.” *Nature Genetics* 10 (July): 360. https://doi.org/10.1038/ng0795-360.

Fukada, Toshiyuki, Masahiko Hibi, Yojiro Yamanaka, Mariko Takahashi-Tezuka, Yoshio Fujitani, Takuya Yamaguchi, Koichi Nakajima, and Toshio Hirano. 1996. “Two Signals Are Necessary for Cell Proliferation Induced by a Cytokine Receptor Gp130: Involvement of STAT3 in Anti-Apoptosis.” *Immunity* 5 (5): 449–60. https://doi.org/https://doi.org/10.1016/S1074-7613(00)80501-4.

Fukada, Yoshitaka, Toshifumi Takao, Hiroshi Ohguro, Tôru Yoshizawa, Toyoaki Akino, and Yasutsugu Shimonishi. 1990. “Farnesylated γ-Subunit of Photoreceptor G Protein Indispensable for GTP-Binding.” *Nature*. https://doi.org/10.1038/346658a0.

Fung, B K, B S Lieberman, and R H Lee. 1992. “A Third Form of the G Protein Beta Subunit. 2. Purification and Biochemical Properties.” *J Biol Chem*.

Galan, Alessandro, Marzio Chizzolini, Elisabeth Milan, Adolfo Sebastiani, Ciro Costagliola, and Francesco Parmeggiani. 2011. “Good Epidemiologic Practice in Retinitis Pigmentosa: From Phenotyping to Biobanking.” *Current Genomics*. https://doi.org/10.2174/138920211795860071.

Galli, L. M., T. L. Barnes, S. S. Secrest, T. Kadowaki, and L. W. Burrus. 2007. “Porcupine-Mediated Lipid-Modification Regulates the Activity and Distribution of Wnt Proteins in the Chick Neural Tube.” *Development*. https://doi.org/10.1242/dev.02881.

Gao, Xinxin, and Rami N. Hannoush. 2014. “Single-Cell Imaging of Wnt Palmitoylation by the Acyltransferase Porcupine.” *Nature Chemical Biology*. https://doi.org/10.1038/nchembio.1392.

Goetz, Sarah C., and Kathryn V. Anderson. 2010. “The Primary Cilium: A Signalling Centre during Vertebrate Development.” *Nature Reviews Genetics*. https://doi.org/10.1038/nrg2774.

Gotthardt, Katja, Mandy Lokaj, Carolin Koerner, Nathalie Falk, Andreas Gießl, and Alfred Wittinghofer. 2015. “A G-Protein Activation Cascade from Arl13B to Arl3 and Implications for Ciliary Targeting of Lipidated Proteins.” *ELife* 4 (NOVEMBER2015). https://doi.org/10.7554/eLife.11859.001.

Grayson, C, F Bartolini, J P Chapple, K R Willison, A Bhamidipati, S A Lewis, P J Luthert, A J Hardcastle, N J Cowan, and M E Cheetham. 2002. “Localization in the Human Retina of the X-Linked Retinitis Pigmentosa Protein RP2, Its Homologue Cofactor C and the RP2 Interacting Protein Arl3.” *Hum Mol Genet* 11 (24): 3065–74. https://doi.org/10.1093/hmg/11.24.3065.

Greaves, Jennifer, and Luke H. Chamberlain. 2011. “DHHC Palmitoyl Transferases: Substrate Interactions and (Patho)Physiology.” *Trends in Biochemical Sciences*. https://doi.org/10.1016/j.tibs.2011.01.003.

Green, Eric S., Michael D. Menz, Matthew M. LaVail, and John G. Flannery. 2000. “Characterization of Rhodopsin Mis-Sorting and Constitutive Activation in a Transgenic Rat Model of Retinitis Pigmentosa.” *Investigative Ophthalmology*

and Visual Science.

Greiner, J V, T a Weidman, H D Bodley, and C a Greiner. 1981. “Ciliogenesis in Photoreceptor Cells of the Retina.” *Experimental Eye Research* 33 (4): 433–46.

Gupta, Nisha, Kimberly E. Brown, and Ann H. Milam. 2003. “Activated Microglia in Human Retinitis Pigmentosa, Late-Onset Retinal Degeneration, and Age-Related Macular Degeneration.” *Experimental Eye Research*. https://doi.org/10.1016/S0014-4835(02)00332-9.

Hafler, Brian P. 2017. “Clinical Progress in Inherited Retinal Degenerations: Gene Therapy Clinical Trials and Advances in Genetic Sequencing.” *Retina*. https://doi.org/10.1097/IAE.0000000000001341.

Hall, Michael O., and Toshka Abrams. 1987. “Kinetic Studies of Rod Outer Segment Binding and Ingestion by Cultured Rat RPE Cells.” *Experimental Eye Research*. https://doi.org/10.1016/S0014-4835(87)80105-7.

Halliwell, Barry. 2006. “Oxidative Stress and Neurodegeneration: Where Are We Now?” *Journal of Neurochemistry*. https://doi.org/10.1111/j.1471-4159.2006.03907.x.

Hamel, Christian. 2006. “Retinitis Pigmentosa.” *Orphanet Journal of Rare Diseases* 1 (October): 40. https://doi.org/10.1186/1750-1172-1-40.

Hamel, Christian P. 2007. “Cone Rod Dystrophies.” *Orphanet Journal of Rare Diseases*. https://doi.org/10.1186/1750-1172-2-7.

Hamer, R.D., S.C. Nicholas, D. Tranchina, P.A. Liebman, and T.D. Lamb. 2003. “Multiple Steps of Phosphorylation of Activated Rhodopsin Can Account for the Reproducibility of Vertebrate Rod Single-Photon Responses.” *The Journal of General Physiology*. https://doi.org/10.1085/jgp.200308832.

Hanke-Gogokhia, Christin, Zhijian Wu, Cecilia D. Gerstner, Jeanne M. Frederick, Houbin Zhang, and Wolfgang Baehr. 2016. “Arf-like Protein 3 (ARL3) Regulates Protein Trafficking and Ciliogenesis in Mouse Photoreceptors.” *Journal of Biological Chemistry* 291 (13): 7142–55. https://doi.org/10.1074/jbc.M115.710954.

Hannoush, Rami N. 2015. “Synthetic Protein Lipidation.” *Current Opinion in*

Chemical Biology 28: 39–46. https://doi.org/10.1016/j.cbpa.2015.05.025.

Hardcastle, A J, D L Thiselton, L Van Maldergem, B K Saha, M Jay, C Plant, R Taylor, A C Bird, and S Bhattacharya. 1999. “Mutations in the RP2 Gene Cause Disease in 10% of Families with Familial X-Linked Retinitis Pigmentosa Assessed in This Study.” *American Journal of Human Genetics* 64 (4): 1210–15. https://www.ncbi.nlm.nih.gov/pubmed/10090907.

He, Wei, Christopher W. Cowan, and Theodore G. Wensel. 1998. “RGS9, a GTPase Accelerator for Phototransduction.” *Neuron*. https://doi.org/10.1016/S0896-6273(00)80437-7.

He, Yinghong, Philipp Esser, Anja Heinemann, Leena Bruckner-Tuderman, and Cristina Has. 2011. “Kindlin-1 and -2 Have Overlapping Functions in Epithelial Cells: Implications for Phenotype Modification.” *American Journal of Pathology*. https://doi.org/10.1016/j.ajpath.2010.11.053.

Heavner, Whitney, and Larysa Pevny. 2012. “Eye Development and Retinogenesis.” *Cold Spring Harbor Perspectives in Biology*. https://doi.org/10.1101/cshperspect.a008391.

Heinrech, Peter C, Iris BEHRMANN, Gerhard MÜLLER-NEWEN, Fred SCHAPER, and Lutz GRAEVE. 1998. “Interleukin-6-Type Cytokine Signalling through the Gp130/Jak/STAT Pathway.” *Biochemical Journal* 334 (2): 297–314. https://doi.org/10.1042/bj3340297.

Hendrickson, Anita. 2005. “Organization of the Adult Primate Fovea.” In *Macular Degeneration*. https://doi.org/10.1007/3-540-26977-0_1.

Hickman, Mark J, and Leona D Samson. 1999. “Role of DNA Mismatch Repair and P53 in Signaling Induction of Apoptosis by Alkylating Agents.” *Proceedings of the National Academy of Sciences* 96 (19): 10764 LP-10769.

Hill, Jeff W., Jennifer J. Hu, and Michele K. Evans. 2008. “OGG1 Is Degraded by Calpain Following Oxidative Stress and Cisplatin Exposure.” *DNA Repair*. https://doi.org/10.1016/j.dnarep.2008.01.003.

Hillig, Roman C, Michael Hanzal-Bayer, Marco Linari, Jörg Becker, Alfred Wittinghofer, and Louis Renault. 2000. “Structural and Biochemical Properties

Show ARL3-GDP as a Distinct GTP Binding Protein." *Structure (London, England : 1993)*. https://doi.org/10.1016/S0969-2126(00)00531-1.

Hirano, Toshio, Katsuhiko Ishihara, and Masahiko Hibi. 2000. "Roles of STAT3 in Mediating the Cell Growth, Differentiation and Survival Signals Relayed through the IL-6 Family of Cytokine Receptors." *Oncogene* 19 (May): 2548.

Hofmann, I. 2006. "An N-Terminally Acetylated Arf-like GTPase Is Localised to Lysosomes and Affects Their Motility." *Journal of Cell Science*. https://doi.org/10.1242/jcs.02958.

Hollander, Anneke I. den, Ronald Roepman, Robert K. Koenekoop, and Frans P M Cremers. 2008. "Leber Congenital Amaurosis: Genes, Proteins and Disease Mechanisms." *Progress in Retinal and Eye Research*. https://doi.org/10.1016/j.preteyeres.2008.05.003.

Hollyfield, Joe G, Vera L Bonilha, Mary E Rayborn, Xiaoping Yang, Karen G Shadrach, Liang Lu, Rafael L Ufret, Robert G Salomon, and Victor L Perez. 2008. "Oxidative Damage–induced Inflammation Initiates Age-Related Macular Degeneration." *Nature Medicine* 14 (January): 194.

Holopainen, Juha M., Christiana L. Cheng, Laurie L. Molday, Gurp Johal, Jonathan Coleman, Frank Dyka, Theresa Hii, Jinhi Ahn, and Robert S. Molday. 2010. "Interaction and Localization of the Retinitis Pigmentosa Protein RP2 and NSF in Retinal Photoreceptor Cells." *Biochemistry*. https://doi.org/10.1021/bi1005249.

Hong, Dong Hyun, Basil S Pawlyk, J Shang, Michael A Sandberg, Eliot L Berson, and T Li. 2000. "A Retinitis Pigmentosa GTPase Regulator (RPGR)-Deficient Mouse Model for X-Linked Retinitis Pigmentosa (RP3)." *Proceedings of the National Academy of Sciences of the United States of America*. https://doi.org/10.1073/pnas.97.7.3649.

Hong, Dong Hyun, Basil Pawlyk, Maxim Sokolov, Katherine J. Strissel, Jun Yang, Brian Tulloch, Alan F. Wright, Vadim Y. Arshavsky, and Tiansen Li. 2003. "RPGR Isoforms in Photoreceptor Connecting Cilia and the Transitional Zone of Motile Cilia." *Investigative Ophthalmology and Visual Science*. https://doi.org/10.1167/iovs.02-1206.

Hoon, Mrinalini, Haruhisa Okawa, Luca Della Santina, and Rachel O.L. Wong. 2014. "Functional Architecture of the Retina: Development and Disease." *Progress in Retinal and Eye Research*. https://doi.org/10.1016/j.preteyeres.2014.06.003.

Howes, K, J D Bronson, Y L Dang, N Li, K Zhang, C Ruiz, B Helekar, et al. 1998. "Gene Array and Expression of Mouse Retina Guanylate Cyclase Activating Proteins 1 and 2." *Invest Ophthalmol Vis Sci*.

Howie, Jacqueline, Louise Reilly, Niall J. Fraser, Julia M. Vlachaki Walker, Krzysztof J. Wypijewski, Michael L. J. Ashford, Sarah C. Calaghan, et al. 2014. "Substrate Recognition by the Cell Surface Palmitoyl Transferase DHHC5." *Proceedings of the National Academy of Sciences*. https://doi.org/10.1073/pnas.1413627111.

Hu, Guang, and Theodore G Wensel. 2002. "R9AP, a Membrane Anchor for the Photoreceptor GTPase Accelerating Protein, RGS9-1." *Proceedings of the National Academy of Sciences of the United States of America*. https://doi.org/10.1073/pnas.152094799.

Hu, Qicong, and W. James Nelson. 2011. "Ciliary Diffusion Barrier: The Gatekeeper for the Primary Cilium Compartment." *Cytoskeleton*. https://doi.org/10.1002/cm.20514.

Huang, K., S. Sanders, R. Singaraja, P. Orban, T. Cijsouw, P. Arstikaitis, A. Yanai, M. R. Hayden, and A. El-Husseini. 2009. "Neuronal Palmitoyl Acyl Transferases Exhibit Distinct Substrate Specificity." *The FASEB Journal*. https://doi.org/10.1096/fj.08-127399.

Huang, Lijia, Katarzyna Szymanska, Victor L. Jensen, Andreas R. Janecke, A. Micheil Innes, Erica E. Davis, Patrick Frosk, et al. 2011. "TMEM237 Is Mutated in Individuals with a Joubert Syndrome Related Disorder and Expands the Role of the TMEM Family at the Ciliary Transition Zone." *American Journal of Human Genetics*. https://doi.org/10.1016/j.ajhg.2011.11.005.

Huang, Shun-Ping, Bruce M Brown, and Cheryl M Craft. 2010. "Visual Arrestin 1 Acts as a Modulator for N-Ethylmaleimide-Sensitive Factor in the Photoreceptor Synapse." *The Journal of Neuroscience : The Official Journal of the Society for Neuroscience* 30 (28): 9381–91. https://doi.org/10.1523/JNEUROSCI.1207-10.2010.

Hubbert, Charlotte, Amaris Guardiola, Rong Shao, Yoshiharu Kawaguchi, Akihiro Ito, Andrew Nixon, Minoru Yoshida, Xiao-Fan Wang, and Tso-Pang Yao. 2002. “HDAC6 Is a Microtubule-Associated Deacetylase.” *Nature* 417 (6887): 455–58. https://doi.org/10.1038/417455a.

Humbert, Melissa C, Katie Weihbrecht, Charles C Searby, Yalan Li, Robert M Pope, Val C Sheffield, and Seongjin Seo. 2012. “ARL13B, PDE6D, and CEP164 Form a Functional Network for INPP5E Ciliary Targeting.” *Proceedings of the National Academy of Sciences of the United States of America* 109 (48): 19691–96. https://doi.org/10.1073/pnas.1210916109.

Hunt, 2005. “Digital Printing.” *The Reproduction of Colour*. Wiley Online Books. https://doi.org/doi:10.1002/0470024275.ch33.

Hurd, T. W., S. Fan, and B. L. Margolis. 2011. “Localization of Retinitis Pigmentosa 2 to Cilia Is Regulated by Importin 2.” *Journal of Cell Science*. https://doi.org/10.1242/jcs.070839.

Hurd, Toby, Weibin Zhou, Paul Jenkins, Chia Jen Liu, Anand Swaroop, Hemant Khanna, Jeffrey Martens, Friedhelm Hildebrandt, and Ben Margolis. 2010. “The Retinitis Pigmentosa Protein RP2 Interacts with Polycystin 2 and Regulates Cilia-Mediated Vertebrate Development.” *Human Molecular Genetics*. https://doi.org/10.1093/hmg/ddq355.

Hurley, J B, and L Stryer. 1982. “Purification and Characterization of the Gamma Regulatory Subunit of the Cyclic GMP Phosphodiesterase from Retinal Rod Outer Segments.” *The Journal of Biological Chemistry*.

Hüttl, Sabine, Stylianos Michalakis, Mathias Seeliger, Dong-Gen Luo, Niyazi Acar, Heidi Geiger, Kristiane Hudl, et al. 2005. “Impaired Channel Targeting and Retinal Degeneration in Mice Lacking the Cyclic Nucleotide-Gated Channel Subunit CNGB1.” *The Journal of Neuroscience : The Official Journal of the Society for Neuroscience* 25 (1): 130–38. https://doi.org/10.1523/JNEUROSCI.3764-04.2005.

Ibañez-Tallon, Inés, Nathaniel Heintz, and Heymut Omran. 2003. “To Beat or Not to Beat: Roles of Cilia in Development and Disease.” *Hum Mol Genet* 12 (1): R27–35. https://doi.org/10.1093/hmg/ddg061.

Imai, Hiroo, Akihisa Terakita, Shuji Tachibanaki, Yasushi Imamoto, Tôru Yoshizawa, and Yoshinori Shichida. 1997. “Photochemical and Biochemical Properties of Chicken Blue-Sensitive Cone Visual Pigment.” *Biochemistry*. https://doi.org/10.1021/bi970809x.

Insinna, Christine, and Joseph C. Besharse. 2008. “Intraflagellar Transport and the Sensory Outer Segment of Vertebrate Photoreceptors.” *Developmental Dynamics*. https://doi.org/10.1002/dvdy.21554.

Insinna, Christine, Narendra Pathak, Brian Perkins, Iain Drummond, and Joseph C. Besharse. 2008. “The Homodimeric Kinesin, Kif17, Is Essential for Vertebrate Photoreceptor Sensory Outer Segment Development.” *Developmental Biology*. https://doi.org/10.1016/j.ydbio.2008.01.025.

Ishiba, Yasutsugu, Tomomi Higashide, Naoki Mori, Akira Kobayashi, Shinya Kubota, Margaret J. McLaren, Hiromasa Satoh, Fulton Wong, and George Inana. 2007. “Targeted Inactivation of Synaptic HRG4 (UNC119) Causes Dysfunction in the Distal Photoreceptor and Slow Retinal Degeneration, Revealing a New Function.” *Experimental Eye Research* 84 (3): 473–85. https://doi.org/10.1016/j.exer.2006.10.016.

Ismail, Shehab A, Yong-Xiang Chen, Mandy Miertzschke, Ingrid R Vetter, Carolin Koerner, and Alfred Wittinghofer. 2012. “Structural Basis for Arl3-Specific Release of Myristoylated Ciliary Cargo from UNC119.” *The EMBO Journal* 31 (20): 4085–94. https://doi.org/10.1038/emboj.2012.257.

Ismail, Shehab a, Yong-Xiang Chen, Alexandra Rusinova, Anchal Chandra, Martin Bierbaum, Lothar Gremer, Gemma Triola, Herbert Waldmann, Philippe I H Bastiaens, and Alfred Wittinghofer. 2011. “Arl2-GTP and Arl3-GTP Regulate a GDI-like Transport System for Farnesylated Cargo.” *Nature Chemical Biology* 7 (12): 942–49. https://doi.org/10.1038/nchembio.686.

Jayasundera, Thiran, Kari E H Branham, Mohammad Othman, William R Rhoades, Athanasios J Karoukis, Hemant Khanna, Anand Swaroop, and John R Heckenlively. 2010. “RP2 Phenotype and Pathogenetic Correlations in X-Linked Retinitis Pigmentosa.” *Archives of Ophthalmology (Chicago, Ill. : 1960)* 128: 915–23. https://doi.org/10.1001/archophthalmol.2010.122.

Jiang, Ke, Katherine L Wright, Ping Zhu, Michael J Szego, Alexa N Bramall, William

W Hauswirth, Qiuhong Li, Sean E Egan, and Roderick R McInnes. 2014. “STAT3 Promotes Survival of Mutant Photoreceptors in Inherited Photoreceptor Degeneration Models.” *Proceedings of the National Academy of Sciences* 111 (52): E5716--E5723. https://doi.org/10.1073/pnas.1411248112.

Jiang, Li, Beatrice M Tam, Guoxing Ying, Sen Wu, William W Hauswirth, Jeanne M Frederick, Orson L Moritz, and Wolfgang Baehr. 2015. “Kinesin Family 17 (Osmotic Avoidance Abnormal-3) Is Dispensable for Photoreceptor Morphology and Function.” *FASEB Journal : Official Publication of the Federation of American Societies for Experimental Biology* 29 (12): 4866–80. https://doi.org/10.1096/fj.15-275677.

Jimeno, David, Leonard Feiner, Concepcion Lillo, Karen Teofilo, Lawrence S.B. Goldstein, Eric A. Pierce, and David S. Williams. 2006. “Analysis of Kinesin-2 Function in Photoreceptor Cells Using Synchronous Cre-LoxP Knockout of Kif3a with RHO-Cre.” *Investigative Ophthalmology and Visual Science*. https://doi.org/10.1167/iovs.06-0032.

Jin, Mingyue, Masami Yamada, Yoshiyuki Arai, Takeharu Nagai, and Shinji Hirotsune. 2014. “Arl3 and LC8 Regulate Dissociation of Dynactin from Dynein.” *Nature Communications* 5: 5295. https://doi.org/10.1038/ncomms6295.

Joly, S., C. Lange, M. Thiersch, M. Samardzija, and C. Grimm. 2008. “Leukemia Inhibitory Factor Extends the Lifespan of Injured Photoreceptors In Vivo.” *Journal of Neuroscience*. https://doi.org/10.1523/JNEUROSCI.5114-08.2008.

Jong, Paulus T V M de. 2006. “Age-Related Macular Degeneration.” *The New England Journal of Medicine*. https://doi.org/10.1056/NEJMra062326.

Jonnal, Ravi S., Jason R. Besecker, Jack C. Derby, Omer P. Kocaoglu, Barry Cense, Weihua Gao, Qiang Wang, and Donald T. Miller. 2010. “Imaging Outer Segment Renewal in Living Human Cone Photoreceptors.” *Optics Express*. https://doi.org/10.1364/OE.18.005257.

Joseph C. BesharseCynthia J. Horst. 1999. *The Photoreceptor Connecting Cilium A Model for the Transition Zone, Cilliary and Flageller Membranes*.

Karan, Sukanya, Houbin Zhang, Sha Li, Jeanne M. Frederick, and Wolfgang Baehr.

2008. “A Model for Transport of Membrane-Associated Phototransduction Polypeptides in Rod and Cone Photoreceptor Inner Segments.” *Vision Research*. https://doi.org/10.1016/j.visres.2007.08.020.

Karpen, J W, A L Zimmerman, L Stryer, and D A Baylor. 1988. “Gating Kinetics of the Cyclic-GMP-Activated Channel of Retinal Rods: Flash Photolysis and Voltage-Jump Studies.” *Proceedings of the National Academy of Sciences of the United States of America* 85 (4): 1287–91.

Kasai, Hiroshi, and Susumu Nishimura. 1984. “Hydroxylation of Deoxyguanosine at the C-8 Position by Ascorbic Acid and Other Reducing Agents.” *Nucleic Acids Research*. https://doi.org/10.1093/nar/12.4.2137.

Kassai, Hidetoshi, Atsu Aiba, Kazuki Nakao, Kenji Nakamura, Motoya Katsuki, Wei Hong Xiong, King Wai Yau, et al. 2005. “Farnesylation of Retinal Transducin Underlies Its Translocation during Light Adaptation.” *Neuron*. https://doi.org/10.1016/j.neuron.2005.07.025.

Kassen, Sean C., Vijay Ramanan, Jacob E. Montgomery, Christopher T. Burket, Chang Gong Liu, Thomas S. Vihtelic, and David R. Hyde. 2007. “Time Course Analysis of Gene Expression during Light-Induced Photoreceptor Cell Death and Regeneration in Albino Zebrafish.” *Developmental Neurobiology*. https://doi.org/10.1002/dneu.20362.

Kawamura, Satoru, and Shuji Tachibanaki. 2008. “Rod and Cone Photoreceptors: Molecular Basis of the Difference in Their Physiology.” *Comparative Biochemistry and Physiology - A Molecular and Integrative Physiology*. https://doi.org/10.1016/j.cbpa.2008.04.600.

Keady, B. T., Y. Z. Le, and G. J. Pazour. 2011. “IFT20 Is Required for Opsin Trafficking and Photoreceptor Outer Segment Development.” *Molecular Biology of the Cell*. https://doi.org/10.1091/mbc.E10-09-0792.

Kennedy, Matthew J., Felice A. Dunn, and James B. Hurley. 2004. “Visual Pigment Phosphorylation but Not Transducin Translocation Can Contribute to Light Adaptation in Zebrafish Cones.” *Neuron*. https://doi.org/10.1016/S0896-6273(04)00086-8.

Keresztes, Gabor, Kirill A. Martemyanov, Claudia M. Krispel, Hideki Mutai, Peter J.

Yoo, Stephane F. Maison, Marie E. Burns, Vadim Y. Arshavsky, and Stefan Heller. 2004. “Absence of the RGS9·Gβ5 GTPase-Activating Complex in Photoreceptors of the R9AP Knockout Mouse.” *Journal of Biological Chemistry*. https://doi.org/10.1074/jbc.C300456200.

Kevany, Brian M, and Krzysztof Palczewski. 2010. “Phagocytosis of Retinal Rod and Cone Photoreceptors.” *Physiology (Bethesda, Md.)*. https://doi.org/10.1152/physiol.00038.2009.

Khan, Saadullah, Imran Ullah, Irfanullah, Muhammad Touseef, Sulman Basit, Muhammad Nasim Khan, and Wasim Ahmad. 2013. “Novel Homozygous Mutations in the Genes ARL6 and BBS10 Underlying Bardet-Biedl Syndrome.” *Gene* 515 (1): 84–88. https://doi.org/10.1016/j.gene.2012.11.023.

Khanna, Hemant, Toby W. Hurd, Concepcion Lillo, Xinhua Shu, Sunil K. Parapuram, Shirley He, Masayuki Akimoto, et al. 2005. “RPGR-ORF15, Which Is Mutated in Retinitis Pigmentosa, Associates with SMC1, SMC3, and Microtubule Transport Proteins.” *Journal of Biological Chemistry*. https://doi.org/10.1074/jbc.M505827200.

Kirschner, Renate, Thomas Rosenberg, Robert Schultz-Heienbrok, Steffen Lenzner, Silke Feil, Ronald Roepman, Frans P.M. Cremers, Hans Hilger Ropers, and Wolfgang Berger. 1999. “RPGR Transcription Studies in Mouse and Human Tissues Reveal a Retina-Specific Isoform That Is Disrupted in a Patient with X-Linked Retinitis Pigmentosa.” *Human Molecular Genetics*. https://doi.org/10.1093/hmg/8.8.1571.

Knodler, A., S. Feng, J. Zhang, X. Zhang, A. Das, J. Peranen, and W. Guo. 2010. “Coordination of Rab8 and Rab11 in Primary Ciliogenesis.” *Proceedings of the National Academy of Sciences*. https://doi.org/10.1073/pnas.1002401107.

Kohl, S, T Marx, I Giddings, H Jägle, S G Jacobson, E Apfelstedt-Sylla, E Zrenner, L T Sharpe, and B Wissinger. 1998. “Total Colourblindness Is Caused by Mutations in the Gene Encoding the Alpha-Subunit of the Cone Photoreceptor CGMP-Gated Cation Channel.” *Nature Genetics*. https://doi.org/10.1038/935.

Kohl, Susanne, Britta Baumann, Martina Broghammer, Herbert Jägle, Paul Sieving, Ulrich Kellner, Robert Spegal, et al. 2000. “Mutations in the CNGB3 Gene Encoding the β-Subunit of the Cone Photoreceptor CGMP-Gated Channel Are

Responsible for Achromatopsia (ACHM3) Linked to Chromosome 8q21." *Human Molecular Genetics*. https://doi.org/10.1093/hmg/9.14.2107.

Kokame, Koichi, Yoshitaka Fukada, Tôru Yoshizawa, Toshifumi Takao, and Yasutsugu Shimonishi. 1992. "Lipid Modification at the N Terminus of Photoreceptor G-Protein α-Subunit." *Nature*. https://doi.org/10.1038/359749a0.

Komeima, K., B. S. Rogers, L. Lu, and P. A. Campochiaro. 2006. "Antioxidants Reduce Cone Cell Death in a Model of Retinitis Pigmentosa." *Proceedings of the National Academy of Sciences*. https://doi.org/10.1073/pnas.0604056103.

Kong, J, S-R Kim, K Binley, I Pata, K Doi, J Mannik, J Zernant-Rajang, et al. 2008. "Correction of the Disease Phenotype in the Mouse Model of Stargardt Disease by Lentiviral Gene Therapy." *Gene Therapy*. https://doi.org/10.1038/gt.2008.78.

Korycka, Justyna, Agnieszka Łach, Elłbieta Heger, Dłamila M. Bogusławska, Marcin Wolny, Monika Toporkiewicz, Katarzyna Augoff, Jan Korzeniewski, and Aleksander F. Sikorski. 2012. "Human DHHC Proteins: A Spotlight on the Hidden Player of Palmitoylation." *European Journal of Cell Biology*. https://doi.org/10.1016/j.ejcb.2011.09.013.

Koskela, Hanna L M, Samuli Eldfors, Pekka Ellonen, Arjan J van Adrichem, Heikki Kuusanmäki, Emma I Andersson, Sonja Lagström, et al. 2012. "Somatic STAT3 Mutations in Large Granular Lymphocytic Leukemia." *New England Journal of Medicine* 366 (20): 1905–13. https://doi.org/10.1056/NEJMoa1114885.

Krispel, C M, C K Chen, M I Simon, and M E Burns. 2003. "Prolonged Photoresponses and Defective Adaptation in Rods of Gbeta5-/- Mice." *J Neurosci*. https://doi.org/23/18/6965 [pii].

Krispel, Claudia M., Desheng Chen, Nathan Melling, Yu Jiun Chen, Kirill A. Martemyanov, Nidia Quillinan, Vadim Y. Arshavsky, Theodore G. Wensel, Ching Kang Chen, and Marie E. Burns. 2006. "RGS Expression Rate-Limits Recovery of Rod Photoresponses." *Neuron*. https://doi.org/10.1016/j.neuron.2006.07.010.

Kühn, H., and U. Wilden. 1987. "Deactivation of Photoactivated Rhodopsin by Rhodopsin-Kinase and Arrestin." *Journal of Receptors and Signal*

Transduction. https://doi.org/10.3109/10799898709054990.

Kühnel, Karin, Stefan Veltel, Ilme Schlichting, and Alfred Wittinghofer. 2006. “Crystal Structure of the Human Retinitis Pigmentosa 2 Protein and Its Interaction with Arl3.” *Structure*. https://doi.org/10.1016/j.str.2005.11.008.

Lai, Cary K, Nidhi Gupta, Xiaohui Wen, Linda Rangell, Ben Chih, Andrew S Peterson, J Fernando Bazan, Li Li, and Suzie J Scales. 2011. “Functional Characterization of Putative Cilia Genes by High-Content Analysis.” *Molecular Biology of the Cell* 22 (7): 1104–19. https://doi.org/10.1091/mbc.E10-07-0596.

Langmann, Thomas. 2007. “Microglia Activation in Retinal Degeneration.” *Journal of Leukocyte Biology*. https://doi.org/10.1189/jlb.0207114.

LaVail, Matthew M., and Gregg M. Gorrin. 1987. “Protection from Light Damage by Ocular Pigmentation: Analysis Using Experimental Chimeras and Translocation Mice.” *Experimental Eye Research*. https://doi.org/10.1016/S0014-4835(87)80050-7.

Law, Ah-Lai, Qi Ling, Katherine A. Hajjar, Clare E Futter, John Greenwood, Peter Adamson, Silene T Wavre-Shapton, Stephen E Moss, and Matthew J Hayes. 2010. “Annexin A2 Regulates Phagocytosis of Photoreceptor Outer Segments in the Mouse Retina.” *Molecular Biology of the Cell*. https://doi.org/10.1091/mbc.E08.

Lee, R H, B S Lieberman, H K Yamane, D Bok, and B K Fung. 1992. “A Third Form of the G Protein Beta Subunit. 1. Immunochemical Identification and Localization to Cone Photoreceptors.” *J Biol Chem*.

Leightner, Amanda, and Peter C Harris. 2013. “Meckel Syndrome.” In *Polycystic Kidney Disease: From Bench to Bedside*, 76–89. Future Medicine Ltd. https://doi.org/doi:10.2217/ebo.12.263.

Lerea, C L, D E Somers, J B Hurley, I B Klock, and A H Bunt-Milam. 1986. “Identification of Specific Transducin Alpha Subunits in Retinal Rod and Cone Photoreceptors.” *Science*.

Léveillard, Thierry, Saddek Mohand-Saïd, Olivier Lorentz, David Hicks, Anne Claire Fintz, Emmanuelle Clérin, Manuel Simonutti, et al. 2004. “Identification and

Characterization of Rod-Derived Cone Viability Factor." *Nature Genetics*. https://doi.org/10.1038/ng1386.

Lewis, Tylor R, Sean R Kundinger, Brian A Link, Christine Insinna, and Joseph C Besharse. 2018. "Kif17 Phosphorylation Regulates Photoreceptor Outer Segment Turnover." *BMC Cell Biology* 19 (1): 25. https://doi.org/10.1186/s12860-018-0177-9.

Li, Linjing, Naheed Khan, Toby Hurd, Amiya Kumar Ghosh, Christiana Cheng, Robert Molday, John R. Heckenlively, Anand Swaroop, and Hemant Khanna. 2013. "Ablation of the X-Linked Retinitis Pigmentosa 2 (Rp2) Gene in Mice Results in Opsin Mislocalization and Photoreceptor Degeneration." *Investigative Ophthalmology and Visual Science* 54 (7): 4503–11. https://doi.org/10.1167/iovs.13-12140.

Li, Linjing, Kollu Nageswara Rao, Yun Zheng-Le, Toby W. Hurd, Concepción Lillo, and Hemant Khanna. 2015. "Loss of Retinitis Pigmentosa 2 (RP2) Protein Affects Cone Photoreceptor Sensory Cilium Elongation in Mice." *Cytoskeleton* 72 (9): 447–54. https://doi.org/10.1002/cm.21255.

Li, Peipei, Jingjing Li, Li Wang, and Li Jun Di. 2017. "Proximity Labeling of Interacting Proteins: Application of BioID as a Discovery Tool." *Proteomics*. https://doi.org/10.1002/pmic.201700002.

Li, Sha, Desheng Chen, Yves Sauvé, Jeremy McCandless, Yu Jiun Chen, and Ching Kang Chen. 2005. "Rhodopsin-ICre Transgenic Mouse Line for Cre-Mediated Rod-Specific Gene Targeting." *Genesis* 41 (2): 73–80. https://doi.org/10.1002/gene.20097.

Li, T, W K Snyder, J E Olsson, and T P Dryja. 1996. "Transgenic Mice Carrying the Dominant Rhodopsin Mutation P347S: Evidence for Defective Vectorial Transport of Rhodopsin to the Outer Segments." *Proceedings of the National Academy of Sciences of the United States of America*. https://doi.org/10.1073/pnas.93.24.14176.

Li, Yawei, William G Kelly, John M Logsdon, Andrew M Schurko, Brian D Harfe, Katherine L Hill-Harfe, and Richard a Kahn. 2004. "Functional Genomic Analysis of the ADP-Ribosylation Factor Family of GTPases: Phylogeny among Diverse Eukaryotes and Function in C. Elegans." *The FASEB Journal* 18 (15):

1834–50. https://doi.org/10.1096/fj.04-2273com.

Li, Yi, Jie Hu, Klemens Höfer, Andrew M.S. Wong, Jonathan D. Cooper, Shari G. Birnbaum, Robert E. Hammer, and Sandra L. Hofmann. 2010. “DHHC5 Interacts with PDZ Domain 3 of Post-Synaptic Density-95 (PSD-95) Protein and Plays a Role in Learning and Memory.” *Journal of Biological Chemistry*. https://doi.org/10.1074/jbc.M109.079426.

Li, Yi, Brent R. Martin, Benjamin F. Cravatt, and Sandra L. Hofmann. 2012. “DHHC5 Protein Palmitoylates Flotillin-2 and Is Rapidly Degraded on Induction of Neuronal Differentiation in Cultured Cells.” *Journal of Biological Chemistry*. https://doi.org/10.1074/jbc.M111.306183.

Li, Yiwen, Weng Tao, Lingyu Luo, Deqiang Huang, Konrad Kauper, Paul Stabila, Matthew M. Lavail, Alan M. Laties, and Rong Wen. 2010. “CNTF Induces Regeneration of Cone Outer Segments in a Rat Model of Retinal Degeneration.” *PLoS ONE*. https://doi.org/10.1371/journal.pone.0009495.

Li, Yujie, and Jinghua Hu. 2011. “Small GTPases and Cilia.” *Protein and Cell*. https://doi.org/10.1007/s13238-011-1004-7.

Li, Yujie, Qing Wei, Yuxia Zhang, Kun Ling, and Jinghua Hu. 2010. “The Small GTPases ARL-13 and ARL-3 Coordinate Intraflagellar Transport and Ciliogenesis.” *Journal of Cell Biology* 189 (6): 1039–51. https://doi.org/10.1083/jcb.200912001.

Linari, Marco, Michael Hanzal-Bayer, and Jörg Becker. 1999. “The Delta Subunit of Rod Specific Cyclic GMP Phosphodiesterase, PDE δ, Interacts with the Arf-like Protein Arl3 in a GTP Specific Manner.” *FEBS Letters*. https://doi.org/10.1016/S0014-5793(99)01117-5.

Linstedt, A D, and H P Hauri. 1993. “Giantin, a Novel Conserved Golgi Membrane Protein Containing a Cytoplasmic Domain of at Least 350 KDa.” *Molecular Biology of the Cell* 4 (7): 679–93. https://doi.org/10.1091/mbc.4.7.679.

Littleton, J. T., R. J. O. Barnard, S. A. Titus, J. Slind, E. R. Chapman, and B. Ganetzky. 2001. “SNARE-Complex Disassembly by NSF Follows Synaptic-Vesicle Fusion.” *Proceedings of the National Academy of Sciences*. https://doi.org/10.1073/pnas.221450198.

Liu, Fei, Jiaxiang Chen, Shanshan Yu, Rakesh Kotapati Raghupathy, Xiliang Liu, Yayun Qin, Chang Li, et al. 2015. “Knockout of RP2 Decreases GRK1 and Rod Transducin Subunits and Leads to Photoreceptor Degeneration in Zebrafish.” *Human Molecular Genetics* 24 (16): 4648–59. https://doi.org/10.1093/hmg/ddv197.

Liu, Fei, Yayun Qin, Shanshan Yu, Dinesh C. Soares, Lifang Yang, Jun Weng, Chang Li, et al. 2017. “Pathogenic Mutations in Retinitis Pigmentosa 2 Predominantly Result in Loss of RP2 Protein Stability in Humans and Zebrafish.” *Journal of Biological Chemistry*. https://doi.org/10.1074/jbc.M116.760314.

Liu, L., K. M. McBride, and N. C. Reich. 2005. “STAT3 Nuclear Import Is Independent of Tyrosine Phosphorylation and Mediated by Importin- 3.” *Proceedings of the National Academy of Sciences*. https://doi.org/10.1073/pnas.0501643102.

Liu, Qin, Jian Zuo, and Eric A Pierce. 2004. “The Retinitis Pigmentosa 1 Protein Is a Photoreceptor Microtubule-Associated Protein.” *The Journal of Neuroscience : The Official Journal of the Society for Neuroscience* 24 (29): 6427–36. https://doi.org/10.1523/JNEUROSCI.1335-04.2004.

Liu, X., O. V. Bulgakov, K. N. Darrow, B. Pawlyk, M. Adamian, M. C. Liberman, and T. Li. 2007. “Usherin Is Required for Maintenance of Retinal Photoreceptors and Normal Development of Cochlear Hair Cells.” *Proceedings of the National Academy of Sciences*. https://doi.org/10.1073/pnas.0610950104.

Liu, Xinran, Keiji Seno, Yuji Nishizawa, Fumio Hayashi, Akio Yamazaki, Hiroyuki Matsumoto, Takashi Wakabayashi, and Jiro Usukura. 1994. “Ultrastructural Localization of Retinal Guanylate Cyclase in Human and Monkey Retinas.” *Experimental Eye Research*. https://doi.org/10.1006/exer.1994.1162.

Lonze, Bonnie E., and David D. Ginty. 2002. “Function and Regulation of CREB Family Transcription Factors in the Nervous System.” *Neuron*. https://doi.org/10.1016/S0896-6273(02)00828-0.

Loscher, Carol J., Karsten Hokamp, John H. Wilson, Tiansen Li, Peter Humphries, G. Jane Farrar, and Arpad Palfi. 2008. “A Common MicroRNA Signature in Mouse Models of Retinal Degeneration.” *Experimental Eye Research*.

https://doi.org/10.1016/j.exer.2008.08.016.

Lowe, D G, a M Dizhoor, K Liu, Q Gu, M Spencer, R Laura, L Lu, and J B Hurley. 1995. “Cloning and Expression of a Second Photoreceptor-Specific Membrane Retina Guanylyl Cyclase (RetGC), RetGC-2.” *Proceedings of the National Academy of Sciences of the United States of America*. https://doi.org/10.1073/pnas.92.12.5535.

Lutticken, C, U M Wegenka, J Yuan, J Buschmann, C Schindler, A Ziemiecki, A G Harpur, et al. 1994. “Association of Transcription Factor APRF and Protein Kinase Jak1 with the Interleukin-6 Signal Transducer Gp130.” *Science* 263 (5143): 89–92. https://doi.org/10.1126/science.8272872.

Luzio, J Paul, Brigitte Brake, George Banting, Kathryn E Howell, P Braghetta, and Keith K Stanley. 1990. “Identification, Sequencing and Expression of an Integral Membrane Protein of the Trans-Golgi Network (TGN38).” *The Biochemical Journal*. https://doi.org/10.1042/bj2700097.

Lyraki, Rodanthi, Mandy Lokaj, Dinesh C Soares, Abigail Little, Matthieu Vermeren, Joseph A Marsh, Alfred Wittinghofer, and Toby Hurd. 2018. “Characterization of a Novel RP2 – OSTF1 Interaction and Its Implication for Actin Remodelling.” https://doi.org/10.1242/jcs.211748.

Lyubarsky, a L, C Chen, M I Simon, and E N Pugh. 2000. “Mice Lacking G-Protein Receptor Kinase 1 Have Profoundly Slowed Recovery of Cone-Driven Retinal Responses.” *The Journal of Neuroscience : The Official Journal of the Society for Neuroscience*.

Maerker, Tina, Erwin van Wijk, Nora Overlack, Ferry F.J. Kersten, Joann Mcgee, Tobias Goldmann, Elisabeth Sehn, et al. 2008. “A Novel Usher Protein Network at the Periciliary Reloading Point between Molecular Transport Machineries in Vertebrate Photoreceptor Cells.” *Human Molecular Genetics*. https://doi.org/10.1093/hmg/ddm285.

Maita, Hiroshi, Hirotake Kitaura, T. Jeffrey Keen, Chris F. Inglehearn, Hiroyoshi Ariga, and Sanae M.M. Iguchi-Ariga. 2004. “PAP-1, the Mutated Gene Underlying the RP9 Form of Dominant Retinitis Pigmentosa, Is a Splicing Factor.” *Experimental Cell Research*. https://doi.org/10.1016/j.yexcr.2004.07.029.

Maki, Hisaji. 2002. “Origins of Spontaneous Mutations: Specificity and Directionality of Base-Substitution, Frameshift, and Sequence-Substitution Mutageneses.” *Annual Review of Genetics*. https://doi.org/10.1146/annurev.genet.36.042602.094806.

Makino, Clint L., R.L. Dodd, J. Chen, M.E. Burns, A. Roca, M.I. Simon, and D.A. Baylor. 2004. “Recoverin Regulates Light-Dependent Phosphodiesterase Activity in Retinal Rods.” *The Journal of General Physiology*. https://doi.org/10.1085/jgp.200308994.

Makino, E R, J W Handy, T Li, and V Y Arshavsky. 1999. “The GTPase Activating Factor for Transducin in Rod Photoreceptors Is the Complex between RGS9 and Type 5 G Protein Beta Subunit.” *Proc Natl Acad Sci U S A*. https://doi.org/10.1073/pnas.96.5.1947.

Marc, Robert E., James R. Anderson, Bryan W. Jones, Crystal L. Sigulinsky, and James S. Lauritzen. 2014. “The AII Amacrine Cell Connectome: A Dense Network Hub.” *Frontiers in Neural Circuits*. https://doi.org/10.3389/fncir.2014.00104.

Marszalek, Joseph R., Xinran Liu, Elizabeth A. Roberts, Daniel Chui, Jamey D. Marth, David S. Williams, and Lawrence S.B. Goldstein. 2000. “Genetic Evidence for Selective Transport of Opsin and Arrestin by Kinesin-II in Mammalian Photoreceptors.” *Cell*. https://doi.org/10.1016/S0092-8674(00)00023-4.

Martinez-Navarrete, G., M. J. Seiler, R. B. Aramant, L. Fernandez-Sanchez, I. Pinilla, and N. Cuenca. 2011. “Retinal Degeneration in Two Lines of Transgenic S334ter Rats.” *Experimental Eye Research*. https://doi.org/10.1016/j.exer.2010.12.001.

Matsuda, Tadashi, Yojiro Yamanaka, and Toshio Hirano. 1994. “Interleukin-6-Induced Tyrosine Phosphorylation of Multiple Proteins in Murine Hematopoietic Lineage Cells.” *Biochemical and Biophysical Research Communications*. https://doi.org/10.1006/bbrc.1994.1525.

McKie, A B, J C McHale, T J Keen, E E Tarttelin, R Goliath, J J van Lith-Verhoeven, J Greenberg, et al. 2001. “Mutations in the Pre-MRNA Splicing Factor Gene PRPC8 in Autosomal Dominant Retinitis Pigmentosa (RP13).” *Human*

Molecular Genetics. https://doi.org/10.1093/hmg/10.15.1555.

Mears, Alan J., Mineo Kondo, Prabodha K. Swain, Yuichiro Takada, Ronald A. Bush, Thomas L. Saunders, Paul A. Sieving, and Anand Swaroop. 2001. “Nrl Is Required for Rod Photoreceptor Development.” *Nature Genetics*. https://doi.org/10.1038/ng774.

Megaw, Roly, Hashem Abu-arafeh, Melissa Jungnickel, Carla Mellough, Christine Gurniak, Walter Witke, Wei Zhang, et al. n.d. “Gelsolin Dysfunction Causes Photoreceptor Loss in Induced Pluripotent Cell and Animal Retinitis Pigmentosa Models.” *Nature Communications*, 1–9. https://doi.org/10.1038/s41467-017-00111-8.

Meindl, A., K. Dry, K. Herrmann, F. Manson, A. Ciccodicola, A. Edgar, M. R.S. Carvalho, et al. 1996. “A Gene (RPGR) with Homology to the RCC1 Guanine Nucleotide Exchange Factor Is Mutated in X-Linked Retinitis Pigmentosa (RP3).” *Nature Genetics*. https://doi.org/10.1038/ng0596-35.

Mendes, Hugo F., Jacqueline Van Der Spuy, J. Paul Chapple, and Michael E. Cheetham. 2005. “Mechanisms of Cell Death in Rhodopsin Retinitis Pigmentosa: Implications for Therapy.” *Trends in Molecular Medicine*. https://doi.org/10.1016/j.molmed.2005.02.007.

Mendez, A., M.E. Burns, I. Sokal, A.M. Dizhoor, W. Baehr, K. Palczewski, D.A. Baylor, and J. Chen. 2001. “Role of Guanylate Cyclase-Activating Proteins (GCAPs) in Setting the Flash Sensitivity of Rod Photoreceptors.” *Proceedings of the National Academy of Sciences of the United States of America*. https://doi.org/10.1073/pnas.171308998.

Mendez, Ana, Marie E. Burns, Angela Roca, Janis Lem, Lan Wing Wu, Melvin I. Simon, Denis A. Baylor, and Jeannie Chen. 2000. “Rapid and Reproducible Deactivation of Rhodopsin Requires Multiple Phosphorylation Sites.” *Neuron*. https://doi.org/10.1016/S0896-6273(00)00093-3.

Mick, David U., Rachel B. Rodrigues, Ryan D. Leib, Christopher M. Adams, Allis S. Chien, Steven P. Gygi, and Maxence V. Nachury. 2015. “Proteomics of Primary Cilia by Proximity Labeling.” *Developmental Cell*. https://doi.org/10.1016/j.devcel.2015.10.015.

Mikami, A. 2002. “Molecular Structure of Cytoplasmic Dynein 2 and Its Distribution in Neuronal and Ciliated Cells.” *Journal of Cell Science*. https://doi.org/10.1242/jcs.00168.

Ming, Ming, Xuping Li, Xiaolan Fan, Dehua Yang, Liang Li, Sheng Chen, Qing Gu, and Weidong Le. 2009. “Retinal Pigment Epithelial Cells Secrete Neurotrophic Factors and Synthesize Dopamine: Possible Contribution to Therapeutic Effects of RPE Cell Transplantation in Parkinson’s Disease.” *Journal of Translational Medicine*. https://doi.org/10.1186/1479-5876-7-53.

Mitchell, David A, Anant Vasudevan, Maurine E Linder, and Robert J Deschenes. 2006. “Protein Palmitoylation by a Family of DHHC Protein S-Acyltransferases.” *J Lipid Res*. https://doi.org/R600007-JLR200 [pii]\n10.1194/jlr.R600007-JLR200.

Moiseyev, Gennadiy, Ying Chen, Yusuke Takahashi, Bill X Wu, and Jian-xing Ma. 2005. “RPE65 Is the Isomerohydrolase in the Retinoid Visual Cycle.” *Proceedings of the National Academy of Sciences* 102 (35): 12413–18. https://doi.org/10.1073/pnas.0503460102.

Molday, Robert S. 1998. “Photoreceptor Membrane Proteins, Phototransduction, and Retinal Degenerative Diseases: The Friedenwald Lecture.” In *Investigative Ophthalmology and Visual Science*.

Mookherjee, Suddhasil, Suja Hiriyanna, Kayleigh Kaneshiro, Yichao Li, Wei Li, Haohua Qian, Tiansen Li, et al. 2015. “Long-Term Rescue of Cone Photoreceptor Degeneration in Retinitis Pigmentosa 2 (RP2)-Knockout Mice by Gene Replacement Therapy.” *Human Molecular Genetics*. https://doi.org/10.1093/hmg/ddv354.

Moritz, O L, B M Tam, L L Hurd, J Peränen, D Deretic, and D S Papermaster. 2001. “Mutant Rab8 Impairs Docking and Fusion of Rhodopsin-Bearing Post-Golgi Membranes and Causes Cell Death of Transgenic Xenopus Rods.” *Molecular Biology of the Cell*. https://doi.org/10.1091/mbc.12.8.2341.

Murakami, Y., H. Matsumoto, M. Roh, J. Suzuki, T. Hisatomi, Y. Ikeda, J. W. Miller, and D. G. Vavvas. 2012. “Receptor Interacting Protein Kinase Mediates Necrotic Cone but Not Rod Cell Death in a Mouse Model of Inherited Degeneration.” *Proceedings of the National Academy of Sciences*.

https://doi.org/10.1073/pnas.1206937109.

Murga-Zamalloa, Carlos A., Stephen J. Atkins, Johan Peranen, Anand Swaroop, and Hemant Khanna. 2010. “Interaction of Retinitis Pigmentosa GTPase Regulator (RPGR) with RAB8A GTPase: Implications for Cilia Dysfunction and Photoreceptor Degeneration.” *Human Molecular Genetics*. https://doi.org/10.1093/hmg/ddq275.

Murphy, Daniel, Benjamin Cieply, Russ Carstens, Visvanathan Ramamurthy, and Peter Stoilov. 2016. “The Musashi 1 Controls the Splicing of Photoreceptor-Specific Exons in the Vertebrate Retina.” *PLoS Genetics* 12 (8). https://doi.org/10.1371/journal.pgen.1006256.

Murphy, Joseph, and Saravanan Kolandaivelu. 2016. “Palmitoylation of Progressive Rod-Cone Degeneration (PRCD) Regulates Protein Stability and Localization.” *Journal of Biological Chemistry*. https://doi.org/10.1074/jbc.M116.742767.

Mustafi, Debarshi, Andreas H. Engel, and Krzysztof Palczewski. 2009. “Structure of Cone Photoreceptors.” *Progress in Retinal and Eye Research*. https://doi.org/10.1016/j.preteyeres.2009.05.003.

Naash, M I, J G Hollyfield, M R al-Ubaidi, and W Baehr. 1993. “Simulation of Human Autosomal Dominant Retinitis Pigmentosa in Transgenic Mice Expressing a Mutated Murine Opsin Gene.” *Proceedings of the National Academy of Sciences of the United States of America*. https://doi.org/10.1073/pnas.90.12.5499.

Nachury, Maxence V., Alexander V. Loktev, Qihong Zhang, Christopher J. Westlake, Johan Peränen, Andreas Merdes, Diane C. Slusarski, et al. 2007. “A Core Complex of BBS Proteins Cooperates with the GTPase Rab8 to Promote Ciliary Membrane Biogenesis.” *Cell*. https://doi.org/10.1016/j.cell.2007.03.053.

Nager, Andrew R., Jaclyn S. Goldstein, Vicente Herranz-Pérez, Didier Portran, Fan Ye, Jose Manuel Garcia-Verdugo, and Maxence V. Nachury. 2017. “An Actin Network Dispatches Ciliary GPCRs into Extracellular Vesicles to Modulate Signaling.” *Cell*. https://doi.org/10.1016/j.cell.2016.11.036.

Nakazawa, Mitsuru, Yuko Wada, Sigrid Fuchs, Andreas Gal and Makoto Tamai. 1997. "Oguchi Disease: Phenotypic Characteristics of Patients with the

Frequent 1147DELA Mutation in the Arrestin Gene." *Retina* 17 (1). https://journals.lww.com/retinajournal/Fulltext/1997/01000/OGUCHI_DISEASE__PHENOTYPIC_CHARACTERISTICS_OF.4.aspx.

Nandrot, E. F., M. Anand, D. Almeida, K. Atabai, D. Sheppard, and S. C. Finnemann. 2007. “Essential Role for MFG-E8 as Ligand for Vbeta5 Integrin in Diurnal Retinal Phagocytosis.” *Proceedings of the National Academy of Sciences*. https://doi.org/10.1073/pnas.0704756104.

Neubert, T. A., R. S. Johnson, J. B. Hurley, and K. A. Walsh. 1992. “The Rod Transducin α Subunit Amino Terminus Is Heterogeneously Fatty Acylated.” *Journal of Biological Chemistry*. https://doi.org/10.1684/bdc.2010.1196.

Oates, Andrew C., Patrik Wollberg, Stephen J. Pratt, Barry H. Paw, Stephen L. Johnson, Robert K. Ho, John H. Postlethwait, Leonard I. Zon, and Andrew F. Wilks. 1999. “Zebrafish Stat3 Is Expressed in Restricted Tissues during Embryogenesis and Stat1 Rescues Cytokine Signaling in a STAT1-Deficient Human Cell Line.” *Developmental Dynamics*. https://doi.org/10.1002/(SICI)1097-0177(199908)215:4<352::AID-AJA7>3.0.CO;2-J.

Ohguro, H., J. P. Van Hooser, A. H. Milam, and K. Palczewski. 1995. “Rhodopsin Phosphorylation and Dephosphorylation in Vivo.” *Journal of Biological Chemistry*. https://doi.org/10.1074/jbc.270.24.14259.

Oliver, Guillermo, Alvaro Mailhos, Roland Wehr, Neal G Copeland, Nancy A Jenkins, and Peter Gruss. 1995. “Six3, a Murine Homologue of the Sine Oculis Gene, Demarcates the Most Anterior Border of the Developing Neural Plate and Is Expressed during Eye Development.” *Development (Cambridge, England)*.

Organisciak, Daniel T., and Barry S. Winkler. 1994. “Retinal Light Damage: Practical and Theoretical Considerations.” *Progress in Retinal and Eye Research*. https://doi.org/10.1016/1350-9462(94)90003-5.

Oslowski, Christine M, and Fumihiko Urano. 2013. “Measuring ER Stress and the Unfolded Protein Response Using Mammalian Tissue Culture System.” *Methods in Enzymology*. https://doi.org/10.1016/B978-0-12-385114-7.00004-0.Measuring.

Ozawa, Yoko, Keiko Nakao, Takuya Shimazaki, Junji Takeda, Shizuo Akira, Katsuhiko Ishihara, Toshio Hirano, Yoshihisa Oguchi, and Hideyuki Okano. 2004. “Downregulation of STAT3 Activation Is Required for Presumptive Rod Photoreceptor Cells to Differentiate in the Postnatal Retina.” *Molecular and Cellular Neuroscience*. https://doi.org/10.1016/j.mcn.2004.02.001.

Padnick-Silver, Lissa, Jennifer J Kang Derwent, Elizabeth Giuliano, Kristina Narfström, and Robert A Linsenmeier. 2006. “Retinal Oxygenation and Oxygen Metabolism in Abyssinian Cats with a Hereditary Retinal Degeneration.” *Investigative Ophthalmology & Visual Science* 47 (8): 3683–89.

Palczewski, Krzysztof. 1994. “Structure and Functions of Arrestins.” *Protein Science*. https://doi.org/10.1002/pro.5560030901.

Papermaster, D. S., B. G. Schneider, D. Defoe, and J. C. Besharse. 1986. “Biosynthesis and Vectorial Transport of Opsin on Vesicles in Retinal Rod Photoreceptors.” *Journal of Histochemistry and Cytochemistry*. https://doi.org/10.1177/34.1.2934469.

Paquet-Durand, Francois, Seifollah Azadi, Stefanie M. Hauck, Marius Ueffing, Theo Van Veen, and Per Ekström. 2006. “Calpain Is Activated in Degenerating Photoreceptors in the Rd1 Mouse.” *Journal of Neurochemistry*. https://doi.org/10.1111/j.1471-4159.2005.03628.x.

Paquet-Durand, François, José Silva, Tanuja Talukdar, Leif E Johnson, Seifollah Azadi, Theo van Veen, Marius Ueffing, Stefanie M Hauck, and Per A R Ekström. 2007. “Excessive Activation of Poly(ADP-Ribose) Polymerase Contributes to Inherited Photoreceptor Degeneration in the Retinal Degeneration 1 Mouse.” *The Journal of Neuroscience*. https://doi.org/10.1523/JNEUROSCI.1514-07.2007.

Pazour, Gregory J., Sheila A. Baker, James A. Deane, Douglas G. Cole, Bethany L. Dickert, Joel L. Rosenbaum, George B. Witman, and Joseph C. Besharse. 2002. “The Intraflagellar Transport Protein, IFT88, Is Essential for Vertebrate Photoreceptor Assembly and Maintenance.” *Journal of Cell Biology*. https://doi.org/10.1083/jcb.200107108.

Pazour, Gregory J., Bethany L. Dickert, and George B. Witman. 1999. “The DHC1b (DHC2) Isoform of Cytoplasmic Dynein Is Required for Flagellar Assembly.”

Journal of Cell Biology. https://doi.org/10.1083/jcb.144.3.473.

Pearring, Jillian N., Raquel Y. Salinas, Sheila A. Baker, and Vadim Y. Arshavsky. 2013. “Protein Sorting, Targeting and Trafficking in Photoreceptor Cells.” *Progress in Retinal and Eye Research*. https://doi.org/10.1016/j.preteyeres.2013.03.002.

Pearring, Jillian N, Jovenal T San Agustin, Ekaterina S Lobanova, Christopher J Gabriel, Eric C Lieu, William J Monis, Michael W Stuck, et al. 2017. “Loss of Arf4 Causes Severe Degeneration of the Exocrine Pancreas but Not Cystic Kidney Disease or Retinal Degeneration.” *PLoS Genetics* 13 (4): e1006740–e1006740. https://doi.org/10.1371/journal.pgen.1006740.

Peng, Changhong, Elizabeth D. Rich, and Michael D. Varnum. 2004. “Subunit Configuration of Heteromeric Cone Cyclic Nucleotide-Gated Channels.” *Neuron*. https://doi.org/10.1016/S0896-6273(04)00225-9.

Peng, Y W, J D Robishaw, M A Levine, and K W Yau. 1992. “Retinal Rods and Cones Have Distinct G Protein Beta and Gamma Subunits.” *Proc Natl Acad Sci U S A*.

Peterson, W M, Q Wang, R Tzekova, and S J Wiegand. 2000. “Ciliary Neurotrophic Factor and Stress Stimuli Activate the Jak-STAT Pathway in Retinal Neurons and Glia.” *The Journal of Neuroscience : The Official Journal of the Society for Neuroscience*. https://doi.org/10.1523/JNEUROSCI.20-11-04081.2000.

Philp, N J, W Chang, and K Long. 1987. “Light-Stimulated Protein Movement in Rod Photoreceptor Cells of the Rat Retina.” *FEBS Lett*. https://doi.org/0014-5793(87)81144-4 [pii] ET - 1987/12/10.

Pilati, Camilla, Mohamed Amessou, Michel P Bihl, Charles Balabaud, Jeanne Tran Van Nhieu, Valérie Paradis, Jean Charles Nault, et al. 2011. “Somatic Mutations Activating STAT3 in Human Inflammatory Hepatocellular Adenomas.” *The Journal of Experimental Medicine* 208 (7): 1359 LP-1366.

Pollard, Victoria W., W. Matthew Michael, Sara Nakielny, Mikiko C. Siomi, Fan Wang, and Gideon Dreyfuss. 1996. “A Novel Receptor-Mediated Nuclear Protein Import Pathway.” *Cell*. https://doi.org/10.1016/S0092-8674(00)80173-7.

Portera-Cailliau, C, C H Sung, J Nathans, and R Adler. 1994. “Apoptotic Photoreceptor Cell Death in Mouse Models of Retinitis Pigmentosa.” *Proceedings of the National Academy of Sciences* 91 (3): 974–78. https://doi.org/10.1073/pnas.91.3.974.

Pruski, Michal, Ann Rajnicek, Zhifu Yang, Hannah Clancy, Yu-qiang Ding, Colin D Mccaig, and Bing Lang. 2016. “The Ciliary GTPase Arl13b Regulates Cell Migration and Cell Cycle Progression.” *Cell Adhesion & Migration* 10 (4): 393–405. https://doi.org/10.1080/19336918.2016.1159380.

Pugacheva, Elena N., Sandra A. Jablonski, Tiffiney R. Hartman, Elizabeth P. Henske, and Erica A. Golemis. 2007. “HEF1-Dependent Aurora A Activation Induces Disassembly of the Primary Cilium.” *Cell* 129 (7): 1351–63. https://doi.org/10.1016/j.cell.2007.04.035.

Qtaishat, Nasser M., Ting Ing L. Okajima, Shihong Li, Muna I. Naash, and David R. Pepperberg. 1999. “Retinoid Kinetics in Eye Tissues of VPP Transgenic Mice and Their Normal Littermates.” *Investigative Ophthalmology and Visual Science*.

Querques, Giuseppe, and Eric H. Souied. 2016. *Macular Dystrophies*. *Macular Dystrophies*. https://doi.org/10.1007/978-3-319-26621-3.

Rácz, Boglarka, Andrea Tamás, Peter Kiss, Gabor Tóth, Balazs Gasz, Balazs Borsiczky, Andrea Ferencz, Ferenc Gallyas, Erzsebet Roth, and Dora Reglodi. 2006. “Involvement of ERK and CREB Signaling Pathways in the Protective Effect of PACAP in Monosodium Glutamate-Induced Retinal Lesion.” In *Annals of the New York Academy of Sciences*. https://doi.org/10.1196/annals.1317.070.

Raymond, Sophie M., and Ian J. Jackson. 1995. “The Retinal Pigmented Epithelium Is Required for Development and Maintenance of the Mouse Neural Retina.” *Current Biology*. https://doi.org/10.1016/S0960-9822(95)00255-7.

Redmond., T Michael, Shirley Yu, Eric Lee, Dean Bok, Duco Hamasaki, Ning Chen, Patrice Goletz, Jian-Xing Ma, Rosalie K Crouch, and Karl Pfeifer. 1998. “Rpe65 Is Necessary for Production of 11-Cis-Vitamin A in the Retinal Visual Cycle.” *Nature Genetics* 20 (December): 344.

Remans, Kim, Marco Bürger, Ingrid R. Vetter, and Alfred Wittinghofer. 2014. “C2 Domains as Protein-Protein Interaction Modules in the Ciliary Transition Zone.” *Cell Reports*. https://doi.org/10.1016/j.celrep.2014.05.049.

Rieke, F., and D. A. Baylor. 1998. “Origin of Reproducibility in the Responses of Retinal Rods to Single Photons.” *Biophysical Journal*. https://doi.org/10.1016/S0006-3495(98)77625-8.

Ripps, Harris. 2002. “Cell Death in Retinitis Pigmentosa: Gap Junctions and the ‘bystander’ Effect.” *Experimental Eye Research*. https://doi.org/10.1006/exer.2002.1155.

Roberts, Anthony J., Takahide Kon, Peter J. Knight, Kazuo Sutoh, and Stan A. Burgess. 2013. “Functions and Mechanics of Dynein Motor Proteins.” *Nature Reviews Molecular Cell Biology*. https://doi.org/10.1038/nrm3667.

Rocks, Oliver, Marc Gerauer, Nachiket Vartak, Sebastian Koch, Zhi Ping Huang, Markos Pechlivanis, Jürgen Kuhlmann, et al. 2010. “The Palmitoylation Machinery Is a Spatially Organizing System for Peripheral Membrane Proteins.” *Cell*. https://doi.org/10.1016/j.cell.2010.04.007.

Roepman, R, N Bernoud-Hubac, D E Schick, a Maugeri, W Berger, H H Ropers, F P Cremers, and P a Ferreira. 2000. “The Retinitis Pigmentosa GTPase Regulator (RPGR) Interacts with Novel Transport-like Proteins in the Outer Segments of Rod Photoreceptors.” *Human Molecular Genetics*.

Rose-John, Stefan. 2018. “Interleukin-6 Family Cytokines.” *Cold Spring Harbor Perspectives in Biology*. https://doi.org/10.1101/cshperspect.a028415.

Rosenbaum, J L, and G B Witman. 2002. “Intraflagellar Transport.” *Nat Rev Mol Cell Biol* 3 (11): 813–25. https://doi.org/10.1038/nrm952.

Roux, Kyle J., Dae In Kim, Manfred Raida, and Brian Burke. 2012. “A Promiscuous Biotin Ligase Fusion Protein Identifies Proximal and Interacting Proteins in Mammalian Cells.” *Journal of Cell Biology* 196 (6): 801–10. https://doi.org/10.1083/jcb.201112098.

Roy, Kasturi, Stephanie Jerman, Levente Jozsef, Thomas McNamara, Ginikanwa Onyekaba, Zhaoxia Sun, and Ethan P. Marin. 2017. “Palmitoylation of the

Ciliary GTPase ARL13b Is Necessary for Its Stability and Its Role in Cilia Formation." *Journal of Biological Chemistry*. https://doi.org/10.1074/jbc.M117.792937.

Sahel, José Alain, Katia Marazova, and Isabelle Audo. 2015. "Clinical Characteristics and Current Therapies for Inherited Retinal Degenerations." *Cold Spring Harbor Perspectives in Medicine*. https://doi.org/10.1101/cshperspect.a017111.

Sakai, Katsunaga, and Jun Ichi Miyazaki. 1997. "A Transgenic Mouse Line That Retains Cre Recombinase Activity in Mature Oocytes Irrespective of the Cre Transgene Transmission." *Biochemical and Biophysical Research Communications*. https://doi.org/10.1006/bbrc.1997.7111.

Salinas, Raquel Y., Jillian N. Pearring, Jin Dong Ding, William J. Spencer, Ying Hao, and Vadim Y. Arshavsky. 2017. "Photoreceptor Discs Form through Peripherindependent Suppression of Ciliary Ectosome Release." *Journal of Cell Biology*. https://doi.org/10.1083/jcb.201608081.

Samardzija, Marijana, Andreas Wenzel, Svenja Aufenberg, Markus Thiersch, Charlotte Remé, and Christian Grimm. 2006. "Differential Role of Jak-STAT Signaling in Retinal Degenerations." *The FASEB Journal : Official Publication of the Federation of American Societies for Experimental Biology*. https://doi.org/10.1096/fj.06-5895fje.

Sancho-Pelluz, Javier, Blanca Arango-Gonzalez, Stefan Kustermann, Francisco Javier Romero, Theo Van Veen, Eberhart Zrenner, Per Ekström, and François Paquet-Durand. 2008. "Photoreceptor Cell Death Mechanisms in Inherited Retinal Degeneration." *Molecular Neurobiology*. https://doi.org/10.1007/s12035-008-8045-9.

Sanges, Daniela, and Valeria Marigo. 2006. "Cross-Talk between Two Apoptotic Pathways Activated by Endoplasmic Reticulum Stress: Differential Contribution of Caspase-12 and AIF." *Apoptosis*. https://doi.org/10.1007/s10495-006-9006-2.

Sanyal, S, and H Jansen. 1989. "A Comparative Survey of Synaptic Changes in the Rod Photoreceptor Terminals of Rd, Rds and Double Homozygous Mutant Mice." *Prog Clin Biol Res*.

Sanz, M. M., L. E. Johnson, S. Ahuja, P. A R Ekström, J. Romero, and T. van Veen. 2007. “Significant Photoreceptor Rescue by Treatment with a Combination of Antioxidants in an Animal Model for Retinal Degeneration.” *Neuroscience*. https://doi.org/10.1016/j.neuroscience.2006.12.034.

Saraiva, Jorge M, and Michael Baraitser. n.d. “Joubert Syndrome: A Review.” *American Journal of Medical Genetics* 43 (4): 726–31. https://doi.org/10.1002/ajmg.1320430415.

Sato, Takashi, Tomohiko Iwano, Masataka Kunii, Shinji Matsuda, Rumiko Mizuguchi, Yongwook Jung, Haruo Hagiwara, et al. 2014. “Rab8a and Rab8b Are Essential for Several Apical Transport Pathways but Insufficient for Ciliogenesis.” *Journal of Cell Science* 127 (Pt 2): 422–31. https://doi.org/10.1242/jcs.136903.

Satoh, A. K. 2005. “Rab11 Mediates Post-Golgi Trafficking of Rhodopsin to the Photosensitive Apical Membrane of Drosophila Photoreceptors.” *Development*. https://doi.org/10.1242/dev.01704.

Schindler, Christian, David E. Levy, and Thomas Decker. 2007. “JAK-STAT Signaling: From Interferons to Cytokines.” *Journal of Biological Chemistry*. https://doi.org/10.1074/jbc.R700016200.

Scholey, Jonathan M. 1996. “Kinesin-II, a Membrane Traffic Motor in Axons, Axonemes, and Spindles.” *Journal of Cell Biology*. https://doi.org/10.1083/jcb.133.1.1.

Schreiber, Valérie, Françoise Dantzer, Jean Christophe Amé, and Gilbert De Murcia. 2006. “Poly(ADP-Ribose): Novel Functions for an Old Molecule.” *Nature Reviews Molecular Cell Biology*. https://doi.org/10.1038/nrm1963.

Schrick, Jeffrey J, Peter Vogel, Alejandro Abuin, Billy Hampton, and Dennis S Rice. 2006. “ADP-Ribosylation Factor-like 3 Is Involved in Kidney and Photoreceptor Development.” *The American Journal of Pathology* 168 (4): 1288–98. https://doi.org/10.2353/ajpath.2006.050941.

Schwahn, Uwe, Steffen Lenzner, Juan Dong, Silke Feil, Bernd Hinzmann, Gerard Van Duijnhoven, Renate Kirschner, et al. 1998. “Positional Cloning of the Gene for X-Linked Retinitis Pigmentosa 2.” *Nature Genetics*.

https://doi.org/10.1038/1214.

Schwartz, Steven D., Carl D. Regillo, Byron L. Lam, Dean Eliott, Philip J. Rosenfeld, Ninel Z. Gregori, Jean Pierre Hubschman, et al. 2015. “Human Embryonic Stem Cell-Derived Retinal Pigment Epithelium in Patients with Age-Related Macular Degeneration and Stargardt’s Macular Dystrophy: Follow-up of Two Open-Label Phase 1/2 Studies.” *The Lancet*. https://doi.org/10.1016/S0140-6736(14)61376-3.

Schwarz, Nele, Amanda Jayne Carr, Amelia Lane, Fabian Moeller, Li Li Chen, Mïnica Aguilï, Britta Nommiste, et al. 2015. “Translational Read-through of the RP2 Arg120stop Mutation in Patient IPSC-Derived Retinal Pigment Epithelium Cells.” *Human Molecular Genetics*. https://doi.org/10.1093/hmg/ddu509.

Schwarz, Nele, Amelia Lane, Katarina Jovanovic, David A. Parfitt, Monica Aguila, Clare L. Thompson, Lyndon da Cruz, et al. 2017. “Arl3 and RP2 Regulate the Trafficking of Ciliary Tip Kinesins.” *Human Molecular Genetics*. https://doi.org/10.1093/hmg/ddx143.

Schwarz, Nele, Tatiana V. Novoselova, Robin Wait, Alison J. Hardcastle, and Michael E. Cheetham. 2012. “The X-Linked Retinitis Pigmentosa Protein RP2 Facilitates G Protein Traffic.” *Human Molecular Genetics* 21 (4): 863–73. https://doi.org/10.1093/hmg/ddr520.

Sergouniotis, Panagiotis I., Christina Chakarova, Cian Murphy, Mirjana Becker, Eva Lenassi, Gavin Arno, Monkol Lek, et al. 2014. “Biallelic Variants in TTLL5, Encoding a Tubulin Glutamylase, Cause Retinal Dystrophy.” *American Journal of Human Genetics*. https://doi.org/10.1016/j.ajhg.2014.04.003.

Shakibaei, Mehdi, Thilo John, Claudia Seifarth, and Ali Mobasheri. 2007. “Resveratrol Inhibits IL-1 Beta-Induced Stimulation of Caspase-3 and Cleavage of PARP in Human Articular Chondrocytes in Vitro.” *Annals of the New York Academy of Sciences*. https://doi.org/10.1196/annals.1397.060.

Sharon, D., G. A P Bruns, T. L. McGee, M. A. Sandberg, E. L. Berson, and T. P. Dryja. 2000. “X-Linked Retinitis Pigmentosa: Mutation Spectrum of the RPGR and RP2 Genes and Correlation with Visual Function.” *Investigative Ophthalmology and Visual Science*.

Sharon, Dror, Michael A. Sandberg, Vivian W. Rabe, Melissa Stillberger, Thaddeus P. Dryja, and Eliot L. Berson. 2003. “RP2 and RPGR Mutations and Clinical Correlations in Patients with X-Linked Retinitis Pigmentosa.” *The American Journal of Human Genetics*. https://doi.org/10.1086/379379.

Shen, Jikui, Xiaoru Yang, Aling Dong, Robert M. Petters, You Wei Peng, Fulton Wong, and Peter A. Campochiaro. 2005. “Oxidative Damage Is a Potential Cause of Cone Cell Death in Retinitis Pigmentosa.” *Journal of Cellular Physiology*. https://doi.org/10.1002/jcp.20346.

Shiells, R. A., and G. Falk. 1990. “Glutamate Receptors of Rod Bipolar Cells Are Linked to a Cyclic GMP Cascade via a G-Protein.” *Proceedings of the Royal Society B: Biological Sciences*. https://doi.org/10.1098/rspb.1990.0109.

Shu, X., A. M. Fry, B. Tulloch, F. D.C. Manson, J. W. Crabb, H. Khanna, A. J. Faragher, et al. 2005. “RPGR ORF15 Isoform Co-Localizes with RPGRIP1 at Centrioles and Basal Bodies and Interacts with Nucleophosmin.” *Human Molecular Genetics*. https://doi.org/10.1093/hmg/ddi129.

Sieving, P. A., R. C. Caruso, W. Tao, H. R. Coleman, D. J. S. Thompson, K. R. Fullmer, and R. A. Bush. 2006. “Ciliary Neurotrophic Factor (CNTF) for Human Retinal Degeneration: Phase I Trial of CNTF Delivered by Encapsulated Cell Intraocular Implants.” *Proceedings of the National Academy of Sciences*. https://doi.org/10.1073/pnas.0600236103.

Singla, Veena, and Jeremy F Reiter. 2006. “The Primary Cilium as the Cell’s Antenna: Signaling at a Sensory Organelle.” *Science* 313 (5787): 629–33. https://doi.org/10.1126/science.1124534.

Siomi, Mikiko C., Paul S. Eder, Naoyuki Kataoka, Lili Wan, Qing Liu, and Gideon Dreyfuss. 1997. “Transportin-Mediated Nuclear Import of Heterogeneous Nuclear RNP Proteins.” *Journal of Cell Biology*. https://doi.org/10.1083/jcb.138.6.1181.

Skiba, N. P., J. A. Hopp, and V. Y. Arshavsky. 2000. “The Effector Enzyme Regulates the Duration of G Protein Signaling in Vertebrate Photoreceptors by Increasing the Affinity between Transducin and RGS Protein.” *Journal of Biological Chemistry*. https://doi.org/10.1074/jbc.C000413200.

Smith, W. Clay, Ann H. Milam, Donald Dugger, Anatol Arendt, Paul A. Hargrave, and Krzysztof Palczewski. 1994. “A Splice Variant of Arrestin. Molecular Cloning and Localization in Bovine Retina.” *Journal of Biological Chemistry*.

Sokolov, Maxim, Arkady L. Lyubarsky, Katherine J. Strissel, Andrey B. Savchenko, Viktor I. Govardovskii, Edward N. Pugh, and Vadim Y. Arshavsky. 2002. “Massive Light-Driven Translocation of Transducin between the Two Major Compartments of Rod Cells: A Novel Mechanism of Light Adaptation.” *Neuron*. https://doi.org/10.1016/S0896-6273(02)00636-0.

Spencer, M., P. B. Detwiler, and A. H. Bunt-Milam. 1988. “Distribution of Membrane Proteins in Mechanically Dissociated Retinal Rods.” *Investigative Ophthalmology and Visual Science*.

Stahl, N, T G Boulton, T Farruggella, N Y Ip, S Davis, B A Witthuhn, F W Quelle, et al. 1994. “Association and Activation of Jak-Tyk Kinases by CNTF-LIF-OSM-IL-6 Beta Receptor Components.” *Science* 263 (5143): 92–95. https://doi.org/10.1126/science.8272873.

Stahl, N, T J Farruggella, T G Boulton, Z Zhong, J E Darnell, and G D Yancopoulos. 1995. “Choice of STATs and Other Substrates Specified by Modular Tyrosine-Based Motifs in Cytokine Receptors.” *Science* 267 (5202): 1349–53. https://doi.org/10.1126/science.7871433.

Stewart, Murray. 2007. “Molecular Mechanism of the Nuclear Protein Import Cycle.” *Nature Reviews Molecular Cell Biology*. https://doi.org/10.1038/nrm2114.

Strauss, Olaf. 2005. “The Retinal Pigment Epithelium in Visual Function.” *Physiological Reviews*. https://doi.org/10.1152/physrev.00021.2004.

Strick, David J., Wei Feng, and Douglas Vollrath. 2009. “Mertk Drives Myosin Ii Redistribution during Retinal Pigment Epithelial Phagocytosis.” *Investigative Ophthalmology and Visual Science*. https://doi.org/10.1167/iovs.08-3058.

Strom, Samuel P., Michael J. Clark, Ariadna Martinez, Sarah Garcia, Amira A. Abelazeem, Anna Matynia, Sachin Parikh, et al. 2016. “De Novo Occurrence of a Variant in ARL3 and Apparent Autosomal Dominant Transmission of Retinitis Pigmentosa.” *PLoS ONE* 11 (3). https://doi.org/10.1371/journal.pone.0150944.

Sullivan, L S, and S P Daiger. 1996. “Inherited Retinal Degeneration: Exceptional Genetic and Clinical Heterogeneity.” *Molecular Medicine Today* 2 (9): 380–86. https://doi.org/10.1016/S1357-4310(96)10037-X.

Sung, C H, C Makino, D Baylor, and J Nathans. 1994. “A Rhodopsin Gene Mutation Responsible for Autosomal Dominant Retinitis Pigmentosa Results in a Protein That Is Defective in Localization to the Photoreceptor Outer Segment.” *The Journal of Neuroscience : The Official Journal of the Society for Neuroscience*.

Szegezdi, Eva, Susan E. Logue, Adrienne M. Gorman, and Afshin Samali. 2006. “Mediators of Endoplasmic Reticulum Stress-Induced Apoptosis.” *EMBO Reports*. https://doi.org/10.1038/sj.embor.7400779.

Tachibanaki, Shuji, Daisuke Arinobu, Yoshie Shimauchi-Matsukawa, Sawae Tsushima, and Satoru Kawamura. 2005. “Highly Effective Phosphorylation by G Protein-Coupled Receptor Kinase 7 of Light-Activated Visual Pigment in Cones.” *Proceedings of the National Academy of Sciences of the United States of America*. https://doi.org/10.1073/pnas.0501875102.

Takahashi, S., K. Kubo, S. Waguri, A. Yabashi, H.-W. Shin, Y. Katoh, and K. Nakayama. 2012. “Rab11 Regulates Exocytosis of Recycling Vesicles at the Plasma Membrane.” *Journal of Cell Science*. https://doi.org/10.1242/jcs.102913.

Takeda, Sen, Yoshiaki Yonekawa, Yosuke Tanaka, Yasushi Okada, Shigenori Nonaka, and Nobutaka Hirokawa. 1999. “Left-Right Asymmetry and Kinesin Superfamily Protein KIF3a: New Insights in Determination of Laterality and Mesoderm Induction by KIF3A(-/-) Mice Analysis.” *Journal of Cell Biology*. https://doi.org/10.1083/jcb.145.4.825.

Tao, Weng, Rong Wen, Moses B Goddard, Sandy D Sherman, Pam J O’Rourke, Paul F Stabila, William J Bell, et al. 2002. “Encapsulated Cell-Based Delivery of CNTF Reduces Photoreceptor Degeneration in Animal Models of Retinitis Pigmentosa.” *Investigative Ophthalmology & Visual Science* 43 (10): 3292–98.

Teigelkamp, S, T Achsel, C Mundt, S F Göthel, U Cronshagen, W S Lane, M Marahiel, and Reinhard Lührmann. 1998. “The 20kD Protein of Human [U4/U6.U5] Tri-SnRNPs Is a Novel Cyclophilin That Forms a Complex with the U4/U6-Specific 60kD and 90kD Proteins.” *RNA (New York, N.Y.)*.

Thomas, Gareth M., Takashi Hayashi, Shu Ling Chiu, Chih Ming Chen, and Richard L. Huganir. 2012. “Palmitoylation by DHHC5/8 Targets GRIP1 to Dendritic Endosomes to Regulate AMPA-R Trafficking.” *Neuron*. https://doi.org/10.1016/j.neuron.2011.11.021.

Thomas, Sophie, Kevin J. Wright, Stéphanie Le Corre, Alessia Micalizzi, Marta Romani, Avinash Abhyankar, Julien Saada, et al. 2014. “A Homozygous PDE6D Mutation in Joubert Syndrome Impairs Targeting of Farnesylated INPP5E Protein to the Primary Cilium.” *Human Mutation* 35 (1): 137–46. https://doi.org/10.1002/humu.22470.

Thoreson W.B. 2017. *The Vertebrate Retina. In: Ikezu T., Gendelman H. (Eds) Neuroimmune Pharmacology*. Springer, Cham. https://doi.org/https://doi.org/10.1007/978-3-319-44022-4_5.

Tian, Lijun, Heather McClafferty, Owen Jeffries, and Michael J. Shipston. 2010. “Multiple Palmitoyltransferases Are Required for Palmitoylation-Dependent Regulation of Large Conductance Calcium- and Voltage-Activated Potassium Channels.” *Journal of Biological Chemistry*. https://doi.org/10.1074/jbc.M110.137802.

Togi, Sumihito, Ryuta Muromoto, Koki Hirashima, Yuichi Kitai, Taichiro Okayama, Osamu Ikeda, Naoki Matsumoto, et al. 2016. “A New STAT3-Binding Partner, ARL3, Enhances the Phosphorylation and Nuclear Accumulation of STAT3.” *Journal of Biological Chemistry* 291 (21): 11161–71. https://doi.org/10.1074/jbc.M116.724849.

Travis, G H. 1998. “Mechanisms of Cell Death in the Inherited Retinal Degenerations.” *American Journal of Human Genetics* 62 (3): 503–8. https://doi.org/10.1086/301772.

Tsang, S H, P Gouras, C K Yamashita, H Kjeldbye, J Fisher, D B Farber, and S P Goff. 1996. “Retinal Degeneration in Mice Lacking the Gamma Subunit of the Rod CGMP Phosphodiesterase.” *Science (New York, N.Y.)*. https://doi.org/10.1126/science.272.5264.1026.

Usui, Shinichi, Brian C Oveson, Sun Young Lee, Young-Joon Jo, Tsunehiko Yoshida, Akiko Miki, Katsuaki Miki, Takeshi Iwase, Lili Lu, and Peter A Campochiaro. 2009. “NADPH Oxidase Plays a Central Role in Cone Cell Death

in Retinitis Pigmentosa." *Journal of Neurochemistry*. https://doi.org/10.1111/j.1471-4159.2009.06195.x.

Valdez-Taubas, Javier, and Hugh Pelham. 2005. "Swf1-Dependent Palmitoylation of the SNARE Tlg1 Prevents Its Ubiquitination and Degradation." *EMBO Journal*. https://doi.org/10.1038/sj.emboj.7600724.

Valenzuela-Fernández, Agustín, J. R. Cabrero, Juan M. Serrador, and Francisco Sánchez-Madrid. 2008. "HDAC6: A Key Regulator of Cytoskeleton, Cell Migration and Cell-Cell Interactions." *Trends in Cell Biology*. https://doi.org/10.1016/j.tcb.2008.04.003.

Veltel, Stefan, Raphael Gasper, Elke Eisenacher, and Alfred Wittinghofer. 2008. "The Retinitis Pigmentosa 2 Gene Product Is a GTPase-Activating Protein for Arf-like 3." *Nature Structural & Molecular Biology* 15 (4): 373–80. https://doi.org/10.1038/nsmb.1396.

Veltel, Stefan, Aleksandra Kravchenko, Shehab Ismail, and Alfred Wittinghofer. 2008. "Specificity of Arl2/Arl3 Signaling Is Mediated by a Ternary Arl3-Effector-GAP Complex." *FEBS Letters*. https://doi.org/10.1016/j.febslet.2008.05.053.

Vervoort, Raf, Alan Lennon, Alan C. Bird, Brian Tulloch, Richard Axton, Maria G. Miano, Alfons Meindl, Thomas Meitinger, Alfredo Ciccodicola, and Alan F. Wright. 2000. "Mutational Hot Spot within a New RPGR Exon in X-Linked Retinitis Pigmentosa." *Nature Genetics*. https://doi.org/10.1038/78182.

Vithana, Eranga N., Leen Abu-Safieh, Maxine J. Allen, Alisoun Carey, Myrto Papaioannou, Christina Chakarova, Mai Al-Maghtheh, et al. 2001. "A Human Homolog of Yeast Pre-MRNA Splicing Gene, PRP31, Underlies Autosomal Dominant Retinitis Pigmentosa on Chromosome 19q13.4 (RP11)." *Molecular Cell*. https://doi.org/10.1016/S1097-2765(01)00305-7.

Volland, Stefanie, Julian Esteve-Rudd, Juyea Hoo, Claudine Yee, and David S. Williams. 2015. "A Comparison of Some Organizational Characteristics of the Mouse Central Retina and the Human Macula." *PLoS ONE*. https://doi.org/10.1371/journal.pone.0125631.

Wada, Yasutaka, Junichi Sugiyama, Toshiyuki Okano, and Yoshitaka Fukada. 2006. "GRK1 and GRK7: Unique Cellular Distribution and Widely Different Activities

of Opsin Phosphorylation in the Zebrafish Rods and Cones." *Journal of Neurochemistry*. https://doi.org/10.1111/j.1471-4159.2006.03920.x.

Wadsworth, P. 1999. "Regional Regulation of Microtubule Dynamics in Polarized, Motile Cells." *Cell Motility and the Cytoskeleton* 42 (1): 48–59. https://doi.org/10.1002/(SICI)1097-0169(1999)42:1<48::AID-CM5>3.0.CO;2-8.

Watanabe, Takashi, Jun Noritake, and Kozo Kaibuchi. 2005. "Regulation of Microtubules in Cell Migration." *Trends in Cell Biology*. https://doi.org/10.1016/j.tcb.2004.12.006.

Wätzlich, Denise, Ingrid Vetter, Katja Gotthardt, Mandy Miertzschke, Yong Xiang Chen, Alfred Wittinghofer, and Shehab Ismail. 2013. "The Interplay between RPGR, PDE?? And Arl2/3 Regulate the Ciliary Targeting of Farnesylated Cargo." *EMBO Reports*. https://doi.org/10.1038/embor.2013.37.

Webb, Tom R., David A. Parfitt, Jessica C. Gardner, Ariadna Martinez, Dalila Bevilacqua, Alice E. Davidson, Ilaria Zito, et al. 2012. "Deep Intronic Mutation in Ofd1, Identified by Targeted Genomic next-Generation Sequencing, Causes a Severe Form of x-Linked Retinitis Pigmentosa (Rp23)." *Human Molecular Genetics* 21 (16): 3647–54. https://doi.org/10.1093/hmg/dds194.

Weiss, Ellen R, Melissa H Ducceschi, Thierry J Horner, Aimin Li, Cheryl M Craft, and Shoji Osawa. 2001. "Species-Specific Differences in Expression of G-Protein-Coupled Receptor Kinase (GRK) 7 and GRK1 in Mammalian Cone Photoreceptor Cells: Implications for Cone Cell Phototransduction." *Cloning*. https://doi.org/21/23/9175 [pii].

Weitz, Dietmar, Nicole Ficek, Elisabeth Kremmer, Paul J. Bauer, and U. Benjamin Kaupp. 2002. "Subunit Stoichiometry of the CNG Channel of Rod Photoreceptors." *Neuron*. https://doi.org/10.1016/S0896-6273(02)01098-X.

Wen, R, Y Song, T Cheng, M T Matthes, D Yasumura, M M LaVail, and R H Steinberg. 1995. "Injury-Induced Upregulation of BFGF and CNTF MRNAS in the Rat Retina." *The Journal of Neuroscience : The Official Journal of the Society for Neuroscience*. https://doi.org/10.1097/00006982-199616020-00027.

Wen, Zilong, Zhong Zhong, and James E. Darnell. 1995. "Maximal Activation of Transcription by Statl and Stat3 Requires Both Tyrosine and Serine

Phosphorylation.” *Cell*. https://doi.org/10.1016/0092-8674(95)90311-9.

Wenzel, a, C Grimm, a Marti, N Kueng-Hitz, F Hafezi, G Niemeyer, and C E Remé. 2000. “C-Fos Controls the ‘Private Pathway’ of Light-Induced Apoptosis of Retinal Photoreceptors.” *The Journal of Neuroscience : The Official Journal of the Society for Neuroscience*. https://doi.org/10.1523/JNEUROSCI.20-01-00081.2000.

Whelan, J. P., and J. F. McGinnis. 1988. “Light- dependent Subcellular Movement of Photoreceptor Proteins.” *Journal of Neuroscience Research*. https://doi.org/10.1002/jnr.490200216.

Whiting, Paul, Julie Kerby, Peter Coffey, Lyndon da Cruz, and Ruth McKernan. 2015. “Progressing a Human Embryonic Stem-Cell-Based Regenerative Medicine Therapy towards the Clinic.” *Philosophical Transactions of the Royal Society B: Biological Sciences*. https://doi.org/10.1098/rstb.2014.0375.

Wilcke, Mona, Ludger Johannes, Thierry Galli, Véronique Mayau, Bruno Goud, and Jean Salamero. 2000. “Rab11 Regulates the Compartmentalization of Early Endosomes Required for Efficient Transport from Early Endosomes to the Trans-Golgi Network.” *Journal of Cell Biology*. https://doi.org/10.1083/jcb.151.6.1207.

Wilden, U., S. W. Hall, and H. Kuhn. 1986. “Phosphodiesterase Activation by Photoexcited Rhodopsin Is Quenched When Rhodopsin Is Phosphorylated and Binds the Intrinsic 48-KDa Protein of Rod Outer Segments.” *Proceedings of the National Academy of Sciences*. https://doi.org/10.1073/pnas.83.5.1174.

Will, C. L., and R. Lührmann. 2001. “Spliceosomal UsnRNP Biogenesis, Structure and Function.” *Current Opinion in Cell Biology*. https://doi.org/10.1016/S0955-0674(00)00211-8.

Wolfrum, Uwe, and Angelika Schmitt. 2000. “Rhodopsin Transport in the Membrane of the Connecting Cilium of Mammalian Photoreceptor Cells.” *Cell Motility and the Cytoskeleton*. https://doi.org/10.1002/1097-0169(200006)46:2<95::AID-CM2>3.0.CO;2-Q.

Wood, Christopher R., Kaiyao Huang, Dennis R. Diener, and Joel L. Rosenbaum. 2013. “The Cilium Secretes Bioactive Ectosomes.” *Current Biology*.

https://doi.org/10.1016/j.cub.2013.04.019.

Wood, Christopher R., and Joel L. Rosenbaum. 2015. “Ciliary Ectosomes: Transmissions from the Cell’s Antenna.” *Trends in Cell Biology*. https://doi.org/10.1016/j.tcb.2014.12.008.

Wright, Kevin J., Lisa M. Baye, Anique Olivier-Mason, Saikat Mukhopadhyay, Liyun Sang, Mandy Kwong, Weiru Wang, et al. 2011. “An ARL3-UNC119-RP2 GTPase Cycle Targets Myristoylated NPHP3 to the Primary Cilium.” *Genes and Development* 25 (22): 2347–60. https://doi.org/10.1101/gad.173443.111.

Wright, Rachel N., Dong Hyun Hong, and Brian Perkins. 2012. “Rpgr ORF15 Connects to the Usher Protein Network through Direct Interactions with Multiple Whirlin Isoforms.” *Investigative Ophthalmology and Visual Science*. https://doi.org/10.1167/iovs.11-8845.

Wright, Zachary C, Ratnesh K Singh, Ryan Alpino, Andrew F X Goldberg, Maxim Sokolov, and Visvanathan Ramamurthy. 2016. “ARL3 Regulates Trafficking of Prenylated Phototransduction Proteins to the Rod Outer Segment.” *Human Molecular Genetics* , no. March: 1–46. https://doi.org/10.1093/hmg/ddw077.

Xu, Jun, Robert L. Dodd, Clint L. Makino, Melvin I. Simon, Denis A. Baylor, and Jeannle Chen. 1997. “Prolonged Photoresponses in Transgenic Mouse Rods Lacking Arrestin.” *Nature*. https://doi.org/10.1038/39068.

Yamashima, Tetsumori. 2004. “Ca2+-Dependent Proteases in Ischemic Neuronal Death. A Conserved ‘calpain-Cathepsin Cascade’ from Nematodes to Primates.” *Cell Calcium*. https://doi.org/10.1016/j.ceca.2004.03.001.

Yan, Denise, Prabodha K. Swain, Debra Breuer, Rebecca M. Tucker, Weiping Wu, Ricardo Fujita, Alnawaz Rehemtulla, David Burke, and Anand Swaroop. 1998. “Biochemical Characterization and Subcellular Localization of the Mouse Retinitis Pigmentosa GTPase Regulator (MRpgr).” *Journal of Biological Chemistry*. https://doi.org/10.1074/jbc.273.31.19656.

Yang, Jun, Xiaoqing Liu, Yun Zhao, Michael Adamian, Basil Pawlyk, Xun Sun, Randy D. McMillan, M. Charles Liberman, and Tiansen Li. 2010. “Ablation of Whirlin Long Isoform Disrupts the USH2 Protein Complex and Causes Vision and Hearing Loss.” *PLoS Genetics*.

https://doi.org/10.1371/journal.pgen.1000955.

Yang, Li Ping, Le Meng Wu, Xiu Juan Guo, and Mark O.M. Tso. 2007. “Activation of Endoplasmic Reticulum Stress in Degenerating Photoreceptors of the Rd1 Mouse.” *Investigative Ophthalmology and Visual Science*. https://doi.org/10.1167/iovs.07-0512.

Yang, R B, S W Robinson, W H Xiong, K W Yau, D G Birch, and D L Garbers. 1999. “Disruption of a Retinal Guanylyl Cyclase Gene Leads to Cone-Specific Dystrophy and Paradoxical Rod Behavior.” *The Journal of Neuroscience : The Official Journal of the Society for Neuroscience*. https://doi.org/10.1523/JNEUROSCI.19-14-05889.1999.

Yang, Wei, Dolores Di Vizio, Marc Kirchner, Hanno Steen, and Michael R. Freeman. 2010. “Proteome Scale Characterization of Human *S* -Acylated Proteins in Lipid Raft-Enriched and Non-Raft Membranes.” *Molecular & Cellular Proteomics*. https://doi.org/10.1074/mcp.M800448-MCP200.

Yang, Xiuwei, Oleg V. Kovalenko, Wei Tang, Christoph Claas, Christopher S. Stipp, and Martin E. Hemler. 2004. “Palmitoylation Supports Assembly and Function of Integrin-Tetraspanin Complexes.” *Journal of Cell Biology*. https://doi.org/10.1083/jcb.200404100.

Yao, Kai, Suo Qiu, Yanbin V. Wang, Silvia J. H. Park, Ethan J. Mohns, Bhupesh Mehta, Xinran Liu, et al. 2018. “Restoration of Vision after de Novo Genesis of Rod Photoreceptors in Mammalian Retinas.” *Nature*. https://doi.org/10.1038/s41586-018-0425-3.

Yasuda-Yamahara, M., M. Rogg, J. Frimmel, P. Trachte, M. Helmstaedter, P. Schroder, M. Schiffer, C. Schell, and T. B. Huber. 2018. “FERMT2 Links Cortical Actin Structures, Plasma Membrane Tension and Focal Adhesion Function to Stabilize Podocyte Morphology.” *Matrix Biology*. https://doi.org/10.1016/j.matbio.2018.01.003.

Yau, K. W. 1994. “Phototransduction Mechanism in Retinal Rods and Cones. The Friedenwald Lecture.” *Investigative Ophthalmology and Visual Science*.

Yoon, Jung Hoon, Junzhuan Qiu, Sheng Cai, Yuan Chen, Michael E. Cheetham, Binghui Shen, and Gerd P. Pfeifer. 2006. “The Retinitis Pigmentosa-Mutated

RP2 Protein Exhibits Exonuclease Activity and Translocates to the Nucleus in Response to DNA Damage." *Experimental Cell Research*. https://doi.org/10.1016/j.yexcr.2005.12.026.

Yu, Dao-Yi, Stephen J Cringle, Er-Ning Su, and Paula K Yu. 2000. "Intraretinal Oxygen Levels before and after Photoreceptor Loss in the RCS Rat." *Investigative Ophthalmology & Visual Science* 41 (12): 3999–4006.

Yu, Hua, Drew Pardoll, and Richard Jove. 2009. "STATs in Cancer Inflammation and Immunity: A Leading Role for STAT3." *Nature Reviews Cancer* 9 (November): 798.

Zach, Frank, Felix Grassmann, Thomas Langmann, Nasrin Sorusch, Uwe Wolfrum, and Heidi Stöhr. 2012. "The Retinitis Pigmentosa 28 Protein FAM161A Is a Novel Ciliary Protein Involved in Intermolecular Protein Interaction and Microtubule Association." *Human Molecular Genetics*. https://doi.org/10.1093/hmg/dds268.

Zeng, Hui Yang, Xiu An Zhu, Cheng Zhang, Li Ping Yang, Le Meng Wu, and Mark O.M. Tso. 2005. "Identification of Sequential Events and Factors Associated with Microglial Activation, Migration, and Cytotoxicity in Retinal Degeneration in Rd Mice." *Investigative Ophthalmology and Visual Science*. https://doi.org/10.1167/iovs.05-0118.

Zhang, H, S Li, T Doan, F Rieke, P B Detwiler, J M Frederick, and W Baehr. 2007. "Deletion of PrBP/Delta Impedes Transport of GRK1 and PDE6 Catalytic Subunits to Photoreceptor Outer Segments." *Proceedings of the National Academy of Sciences of the United States of America* 104 (21): 8857–62. https://doi.org/10.1073/pnas.0701681104.

Zhang, Houbin, Ryan Constantine, Sergey Vorobiev, Yang Chen, Jayaraman Seetharaman, Yuanpeng Janet Huang, Rong Xiao, et al. 2011. "UNC119 Is Required for G Protein Trafficking in Sensory Neurons." *Nature Neuroscience* 14 (7): 874–80. https://doi.org/10.1038/nn.2835.

Zhang, Houbin, Jie Fan, Sha Li, Sukanya Karan, Baerbel Rohrer, Krzysztof Palczewski, Jeanne M Frederick, Rosalie K Crouch, and Wolfgang Baehr. 2008. "Trafficking of Membrane-Associated Proteins to Cone Photoreceptor Outer Segments Requires the Chromophore 11-Cis-Retinal." *The Journal of*

Neuroscience : The Official Journal of the Society for Neuroscience. https://doi.org/10.1523/JNEUROSCI.0317-08.2008.

Zhang, Houbin, Jeanne M. Frederick, and Wolfgang Baehr. 2014. “Unc119 Gene Deletion Partially Rescues the GRK1 Transport Defect of Pde6d$^{-/-}$ Cones.” *Advances in Experimental Medicine and Biology* 801: 487–93. https://doi.org/10.1007/978-1-4614-3209-8_62.

Zhang, Houbin, Christin Hanke-Gogokhia, Li Jiang, Xiaobo Li, Pu Wang, Cecilia D. Gerstner, Jeanne M. Frederick, Zhenglin Yang, and Wolfgang Baehr. 2015. “Mistrafficking of Prenylated Proteins Causes Retinitis Pigmentosa 2.” *FASEB Journal* 29 (3): 932–42. https://doi.org/10.1096/fj.14-257915.

Zhang, Houbin, Xiao Hui Liu, Kai Zhang, Ching Kang Chen, Jeanne M. Frederick, Glenn D. Prestwich, and Wolfgang Baehr. 2004. “Photoreceptor CGMP Phosphodiesterase ?? Subunit (PDE??) Functions as a Prenyl-Binding Protein.” *Journal of Biological Chemistry* 279 (1): 407–13. https://doi.org/10.1074/jbc.M306559200.

Zhang, Qing, Jinghua Hu, and Kun Ling. 2013. “Molecular Views of Arf-like Small GTPases in Cilia and Ciliopathies.” *Experimental Cell Research*. https://doi.org/10.1016/j.yexcr.2013.03.024.

Zhang, Samuel Shao-Min, Mu-Gen Liu, Arihiro Kano, Chun Zhang, Xin-Yuan Fu, and Colin J Barnstable. 2005. “STAT3 Activation in Response to Growth Factors or Cytokines Participates in Retina Precursor Proliferation.” *Experimental Eye Research*. https://doi.org/10.1016/j.exer.2005.01.016.

Zhang, Samuel Shao Min, Jiye Wei, Hua Qin, Lixin Zhang, Bing Xie, Pei Hui, Albert Deisseroth, Colin J. Barnstable, and Xin Yuan Fu. 2004. “STAT3-Mediated Signaling in the Determination of Rod Photoreceptor Cell Fate in Mouse Retina.” *Investigative Ophthalmology and Visual Science*. https://doi.org/10.1167/iovs.04-0003.

Zhang, T., N. Zhang, W. Baehr, and Y. Fu. 2011. “Cone Opsin Determines the Time Course of Cone Photoreceptor Degeneration in Leber Congenital Amaurosis.” *Proceedings of the National Academy of Sciences*. https://doi.org/10.1073/pnas.1017127108.

Zhang, Xinmin, Duncan T Odom, Seung-Hoi Koo, Michael D Conkright, Gianluca Canettieri, Jennifer Best, Huaming Chen, et al. 2005. “Genome-Wide Analysis of CAMP-Response Element Binding Protein Occupancy, Phosphorylation, and Target Gene Activation in Human Tissues.” *Proceedings of the National Academy of Sciences of the United States of America*. https://doi.org/10.1073/pnas.0501076102.

Zhao, Yun, Dong-Hyun Hong, Basil Pawlyk, Guohua Yue, Michael Adamian, Marcin Grynberg, Adam Godzik, and Tiansen Li. 2003. “The Retinitis Pigmentosa GTPase Regulator (RPGR)- Interacting Protein: Subserving RPGR Function and Participating in Disk Morphogenesis.” *Proceedings of the National Academy of Sciences* 100 (7): 3965–70. https://doi.org/10.1073/pnas.0637349100.

Zheng, Jie, Matthew C. Trudeau, and William N. Zagotta. 2002. “Rod Cyclic Nucleotide-Gated Channels Have a Stoichiometry of Three CNGA1 Subunits and One CNGB1 Subunit.” *Neuron*. https://doi.org/10.1016/S0896-6273(02)01099-1.

Zhong, Haining, Laurie L Molday, Robert S Molday, and King-Wai Yau. 2002. “The Heteromeric Cyclic Nucleotide- Gated Channel Adopts a 3A : 1B Stoichiometry.” *Nature*. https://doi.org/10.1038/nature01166.1.

Zhou, C, L Cunningham, AI Marcus, Y Li, and RA Kahn. 2006. “Arl2 and Arl3 Regulate Different Microtubule-Dependent Processes.” *Molecular Biology of the Cell*. https://doi.org/10.1091/mbc.E05-10-0929.

Zhu, X, K Wu, L Rife, B Brown, and C M Craft. 2005. “Rod Arrestin Expression and Function in Cone Photoreceptors .” *Investigative Ophthalmology & Visual Science* 46 (13): 1179.